A study of mechanisms of genotoxicity in mammalian cells by retrovirus vectors intended for gene therapy

A thesis submitted for the degree of

Doctor of Philosophy

By

Safia Reja

Biosciences, School of Health Sciences and Social Care

Brunel University

September 2013

Abstract

Retrovirus gene therapy vectors can deliver therapeutic genes to mammalian cells in a permanent manner by integrating their genome into host chromosomes and therefore provide the potential for long term therapeutic gene expression. Retrovirus integration, however, can be oncogenic. Apart from insertional mutagenesis (IM) genotoxicity may be caused by other factors including DNA damage following infection and integration and epigenetic effects related to incoming viral particles. Thus, using retrovirus and lentivirus infected murine tumour tissue and infected cell lines *in vitro* this thesis was directed at investigating whether virus infection and integration could cause genotoxicity by alternative route(s) other than IM.

Using clonally derived liver tumours that developed in mice, and normal liver and kidney tissues, following EIAV and HIV delivery *in utero*, comparative genome hybridisation methodology was used to examine for copy number variation. This showed amplification and deletions only in EIAV derived tumours. Real time Q-PCR analysis was then used to measure gene expression changes relating to genes contained within or near to amplifications observed in two tumours of individual mice. The STRING database was then used to find networks linking genes with differential expression profiles and genes in one of these tumours identified with provirus insertions that were also differentially expressed. These data provided preliminary data implicating a role for LV in Hepatocellular carcinoma (HCC).

DNA damage is known to cause chromosomal instability that can lead to tumour development. The relationship between double strand breaks (DSB) and virus infection was also investigated *in-vitro* to find alternative routes to genotoxicity other than IM. Cell viability analysis demonstrated cells with a defective DNA damage response (DDR) have decreased cell viability compared with cells with intact DDR when infected with RV or LV vectors. DSB assays showed RV and LV infection to generate foci over a 6 hour period followed by DDR. Where no viral integrase is present, no DDR appears, however, where the vector is used with or without a genome to infect cells, DDR occurs as shown by the presence of 53BP1 foci indicative of DNA damage.

The relationship between DNA damage and methylation was also investigated. Global methylation was found elevated in the genomic DNA of LV and RV infected cells and not in control uninfected cells. In contrast, methylation changes were not found in

infected cells lacking the NHEJ repair pathway. These data suggest the DNA damage response is linked to genome methylation. The E2F transcription factor plays a key role in regulating expression of genes known to control oncogenesis and cancer, and E2F is regulated by methylation of its related target gene promoters. Taking into account all genes in the human genome the number of genes that bind E2F is 32.77%. However, using microarray to represent genes differentially expressed after infection, 59% of these were E2F targets.

Overall, taking the data obtained in this thesis into account it may be suggested that RV and LV infection causes a number of potentially related changes to cells that include DNA damage and repair and methylation changes that could influence E2F that is an important factor involved in oncogenesis. Combining this with IM, attenuated RV and LV currently in use for gene therapy may cause genotoxicity to infected cells and increase the risk of oncogenesis especially where DNA damage is not correctly repaired. Further work is required to show in greater detail the extent of this genotoxicity, possible by whole genome sequencing of treated host genomes or cell transformation assays linked to the genotoxicity assays presented here.

Collectively these data show that alternative factors to IM might exist that could act independently or synergistically to IM.

Declaration

I hereby declare that all the work presented in this thesis has been performed by me unless otherwise stated.

Safia Reja

Acknowledgements

I would like to first of all thank my supervisor, Dr Michael Themis for his guidance, support, strength, and encouragement throughout my PhD. The pure passion and enthusiasm he conveys has been the keystone for my morale and has kept me going for the last 4 years. I am highly grateful for this special experience that I will always treasure and thank him for giving me this opportunity.

I would like to express my sincere thanks to Dr Matthew Themis and Dr Christopher Parris for the trainings, support, and advice they have always given me since the beginning of my PhD.

I would like to acknowledge the generosity of several collaborators; in particular our collaborators from the Wellcome Trust, Dr Ruby Banerjee and Dr Nathalie Conte for their help in mFISH and CGH. I am also grateful to Dr Martin Spitaler from Imperial college, London. I would also like to thank Professor Penny Jeggo from the University of Sussex, UK for supplying the 53BP1 -/- cell line. I specially would like to thank Dr Annette Payne for her contribution to Microarray analysis.

I would also very much like to thank Dr Viacheslav Bolshakov for his guidance, assistance, training, and use of equipment when carrying out Microarray.

I would like to express my gratitude to my fellow group member Hassan Khonsari for his advice and assistance pertaining to PCR and cell culture.

I reserve a special thank you to the members of the Centre for cell and chromosome biology, the cancer institute and the PhD office for their helpful advice and support but most of all for their friendship and making my PhD an enjoyable experience. I would particularly like to acknowledge Dr Emma Osejindu for her help with many things including Q-PCR training. Thank you for your friendship and support.

Thank you to my friends outside of the PhD bubble who despite my absence still encouraged me to stay focus.

Also a big thank you, to my best friend and PhD “sister” Halime Arican, for always being there for me and knowing all the right things to say. I am grateful I got to

experience this with you and will treasure our time together not only in the lab but also in your aptly named car, the dirty princess.

I would like to say a huge thank you to my beautiful parents for their infinite love and support. Mom and Dad you have been my constant support system throughout my studies without you both I would have lost my mind. Last but not least I would like to thank my lovely husband Musawir for not least his words of support and encouragement but his ability to make me laugh when things got tough. Thank you all for believing in me and keeping me as sane as possible. I love you all!!

To my parents, my greatest inspiration of all, who have always shown me the light, I dedicate this thesis to you.

Abbreviations

ADA	adenosine deaminase
AIDS	acquired immune deficiency syndrome
ALV	avian leucosis virus
ASLV	avian sarcoma leucosis virus
ATM	ataxia-telangiectasia
β-gal	beta- galactosidase
β-ME	beta-mercaptoethanol
BSA	bovine serum albumin
CA	capsid protein
CAEV	caprine arthritis-encephalomyelitis
CAT	cationic amino acid transporter-1
CCR5	C-C chemokine receptor type 5
CD34+	haematopoietic progenitor cells
cDNA	complementary deoxyribonucleic acid
CGD	chronic granulomatous disease
CIN	chromosome instability
CIS	common insertion sites
CMV	cytomegalovirus
CpG	cytomegalovirus
cPPT	central polypurine tract
CT	cycle threshold
CXCR4	C-X-C chemokine receptor type 4
DDR	DNA damage response
dH_2O	distilled water
DMEM	Dulbecco's modified eagle's medium
DMSO	dimethyl sulfoxide
DNA	deoxyribonucleic acid
DNMT	DNA methyl transferase
dNTPs	deoxynucleotide triphosphates
DSB	double strand break
dsDNA	double stranded DNA
DTT	dithiothreitol

DU/dUTPase	deoxnucleotide triphosphates
EB	elution buffer
EDTA	ethylene diamine tetraacetic acid
EIA	equine infectious anaemia
EIAV	equine infectious anaemia virus
Env	viral envelope
EVI1	ecotropic viral integration site
FDA	US food and drug administration
FIV	feline immunodeficiency virus
FIX	clotting factor IX
GAPDH	glyceraldehyde-3-phosphate dehydrogenase
GFP/eGFP	green florescent protein
Go	gene ontology
GP	glycoprotein
gp120	envelope glycoprotein
hrs	Hours
HBV	hepatitis B virus
HCC	hepatocellular carcinoma
HepG2	hepatocellular carcinoma cell line
hFIX	human clotting factor
HIV	human immunodeficiency virus
HLA	human leukocyte antigen
HPRT	hypoxanthine-guanine phosphoribsyltransferase
HR	homologous recombination
HR'SIN-CPPT-S-FX-W	HIV vector construct containing SFFV promoter
HSC	haematopoietic stem cell
HSV	herpes simplex virus
IDDb	insertional dominance database
IL2	interleukin 2
IL2RG	interleukin 2 receptor, gamma
IM	insertional mutagenesis
IN	integrase
IS	insertion site

Kb	kilobase pairs
LacZ	β-galactosidase gene
LAM-PCR	linear amplification mediated polymerase chain reaction
LB	Luria-Bertani
LCMV	lymphocytic choriomengitis virus
LEDGF	lens epithelium- derived growth factor
LTR	long terminal repeat
LV	lentivirus
MA	matrix protein
MDR1	multiresistance gene 1
$MgCl_2$	magnesium chloride
MIN	mutational instability
MLV	murine leukaemia virus
MOI	multiplicity of infection
Mo-MLV	Moloney murine leukaemia virus
mRNA	messenger ribonucleic acid
NC	Nucleoplasmid
NHEJ	non homologous end joining
NK	natural killer cell
P1	re-suspension buffer
P2	lysis buffer
P3	neutralising buffer
PB	binding buffer
PBL	peripheral blood lymphocytes
PBS	phosphate buffer solution
PCR	polymerase chain reaction
PE	wash buffer
PEG	polyethylene glycol-conjugates bovine
PIC	preintegration complex
pLIONhAATGFP FIV	construct containing eGFP reporyter gene
POL	polymerase
PPT	polypurine tract
PR	protease

PSI/Ψ	packaging signal
QPCR	quantitative real time polymerase chain reaction
R	repeat region
RB	retinoblastoma
RCL	replication competent lentivirus
RCR	replication competent retrovirus
RCV	replication competent virus
RDV	replication defective retrovirus
RefSeq	reference sequence
REV	regulatory of viron
RIS	retroviral insertion site
RNA	ribonucleic acid
rpm	rotations per minute
RQ	relative quantification level
RRE	rev response element
rRNA	ribosomal ribonucleic acid
RT	reverse transcriptase
RTCGD	retroviral tagged cancer gene database
RT-PCR	reverse transcription polymerase chain reaction
RV	retrovirus
SAHA	suberoylanilide hydroxamic acid
SCID	severe combined immunodeficiency
SD	splice donor
SEM	standard error of the mean
SFFV	spleen focus forming virus
SIN	self-inactivating
SIV	simian immunodeficiency virus
SMART2Z EIAV	vector construct containing lacZ transgene
ssRNA	single strand RNA
STRING	search tool for interacting genes/proteins
SU	surface unit
TAR	transactivator responsive element
TAT	transcriptional activator

TBE	tris borate acid
TE	tris-EDTA
TM	transmembrane subunit
tRNA	transfer ribonucleic acid
U3	unique 3'
U5	unique 5'
VSG-G	vesicular stomatitis virus G glycoprotein
WHO	world health organization
WPRE	woodchuck hepatitis virus posttranscriptional regulatory
X-gal	5-bromo-4-chloro-3-indolyl-β-D-galactopyranoside
X-SCID	x-linked severe combined immunodeficiency
6TG	6-thiguanine
18SRNA	18S ribosomal RNA

Table of Contents

Abstract.....i-ii

Declaration.....iii

Acknowledgements.....iv-v

Abbreviations.....vi-x

Table of contents.....xi-xv

List of figures.....xvi-xviii

List of tables.....xix-xx

Chapter 1: Introduction **1-49**

1.1: Gene therapy……...1

1.2: Retroviruses……2-5

1.2.1: Life cycle of the RV…….....6-11

1.3: Lentivirus……..……...12-14

1.3.1: HIV…….....14

1.4: Optimizing vectors and vector packaging……..……..……...14-17

1.5: Gene therapy success……18

1.6: Gene therapy trials involving retrovirus vectors…….……19-20

1.7: Safety of gene therapy vectors…….……..21

1.8: Genotoxicity……...……21

1.8.1: Insertion site (IS) selection…….……22-23

1.8.2: Insertional mutagenesis (IM)…….……...24

1.9: Identification of IM during gene therapy of X-SCID…….……24-26

1.10: Chronic granulomatous (CGD) trial…….……26-27

1.11: Models of genotoxicity…….……28

1.11.1: *In Vitro* models of genotoxicity…….……28-30

1.11.2: *In Vivo* models of genotoxicity…….……..30-31

1.12: Alternative routes to genotoxicity not involving IM……..32

1.12.1: DNA damage……..32-33

1.12.2: DNA DSB repair……..34
1.12.2.1: DNA repair by Homologous recombination (HR)..34-35
1.12.2.2: DNA repair by non-homologous recombination (NHEJ)……35-36
1.12.3: Genome instability due to DSB……..36-38
1.12.4: Proteins used to determine the presence of DSBs……..38-39
1.12.5: Methods for determining DNA DSBs……..…40
1.12.6: Retrovirus integration mediated DSBs……...41-42
1.13: Epigenetic modifications leading to genotoxicity……43-45
1.14: Viral integration and methylation……....45-46
1.15: Methylation and DNA damage……47
1.16: E2F and DNA damage…….....48-49
1.17: Hypothesis……..……....49
1.17.1: Aims and objectives……49

Chapter 2: Materials and Methods 50-80

2.1: Materials…….. 50-60
2.1.1: General chemicals and reagents…….....50
2.1.2: Tissue culture reagents……..51
2.1.3: X-gal reagents……...51
2.1.4: Cell viability reagents……...51
2.1.5: Immunofluorescence reagents……..52
2.1.6: DNA extraction reagents……..52
2.1.7: Reagents for global methylation assay using Imprint® methylated DNA quantification kit……52
2.1.8: Pre designed and custom made TaqMan probes for gene expression analysis……...53
2.1.9: RNA extraction reagents……..53
2.1.10: cDNA synthesis for real time quantitative (Q)-PCR reagents...54
2.1.11: Q-PCR reagents for gene expression analysis……...54
2.1.12: mFISH reagents……54-55
2.1.13: Microarray reagents……..55
2.1.14: Compositions of buffers and solutions…….56-58

2.1.15: Cell lines……....60
2.1.16: Viral vectors……60
2.2: Methods…….. 61-80
2.2.1: Mammalian cell culture methods…….....61
2.2.1.1: Growth and maintenance……...61
2.2.1.2: Long term storage of cells in liquid nitrogen…….62
2.2.1.3: Seeding cells into cell culture dishes……..62
2.2.1.4: Infection of cells with viral vectors……62
2.2.2: X-gal staining- Percentage of infectibility……...62-63
2.2.2.1: Image capture and processing……63
2.2.3: Cell viability assay……63
2.2.4: Immunofluorescence……64
2.2.4.1: Immunofluorescence image analysis……64
2.2.5: DNA extraction from cultured cells……64-65
2.2.6: Quantification of nucleic acids……65
2.2.7: Agarose gel electrophoresis……..66
2.2.8: Global methylation assay using Imprint® methylated DNA quantification kit……..66-67
2.2.9: RNA extraction from cultured cells…….67-68
2.2.9.1: *DNase I* treatment…….68-69
2.2.10: cDNA synthesis for Q-PCR……...69-70
2.2.10.1: Q-PCR for gene expression analysis……..70-71
2.2.11: Microarray……..72
2.2.11.1: cDNA synthesis from RNA……72-73
2.2.11.2: Degradation of the RNA……..73
2.2.11.3: Pre-slide scanning and wash……74
2.2.11.4: Pre-hybridisation of slides……...74
2.2.11.5: Preparation of Slidebooster…….75
2.2.11.6: cDNA hybridisation……...75-76
2.2.11.7: Post cDNA hybridisation wash……76
2.2.11.8: Hybridisation of the fluorescently labelled 3DNA to the microarray slide……..76-77
2.2.11.9: Post 3DNA hybridisation wash……...77

2.2.11.10: Microarray image acquisition……78
2.2.11.11: Microarray image analysis……..78
2.2.11.12: Microarray data analysis……78
2.2.12: mFISH……78
2.2.12.1: Slide preparation and metaphase spreads…….79
2.2.13.2: Slide pre-treatment prior to hybridisation……...79
2.2.13.3: Hybridisation……...79
2.2.12.4: Post-hybridisation wash and detection……...79-80
2.2.12.5: mFISH imaging……...80

Chapter 3: Results **81-95**

3.1: Background…….....81-82
3.2: Investigation of mouse tumour DNA compared to non-tumour liver using CGH……..82-95

Chapter 4: Results **96-149**

4.1: Investigation of vector associated genotoxicity in cells following *in vitro* delivery of RV and LV…….…….....96
4.1.1: Cell Infectibility…….96-104
4.1.2: Survival of cells following infection……...104-112
4.1.3: The effect of infection by RV and LV on DNA DSB…….113-142
4.2: An investigation of chromosome integrity using multicolour florescent *in situ* hybridisation (mFISH) and G-banding following infection…..143-149

Chapter 5: Results **150-172**

5.1: Epigenetic modification and E2F regulation of host genes following RV and LV vector delivery…….…….....150
5.1.1: The effects of RV and LV infection on host epigenetics via Methylation…….150-166
5.2: Microarray analysis of cells infected with RV and LV vectors…..167-170
5.2.1: Analysis of differential expression of target genes associated with the E2F transcription factor……..170-172

Chapter 6: Discussion **173-187**

6.1: Conclusion…….....187

References..... *188*

Appendix 1 ..... *213*

List of Figures

Figure 1. Schematic representation of a retroviruses particle 4

Figure 2. A schematic overview of the retrovirus genome 5

Figure 3. Schematic illustration of the general stages of the RV lifecycle ... 6

Figure 4. Retrovirus replication 8

Figure 5. Integration of retroviral DNA into the host cell genome 10

Figure 6. Schematic representation of the HIV genome 13

Figure 7. CGH ideograms representing pooled CNV of tumours 83-86

Figure 8. CGH ideograms representing CNV in EIAV tumour 2 87-89

Figure 9. CGH ideogram representing amplification of part of chromosome 2 in EIAV derived tumour 1 90

Figure 10. Ideogram comparing tumours 1 and 2 CNV in chromosome 2 ... 91

Figure 11. RT-PCR of Hnf4α, Hnf1α and Foxa2 genes in tumours one and tumour two 93

Figure 12. Analysis of the relationship between genes found by CGH and IM of tumour 2 94

Figure 13. Mcf10a cells infected with RV and LV vectors 97

Figure 14. Mrc5 cells infected with RV and LV vectors 98

Figure 15. At5biva cells infected with RV and LV vectors 99

Figure 16. Xp14br cells infected with RV and LV vectors 100

Figure 17. Mcf10a, Mrc5, At5biva and Xp14br cells infected with an HIV deprived integrase negative (IN-ve) vector at high and low MOI 101-102

Figure 18. Mcf10a and Mrc5 percentage cell survival following infection with RV and LV at high MOI 105

Figure 19. At5biva and Xp14br percentage cell survival on infection with RV and LV at high MOI 106

Figure 20. Mcf10a and Mrc5 percentage cell survival following infection with RV and LV at low MOI 107

Figure 21. At5biva and Xp14br percentage cell survival on infection with RV and LV at low MOI 108

Figure 22a & b. Photomicrographs of immunofluorescence of 53BP1 in Mcf10a cells infected by RV and LV at high and low MOI 114-116

Figure 23a & b. Histograms of the mean number of 53BP1 foci in Mcf10a cells infected at high and low MOI.....117-118
Figure 24a & b. Histograms of the mean number of 53BP1 foci in Mrc5 cells infected at high and low MOI.....121-122
Figure 25a & b. Histograms of the mean number of 53BP1 foci in At5biva cells infected at high and low MOI.....125-126
Figure 26a & b. Histograms of the mean number of 53BP1 foci in Xp14br cells infected at high and low MOI.....129-130
Figure 27. Pie charts representing frequency of 53Bp1 foci in Mcf10a nuclei at 6 hours post treatment with IR, MLV, HIV, EIAV, FIV, IN- and MLV without genome 134-135
Figure 28. Pie charts representing frequency of 53Bp1 foci in Mrc5 nuclei at 6 hours post treatment with IR, MLV, HIV, EIAV, FIV, IN- and MLV without genome 136-137
Figure 29. Pie charts representing frequency of 53Bp1 foci in At5biva nuclei at 6 hours post treatment with IR, MLV, HIV, EIAV, FIV, IN- and MLV without genome 138-139
Figure 30. Pie charts representing frequency of 53Bp1 foci in Xp14br nuclei at 6 hours post treatment with IR, MLV, HIV, EIAV, FIV, IN- and MLV without genome 140-141
Figure 31. mFISH and pseudo G-banding of un-infected Mcf10a 144-145
Figure 32. mFISH and pseudo G-banding of EIAV, HIV and MLV infected Mcf10a cells 146-149
Figure 33. Global methylation levels in RV and LV infected Mcf10a cells 152
Figure 34. Global methylation levels in RV and LV infected HepG2 cells 154
Figure 35. Global methylation levels in RV and LV infected 53BP1-/- cells 156
Figure 36. Dnmt1, 3a and 3b expression in Mcf10a cells following RV and LV infection.....159-160
Figure 37. Dnmt1, 3a and 3b expression in HepG2 cells following RV and LV infection.....162-163

Figure 38. Dnmt1 and 3a expression in 53BP1 -/- cells following RV and LV infection 165-166

List of Tables

Table 1. Classification of retrovirus 3
Table 2. Basic components of the retrovirus genome 5
Table 3. General chemicals and reagents 50
Table 4. General reagents used for tissue culture 51
Table 5. General chemical and reagents used in x-gal procedure 51
Table 6. General chemical and reagents used in cell viability assays 51
Table 7. Reagents used in immunofluorescence 52
Table 8. Reagents used for DNA extraction of cells 52
Table 9. General reagents used for global methylation assays 52
Table 10. TaqMan gene expression assays used to quantify DNA methyltransferase activity 53
Table 11. Reagents used for isolation of total RNA from cell lines, Dnase1 treatments and RNA purification 53
Table 12. General chemicals and regents used for cDNA synthesis of total RNA for Q-PCR 54
Table 13. General chemicals and reagents for TaqMan PCR reactions 54
Table 14. General chemicals and reagents for mFISH 54-55
Table 15. General chemicals and reagents used for Microarray 55
Table 16. Preparation of one reaction mixture for *DNase* I treatment 68
Table 17. General reagents used for cDNA synthesis of total RNA for Q-PCR .. 69
Table 18. PCR parameters used for cDNA synthesis using the MultiScibe reaction kit 70
Table 19. Reagents used for preparation of TaqMan PCR mastermix for amplifications 70
Table 20. PCR parameters required for Q-PCR 71
Table 21. Samples used for the reaction master mix for cDNA synthesis 72
Table 22. Reagents used for the reaction master mix of cDNA synthesis. 73
Table 23. Reagents used to make pre-hybridisation solution for Microarray 74
Table 24. Reagents used for cDNA hybridisation for Microarray. 75
Table 25. Reagents used for 3DNA hybridisation mix for one slide for Microarray 77

Table 26. Real time PCR relative change in gene expression of *Hnf4α, Hnf1α* and *Foxa2* in tumour 1 and 2 92
Table 27. Percentage level of infection in Mcf10a, Mrc5, At5biva and Xp14br cells..... 103
Table 28. Percentage of viable cells on infection with high MOI RV and LV 109-110
Table 29. Percentage of viable cells on infection with low MOI RV and LV 111
Table 30a. Mean number of foci in Mcf10a nuclei at high MOI..... 119
Table 30b. Mean number of foci in Mcf10a nuclei at low MOI..... 120
Table 31a. Mean number of foci in Mrc5 nuclei at high MOI..... 123
Table 30b. Mean number of foci in Mrc5 nuclei at low MOI..... 124
Table 32a. Mean number of foci in At5biva nuclei at high MOI 127
Table 30b. Mean number of foci in At5biva nuclei at high MOI 128
Table 33a. Mean number of foci in Xp14br nuclei at low MOI 131
Table 33b Mean number of foci in Xp14br nuclei at high MOI 132
Table 34. Measurement of global methylation in Mcf10a cells infected with RV and LV vectors 151
Table 35. Measurement of global methylation in HepG2 cells infected with RV and LV vectors 153
Table 36. Measurement of global methylation in 53BP1-/- cells infected with RV and LV vectors 155
Table 37. DNA methyltransferase gene expression in Mcf10a cells following RV and LV infection..... 158
Table 38. DNA methyltransferase gene expression in HepG2 cells following RV and LV infection..... 161
Table 39. DNA methyltransferase gene expression in 53BP1 -/- cells following RV and LV infection 164
Table 40. Genes up-regulated by 1.2 following infection of Mcf10a cells by MLV, EIAV and MLV without viral genome vectors 168
Table 41. Genes down-regulated by 1.2 following infection of Mcf10a cells by MLV, EIAV and MLV without viral genome vectors 169-170
Table 42. Genes associated with E2F binding from virus treated Mcf10a cell..... 171-172

INTRODUCTION Chapter 1

1.1 Gene therapy

Gene therapy refers to the transfer of genetic material to cells to modify specific gene expression to treat or correct the progression of a genetic disease. Whilst traditional pharmacological therapies aim to cure the symptoms of a disease, gene therapy aims to treat or remove the cause of disease by correcting the defective genetic information contained within the cells of the patient. For some diseases stem cell therapy is possible, however, the complications associated with HLA-mismatched bone marrow transplantation have meant that the use of stem cells in an autologous manner is of importance. Thus, gene therapy should be used somatically or on patient stem cells in an *ex-vivo* manner.

Gene therapy is applicable to the "classic" diseases such as the inherited monogenic disorders that result from the absence or dysfunction of a specific gene product. It is also applicable to the treatment of rheumatoid arthritis, infection of pathogens, atherosclerosis and cancer.

Studies in the 1960's by Borenfreund and Bendich first demonstrated gene transfer of exogenous DNA and found that incorporation of genetic material into the nucleus of the mammalian cell occurred 6-24 hours post treatment (Borenfreund and Bendich, 1961). Interest in gene therapy increased when between 1961 and 1966 it was made possible to characterize and deliver therapeutic genes (Rieke1962; Borenfreund and Bendich, 1961; Bendich, 1961).

Gene therapy has been improved by the use of viruses as vectors to carry therapeutic genes into host cells defective of a genetic function as they have evolved intricate mechanisms for overcoming the defensive barriers of their target cells. One such virus is the retrovirus (RV) and our understanding of RV biology has helped us use these viruses to deliver genes in an efficient manner.

1.2 Retroviruses

The term RV is used to describe a large and diverse family of RNA viruses (Figure 1 and 2). RV were discovered more than 20 years ago. They have a small and simple genome that can provide stable co linear integration into host genome whilst also accommodating about 10kb of foreign DNA for high transfer efficiency (Bouard, Alazard-Dany and Cosset, 2009).

Retrovirus particles are typically 80-100nm in size and consist of enveloped glycoprotein particles and a lipid envelope (Coffin, Huges and Varmus, 1997). The retrovirus genome consists of two copies of single stranded linear RNA genome of positive polarity that are able to create double stranded complementary DNA (cDNA) copies of their RNA genomes in the nucleus of the host cell using reverse transcriptase. The DNA is then incorporated into the host's genome via a virally encoded protein called integrase. It is this process of alternating genetic material between RNA in the virion and DNA in infected cells which is the vital feature of the life cycle (Somia and Verma, 2000; Zhang and Temin, 1993). Also due to their ability to integrate into the host genome they can provide permanent gene transfer to the host cells (Bushman, 2007).

Retroviruses are broadly divided into simple and complex classes based on their genome organisation and can be further subdivided into seven groups (Table 1). Simple retroviruses encode only the basic viral functions such as the structural, enzymatic and envelope proteins. The complex retroviruses, code for additional regulatory proteins that help to accurately control the level and timing of expression of the viral genes (Brenner and Malech, 2003; Coffin, 1992).

Genome	Sub-Division	Genus	Example
Simple	1	Avian sarcoma and leukosis viral group	Rous sarcoma virus
	2	Mammalian B-type viral group	Mouse mammary tumour virus
	3	Murine leukemia-related viral group	Moloney murine leukaemia virus (Mo-MLV)
	4	D-type viral group	Mason-Pfizer monkey virus
Complex	5	Human T-cell leukemia–bovine leukemia viral group	Human T-cell leukemia virus
	6	Spumaviruses	Human foamy virus
	7	Lentiviruses (LV)	Equine Infectious Anaemia virus or Human Immunodeficiency Virus

Table 1. Classification of RV's. Seven genesis of RV's are listed along with examples from each group. Note, five of these groups display oncogenic potential (1-5) and are known as oncoretroviruses.

The genome common to all RVs consists of three coding genes called *gag*, *pol* and *env* which are required in supplying multiple components of the virus structure, enzymes and envelope proteins respectively, in both simple and complex retroviruses (Figure 1, Table 2) (Vogt, 1997; Coffin, 1996).

The *Gag* gene encodes and directs the synthesis of internal virion proteins that form the matrix, capsid and nucleocapsid proteins that make up virions. *Pol* encodes the viral protease, reverse transcriptase, RNase H and integrase responsible for transcribing viral RNA into double stranded DNA and for integration, respectively. The *env* gene encodes the proteins needed for receptor recognition and envelope anchoring. The viral envelope is formed by a cell derived lipid bilayer where proteins encoded by the *env* region of the viral genome are inserted. These consist of the transmembrane and the surface components linked together by disulphide bonds (Cardone *et al.*, 2009; Benit, Dessen and Heidmann, 2001; Erlwein, Bieniasz and McClure, 1998).

Duplicated regions in the 5' and 3' ends known as Long Terminal Repeats (LTR) flank the *gag*, *pol* and *env* genes. The LTR consists of the U3 (unique 3), R (repeat) and U5

(unique 5) sequences and acts as the control centre for gene expression (Wilk *et al.*, 2001; Zhang and Temin, 1993).

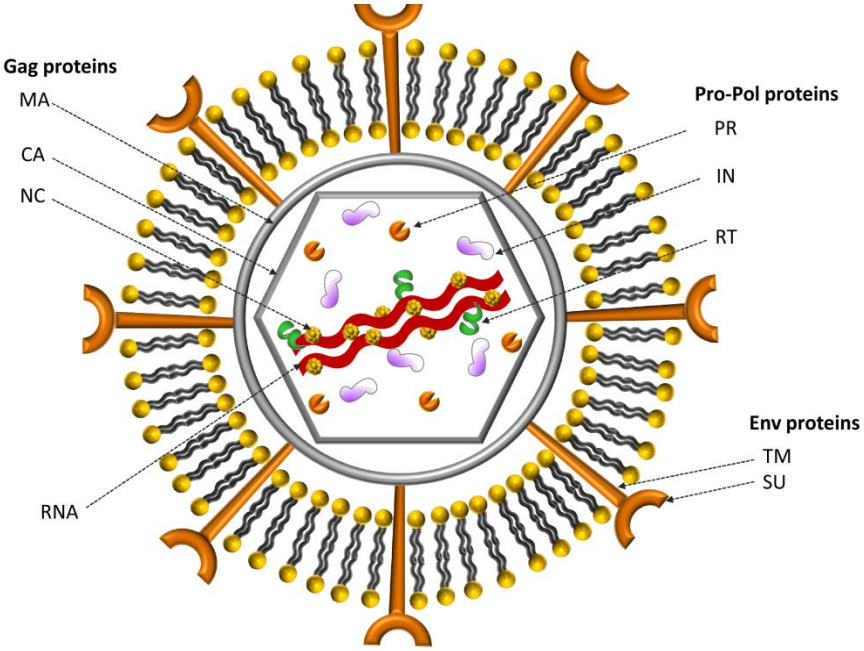

(Rodrigues, M. and Coroadinh, Chapter 2, 2011)

Figure 1. Schematic representation of a retrovirus particle. Retrovirus particles vary in size from 80–100nm in diameter and have an outer envelope consisting of a lipid bilayer that is obtained from the host plasma membrane during the budding process. The protein core of the virus consists of viral enzymes and the viral RNA genome consisting of two RNA strands. *Gag* encodes the structural proteins that form the matrix capsid, and the nucleoprotein complex. *Pol* encodes for the essential viral enzymes, reverse transcriptase and integrase and is responsible for synthesis of viral DNA and integration into host DNA after infection. *Env* encodes the viral glycoproteins and transmembrane proteins that are displayed on the surface of the virus and are responsible for association and entry of virion into host cell.

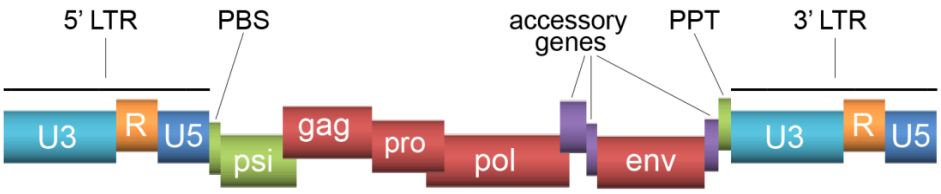

(Fouty and Solodushko, Chapter 4, 2011)

Figure 2. A schematic overview of the retrovirus genome. The virion RNA is typically 7-12kb in size and consists of the *gag, pol* and *env* genes. The LTR regions flank the genome. The gag gene encodes the Matrix protein (MA), capsid protein (CA) and nucleoplasmid (NC). The pol gene encodes reverse transcriptase (RT), protease (PR), integrase (IN) and deoxyuridine triphosphatases (duTPases). The *env* gene encodes the surface subunit (SU) and transmembrane subunit (TM).

Gene	Function
Gag	Directs the synthesis of internal virion proteins that form the matrix, the capsid, and the nucleoprotein structures.
Pol	Contains the information for the reverse transcriptase and integrase enzymes.
Env	Provides surface and transmembrane components of the viral envelope protein.
LTR	Regulate viral gene expression and therefore replication and pathogenesis.
Repeat -R	Essential for reverse transcription and replication.
Unique 3 - U3	Comprises of transcriptional enhancer and promoter sequences.
Unique 5 – U5	Contains sequences involved in initiation of reverse transcription.

Table 2.Basic components of the RV genome.

1.2.1 Life cycle of the RV

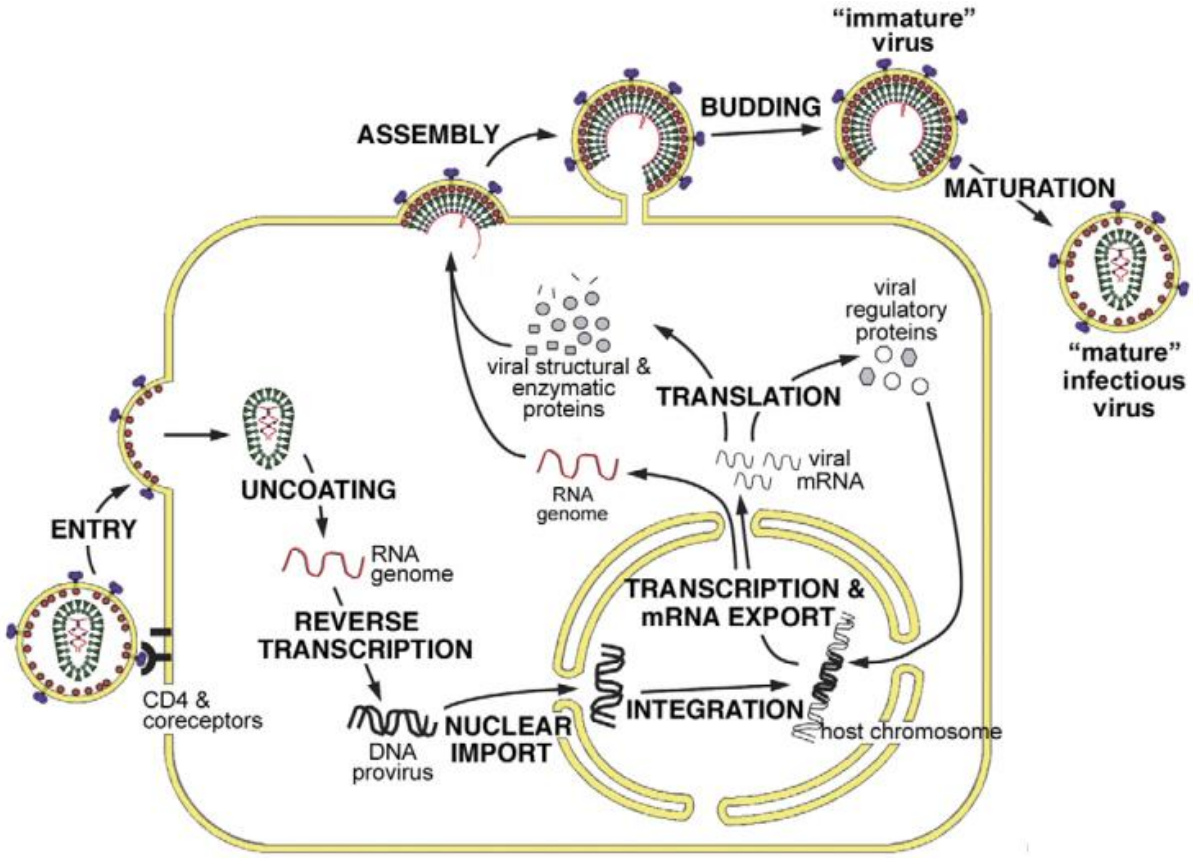

(Ganser-Pornillos, Yeager and Sundquist, 2008)

Figure 3. Schematic illustration of the general stages of a RV life cycle. Cell entry is facilitated by fusion of the virus with host cell membrane. The virus particle uncoats and releases its proteins. Reverse transcription and integration of viral cDNA take place. Virus proteins are assembled and viral particles are released from the host cell.

Cell binding and entry

The lifecycle of a generic retrovirus is shown in Figure 3 and begins with its attachment to a suitable host cell membrane via virally encoded glycoproteins and specific cell surface molecules. These viral glycoproteins, that are embedded in the surface unit lipid envelope, recognize receptors displayed on the target cell plasma membrane such as, CD4, CD8 and CAT-1, and then mediate viral attachment (Suzuki and Craigie, 2007; Ugolini, Mondor and Sattentau, 1999).

Membrane fusion is carried out by the viral *env* protein. The *env* protein is an oligomer composed of three surface unit (SU)-transmembrane (TM) subunit complexes (Sharma, Miyanohara and Friedmann, 2000). TM is integrated into the cellular membrane. SU is located extracellularly and linked to TM by non-covalent interaction. Consequently, SU mediates receptor binding and TM mediates membrane fusion. The SU highly specific receptor mediated interaction is thought to activate a conformational change of the SU proteins leading to the fusion or endocytosis of the viral and cell lipid bilayers. This process is dependent on the virus envelope ligand and cell receptor used for entry (Damico and Bates, 2000; Sharma, Miyanohara and Friedmann, 2000).

Viral particles have two mechanisms of cell entry; membrane fusion or receptor-mediated endocytosis. This is supported by recent compelling research by Miyauchi *et al* in 2011 who used a pH sensitive green fluorescent protein (GFP) tag to successfully visualize the preferential uptake of HIV into acidic endosomes upon entry. This, along with other evidence confirms HIV and other retroviruses do not only rely on lipid membrane fusion, but also receptor-mediated endocytosis followed by pH mediated endosomal fusion for viral entry (Miyauchi, Marin and Melikyan, 2011). In contrast in ASLV-A, *Tva* serves as the cellular receptor and interacts with the ASLV-A specific protein *EnvA* and requires low pH conditions to carry out receptor-mediated endocytosis (Katen *et al.*, 2001; Wang *et al.*, 1999). Binding of the HIV envelope glycoprotein gp120, which is found on the surface of the viral particle, to the primary receptor CD4 in the host cells leads to conformational changes in both CD4 and gp120. This results in exposure of co-receptors belonging to the chemokine receptor family, mainly CXCR4 and CCR5, which allow viral entry (Zhang *et al.*, 1999). Entry of virions into the cell results in the release of the retroviral core into the cytoplasm of the host cell.

Reverse Transcription

Once the retrovirus virions have entered the cytoplasm, the virion nucleocaspid releases the enzyme reverse transcriptase (RT). At this stage a positive sense (5' to 3') ssRNA is transcribed into a double strand complementary DNA (cDNA) via a series of molecular events (Fig 4) (Telesnitsky A, 1997; Palaniappan *et al.*, 1996) The RNAse H activity of RT hydrolyses and displaces the ssRNA template so that RT can transcribe a second complementary DNA strand using the previously generated DNA as a template (Telesnitsky A, 1997; Palaniappan *et al.*, 1996).

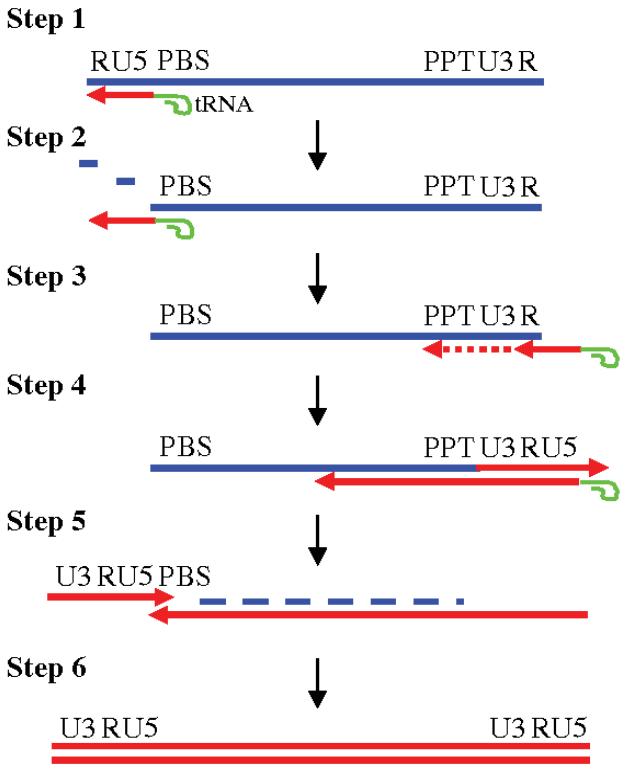

(Delviks-Frankenberry *et al.*, 2011)

Figure 4. Retrovirus replication. Representation of the key steps in retrovirus replication. Negative polarity DNA synthesis (red) is initiated using a partially unwound tRNA annealed to the primer-binding site (PBS) at the 5′-end of the viral genomic RNA (Step 1). Complementary DNA then binds to the U5 (non-coding region) and R region (a direct repeat found at both ends of the RNA molecule) of the viral RNA (Step 2). RT continues copying U3 located at 3' end of viral DNA (Step 3). RT uses the polypurine tract (PPT) to initiate plus strand synthesis by copying the 3'LTR (Step 4). The first

strand of complementary DNA (cDNA) is extended (Step 5). Provirus used for integration into the host genome of the target cells (Step 6).

Nuclear Entry

The double stranded DNA (dsDNA) is now shuttled into the nucleus remaining associated with some of the viral structural proteins in a pre-integration complex (PIC). It has been demonstrated that PIC interacts with the cellular microtubule network to transport itself through the cytoskeleton towards the nucleus. Simple retroviruses cannot gain access to the cellular genome until the disassembly of the nuclear envelope during mitosis. Once this occurs, transportation of PIC's to the cytoplasm can take place (Nisole, Stoye and Saib, 2005; Roe *et al.*, 1993). Consequently, retroviruses such as MLV are dependent on the cell cycle and cannot replicate in non-dividing cells. In comparison, the PIC's of lentiviral complexes, such as HIV-1 are able to productively infect non-dividing cells. Here, the import of the viral genome and its associated proteins is mediated by the interaction of the nuclear pore complex with the protein components of the lentiviral PIC's (Fouchier and Malim, 1999; Miller, Farnet and Bushman, 1997).

Integration

Once nuclear entry has been achieved the viral DNA is transported into the nucleus and integrated into the cellular genome by the viral integrase in order to form a provirus (Mitchell *et al.*, 2004; Bukrinsky *et al.*, 1993). This is shown in figure 5.

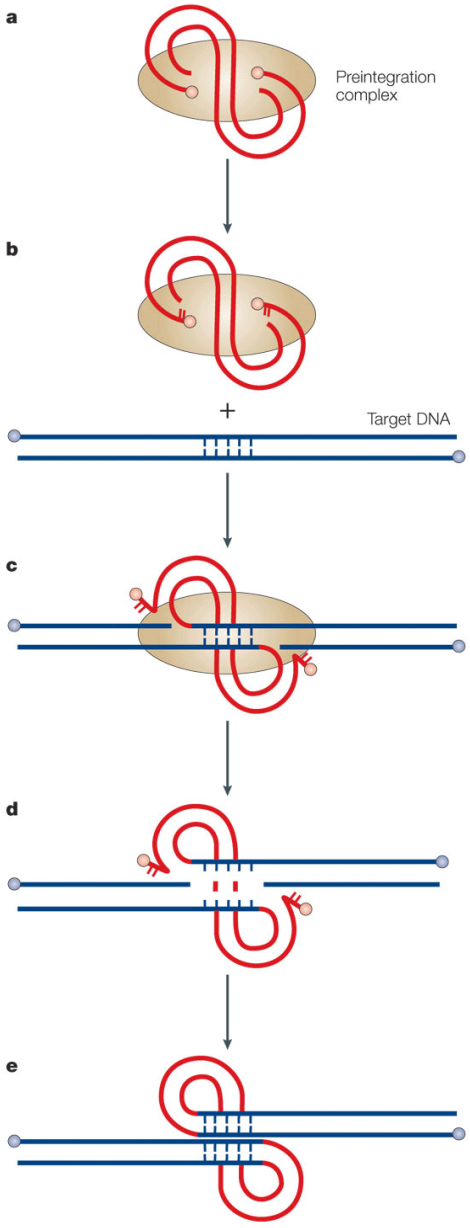

(Bushman *et al.*, 2005)

Figure 5. Integration of retroviral DNA into the host cell genome

a) The pre-integration complex (PIC) is composed of a double stranded complementary DNA molecule (cDNA). b) Complexed to the viral integrase and other proteins (beige

oval) integrase cleaves 2 nucleotides from the 3' end of each strand exposing recessed 3' –OH groups. c) The recessed 3' hydroxyl groups are joined with the 5' ends of the target DNA. This reaction is mediated by a transesterification reaction. d) Gaps at host-virus DNA junctions are caused due to unpairing of the integration intermediate reaction. e) Once the gap is repaired this accomplishes the formation of the integrated proviral DNA.

Viral gene expression, particle assembly and budding

Once integrated the viral DNA can produce full length RNA and spliced RNA using the cellular transcription machinery. Using RNA sequence known as packaging signal (Ψ) part of the full length viral transcripts are packaged into new virions to become the next generation of viruses (McBride, Schwartz and Panganiban, 1997; McBride and Panganiban, 1997). The remainder of the full-length transcripts are used as templates for the translation of the viral proteins. Progeny virions are then packaged using these proteins and become ready to leave the host by one of two mechanisms. These are; budding from the surface membrane thereby preserving the host cell, or the more destructive lytic pathway often destroying the host cell. Following release, some retroviruses undergo a post-release maturation phase. This coincides with morphological changes of the viral core, ultimately culminating in mature progeny virion capable of infecting new target host cells.

1.3 Lentivirus

Lentiviruses are a sub group of the retroviridae family. They are among the most intensely studied group of viruses. Lentivirus vectors based on HIV-1 can transduce a broad spectrum of non-dividing cells *in vivo*, such as retinal cells, muscle cells, neurons and hepatocytes (Bouard, Alazard-Dany and Cosset, 2009). Their ability to efficiently deliver large and complex transgenes (up to 10kb) to target cells and tissues is the main reason lentiviruses are used for gene therapy (Verma and Weitzman, 2005). The lentiviral genome (Fig 6) also carries the three main genes coding for the viral proteins (*gag, pol* and *env)* however the lentiviral genome is more complex than simple retroviruses in that is has additional genes that include regulatory genes (*tat* and *rev*) and auxiliary genes (*vpr, nef, vpu* and *vif*). These genes produce products involved in regulation of synthesis and processing viral RNA and also enable efficient viral replication (Pfeifer and Verma, 2001; Coffin, 1996).

Lentiviruses have been found capable of infecting several cell types (Tang, Kuhen and Wong-Staal, 1999; Narayan and Clements, 1989). There are five serotypes of lentiviruses such as primate (Human immunodeficiency virus, HIV), sheep and goats, (caprine arthritis-encephalomyelitis, CAEV) horses (equine infectious anemia virus, EIAV), cats (Feline Immunodeficiency Virus, FIV) and cattle (Bovine Immunodeficiency Virus, BIV).

Due to the long incubation periods of lentiviral vectors they take a toll on the immune system resulting in a slowly developing multi-system diseases (Tang, Kuhen and Wong-Staal, 1999). The disease associated with lentiviral infections range from benign and subclinical to severely debilitating and lethal. A common feature of lentiviruses is their tropism for cells of the monocyte or macrophage lineages. Infection of macrophages provide a hiding place for the virus from the infected host immune system (Trono, 2000).

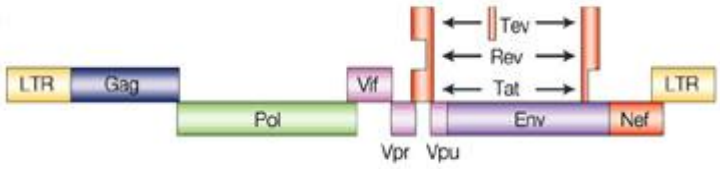

(Chang, Liu and He, 2005)

Figure 6. Schematic representation of the HIV genome. HIV has several major genes coding for structural proteins that are found in all retroviruses (*gag, pol, env)* and several nonstructural/ accessory genes that are unique to HIV genome.

An important genetic difference between simple retroviruses and lentiviruses are regulatory (*tat* and *rev*) and auxiliary genes (*vpr, vif, vpu* and *nef)* that have important functions during the viral life cycle and viral pathogenesis (Brügger *et al.*, 2007).

The *tat* (transactivator of transcription) gene binds to the TAR region of viral RNA and to host proteins and acts as an activating element by binding to cellular factors and mediating their phosphorylation thereby resulting in an increased transcription of all HIV genes. *Tat* is also involved in LTR activation and therefore important in the production of viral genomes and for gene expression (Kim and Sharp, 2001).

The *rev* (regulator of expression of virion proteins) gene allows fragments of HIV mRNA containing a Rev Response element (RRE) to be exported from the nucleus to the cytoplasm so that structural proteins and RNA genome can be produced. This mechanism provides time-dependent regulation of replication (Strebel, 2003).

The *vpr* gene plays an important role in regulation of nuclear import of the HIV-1 pre-integration complex and is required for viral replication in non-dividing cells (Muthumani *et al.*, 2006).

The *vif gene,* which overlaps the 3' end of the pol gene, affects the assembly of the virions and infectivity in certain cell types, while also stabilizing the pre-integration complex.

The *vpu* gene is involved in viral budding following infection and is necessary for down regulation in CDF molecules. In addition *vpu* stimulates viral release (Lindwasser, Chaudhuri and Bonifacino, 2007).

The *nef* gene is expressed by primate lentiviruses, HIV. It is known as a virulence factor as it manipulates the host's cellular machinery to aid infection, survival and viral

replication. *Nef* also promotes the survival of infected cells by down modulating the expression of several surface molecules important in host immune function such as the CD4 receptor (Das and Jameel, 2005).

1.3.1 HIV

The first lentiviral vectors developed were derived from HIV-1, the most extensively studied lentivirus (Naldini *et al.*, 1996). Two variants of HIV have been described; HIV-1 presents more pathogenic properties with greater virulence and infectivity than HIV-2 (Gilbert *et al.*, 2003). HIV causes acquired immunodeficiency syndrome (AIDS) a condition that resulted in the deaths of 1.9 million people in 2009 http://www.who.int/hiv/data/2009_global_summary.png. This is a condition whereby the immune system is compromised allowing cancers and opportunistic infections to thrive. This is achieved by the presence of HIV within infected immune cells or as free virus particles. The HIV genome is approximately 10kb in size and primarily infects macrophages and $CD4^+$ T cells and dendritic cells (Delassus, Cheynier and Wain-Hobson, 1991).

In contrast to the epidemic nature of HIV-1, HIV-2 has diminished transmission efficiency due to its lower viral loads. HIV-2 is also less pathogenic and therefore has a reduced progression rate to AIDS (Gilbert *et al.*, 2003).

1.4 Optimizing vectors and vector packaging

Retroviruses have been shown to be the second mostly used viral vectors for gene therapy (Edelstein, Abedi and Wixon, 2007). In order to use these viruses as vectors safety considerations must be met so they can enter the host without causing adverse effects. To do this, vectors need to be structurally and genetically stable, have no ability to recombine, and not cause insertional mutagenesis (Goverdhana *et al.*, 2005).

To prevent pathogenicity, replication incompetence has been engineered into vectors so that only defective particles deliver therapeutic genes without spread (Buchschacher and Wong-Staal, 2000). To do this, the *gag, pol* and *env* genes that provide viral proteins needed to package, reverse transcribe and integrate the vector genome, and target the

virus to the cell's receptors have been removed from the vector and placed on plasmids. Hence, packaging proteins are then provided in *trans* in packaging cells. Homology between packaging constructs has also been kept to a minimum to reduce the chance of creating replication competent viruses (RCV) through recombination in the packaging cells.

The remaining sequences on the retroviral genome are called 'cis' elements and composed of the LTRs, part of *gag* needed for genome packaging, the primer-binding site (PBS) that is recognized by reverse transcriptase and the genome packaging sequence required for efficient packaging of the genome into the viral core. During vector production, the genome carrying the *cis* sequences that also include an internal promoter to drive transgene expression, are packaged leaving behind in the packaging cells the plasmids carrying the trans sequences that do not have packaging sequences (Otto *et al.*, 1994). To generate viral particles that can transfer their RNA genomes, the *cis* and *trans* components are transfected as plasmids into packaging cells. However, there is still the problem that a single recombination event between these two packaging constructs can occur to generate replication competent virus particles. To avoid this trans-acting viral genes have been further split and placed on separate plasmids (Miller and Buttimore, 1986). These two packaging constructs contain the *gag* and *pol* on one plasmid and the *env* gene on the other. This also enables switching of the *env* genes called pseudotyping. (Danos and Mulligan, 1988).

This exchange generates new viral vectors with altered tropism to the host cells. Examples of this are: The ecotropic envelope (limited to one species), xenotropic envelope (infecting most mammalian cells except rodent cells), amphotropic enveope (infecting all mammalian cells) and the pantropic envelope (infecting various species) (Gaspar *et al.*, 2004; Danos and Mulligan, 1988). The envelope from the vesicular stomatis virus (VSV) is now often used because the G protein of the VSV substitutes for the viral *env* protein to enable efficient cell entry (Chen *et al.*, 1996). It does this by mediating virus attachment to the cell surface that results in endocytosis of the virus. VSV-G also mediates fusion of the viral envelope with the endosomal membrane (Barraza and Poeschla, 2008; Douar, Themis and Coutelle, 1996). Previously a major limitation to the production of high titre retrovirus was believed to be due to the labile nature of the virus envelope that prevented increasing its titre using centrifugation. The VSV-G envelope not only enables broad-range host infection but also provides stability

to the virus thus allowing concentration by ultracentrifugation. This leads to an increased viral titre of up to two orders of magnitude, reaching 10^9 particles per ml, suitable for *in-vivo* gene transfer (Chen *et al.*, 1996) Examples of alternative pseudotypes used successfully with lentiviral vectors include the influenza haemagglutinin, the Ross River Virus glycoprotein (offers enhanced liver transduction), lymphocytic choriomeningitis virus envelope and a rabies-G envelope (that successfully achieves gene delivery to the central nervous system) (Cronin, Zhang and Reiser, 2005).

Retroviruses do however have several other disadvantages when being considered for gene therapy. They require cell division for infection since they are unable to reach the nucleus without nuclear breakdown that occurs during mitosis. Hence, tissues such as brain, lungs, eyes and pancreas may not be efficiently infected using these vectors (del Pozo-Rodriguez *et al.*, 2008). Also, retroviral insertion into the host genome is non-random and this can cause problems of genotoxicity by insertional mutagenesis (Baum *et al.*, 2006). This is because the LTRs act as promoters and enhancers and can activate genes close to or far away from where they insert. If the gene close to insertion is an oncogene this 'promoter' insertion' can lead to oncogenesis. LTRs have also been shown to be involved in splicing with cellular genes and can be subjected to promoter shut down by host methylation.

To circumvent some of these disadvantages and with the emergence of new knowledge on the HIV virus, lentiviruses based on HIV-1 have been optimized for gene transfer (del Pozo-Rodriguez *et al.*, 2008; Nisole and Saib, 2004) To overcome the problem of 'promoter' or 'enhancer' insertion self-inactivating (SIN) vectors were developed (Miyoshi *et al.*, 1998). SIN is achieved by deleting the promoter/enhancer sequences in the U3 region of the 3' LTR of the viral vector. This mutation is carried over to the 5' LTR during reverse transcription. (Baum *et al.*, 2003; Zufferey *et al.*, 1998; Miyoshi *et al.*, 1998; Yu *et al.*, 1986). This design is a significant development for gene therapy because it reduces or prevents endogenous oncogene activation following integration.

In addition, replacement of the 5' LTR (U3 region) with the human cytomegalovirus (CMV) promoter results in a CMV driven packaging system which is compatible with the CMV/LTR hybrid vectors and high titre virus preparation. The cells used to generate these vectors are again human embryonic kidney (HEK) 293 cells (Dull *et al.*, 1998; Finer *et al.*, 1994).

Additional elements used to improve lentiviral design are repositioning of the central polypurine tract (cPPT). This cPPT improves entrance of the vector into the nucleus (Barraza and Poeschla, 2008). The inclusion of a cPPT element has also shown significant improvement in transduction efficiency *in vitro* and *in vivo*. HIV and SIV based vectors that contain a cPPT also show a two to threefold enhancement in transduction efficacy (Follenzi *et al.*, 2000).

The woodchuck post-transcriptional regulatory element (WPRE) further improves transduction and translational efficiency of lentiviral vectors via increasing virus titre by improving RNA stability and export of virus genomes from the nucleus. Incorporating the WPRE in the HIV-derived vector increases reporter gene expression up to 5-8 fold higher after transduction of both dividing and arrested 293T cells (Zufferey *et al.*, 1999).

Following these modifications the vector packaging cell along with the transgene cassette is introduced into the packaging cell line. The transient infection method is rapid and flexible due to the virus particles being harvested a few days after infection of 293T cells. The vector will then undergo a series of analytical tests for infection and titre before being either used for further research or delivered therapeutically to a patient (Coffin et al, 1997).

1.5 Gene therapy success

The idea of delivering genes to human cells for beneficial therapeutic effect has been in the mind of scientists since the landmark paper by Friedman and Roblin in 1972 (Friedmann and Roblin, 1972). However there was skepticism because of lack of information on gene regulation, lack of knowledge of the gene causing the disease, the potential side effects and the safety of this approach. However, due to advances in gene therapy technologies as well as in molecular therapy and the discovery of new genes by the human genome project in 2003, gene therapy has become closer to reality to treat many diseases.

Efficient delivery of genes is an enormous hurdle for gene therapy. Synthetic expression vectors such as liposomes have been used to transfer genes into the host cell however, this has proved to be inefficient, produced low level and short lived expression. Entering the hydrophobic membrane of the host cell may still be problematic even if these issues are overcome and gene transfer occurs there is still the problem of low level gene transfer dosage (Conese, 2004).

Gene therapy of hematopoietic stem cells (HSC) has received much attention. It is relevant to a broad range of human diseases, ranging from cancer to haematological disorders. It also allows the use of *ex vivo* transduction protocols that minimize the exposure of the entire patient to viral particles. However, the use of retroviral vectors in this setting is still hampered by the low frequency of gene delivery, as transduction by retrovirus vectors occurs only in cells that are replicating at the time of infection (Miller and Buttimore, 1986). A promising approach is the finding that a number of growth factor combinations can be used to pre-stimulate hematopoietic stem/progenitor cells to increase transduction efficacy (Pfeifer and Verma, 2001; Nolta, Smogorzewska and Kohn, 1995)

1.6 Gene therapy trials involving retrovirus vectors

Worldwide, over 400 gene therapy clinical trials have been carried out or are underway. 70% are cancer related and mainly used on terminally ill patients. The most common used vectors are the retroviral-based vectors (Blaese *et al.*, 1995).

Blaese and Anderson, from the National Institute of Health, performed the first human gene therapy trial in 1990. The therapy treated two children for the primary immunodeficiency disorder, adenosine deaminase (ADA) deficiency. ADA is a rare genetic disease in which children are born with severe immunodeficiency and are prone to repeated serious infections (Aiuti *et al.*, 2002). ADA is an enzyme needed to convert nucleoside inosine and it is this deficiency that prevents the body from producing enough lymphocytes (B-cells and T-cells) that are required to fight off infections (Joachims *et al.*, 2008). Mutations in ADA in mice have shown the progression of severe combined immunodeficiency disease (SCID) due to the severely low levels of B, T and natural killer (NK) cells (Blackburn *et al.*, 1996). Before gene therapy the only way to treat ADA deficiency was regular injection with the ADA enzyme and bone marrow transplant from a compatible donor. If neither of these treatments were possible then the child would have to be isolated in a germ free environment in order to survive. Hence the term "bubble babies". Blaise and Anderson drew blood from the girls and induced the T cells from the blood to replicate in culture. Then retroviral mediated transfer of ADA gene into the cultured T cells took place allowing enough time for the vector to integrate into the patient genome and transfer the gene. Blasie and Anderson then injected the enhanced T cells back into the patients via the bone marrow. This restored ADA gene expression and subsequently a viable T cell population. Within the first 6 months one of the patients T-cell count rose and she had developed a steady increase of ADA while the other patient also showed a rapid rise in T cells and showed improvements in immune function tests (Muul *et al.*, 2003; Blaese *et al.*, 1995; Culver *et al.*, 1991; Kohn *et al.*, 1989).

The year 2000 saw Alan Fischer and Marina Cavazzana-Calvo successfully treat 3 young children suffering from the fatal X-Linked Severe Combined Immuno-Deficiency (X-SCID) disorder. This was achieved by the reinfusion of hematopoietic

stem cells that were transduced *ex vivo* with an MLV vector (Cavazzana-Calvo, M. and Hacein-Bey-Abina, S., 2001; Cavazzana-Calvo *et al.*, 2000). Other successful developments in gene therapy include treatments for cancer, chronic granulomatous disorder (CGD) (Seger, 2008; Ott *et al.*, 2006), viral infections (von Laer, Baum and Protzer, 2009) and ADA SCID (Aiuti *et al.*, 2002). However gene therapy again saw a setback when 2-6 years after the treatment of X-SCID 4 patients in the French trial and one patient in the English trial developed clonal T-cell proliferation (Dave *et al.*, 2009; Hacein-Bey-Abina *et al.*, 2003). The main concern here was that there was no control of where the gene was inserted in the genome carried by the retroviral vector. As a consequence, the retroviral vector was later found to be in the LMO-2 gene resulting in its dysregulation and leukaemogenesis. This was soon proven as insertional mutagenesis.

1.7 Safety of gene therapy vectors

The introduction of genetic material into the host where integration takes place may result in disruption of host gene causing insertional mutagenesis and may lead to oncogenesis. This problem has hampered many clinical trials and requires a clear understanding of the mechanisms that contribute to oncogenesis in order that safety gene therapy vectors can be designed.

1.8 Genotoxicity

Genotoxicity can be defined as a process that has a particular effect on the genome of any individual that can result in a phenotypic change due to mutation (Ramezani, Hawley and Hawley, 2008). The potential for insertional mutagenesis during permanent gene transfer offered by retrovirus vectors present a genotoxic risk to the host.

One of the defining features of retroviral life cycle is the covalent integration of the double stranded viral DNA into the host chromosomal DNA. Retroviral integration is semi-random occurring in genes with open chromatin configuration that are being actively transcribed (Albanese *et al.*, 2008; Baum *et al.*, 2004; Mitchell *et al.*, 2004; Wu *et al.*, 2003; Schroder *et al.*, 2002). This can disrupt host genomic sequences and lead to genotoxicity as a result of gene activation or inactivation (Nienhuis, Dunbar and Sorrentino, 2006). Insertional mutagenesis mediated by wild type viruses has been known for some time and was found to cause tumor development in several animal species as a result of proviruses either carrying a truncated oncogene that becomes expressed uncontrollably or by altering the expression of oncogenes found near to the virus integration site. Indeed, retrovirus mediated mutagenesis can be valuable to study a range of mechanisms associated with deviations from normal cellular function since the gene involved in causing a phenotypic change can be found (Varmus, 1982; King *et al.*, 1985). However, very few studies have reported using attenuated vectors as tools to discover new genes involved in cellular processes since the likelihood of insertional mutagenesis by these viruses was considered to be remote, with estimations of the frequency of mutations to be in the region of 10^{-7} for a haploid locus (Stocking *et al.*, 1993).

1.8.1 Insertion site (IS) selection

Most DNA sequences can act as sites for retrovirus integration acceptor sites, however primary sequences may influence integration. It has been shown that if DNA is placed into nucleosomes *in vitro* it will not reduce integration but instead this creates new "hot spots" for integration. This is thought to be due the IS that are distorted due to wrapping of the DNA around nucleosomes making the DNA accessible in places to viral integration (Pruss, Bushman and Wolffe, 1994). Hence, viral integration appears to be influenced by target site selection and this may influence the likelihood of insertional mutagenesis.

In order to analyze IS, infected cells can be subjected to molecular techniques that retrieve the DNA where integration occurred. This allows sequences of several thousand integration sites to be analyzed (Mitchell *et al.*, 2004; Schmidt *et al.*, 2002; Schroder *et al.*, 2002).

Early studies on MLV indicated preference for integrating in open chromatin as a positive correlation was detected between DNase I-hypersensitive sites and integration frequency (Rohdewohld *et al.*, 1987; Vijaya, Steffen and Robinson, 1986). More recently, due to the sequencing of the human genome, it has been found that roughly 25% of integration events are near transcription start sites and are associated with CpG islands (Bushman *et al.*, 2005b; Wu *et al.*, 2003; Scherdin, Rhodes and Breindl, 1990). Wu *et al* in 2003, looked at 903 MLV insertion sites and found that 80% of integration sites were distributed in the genome in a random fashion but that 20% of these were within the 5' end of a transcriptional unit (Wu *et al.*, 2003). These insertion profiles have been supported by studies of IS in hematopoietic cells of rhesus macaques by Hematti *et al* in 2004, (Bushman *et al.*, 2005b; Hematti *et al.*, 2004). Hematti *et al* showed the same integration site preferences from both human cells and rhesus macaques indicating that integration patterns are similar a (Hematti *et al.*, 2004).

Vectors based on lentiviruses are considered to be less genotoxic than gamma retroviruses as lentiviruses such as HIV-1 and EIAV prefer insertion within the gene transcription units whereas retroviruses such as MLV show an obvious bias for promoters and selected gene classes involved in growth control and cancer which may

increase probability of oncogene activation and consequently cancer development (Montini *et al.*, 2009; Cherepanov, 2007; Bushman *et al.*, 2005b; Schroder *et al.*, 2002). Montini *et al* proved that using lentiviral vectors reduces the risk of cell transformation by a factor of 10 as compared with gamma retroviruses due to IS selection (Modlich and Baum, 2009; Montini *et al.*, 2009) (Modlich and Baum, 2009; Montini *et al.*, 2009)

A study by Lewinski *et al* in 2006, used HIV chimeras with MLV *gag* and *pol* genes substituted for their HIV counterparts and found this to cause the hybrid vectors to shown MLV integration profile (Lewinski *et al.*, 2006). Overall, this study showed how viral sequences such as *gag* and integrase have a direct role in target site selection. Tethering interactions between cellular proteins and retroviral proteins may also effect integration targeting. HIV integrase binds lens epithelium-derived growth factor (LEDGF)/p75, a nuclear chromatin which is believed to be a cellular component that influences IS preference. Cells lacking LEDGF/75 show reduced frequency of insertion in transcription units demonstrating that LEDGF/p75 may play a role in integration targeting in HIV (Engelman and Cherepanov, 2008; Lewinski *et al.*, 2006; Kang *et al.*, 2006).

Analysis of the clonal dynamics of genetically modified lymphocytes *in vivo* is of crucial importance to understand the potential genotoxic risk of using retroviral vectors for gene therapy of haematological disorders. Molecular techniques such as linear amplification-mediated PCR and pyrosequencing have provided a genome-wide, high-definition map of retroviral IS in the genome of peripheral blood T cells from several donors treated this way. This, in parallel to gene expression profiling and bioinformatics has enabled a comparison to be drawn with matched random controls and with integrations obtained from $CD34^+$ hematopoietic stem/progenitor cells. Analysis of integration sites in T cells obtained *ex vivo* two months after infusion showed no evidence of integration-related clonal expansion or dominance, but rather loss of cells harboring integration events interfering with RNA post-transcriptional processing (Cattoglio *et al.*, 2010). The study shows that high-definition maps of retroviral integration sites are a powerful tool to analyze the fate of genetically modified T cells in patients and the biological consequences of retroviral transduction.

1.8.2 Insertional mutagenesis (IM)

As previously mentioned retroviral mediated insertional mutagenesis can lead to malignancy via altering the expression of host genes in the vicinity of the IS. Virus insertion can also alter gene products following aberrant splicing between virus and host genes. If the affected gene is cancer related such as a tumor suppressor gene or proto-oncogene, inactivation and activation respectively, can cause uncontrolled cell division and promote tumor development (Modlich and Baum, 2009; Uren *et al.*, 2005; Baum *et al.*, 2004). Various bodies of research have demonstrated vector integration affecting flanking genes as far as 10kb away, leading to production of aberrant transcripts and ultimately clonal proliferation.

1.9 Identification of IM during gene therapy of X-SCID

X-SCID is an X-linked monogenic disorder characterized by disruption of T and natural killer cells signaling and activation due to mutations in the cytokine IL2 receptor γ-chain (IL2RG) (Howe *et al.*, 2008; Thomas, Ehrhardt and Kay, 2003; Cavazzana-Calvo *et al.*, 2000). IL2RG encodes a subunit of a cell surface receptor that allows developing immune cells to respond to growth signals called cytokines. Without this subunit children fail to develop the mature T lymphocytes so B-lymphocytes fail to make antibodies to fight infection. (Hacein-Bey-Abina *et al.*, 2008; Thrasher *et al.*, 2006). A mutation in the IL2RG receptor subunit can lead to lower rates of T and B lymphocytes and natural killer cells which can in turn lead to lack of signalling required for growth and survival of progenitor cells. Young patients with X-SCID are particularly vulnerable to recurrent infections, as reduced lymphocyte function cannot compensate for the already low immunoglobulin levels during early infancy. Hence, SCID is often fatal within the first year (Thrasher *et al.*, 2006).

Bone marrow transplant from HLA matched donors is the most common way to treat X-SCID, however, it is often difficult to find matched cells to circumvent immune rejection. Thus, in order to compensate this problem gene therapy has been used in an autologous manner on patient haematopoietic stem cells. Gene therapy for X-SCID was initiated around the year 2000, following promising *in vitro* results and a trial by Lo *et*

al in 1999 whereby T, B and NK cells were restored in γC deficient mice via a retroviral vector containing the γC gene (Lo *et al.*, 1999). However, the main concern was that there was no control over where retroviral vector integration occurred and the ramifications of this. Hence, the risk of cancer development by IM was always under consideration (Check, 2002).

Following on from the initial preclinical trial *in vivo* clinical trials took place in Paris and (Cavazzana-Calvo et al, 2000; Hacein-Bey-Abina et al, 2002) and London (Gaspar et al, 2004) for the treatment of X-SCID. Haematopoietic stem cells ($CD34^+$) isolated from children suffering from X-SCID were transduced *ex vivo* with an MLV gamma retroviral vector carrying the γC receptor gene before reinfusion back into the patients. Several months after returning the treated cells cellular and humoral immunity was restored and it was noted that T and NK cell counts and function were at near normal levels to those found in normal children of the same age. Unfortunately, in 5 patients clonally dominant cells emerged leading to leukaemnia 3-5 years after treatment (Hacein-Bey-Abina *et al.*, 2010; Qasim, Gaspar and Thrasher, 2009). This resulted in premature cessation of the trials and investigations into the cause(s) of the leukaemias. To investigate for suspected IM, patient cells were isolated and genomic DNA examined for virus IS. Lam-PCR using specifically designed primers recognizing retroviral sequences and linkers to capture genomic DNA containing the inserted vector enabled IS detection. In 4 out of 5 patients that developed leukaemia, 3 from the Paris trial and 1 from the London trial showed integrative events occurred in or near to the proto-oncogene LIM domain only 2 (LMO2) gene. It was subsequently shown that this led to elevated LMO-2 expression and uncontrolled proliferation of mature T cells (Hacein-Bey-Abina *et al.*, 2010; Qasim, Gaspar and Thrasher, 2009; Nam and Rabbitts, 2006; Hacein-Bey-Abina *et al.*, 2003). What remains vague is why the viral vector inserted itself near the LMO2 promoter locus in 4 of the 11 children treated with the same protocol. One suggestion is that it was due to gene expression promoting IS selection (Kaiser, 2003; Coutelle *et al.*, 2003).

A number of studies were performed following the X-SCID trials. One study by Li *et al*, (2002) echoed the findings of the original French trial by showing that the transplantation and expansion of clones from retroviral transduced bone-marrow cells also induced leukaemia in mice (Li *et al.*, 2002). The transgene used in this study was

thought to have had growth promoting activities however, the authors also suggested that the cancer may have developed due to the consequence of co-operation between the transgene product and the MLV retroviral integration event that disrupted and up-regulated the proto-oncogene (Baum *et al.*, 2003).

A later study by Modlich *et al* in 2005 also showed the development of leukemia in mice that were treated by infection of bone marrow derived stem cells at high retroviral MOI. In this case the retroviral vectors were carrying the multi resistance gene 1 (MDR1). Even though several other studies reported no complications of using MDR1 in the transduction of bone marrow cells Modlich found multiple insertions in proto-oncogenes (Modlich *et al.*, 2005) in clonally derived cells.

1.10 Chronic granulomatous (CGD) trial

X-Linked chronic granulomatous disease is an inherited disorder caused by abnormal *p22phox (CYBA), P67phox (NCF2)* and *gp91phox (CYBB)* genes. Two thirds of CGD's are however caused mostly by mutations in the *gp91phox* genes. This group of genes work together to create the NADPH oxidase enzyme which catalases the production of superoxide from oxygen and NADPH (Kang and Malech, 2009; Seger, 2008). Thus, CGD occurs via the absence of NADPH oxidase activity that results in neutrophils, monocytes and other phagocytes being incapable of producing the reactive oxygen species to destroy bacteria. Thus failure of the production of *dp91phox* causes frequent life threatening infections (Stein *et al.*, 2010; Malech *et al.*, 1997; Bjorgvinsdottir *et al.*, 1997). CGD is usually treated with bone marrow transplantation, however, as the gene responsible for CGD is known, it has therefore been possible to apply gene therapy to attempt CGD correction.

A study by Dinauer *et al* in 2001 showed successful retroviral transduction of rats that had a mutation in the *gp91phox* gene. This resulted in the phagocytes of these rats being able to return to producing reactive oxygen radicals (Dinauer *et al.*, 2001). Lee *et al* in 2008 transduced murine bone marrow stem cells with the *MT-gp91phox* gene and evaluated the possibility for toxicity to occur in the treated mice. Although white blood cell counts increased no toxicity was found (Lee *et al.*, 2008). Hence, in comparison to the X-SCID trial, the gamma retroviruses used in these studies did not create any clonal imbalance.

In 2004, two adolescent X-CGD patients were infused with $CD34^+$ blood stem cells containing the *gp91phox* gene after retroviral mediated gene transfer and initially clear benefits were found. In the follow up of patients from this trial, hematopoietic clones carrying insertions in certain gene loci became dominant (Gaspar *et al.*, 2004). Research into gene insertions and their differential expression suggested that this clonal dominance was due to growth and or survival advantage conferred by gene-activating or suppressing effects of the integrated retroviral vector. Clonal dominance had already been thought to be a natural property of hematopoiesis (Fehse and Roeder, 2008; Ott *et al.*, 2006; 2006). As a result of this work and that of others it is generally accepted that having a low copy number of vector integrants per cell is clearly favorable to reduce the likelihood of oncogenesis (Ramezani, Hawley and Hawley, 2008). In addition to this, the vector configuration, the transgene carried by the vector, the proliferation status of the host cells during infection and most recently synergy between the transcription status and the mutational potential of the vector are considered as factors associated with clonal dominance (Nowrouzi *et al.*, 2012; Baum *et al.*, 2006). These findings clearly highlight the need to understand more about the association between vector insertion and genotoxicity in the host to develop safer integrating vectors for gene therapy.

1.11 Models for genotoxicity

The study of retrovirus mediated genotoxicity may still be considered in its infancy and so it is important that we attempt to understand vector associated adverse effects on the host in greater detail. To do this, *in vitro* and *in vivo* models need to be established that either expose the causes of genotoxicity by retrovirus vectors and/or predict their genotoxic risk.

1.11.1 *In Vitro* models of genotoxicity

One *in vitro* assay designed to measure the risk of vector-related genotoxicity is an adaptation of the *hrpt in vitro* assay in V79 Chinese hamster male cells. This assay has previously been used to test for carcinogenicity and genotoxicity caused by radiation and UV light. The *hprt* gene encodes the hypoxanthine-guanine phosphoribosyltransferase (HPRT) and catalyzes purines to monophosphates that are toxic to cells. V79 cells are used as they are male in origin and carry a single copy of the *hprt* gene that is present in the X-chromosome (Zhang *et al.*, 1994). The advantages of using this gene is that existing *hprt*$^-$ mutants can be purged from culture populations using HAT treatment so that any new mutants are likely caused as a result of virus associated induction to *hprt*$^-$ via mutagenesis. Mutants can be isolated following selection using 6-thioguanine (6TG)

Themis *et al* (2003) adapted this model to determine whether retroviral insertional mutagenesis could mediate loss of *hprt* activity by gene inactivation following selection for *hprt*$^-$ mutants in a similar manner to that carried out previously in mouse ES cells (Themis *et al.*, 2003; King *et al.*, 1985).

Goff predicted the frequency of mutagenesis by a single provirus insertion in the mammalian genome at a haploid locus such as *hprt* to be about one inactivating mutation in 10^6 virally exposed cells (Goff, 1987) however, King *et al* (1985) established that only one in 10^8 provirus insertions can cause *hprt* mutagenesis (King *et al.*, 1985). The work by Themis *et al*, in 2003, however, showed *hprt* mutagenesis by attenuated retroviruses occurs at a similar frequency using replication competent vectors at $3.6x10^6$ and only if high MOI is used. This group also showed that a 2.3 fold increase in the risk of mutagenesis only occurred where the infection resulted in multiple provirus insertions per host genome (Themis *et al.*, 2003).

Kustikova *et al* (2003) also investigated the relationship between vector copy numbers and gene transfer efficiency using K562 leukemia cells and primary $CD34^+$ cells. This group also found insertional mutagenesis closely linked with vector copy number.. From their study, they also found an increase in copy number is accompanied by high gene transfer rates. A single transduced cell with one vector insertion occurs when a gene transfer of less than 30% is reached. The use of insertion of 3 vectors/cell (MOI of 3) increased the transduction efficacy to 60% and an MOI of 9 increased gene transfer efficacy to 90% (Kustikova *et al.*, 2003).

Kustikova *et al* in 2007 studied the cause of clonal dominance leading to malignancy by cultivating bone marrow stem cells *ex vivo* and transporting them to primary then secondary mice. They then produced a database showing which retroviral IS are related to malignancy. This insertional dominance database (IDDb) showed retroviral insertions into genes with ontologies associated with apoptosis, cell cycle control, proliferation and transcription (Kustikova *et al.*, 2007). In 2009 this group then showed the influence of purifying haemopoietic stem cells and cell sorting on insertional mutagenesis. They found that when stem cells were purified this did not necessarily reduce the genotoxic effect of γ-retroviral transduction. However, reducing the number of transduced haemopoietic stem cells did reduce the genotoxic risk. They also found that the risk of clonal imbalance (Kustikova, Modlich and Fehse, 2009)caused by provirus insertion into proto-oncogenes could be reduced by using lentiviruses instead of γ-retroviral vectors to transduce purified haemopoietic stem cells (Kustikova, Modlich and Fehse, 2009).

The effect of vector dosage on retroviral transduction was studied further by Modlich *et al* in 2005 where it was found that increasing vector dose contributes to increasing insertional mutagenesis. This was demonstrated by transducing bone marrow cells *ex vivo* with the RV vectors containing the MDR1 gene. The cells were then returned to the C57BL/6J mice. Development of leukemia was shown to be associated with clones that gave high retroviral expression of MDR1 as a result of high vector copy numbers achieved by high MOI infection. These clones were also over-represented with multiple RV insertion into proto-oncogenes and other signaling genes (Modlich *et al.*, 2005). In

2006 Modlich *et al* also developed a cell culture model assay to test genotoxicity by RV or LV mediated gene up regulation in haematopoietic cells (Modlich *et al.*, 2006). Interestingly, results suggested the idea that genotoxicity could be due to the architecture of the vector used, and by re-locating the strong enhancer regions from the LTR region this could significantly decrease genotoxic outcome (Josephson and Abshire, 2006; Modlich *et al.*, 2006; Wang *et al.*, 1999). Importantly there was a correlation between insertion into the *Evil* gene and the MOI used (Modlich *et al.*, 2006). The same principle could therefore be applied to other viral vectors to deduce if these same changes to the architecture of the vector could lower genotoxicity levels, thus improving the safety of viral gene therapy.

1.11.2 *In Vivo* models of genotoxicity

In genotoxic research studies the mouse is the most used mammalian model as it is small, reproduces quickly and has many genetic, biological and behavior characteristics that closely resemble those of humans. Larger models of gene therapy include sheep, pigs (Amsterdam *et al.*, 1999), rhesus monkeys (Tarantal *et al.*, 2001) and dogs.

One particular mouse model for genotoxicity has been developed in our laboratory. This model was originally based on gene therapy before birth. Numerous genetic disorders may manifest in the fetus before birth and hence *in utero* gene therapy has been researched to treat individuals at this early time point in development. *In utero* gene therapy therefore aims at early intervention for prevention of fatal genetic diseases by targeting stem cells, gene delivery circumventing immune rejection to the vector and transgene product, tolerance to the vector and permanent correction (Coutelle *et al.*, 2005). In 2004 Waddington *et al* corrected human factor IX (hFIX) deficiency using HIV-1 lentiviral vector in hFIX knock out mice. Plasma FIX antigen levels increased and delivery of hFIX did not cause an immune response (Waddington *et al.*, 2004).

In utero studies have been shown in both small and large animal models (Tarantal *et al.*, 2005; Themis *et al.*, 2005; Walsh, 1999). However, since virus IS are believed to target genes that are actively dividing as in the case of rapidly replicating fetal cells this could increase the risk of insertional mutagenesis. The potential for IM in the mouse fetus was hypothesized by Dr Themis. Using the fetal mouse model this group published the observation of liver cancers in mice treated *in utero* with lentivirus

vectors. Hence, the *in utero* mouse genotoxicity model was developed (Themis *et al* 2005;2012). The original study to establish this model involved the use of both primate HIV (HR'SIN-cPPT-S-FIX-W) and non-primate EIAV (SMART2) viral vectors each driving hFIX gene expression. Although both vectors resulted in correction of the KO mouse for haemophilia B, in the EIAV treated mice hepatocellular carcinoma (HCC) developed (n=8/10) (Themis *et al.*, 2005). These tumours were easily predicted by high level HFIX expression in mouse blood. Isolation of DNA from these tumours followed by Southern analysis showed each to be of clonal origin with 1 to 10 integrated proviruses per genome. Next LAM PCR allowed mapping of EIAV IS relative to genes in the mouse genome. Fifty-six percent of these were found to be oncogenes or genes associated with oncogenes. Ninety-nine of these were then found reduced in expression indicative of IM. Furthermore, 11 of were listed in the mouse retroviral tagged cancer gene database (RTCGD) that carries already known genes found involved in tumorigenesis in mice that developed tumours following retroviral infection (Themis *et al.*, 2005; Akagi *et al.*, 2004). Interestingly, the primate HIV vector was not associated with tumour development that indicates this vector could be suitable for prenatal and post natal gene therapy (Waddington *et al.*, 2004).

This *in vivo* model is a valuable tool to enable the evaluation of lentiviral genotoxicity and most importantly for the discovery of genes involved in liver tumour development using the HCC phenotype. The model circumvents the need for cell engraftment and proliferation such is the case for *ex-vivo* models of genotoxicity and is useful to identify molecular pathways for immortalisation and malignant progression that differ from those specific to leukaemia. Most recently, this group used the fetal model to show IS preference to actively transcribing genes and the different IS profiles between the primate HIV and non-primate EIAV vectors (Nowrouzi *et al.*, 2012).

1.12 Alternative routes to genotoxicity not involving IM

1.12.1 DNA Damage

A DNA double strand break (DSB) is a severe form of DNA lesion. Our genomes experience thousands of DNA lesions per cell each day. Some of these lesions are quite benign while others can be genotoxic. DNA DSBs are regarded as one of the most dangerous, toxic and mutagenic forms of DNA damage. A single DSB may lead to the loss of 100 million base pairs of genetic information. The breaks in the covalent bond of both the phosphate backbone of the DNA molecule leads to DNA DSB in eukaryotic cells. After dissociation of the two ends of DNA double stands, repairing becomes difficult and may lead to inappropriate recombination with other broken sites. If DSB's are misrepaired it can cause chromosomal translocations, which is an early step to developing carcinogenesis, and if left unrepaired it can cause cell death (Helleday *et al.*, 2007; Bassing and Alt, 2004).

DSB can form in response to exogenously or endogenously produced DNA damaging agents. Endogenous sources such as reactive oxygen species and free radicals are generated from cellular metabolic reactions, class switch recombination, and replication fork collapse during DNA replication and physical stress during meiosis can cause DSB (van Gent, Hoeijmakers and Kanaar, 2001).

Interestingly despite the danger of DSB, mammals have found ways of using this process for their own benefit in controlling biological processes. Programmed DSB occur in the steps involved in maturation of immunoglobulin genes by initiating rearrangements. V (D) J recombination is involved in the early development of B and T-lymphocytes and is important in generating diverse groups of antigens receptors occurring in lymphocytes. The rearrangement of exons that encode immunoglobulin and T cell receptors occur during B or T lymphocyte development by variable (V), diversity (D) and joining (J) gene segments. These programmed temporary DNA DSB are induced in the cell nucleus by proteins such as RAG1 and RAG2 (Bassing, Swat and Alt, 2002). DSB are also essential for the maintenance of DNA synthesis. DSB occur behind the replication fork by enzyme topoisomerase, which relieves the tension of unwinding (Shin *et al.*, 2004a; Jackson, 2002). The enhanced levels of endogenous chromosome breakage or chromosomal rearrangement, which have been seen in cells

that do not repair DSBs, show that they represent frequent encounters of endogenous lesions (van Gent, Hoeijmakers and Kanaar, 2001).

Exogenous factors that cause DSB include ionizing radiation, chemicals and chemotherapy agents. Cellular responses to these exogenous factors are variable depending on cell type, dose and exposure length.

The early work on DNA damage and repair in the 1930's was stimulated by a prominent group of physicists (Friedberg, 2002). It was the work of geneticist Hermann Muller who while working on the *Drosophilla* fruitfly first demonstrated mutations occurring when external agents such as ionizing radiation were involved (Muller, 1927). Ionizing radiation is energy that is carried by electromagnetic rays or by particles emitted from radioactive materials, nuclear reactions and medical X-ray equipment. Living organisms experience ionizing radiation from natural sources at low doses and at high doses via x-rays and radiation therapy. Understanding how cells respond to radiation exposure is therefore critical. DNA damage is caused directly by energy transfer of the DNA molecule or indirectly by the production of hydroxyl radicals from the ionization of water molecules that subsequently attack DNA. Exposure to ionizing radiation activates the signaling pathway of DNA damage in the nucleus and the result could be therapeutic depending on exposure conditions such as cell cycle, cell cycle stage an dose of radiation (Kastan and Bartek, 2004; Qvarnstrom *et al.*, 2004).

DNA stressing agents induce DNA DSBs that initiate complex set of responses in the cell. First, DNA damage sensing and signaling mechanisms will alert the cell of DNA DSB taking place. Then mediators and transducers will transmit the damage signals to effector molecules that arrest cell cycle if necessary until the DSB is repaired. DNA damage signals can induce apoptosis when the cell suffers from high levels of genomic instability (Mills, Ferguson and Alt, 2003; Paull *et al.*, 2000).

1.12.2 DNA DSB repair

All eukaryotic cells have evolved mechanisms to deal with DSBs. The two main mechanisms of DDR repair are homologous recombination (HR) and non-homologous end joining (NHEJ). HR uses replication to generate an identical copy of the cellular DNA and the undamaged copy can be used as a template for repair and resynthesize of a DSB. This pathway exploits a sister chromatid which is present following replication, consequently HR is restricted to the S phase of the cell cycle. When a replication fork stalls due to its production of unfavorable DNA structures the HR pathway restarts the replication machinery. This pathway is deemed a very accurate method of repair. In contrast, NHEJ is less reliable but more robust as the broken ends of a DSB are fused together. This may result in the removal or addition of a few nucleotides at the repair site and may be error prone. The NHEJ repair mechanism is preferred at the G1 phase of the cell cycle where (Shrivastav, De Haro and Nickoloff, 2008; Jeggo and Lobrich, 2007; Essers *et al.*, 2000).

1.12.2.1 DNA repair by Homologous recombination (HR)

HR is meditated though a set of proteins including RAD50, RAD51, RAD52, RAD54, RAD55, RAD57, RAD59, MRE11 and XRS2 which are all essential in repairing DSB (Thompson and Schild, 1999; Kanaar, Hoeijmakers and van Gent, 1998). The first step in the HR pathway is the resectioning of the broken DNA ends beginning with the 5' to 3' end processing by the MRN complex consisting of Mre11p, Rad51p and NBS1 (Shin *et al.*, 2004). Next the replication protein A (RPA) binds the 3' single stranded DNA (ssDNA) ends. RPA is phosphorylated and replaced with Rad52 to allow Rad51 binding. A homologous sequence that is complementary to broken DNA sequence is found and invaded by Rad51 that binds to the ssDNA end forming a nucleoprotein. Rad51 is the dissociated from the ssDNA to allow normal base pairing by DNA polymerase and extend the ssDNA strand according to the host complementary DNA sequence. This process termed synthesis-dependent strand annealing can occur by annealing extended ssDNA strand with non-invading DNA strand on opposite side of DSB or HR can produce a double holiday junction by invading both strands which are then resolved by crossover or by non-crossover recombinants. Finally, DNA

polymerase and DNA ligase resolve the nicks and gaps by ligation of two DNA ends (Shrivastav, De Haro and Nickoloff, 2008; Shin *et al.*, 2004; van Gent, Hoeijmakers and Kanaar, 2001).

1.12.2.2 DNA repair by non-homologous end joining (NHEJ)

NHEJ require the concerted action of a series of proteins. Such as Ku heterodimer (Ku70 and Ku80), DNA-PKcs, Artemis, XRCC4, DNA ligase IV and XLF (known as Cernunnos). Firstly, the overhanging ends are detected by Ku protein that consists of two subunits Ku70 and Ku80. The broken ends of the DNA are attached with Ku dimer proteins to protect the DNA ends from further collapse and provide access to other repair proteins such as DNA-dependent kinase (DNA-PKcs) (DS, 2005). The second step of NHEJ pathway is the processing of the DNA ends to remove non-ligatable end groups. Different enzymes may be used depending on the nature of the breaks. Artemis, DNA polymerases, MRN complex, RPA and WRN are candidate-processing enzymes. Lastly, XLF stimulate the XRCC4/DNA ligase IV to ligate the DNA ends (Summers *et al.*, 2011; Shrivastav, De Haro and Nickoloff, 2008; Barnes, 2001).

NHEJ is not precise due to synapsis occurring between two broken DNA ends and the trimming that occurs at each end. If two breaks occur at the same time the ends may get mixed up when DNA repair is taking place and genes may be translocated from one place to another. These errors can be deleterious in some cases leading to cancer such as Burkett's lymphoma which moves an inactive c-myc genes into a very active area thereby causing uncontrolled growth in the cell by an over expression of the gene (Rowh *et al.*, 2011).

In the late 1960s James Cleaver reported individuals with xeroderma pigmentosum (XP) to be prone to skin cancers. Cleaver then went on to look for a mammalian cell line deficient in excision repair and found that XP individuals who were genetically defective in excision repair were sunlight sensitive and more prone to cancer. This defect in nucleotide excision repair represented a triumph in the field of genetics as it provided insight into defining DNA repair and hereditary human diseases (Cleaver, 1968).

The first known DSB repair defective mouse mutant was the SCID mouse. These mice carried a mutation which prevented the production of mature B and T cells, due to a defect in V (D) J recombination. These mice were also found to be sensitive to ionizing radiation, which is caused by a mutation in the PRKDC gene resulting in the deletion of parts of the DNA-PKcs (Smith and Jackson, 1999).

Deficiencies in NHEJ leads to increased risk of cancer with chromosomal instability partially in cells consisting of a mutation in the tumor suppressor gene p53. This could be possibly due to the decrease in the cell undergoing apoptosis (Helleday *et al.*, 2007; van Gent, Hoeijmakers and Kanaar, 2001). Patients with mutations in the Artemis gene have been found to develop thymic lymphomas. This shows that a decrease in NHEJ end capacity may increase the incidence of cancer (Moshous *et al.*, 2003).

1.12.3 Genome instability due to DSB

Elevated levels of spontaneous genomic instability, increased sensitivity to ionizing radiation and other factors, which contribute to DSBs, are some of the phenotypes that are associated with mutation or inactivation of either the NHEJ or HR pathway (Jackson, 2002).

Incorrect repair of DSB can cause genome instability in the form of chromosomal loss, rearrangements, or amplifications that could potentially lead to cancer (Shrivastav, De Haro and Nickoloff, 2008). Mutations which alter the function of a specific gene i.e. oncogenes and tumor suppressor genes, which are essential for cell division give rise to neoplasmic transformations. This is known as the somatic mutation hypothesis that shows correlation between chromosomal abnormalities and cancer. This was first observed by Theodore Boveri, who reported abnormal number of chromosomes in cancerous cells (Boveri, 2008).

There are two main forms of genomic instability that are linked to tumours. One is mutational instability (MIN) phenotype that is connected to mismatch repair defects and is portrayed by small deletions or point mutations. The other genomic instability is the chromosomal instability (CIN) phenotype, which is characterized by rearrangements of chromosomes. Unrepaired DNA DSB can lead the cellular genome towards gene deletion, chromosome aberrations including chromosome segment amplification and the loss or gain of whole chromosome (Ricke, van Ree and van Deursen, 2008).

Amplification of a chromosome region may initiate tumorigenesis by the activation of proto-oncogenes whereas inactivation of tumor suppressor genes can be activated by the loss of large regions of a chromosome. Studies involving ionizing radiation of mammals or cells involving DSB have been shown to be involved in chromosome aberrations (van Gent, Hoeijmakers and Kanaar, 2001).

Chromosome instability stems from the inability to correct sister chromatids during mitosis. Failure of this mitotic checkpoint has been shown to be involved in chromosome instability. If the mitosis is prolonged it results in mitotic checkpoint over activation and is a frequent observation in tumours (Schvartzman, Sotillo and Benezra, 2010). Most of the main regulators of the mitotic checkpoints are downstream targets of the retinoblastoma (Rb) tumor suppressor pathway which is up regulated in most human tumors (Iovino *et al.*, 2006; Zheng *et al.*, 2002; Lentini, Pipitone and Di Leonardo, 2002). Mitotic checkpoint genes are essential in each mammalian cell division, however, unlike DNA damage checkpoint their loss is unlikely to cause a buildup of genomic damage in tumors (Schvartzman, Sotillo and Benezra, 2010).

Several genes are involved in the mitotic checkpoint and mitosis. These genes are under the control of the E2F family of transcription factors and are partially dependable on the on the level of inhibition of the Rb pathway (Lentini, Pipitone and Di Leonardo, 2002). Several cancers result from the mutations in genes that are essential for DNA damage checkpoint and DNA repair pathways such as hereditary non-polyposis colorectal cancer caused by the MLH1 and MSH2 gene, xeroderma pigementosum (Xp family) and ataxia-telangiectasia (ATM mutated) (O'Driscoll and Jeggo, 2006). In most cases genes that are essential for mitotic checkpoint are up regulated, this may be due to the absence of the Rb pathway. This overexpression of key genes and an inhibition of the Rb pathway can lead to tumor formation. Interestingly gene expressions from human tumors have shown that genes, which are involved in DNA damage repair pathways, are overexpressed in DNA damage pathways (Swanton *et al.*, 2009).

If a DSB is repaired incorrectly by non-homologous end joined (NHEJ) pathway this can result in mutation or oncogenic rearrangement. V (D) J recombination can lead to rearrangements of oncogene chromosome resulting in lymphoid cancers such as Burkitt's lymphoma and B-cell malignancy which are caused partially due to rearrangements of the c-MYC gene (Jackson, 2002). In conclusion, agents that cause DSB should be considered as potential mutagens. Indeed, integration by retroviruses

also cause DSB due to the viral integrase cutting and ligating the virus genome with that of the infected host (Sakurai *et al.*, 2009).

1.12.4 Proteins used to determine the presence of DSBs

It is vital to spread the alert signal efficiently to the cell when a DSB occurs. Checkpoint mediators or adaptors and transducer kinases CHK1 and CHK2 are linked to proximal checkpoint kinases such as ATM and ATR to organize the global cellular response to DSBs. These transducers (CHK1 and CHK2) regulate the phosphorylation of the downstream checkpoint targets such as effector proteins that play a vital role in cell cycle controls, DNA repair and apoptosis (Jeggo and Lobrich, 2007).
In addition to ATM and MRN other key effectors of the DSB response include histone H2AX and 53BP1. These proteins respond to the site of DSB and initiate in the ATM dependent signaling cascade that leads to DNA repair, or apoptosis.
The proteins function as key regulators in the DNA damage response as an inactivation of any will render the cell sensitive to DSB (van Attikum and Gasser, 2009).

H2AX

H2AX is found exclusively at sites of DNA DSBs and is a key component of chromatin (McKinnon and Caldecott, 2007; Rogakou *et al.*, 1998). H2AX is at the heart of ionizing radiation induced foci and contains a serine residue that is rapidly phosphorylated by protein kinase family ATM in response to DNA damage. This modified form is then referred to as γH2AX (Bassing *et al.*, 2003; Rogakou *et al.*, 1998). It is readily phosphorylated on chromatin surrounding DNA DSBs. It does not diffuse freely in the cell this may explain why their phosphorylation appears to be important for DNA repair and is not required in cell cycle arrest (Zgheib *et al.*, 2005). γH2AX regulates the recruitment and accumulation of a multitude of DNA damage repair factors (DDR) and is critical for repair of DNA lesions. One study using mice found H2AX deficiency results in genome instability and is associated with cancer predisposition (Celeste *et al.*, 2002).

53BP1

53BP1 is a DDR protein phosphorylated by ATM as an early signal of DNA DSBs. 53BP1 is a nuclear protein which rapidly localizes to discrete foci followed by lesions in the cell. The evidence of involvement of 53BP1 in DNA DSBs is the localization of 53BP1 to the sites of DSB after exposure to Ionizing radiation. Its recruitment to sites of DSBs is facilitated by histone H2AX phosphorylation and ubiquitination indirectly (Fernandez-Capetillo *et al.*, 2002). 53BP1 is involved in ATM activation since suppression of 53BP1 leads to a reduction in ATM phosphorylation (Wu *et al.*, 2009). The interaction of 53BP1 with histone H3 methylated on Lys79 also mediates the recruitment of 53BP1 to sites of DNA DSBs (Zgheib *et al.*, 2005; Huyen *et al.*, 2004). Importantly, 53Bp1 undergoes nuclear relocalization to focal structures following irradiation. This molecule facilitates both checkpoint and repair functions. Relocation of 53BP1 to the DNA damage sites is also dependent on its tudor domain that recognizes methylated histones (Kim *et al.*, 2006). Knockdown of 53BP1 results in instability represented by increased levels of chromatid gaps and aneuploidy indicating that 53BP1 is involved and much needed in DNA repair (FitzGerald, Grenon and Lowndes, 2009; Ward *et al.*, 2003).

Since ATM assists in γH2AX spreading and in turn is required for the accumulation of additional DDR factors such as 53BP1, together these events trigger and amplify the DDR signal (Zgheib *et al.*, 2005; Lukas, Lukas and Bartek, 2004). Translocation of these proteins to DNA DSBs facilitates DNA damage checkpoint activation and enhances efficiency of the DNA damage repair.

1.12.5 Methods for determining DNA DSBs

There are a number of methods to measure DNA DSBs such as sucrose density gradients, neutral elution, pulse field gel electrophoresis (PFGE) and nuclear foci analysis. PGFE and nuclear foci analysis are the most common methods of detecting DSBs. In PGFE DNA DSBs is quantified according to the fraction size of DNA released. Because γH2AX and 53BP1 are involved in signaling pathways of DNA damage and repair and accumulate in large nuclear domains after DNA damage, their recruitment to DSBs can be exploited to enable in situ visualization of DSBs. To do this, γH2AX and 53BP1 proteins are stained with specific antibodies then subjected to immunofluorescence. This allows quantification of foci representative of DSB in the cell nucleus after DNA damage (Qvarnstrom *et al.*, 2004; Paull *et al.*, 2000). Quantification can be done either manually or via an automated computational analyzing system (Bourton *et al.*, 2012).

1.12.6 Retrovirus integration mediated DSB

As previously described, retroviral integration into the host genome is critical for retroviral replication using the virus integrase enzyme. The integrase removes two nucleotides from the 3' ends of the viral DNA in the cytoplasm. It then catalyzes the joining of these ends to staggered phosphorous atoms in the backbone of the complementary strands of the host DNA (Skalka and Katz, 2005). Single strand gaps are produced between the viral DNA and the target DNA (Miller, Wang and Bushman, 1995). During this process the host cell DNA suffers a DSB. Insertion of 3-10kb of newly synthesized DNA is likely to be sensed as a major assault on genomic integrity that leads to a DDR. Additionally, unintegrated viral DNA can be is circularized by ligation of LTR sequences to form a 2LTR circle. One LTR circles can also be generated (Goff, 2001; Li *et al.*, 2001). Presumably, this limits recognition of free DSB to reduce a DDR. Completion of the integration is highly important to virus survival as DSB can lead to apoptosis

Indeed, retroviral transduction into cells which lack the DNA-PK or ligase IV repair enzymes undergo apoptosis. This suggests the requirement of NHEJ to complete retroviral integration (Daniel, Katz and Skalka, 1999). Lau *et al* showed that ATM dependent DNA damage response is stimulated by the HIV-1 integrase and that deficiency of the ATM also triggers apoptosis.

Sakurai *et al* in 2009 found that ATM, Artemis and the MRN complex play vital roles in protecting the ends of viral DNA before strand transfer and the 3' processing activity of the integrase as in the cells deficient in ATM, Artemis and the MRN complex could not completely process terminal dinuclotides (Sakurai *et al.*, 2009). Sakuirai *et al* also found in the same study that their sequence analysis indicated lack of DSB repair enzymes influenced HIV-1 integration site selection. They used the data of Holman *et al* (2005) to show that HIV-1 integration preference is slightly influenced by ATM as cells deficient in ATM have different IS profiles to cells that have normal ATM levels (Sakurai *et al.*, 2009; Holman and Coffin, 2005).

Daniel *et al* in 1999 first suggested the role of the NHEJ pathway in post integration repair by showing DNA-PK to be involved in the RV DNA integration process. When

DNA-PK deficient murine SCID cells were infected with 3 different RV, integration is reduced and death via apoptosis occurred. Furthermore, SCID cells infected with the avian retrovirus have reduced viability by 40-50% compared to control cells and this appeared dependent on the virus MOI. In the same study, they observed death of SCID cells after infection with integration competent virus but not with integration defective viruses (Daniel, Katz and Skalka, 1999). A study (Weller, Joy and Temin, 1980) showed that RV infection induced apoptosis in 80-90% of NHEJ deficient cells. They also found the NHEJ system to be responsible for the circulization of some of the viral cDNA to produce 2LTR circles. This is also in agreement with studies by Howard Temin *et al* (1980) who also observed a correlation between the degree of cytopathic effect after infection and the number of integrated RV. Overall, these data suggest that RV integrations cause DNA damaging events and that a failure of post integration repair to these can lead to apoptosis (Skalka and Katz, 2005; Daniel, Katz and Skalka, 1999; Weller, Joy and Temin, 1980).

Daniel *et al* in 2004 established that RV infection induces the formation of γH2AX foci and that H2AX phosphorylation occurred at sites of RV DNA integration. They also established that cells respond to DNA integration in a similar manner to DSBs.
This group also found that efficient transduction of MEF's by HIV- 1 requires DNA-PKcs and that XRCC4 deficient CHO cells infected with HIV-1 have a transduction efficiency 5-10 fold lower than control cells. Furthermore, they found a sharp decrease in viability of cells infected with integration competent virus compared with integration defective vectors (Daniel *et al.*, 2004).

1.13 Epigenetic modifications leading to genotoxicity

Epigenetic modifications determine where and how genetic information is used by the cell to maintain homeostasis (Waddington, 2012). It is important in the normal development of a cell, cell proliferation, gene expression and aetiology of disease (Matouk and Marsden, 2008; Devaskar, S.U. & Raychaudhuri, S., 2007). Making sure genes are active or inactivated at the correct time is essential to prevent abnormal gene expression that could potentially lead to disease and cancer (Sarkies and Sale, 2012; Klose and Bird, 2006; Robertson and Wolffe, 2000).

Epigenetic changes can influence chromatin structure and regulate transcription. Such changes regulate chromatin remodeling and mediate histone modification and DNA methylation (Dolinoy, Weidman and Jirtle, 2007).

DNA methylation is a post replication modification involving the covalent addition of a methyl group to the 5 position of cytosine (Robertson, 2001). DNA methylation itself can result in transcriptional repression, chromatin modulation, genomic imprinting, X chromosomal inactivation and governs genomic integrity. Research has revealed its importance in many processes such as DNA repair, genome stability as well as chromatin architecture (Robertson and Wolffe, 2000; Baylin and Herman, 2000; Jones and Laird, 1999). Globally, DNA methylation patterns in mammals are established by at least three independent DNA methyltransferases: DNMT1, DNMT3A and DNMT3B (Klose and Bird, 2006; Robertson, 2001).

DNMT1

DNMT1 was the first methyltransferase to be discovered and is the most abundant in somatic cells (Bestor *et al.*, 1988). It is primarily the enzyme responsible for copying pre-existing methylation patterns onto new DNA strand during DNA replication (Klose and Bird, 2006). However, under carcinogenic conditions DNMT1 has been found to perform *de novo* methylation (Vertino *et al.*, 1996).

DNMT1 identifies methylated and non-methylated DNA in its regulatory region and carboxy-terminal domain (Fang *et al.*, 2001). DNMT1 is associated with the tumour suppressor Rb that interacts with the N-terminal region of DNMT1 (Robertson and

Wolffe, 2000). DNMT1 also interacts with the Rb associated DNA binding protein and transcriptional activator E2F1. DNMT1 homozygous knockout of embryonic stem cells lead to only 30% of normal methylation levels and have a tenfold increase in the rate of mutations and gene rearrangements compared with the wild type strain of this mouse. Embryonic stem cells deficient in DNMT1 also have high levels of transcription that may be influential to increased genome instability (Chen *et al.*, 1998). Several cancers are associated with disruption of DNMT1, E2f1 and Rb DNA binding activity (Robertson and Wolffe, 2000). Methylation defects observed in tumour cells are believed to be associated with loss of function of Rb either via direct loss of the Rb gene or genes associated with Rb which can include improper nuclear localization of Rb with DNMT1 (Robertson, 2001). Studies have shown that loss of pRb results in increased DNMT1 expression (McCabe, Davis and Day, 2005). The interaction between Rb, E2F and DNMT1 is facilitated by the existence of E2F binding sites in the DNMT1 promoter. During cell division Rb is phosphorylated and no longer binds E2F1. This releases DNMT1 to perform its functions. It has been postulated that loss of Rb may grant DNMT1 free access to the genome that could potentially lead to *de novo* methylation (Robertson, 2001). DNMT1 is required for embryonic development, imprinting and X-activation and is involved in several biological processes that include cell cycle control, chromosomal instability and DNA damage and repair (Tan and Porter, 2009; Brown and Robertson, 2007).

DNMT3A and DNMT3B

DNMT3a and DNMT3b are responsible for *de novo* methylation and are mainly responsible for introducing cytosine methylation at previously unmethylated sites. These enzymes are also required following *de novo* methylation following embryo implantation for the *de novo* methylation of integrated retroviral sequences in mouse embryonic stem cells (Robertson and Wolffe, 2000; Okano *et al.*, 1999). Increased levels of DNMT3a has been shown to promote polyposis and may be involved in several cancers such as HCC. DNMT3a knockout mice survive to birth but die soon after at about 4 weeks of age (Okano *et al.*, 1999). Zhao *et al* in 2010 found in DNMT3a depleted cells suppression of cell proliferation (Zhao *et al.*, 2010). In HCC

cell lines with low DNMT3a cellular proliferation is also suppressed (Shafiei *et al.*, 2008).

DNMT3b knockout mice are not viable and mutant embryos have multiple organ failure, growth impairment and developmental defects (Li, Bestor and Jaenisch, 1992). In patients with ICF syndrome mutations in the catalytic domain of DNMT3b results in immunodeficiency, centromere instability and facial anomalies (Okano *et al.*, 1999; Gartler *et al.*, 1999). Studies have shown the interaction of dnmt1 with dnmt3b to inactive gene expression (Robertson and Wolffe, 2000b).

1.14 Viral integration and methylation

DNA methylation is widely seen to function as a host defense mechanism against the uptake, integration or expression of foreign DNA into chromosomes, to prevent foreign agents from influencing the transcription of cellular genes (Tao and Robertson, 2003). This includes incoming virus elements in infected cells. Methylation of the viral genome usually takes place in LTR to reduce or prevent viral replication. Hence, methylation can act as a mechanism of suppression of viral expression where the LTR drives gene expression. It also affects virus latency (Fang *et al.*, 2001; Mikovits *et al.*, 1990).

Harbers *et al* in 1981 first showed a relationship between retroviral replication and DNA methylation of the MLV virus. In this study, viral expression was silenced by the hypermethylation of sequences in the MLV LTR. Suppression of expression and latency of HIV-1 and HTLV-1 has also been shown following methylation of virus genomes (Harbers *et al.*, 1981).

As RV integration is known to favour promoter regions that are composed of CpG regions and these regions are used for methylation, MLV insertion is often accompanied by methylation of the virus and shut-down of virus expression. LV appears to favour the transcription unit rather than the promoter region and is less susceptible to inactivation of gene expression. (Hacker *et al.*, 2006).

There have been a number of studies that have highlighted the role of viral infection on stimulating the cellular methylation machinery. Leonard *et al* (2011) showed an up regulation of DNMT3a and a down regulation of DNMT3b and DNMT1 following EBV infection of B cells (Leonard *et al.*, 2011)

Fang *et al* (2001) investigated the relationship of HIV-1 infection and methylation levels in lymphoid cells. An increase in DNMT1 levels was reported when lymphoid cells were infected with either HIV-1 wild type or an integrase (IN) mutant (replication defective) 3 to 5 days post infection. This was accompanied by an overall increase in genome methylation and *de novo* methylation of a CpG dinucleotides in gene promoters resulted in promoter shutdown. Importantly, this was reported following infection by a defective HIV vector where increased methylation of CpG nucleotides in the promoter of the $p16^{INK4A}$ gene occurred. The $p16^{INK4A}$ is frequently methylated in non-Hodgkin's leukaemia (Fang *et al.*, 2001) and this finding suggests that changes in methylation patterns following HIV infection could lead to disease. Lee *et al* (2003) also reported similar methylation patterns in non integrating viruses such as HCV and integration HBV virus (Lee *et al.*, 2003).

Yamagata *et al* (2012) investigated the epigenetic effects of transduction of $CD34^+$ cells by a defective lentiviral vector. This group was the first to show that gene transfer into somatic and progenitor cells could influence the methylation state of the genome *in vitro* by gene therapy vectors. The study cultured $CD34^+$ cells in the presence of cytokines for 24hours followed by 2 consecutive incubations with LV. The study found that on exposure to cytokines $CD34^+$ cells had genome wide DNA methylation changes accompanied by an increase in DNMT1 expression only 24 hours after infection. The study then went on to show up to 900 host genes to be differentially expressed following infection compared to just 200 genes in cells cultured in presence of cytokines only (Yamagata *et al.*, 2012).

Surprisingly, little is still known about the overall effects on the host following methylation changes influenced by infection by defective LV. It is of paramount importance, therefore to understand the association between virus integration and host DNA methylation and to what extent gene expression in the host is altered to avoid complications when applying these vectors to patients in the clinic.

1.15 Methylation and DNA damage

A study by Cuozzo *et al* (2007) demonstrated DNA methylation to mark homologous repair (HR) segments and protects cells against DNA damaged up-regulated gene expression. They found this by inducing a single break in the genome of mouse or human cells. This was repaired via HR. DSB repair by HR and gene alteration is linked to methylation changes in the area that DSB occurs and this requires the activity of DNMT1 (Cuozzo *et al.*, 2007).

Armstrong *et al* (2012) showed an inverse correlation between hypomethylation and radiation induced genomic instability. This group found DNMT1 deficient mESCs to have a 10 fold increase in *de novo* mutation of the *hprt* locus (Armstrong *et al.*, 2012). Thereby, suggesting a role in DNMT1 in hindering efficient function of DNA repair resulting in this increase rate of mutation.

Several studies have showed a connection between DNA methylation, genomic instability and DSB and DNA repair. It has also been suggested that DNMT1 is important in sensing or repairing DNA damage (Palii *et al.*, 2008; Guo, Wang and Bradley, 2004).

Chen *et al* (1998), showed DNMT1 deficiency to result in a mutator phenotype by showing DNMT1 deficient ES mice have a ~10 fold increase in mutation frequency (Chen *et al.*, 1998). Okano et al (1999) also showed mice lacking in DNMT1 to be genetically unstable (Okano *et al.*, 1999). Guo *et al* (2004) used a genetic screen to find genes involved in mismatch repair (MMR) and found DNMT1 to be one of these genes. They then found that murine ES cells deficient in DNMT1 exhibited a 4-fold increase in microsatellite instability (Guo, Wang and Bradley, 2004). Mortusewicz *et al* (2005) also found DNMT1 plays a role in regulating genome integrity by inducing DNA damage using ultraviolet light showing DNMT1 and proliferating cell nuclear antigen PCNA accumulates at sites of DNA damage (Palii *et al.*, 2008; Mortusewicz *et al.*, 2005). Palii *et al* (2008) then confirmed this using immunofluorescence to demonstrate DNMT1 to be present at γH2AX positive foci in cells treated with the DNA methylation inhibitor, 5-aza-2'-deoxycytidine. They also showed in DNMT1 deficient cells severe defects in the activation of key DSB responses such as lack of γ-H2AX induction and reduced phosphorylation of p53 and CHK1 (Palii *et al.*, 2008). Taken together these studies show a role for DNMT1 in the DNA DSB response pathway.

1.16 E2F and DNA damage

E2F is a group of proteins (E2F 1-8). They are transcription factors which have a heterodimeric complex which contains an E2F component and a DP1/2 subunit, with the exception of E2F7 and 8. Three of E2Fs act as activators and 6 others as suppressors of gene expression by acting on specific promoter TTTCCCGC sequences. It is this dual activity that allows both oncogenic and tumour suppressor activity (Polager *et al.*, 2002; Dyson, 1998). E2F target genes are involved in cell cycle regulation, cellular differentiation, DNA synthesis, and DNA damage and repair mechanisms (Frame *et al.*, 2006; Polager *et al.*, 2002).

E2Fs are specifically regulated by the Rb tumour suppressor protein (pRb). pRb belongs to the pocket protein family that consist of p107 and p130 (Lee *et al.*, 2002). They inhibit cell cycle progression by regulating the G1 to S phase of the cell cycle, until the cell is ready to divide thereby preventing excessive cell growth (DeGregori *et al.*, 1997). In G0 and early G1, E2F is transcriptionally repressed by complexing with pRb. Transcription of E2F target genes takes place when pRb is phosphoralated causing the E2f-Rb complex to disassociate and release E2F (Lee *et al.*, 2002). Chellapan *et al* in 1991 found that the disassociation of the E2f-Rb complex correlated with an increase in adenovirus infection, as pRb is targeted by the adenovirus E1A (early region 1 A) oncoprotein (Chellappan *et al.*, 1991).

Polagar *et al* (2002) studied the expression of genes involved in DNA replication, repair and mitosis. They found that E2F1 and E2F3 activity up-regulates the expression of genes involved in all 3 groups. Their findings also indicate that E2F gene activation may contribute to the cell response to DNA damage as they found PCNA and BRCA-1 to be controlled by E2F (Polager *et al.*, 2002).

Frame *et al* (2006) established that the deregulation of Rb/E2F pathways in human fibroblast cells caused E2F1 mediated apoptosis and that the MRN complex, 53BP1 and γH2AX relocalize into discrete foci following deregulation of E2F1. E2F has also been shown to play a vital role in maintaining cell cycle and apoptotic cell death in response to oncogene activation and DNA damage (Frame *et al.*, 2006). DeGregori *et al* (1997) found E2F genes rapidly induce apoptosis when E2F is highly expressed (DeGregori *et*

al., 1997). In agreement with this Tsai *et al* (1998) showed that mutations in E2F caused suppression in apoptosis (Tsai *et al.*, 1998).

Hence E2F appeares closely linked to DNA damage, is controlled by methylation and has an important role in cancer development. It may, therefore be suggested that RV infection that causes DSBs may also be involved in mediating E2F activity. DSB, methylation and E2F activity may all be considered as contributors of genotoxicity if stimulated by RV infection and this may occur independent of IM and be synergistic to IM in early on in oncogenesis.

1.17 Hypothesis

Genotoxicity by RV and LV may be caused by several factors. Apart from IM these factors also include DNA damage following infection and integration, and epigenetic effects related to incoming virus particles. These effects may ultimately influence the control of E2F on its target genes. The hypothesis of this work is that DNA damage mediated by RV may lead to epigenetic changes in the form of methylation of genes in the host and changes in E2F target gene expression.

1.17.1 Aims and Objectives

- Mouse tumours will be examined for genetic changes in the form of gene amplifications and deletions
- An *in vitro* model cell line will be used to investigate the DDR to infection by retrovirus and lentivirus vectors
- Epigenetic changes will be measured *in vitro* following infection
- The relationship between DDR and methylation will be investigated using cells mutated at 53BP1, a gene important to the DDR pathway
- Gene expression pathways will be investigated for DNA damage and repair pathways and genes known to be controlled by the E2F transcription factors

2.1 MATERIALS

The materials used in these experiments are listed below, along with details of the suppliers from which they were purchased.

2.1.1 General chemicals and reagents

Chemical/ Reagent	Company name
Agar	Fisher Scientific (Loughborough, UK)
Agarose	
Ampicillin	Sigma-Aldrich (Dorset, UK)
BSA (Bovine Serum Albumin)	
Chloroform	Fisher Scientific
Double distilled water (ddH_2o)	Autoclaved purite water[1]
DMSO (dimethyl Sulfoxide)	Sigma-Aldrich
Ethanol	Hayman LTD (Essex, UK)
Ethidium Bromide	Sigma- Aldrich
Glycerol	Fisher Scientific
IMS (industrial methylated spirit)	Hayman LTD
Isopropanol	Fisher Scientific
Magnesium Chloride	Sigma-Aldrich
Paraformaldehyde	
Phenol	
Potassium Ferrocyanide	
Potassium Ferricyanide	
SDS (sodium dodecyl sulfate)	
Sodium chloride	Fisher Scientific
Sodium citrate	Sigma Aldrich
Sodium hydroxide	BDH
Tris Borate Acid (TBE)	Fisher Scientific

Table 3. General chemicals and reagents used in experiments [1] represent ddH_2O

2.1.2 Tissue culture reagents

Chemical/ Reagent	Company name
DMEM (Dulbecco's modified Eagle's medium) containing GlutaMax™, 1000mg/L and sodium pyruvate	Fisher Scientific
Pen/Strep (penicillin/streptomycin)	
Fetal Bovine Serum	
DMEM-F12	
Hydrocortisone	
Insulin	
Penicillin/streptomycin/glutamine	
Epidermal growth factor	Sigma- Aldrich
10X Trypsin-EDTA (containing 0.5% trypsin in 5.3mM EDTA)	Fisher Scientific
DMSO (dimethyl sulfoxide)	Sigma-Aldrich
1X PBS (Phosphate Buffered Saline)	
Trypan Blue	Invitrogen
Virkon disinfectant	Fisher Scientific

Table 4. General reagents used for tissue culture

2.1.3 X-gal reagents

Chemical/ Reagent	Company name
1X PBS	Sigma- Aldrich
4% Paraformaldehyde	
Potassium Ferrocyanide	
Potassium Ferricyanide	
Magnesium Chloride	
X-gal (5-bromo-4-chloro-3-indoyl b-d-galactopyranoside)	Fisher Scientific

Table 5. General chemicals and reagents used in x-gal staining procedure

2.1.4 Cell viability reagents

Chemical/ Reagent	Company name
Countess® Cell Counting Chamber Slides	Invitrogen
Trypan blue stain (0.4%)	
1X PBS (Phosphate Buffered Saline)	Sigma-Aldrich

Table 6. General chemicals and reagents used in cell viability assays

2.1.5 Immunofluorescence reagents

Chemical/ Reagent	Company name
1X PBS	Sigma- Aldrich
4% Paraformaldehyde	
Permeabilization buffer	See 2.13
Blocking buffer	See 2.13
Washing buffer Solution	See 2.13
Mouse anti-human 53BP1 IgG2b (1:200)	BD Transduction Laboratories™ (Oxford, UK)
Rabbit anti-mouse 53BP1 (1:200)	
Vectashield® Mounting Media containing Dapi	Vector Laboratories (Peterborough, UK)

Table 7. Reagents used in immunofluorescence

2.1.6 DNA Extraction reagents

Chemical/ Reagent	Company name
Phenol	Sigma-Aldrich
Chloroform	Fisher Scientific
Extraction buffer	See 2.13
Proteinase K	Fisher Scientific
RNase A	
Ethanol	Hayman LTD
70% Ethanol	See 2.13

Table 8. Reagents used for DNA extraction of cells

2.1.7 Reagents for global methylation assay using Imprint ® Methylated DNA quantification kit

Chemical/ Reagent	Company name
10X wash buffer	Sigma- Aldrich
DNA Binding Solution	
Methylated Control DNA (50 ng/µl)	
Block Solution	
Capture Antibody	
Detection Antibody	
Developing Solution	
Stop Solution	

Table 9. General reagents used for global methylation assays.

2.1.8 Pre designed and custom made TaqMan probes for gene expression analysis- Applied Biosystems

Gene Name	Assay ID	Exons amplified	Amplificon product size
18sRNA	4310893E	n/a	187
Dnmt1	Mm00599763_m1	1-2	68
Dnmt3a	Mm00432870_m1	6-7	75
Dnmt3b	Mm00599800_m1	1-2	61

Table 10. TaqMan gene expression assays used to quantify DNA methyltransferase activity

2.1.9 RNA extraction reagents

Chemical/ Reagent	Company name
RNA extraction	
TRIzol® reagent	Invitrogen
Chloroform	Fisher Scientific
2-propan-1-ol (isopropanol)	Sigma-Aldrich
75% ice cold ethanol	See 2.13
Nuclease free ddH_2O	Qiagen (West Sussex, UK)
***DNase I* Treatment**	
10X reaction buffer	Sigma- Aldrich
Amplification Grade DNase I (1,0000 units)	
Stop solution	
RNA purification	
β-ME (2-Mercaptoethanol)	Agilent technologies, Stratagene
Lysis solution	
1 x low salt wash solution	
Elution buffer	

Table 11. Reagents used for isolation of total RNA from cell lines, *DNase I* treatments and RNA purification

2.1.10 cDNA synthesis for Real Time Quantitative (Q)- PCR reagents

Chemical/ Reagent	Company name
ddH_2O	
10X RT buffer	Applied Biosystems
10X RT random Primers	
25X dNTP mix (100mM)	
MultiScribe™, Reverse Transcriptase, 50U/μl	
RNase Inhibitor	

Table 12. General chemicals and reagents used for cDNA synthesis of total RNA for QPCR

2.1.11 Q-PCR reagents for gene expression analysis

Chemical/ Reagent	Company name
ddH_2O	
2X TaqMan universal PCR Master Mix containing AmpliTaq Gold®DNA polymerase, Amperase UNG, dNTP's and dUTP	Applied Biosystems
20X TaqMan gene expression assay	

Table 13. General chemicals and reagents for TaqMan PCR reactions

2.1.12 mFISH reagents

Chemical/ Reagent	Company name
Metaphase Spreads	
Carnoy's Fixative	See 2.13
Slide pre-treatment prior to hybridization	
50% Acetic acid	See 2.13
100% methanol	Sigma- Aldrich
0.1M HCL	See 2.13
2X SSC	Sigma- Aldrich
Hybridisation	
70% Formamide	See 2.13
Human M-FISH paint	MetaSystems (Houston, USA)
70% Ethanol	See 2.13
90% Ethanol	See 2.13
100% Ethanol	Hayman LTD (Essex, UK)
Fixogum	Tesco (UK)
Post- Hybridisation	

2X SSC	Sigma- Aldrich
50% formamide/ 2X SSC	See 2.13
4X SSCT	See 2.13
Anti biotin Cy5.5 (Cy5.5 conjugated Affinity purified anti-biotin [goat]	Rockland Immunochemicals (Pennsylvania, USA)
Counterstain DAPI (*SlowFade*® Gold antifade reagent with DAPI	Invitrogen

Table 14. General chemicals and reagents used for mFISH experiments

2.1.13 MicroArray reagents

Chemical/ Reagent	Company name
cDNA synthesis- 3DNA 900	
RT primer- Cy3 (1.0 pmole/µl)	Genisphere (Pennsylvania, USA)
RT primer- Cy5 (1.0 pmole/µl)	
SuperaseIn	
dNTP mix (10mM each)	
cDNA synthesis- SuperScript III	
SuperScript III RT (200 U/µl)	Invitrogen
5X First Strand Buffer	
0.1M DTT	
Pre-hybridization solution	
BSA (100mg/ml)	Sigma- Aldrich
10% SDS	
20X SSC	
cDNA Hybridization	
LNA dT blocker	Genisphere
2X SDS-based hybridization buffer	
Nuclease free water	
Hybridization Wash	
2x SSC, 0.2% SDS wash buffer	Sigma- Aldrich
2x SSC wash buffer	
0.2x SSC	
Hybridization	
3DNA capture reagent- Cy3	Genisphere
3DNA capture reagent- Cy5	
SlideBooster	
Hydration solution- MilliQ water	
Coupling solution- 25% glycerol	
70% ethanol	See 2.13

Table 15. General chemicals and reagents used for Microarray experiments

2.1.14 Compositions of buffers and solutions

General buffers and solutions

75% Ethanol for RNA use

750ml nuclease free ddH_2O

250ml Absolute ethanol solution

70% Ethanol

750ml ddH_2O

250ml Absolute ethanol solution

90% Ethanol

900ml ddH_2O

100ml Absolute ethanol solution

DNA Extraction buffer

50mM Tris pH 8.0

100mM EDTA pH 8.0

100mM NaCl

0.1% SDS

Permeabilization Buffer

50ml X1 PBS

0.5% Triton X100

Blocking Buffer

0.2% skimmed dry milk

0.1% Triton X100

50ml X1PBS

Washing Buffer Solution

0.1% Triton X100

50ml X1 PBS

5X TBE (tris-borate EDTA) buffer

500ml ddH_2O

27g Tris base

137.5g boric acid

10ml 0.5M EDTA pH 8.0

1X TBE

700ml ddH_2O

300ml of 5X TBS solution

X-Gal staining solution

PBS containing :

4mM $K_3FE(CN)_6$

4mM $K_4FE(CN)_6$

0.1mM $MgCl_2$

0.4mg/ml X-Gal (from 40mg/ml stock dissolved in DMSO) Make up fresh immediately before use, protect from light before and during staining. If solution is to be used to stain cells in tissue culture plates it should be filtered through a 0.22μm pore size filter unit before use to eliminate any un dissolved crystals that would hamper subsequent microscopic inspection.

Paraformaldehyde Solution

4% (w/v) paraformaldehyde in PBS.

Stir under gentle heat to dissolve, store frozen in 20ml aliquots.

Carnoy's Fixative

3:1methanol/ glacial acetic acid

50% Acetic acid

50ml acetic acid in 50ml ddH_2O

4X SSCT

80µl Tween 20 in 400ml of 4XSSC

0.01 HCL

50µl 38% HCL, concentrated grade

50ml HPLC water containing 500µl of 1% pepsin.

70% Formamide

30% 2X SSC

2.1.15 Cell Lines

The cell lines utilized in these experiments are listed below.

HepG2

HepG2 cells are a human hepatocellular carcinoma cell line used for mammalian tissue culture. These cells were kindly provided by Dr Amanda Harvey (Brunel University, Uxbridge, UK)

HepG2 cells have been isolated from human liver cancer patients. These cells are frequently used in genotoxicity studies and identification of reactive components. (Knasmuller *et al*, 2004)

Mcf10a

Mcf10a cells are an immortalized non transformed human mammary epithelial cell line. These cells were kindly provided by Dr Amanda Harvey (Brunel University, Uxbridge, UK)

Mcf10a cells were derived from the breast tissue of a 36 year old patient with fibrocystic changes. It exhibits numerous features of normal breast epithelium, including lack of tumorigenicity in nude mice, lack of anchorage-independent growth and is dependable on growth factors and hormones for proliferation and growth. It is also one step away from being metastic (Yang *et al*., 2006).

MRC5-SV1

Is a SV40 immortalized lung fibroblast which when undergone DNA damage, repairs normally (Arlett *et al*., 1988).

These cells were kindly provided by Dr Christopher Parris (Brunel University, Uxbridge, UK)

AT5BIVA

AT5BIVA is an SV40 immortalized classic ataxia telangiectasia fibroblast cell line and are derived from an ataxia telangiectasia patient. It is DNA DSB repair deficient and is deficient in the ATM gene at the cell cycle check point (Murnane *et al*., 1985).

These cells were kindly provided by Dr Christopher Parris (Brunel University, Uxbridge, UK)

XP14BRneo17

Is an SV40 immortalized fibroblast cell line, derived from a human subject defect in the NHEJ pathway particularly deficient in DNA PKcs (Abbaszadeh *et al.*, 2010).

These cells were kindly provided by Dr Christopher Parris (Brunel University, Uxbridge, UK)

53BP1 -/-

Is a 53BP1 deficient mouse embryonic fibroblast (MEF) cell line (Shibata *et al*, 2010).

These cells were kindly provided by Professor Penny Jeggo (University of Sussex, Brighton, UK)

TELCeB/ AF-7

TELCeB/ AF-7 cells contain pCeB (*gag/pol*), pAF7 (amphotropic envelope) and the pMfGns Laz-Z backbone (Cossett *et al*., 1995). For the purpose of this study this virus producing cell line was called MLV.

PA317

Pa317 cells were derived from NIH 3T3 TK^- cells by co-transfection of the defective viral DNA. DNA construct consist of the promoter, *gag*, *pol* and *env* sequences of a helper virus useful for making retrovirus packaging cell line that do not transfer the

packaging function (Miller and Rosman, 1989). For the purpose of this study these cells were called, Empty vector.

These cells were kindly provided by Dr Michael Themis (Brunel University, Uxbridge, UK)

2.1.16 Viral vectors

The Smart2Z (**EIAV**), HR'SIN-CPPT-S-FX-W (**HIV**), HR'SIN-CPPT-S-FX-W (**HIV containing defective integrase**) and pLIONhAAThFIX FIV (**FIV**) vectors used in this study were originally provided by Dr Themis. These vectors were used to infect cell lines.

2.2 METHODS

2.2.1 Mammalian cell culture methods

All cell culture protocols were performed under a laminar class II cell culture hood (Heraeus).

HepG2, TELCeB/ AF-7, PA317, MRC-5 SV1, AT5BIVA, XP14BRneo17 and 53BP -/- cells were maintained in the same growth medium: DMEM containing 15% FBS, supplemented with 1% penicillin/streptomycin.

Mcf01a cells were cultured in DMEM-F12 containing 10% FBS, 1% penicillin/streptomycin/ glutamine, 0.5µg/ml hydrocortisone, 20ng/ml epidermal growth factor and 5µg/ml insulin.

2.2.1.1 Growth and Maintenance

Cells were grown as a monolayer in sterile tissue culture flasks or cell culture dishes in a CO_2 incubator (Sanyo) maintained at 37ºC, in a humidified, 5% CO_2 atmosphere. Once the cells had reached 70% confluence, growth medium was aspirated and the monolayer washed once with 1 x PBS warmed to 37 ºC. Cells were detached from the culture dish using 1 x Trypsin- EDTA. The cell culture dishes were then incubated at 37ºC for no more than 5 minutes. Trypsin activity was neutralized by the addition of >5 volumes of growth medium, and the cells were gently mixed by pipetting up and down. The neutralised cell suspension was centrifuged at 1000rpm for 5 minutes. The clear supernatant formed was discarded. The pellet was re-suspended in 1ml of fresh growth medium and mixed by pipetting up and down until a homogenous single cell suspension was achieved. An aliquot of this was transferred to a cell culture dish containing fresh growth medium and cell culture dishes were placed in the incubator Cells were passaged 2 or 3 times per week at a ratio of 1:3 – 1:8 depending on the growth characteristics of each individual cell line.

2.2.1.2 Long term storage of cells in liquid nitrogen

Cells were frozen in liquid nitrogen (-196ºC) for long term storage. Cell pellet achieved from centrifugation after passaging were re-suspended in freezing medium containing DMEM including 20% FBS and 10% DMSO. 1ml aliquots were transferred to labelled cryotubes, packed in insulated boxes then frozen slowly at -80ºC for 24 hours. After this time the vials were transferred to a liquid nitrogen dewar.

2.2.1.3 Seeding cells into cell culture dishes

Cells were trypsinised and re suspended in a small volume of growth medium as described for passaging, then counted using a haemocytometer to determine the cell density. The suspension was adjusted to 1.5 x 10^5 cells/ml before being added to cell culture dishes at a total volume of 10ml/ dish (i.e. 2ml /well for a 6 well plate, 1ml/ well for a 12 well plate, etc.). Dishes were then replaced at 37ºC until the cells had re-adhered. At this seeding density the cells could be infected the next day.

2.2.1.4 Infection of cells with viral vectors

Cells were plated as described above and left at 37ºC to reattach. Growth medium was aspirated from the cells and replaced with the medium containing the diluted virus. Un-concentrated vector preparations were often applied to the cells without dilution. Plates were replaced at 37ºC for infection to proceed, and in most cases were analysed for gene expression after 6, 24 and 72 hours.

2.2.2 X-Gal Staining - Percentage of infectibility

Cell lines to be stained with x-gal solution were washed with X1 PBS three times, fixed in 4% paraformaldehyde for 8 minutes at room temperature, then washed in x1 PBS three times to remove all traces of paraformaldehyde. Fresh X-gal staining solution was prepared and enough was added to each sample to completely cover the cell monolayer. The samples were wrapped in aluminium foil to exclude light, then left to stain at room temperature for up to 24 hours. The x-gal compound is a chromogenic substrate of β-

galactosidase, and hydrolysis of the β 1-4 bond between galactose and the 5-bromo-4-chloro-3-indolyl parts of the molecule results in the production of an insoluble blue precipitate. The distribution of any β- galactosidase enzyme within the sample is therefore revealed by the appearance of blue pigment. After staining samples were washed with X1 PBS and stored in X1 PBS.

In samples with high levels of β-gal expression, blue colorations could be seen with the naked eye after as little as 30 minutes in staining solution. For the majority of samples, however, inspection under magnification was required. Stained samples were viewed under the Olympus inverted light microscope.

2.2.2.1 Image capture and processing

Samples of interest were photographed using a canon digital camera attached to the Olympus microscope. The numbers of blue cells in each well counted were recorded using a tally counter and all wells from each infection were averaged.

2.2.3 Cell viability asssay

The dye exclusion test is used to determine the number of viable cells present in a cell suspension.

An aliquot of cell suspension being tested for viability was centrifuged for 5 minutes at 1000rpm and its supernatant discarded. The pellet was then re-suspended in 50µl- 1ml of PBS. 10µl of this cell suspension was added into a sterile epindorph tube with 10µl of 0.4% trypan blue. This mixture was allowed to incubate for 5 minutes at room temperature. 20µl of this mixture was then pipetted into one of the chambers of the Countess® slides. The slide was then inserted into the Countess® Automated cell counter and focused. Unstained (viable) and stained (nonviable) cells were counted separately in the Countess® Automated cell counter and a percentage of viable cells were produced.

Cell Viability assays were carried out 24 hours after infection and every day for the next 5 days.

2.2.4 Immunofluorescence

Cell monolayers were grown on 15mm coverslips in 35mm culture dishes. At 70-75% confluency cell monolayers were washed with cold PBS twice. Cells were fixed with 4% paraformaldehyde for 8 minutes at room temperature in order to retain the shape and location of all cellular proteins. After the cell monolayer was washed in 1x PBS three times, 2ml permeabilization buffer was added to each dish to permeabilize the cells and incubated for 5 minutes at room temperature.2 ml of blocking buffer was then added to each dish and left to incubate for 1 hour at room temperature. After this time the coverslips were transferred from the dishes to humidity chamber via sterile tweezers and placed on damp sterile tissue paper. A dilution of primary antibody in blocking buffer was added to the coverslips. The primary antibody was a mouse anti-human 53BP1 IgG2b and was used at a 1/200 dilution. Coverslips were incubated at room temperature for 1 hour. The secondary antibody was a preparation of rabbit anti-mouse 53BP1, diluted 1/200 in blocking buffer. Coverslips were incubated at room temperature for 1 hour in the dark. All steps after this were done in the dark. The secondary antibody was washed off to remove unbound reagents and background. This was done by dipping the coverslips in 3 beakers containing washing buffer solution. Vector shied containing dapi was placed on sterile slides. Each coverslip was then mounted on the slide and sealed with clear nail polish. Slides were then inspected using a Zeiss microscope and photographed using the Metapher softwares: Msearch and AutoCapt.

2.2.4.1 Immunofluorescence image analysis

Nuclei images were imported into and analysed by the Definiens software in collaboration with Dr Martin Spitaler of Imperial College, London.

2.2.5 DNA extraction from cultured cells

All surfaces and equipment were wiped down with 2% trigene and 70% ethanol. From a cell culture dish, standard trypsinization protocol was performed and the cells were pelleted by centrifugation in a 15ml tube. The supernatant was decanted and the pellet

resuspended in 0.5-1 ml of extraction buffer until a thick gloopy solution was generated. The reaction mixture was transferred into a sterile epindorph tube using a pipette, 20µg/ml RNAase was added and the reaction mixture was incubated at 37°C for an hour. Proteinase K at a concentration of 100µg/ml was added to the reaction tubes and incubated at 55°C for two hours. An equal amount of (0.5-1 ml) of phenol was then added to the reaction mixture and mixed gently by inverting the tube sideways until a white solution was formed. The reaction mixture was spun in a centrifuge at 13,000 *g* for 20 minutes at 4°C. The reaction mixture yielded 2 phases separating DNA between the phenol- protein solution. The top layer was DNA in aqueous solution. The aqueous DNA solution was transferred to a sterile centrifuge tube and an equal volume of chloroform was added. The solution was the mixed carefully by inversion. The reaction mixture was spun down at 13,000 *g* for 20 minutes at 4°C. The supernatant was removed and transferred to a sterile centrifuge tube. 1.5 ml of ice cold 100% ethanol was added to wash the reaction mixture and the tube gently mixed by tilting until a clear solution with DNA precipitate was formed. The solution containing DNA precipitate was spun down to form a pellet. The ethanol solution was poured off by tilting the tube in the opposite direction of the DNA pellet. The DNA pellets were washed in 70% ethanol twice to remove excess salt. The tubes were air dried in a sterile hood and the pellets re-suspended in 300µl of double distilled water. The reactions mixtures were left to dissolve at 4°C overnight.

2.2.6 Quantification of nucleic acids

Nucleic acids (dsDNA, cDNA and RNA) were quantified and absorbance values measured at several wavelengths (260, 280 and 260:280) using the Nanodrop spectrophotometer. The 260 absorbance reading was used to determine the concentration of nucleic acids present in uninfected, normal and infected cell line samples. The 280 absorbance reading was used to detect protein contamination in the samples. ddH_20/TE nucleic acids buffer was used as a reference sample. 1.5µl of this reference sample was applied to the Nanadrop using a sterile pipette and this was used to read a zero absorbance for the 'blank'. 1.5µl of DNA, plasmid DNA, cDNA and RNA samples were then measured using the Nanadrop. For pure DNA and RNA samples the 260/280 ratio given were approximately 1.8 and 2.0 respectively.

2.2.7 Agarose gel electrophoresis

Electrophoresis allows the detection and separation of macromolecules (DNA and RNA) based on their size. This was performed through 1 or 2% agarose gels supplemented with 0.5µg/ml ethidium bromide using a casting tray with well-forming combs depending on sample number. Each sample DNA was mixed with 6 x Loading buffer and run alongside a 1Kb DNA ladder containing marker fragments of known size. A constant voltage of 50V was applied to move the DNA or RNA fragment through the gel. The electric field causes the negatively charge DNA or RNA molecules to migrate from negative to positive poles, whilst the ethidium bromide intercalates within DNA or RNA molecules allowing the visualization of the restriction digest sample. DNA or RNA fragments were visualized using ultraviolet illumination of the gel. Gel images were captured using the BIO RAD Chemi Doc ^{TM} XRS.

2.2.8 Global methylation assay using Imprint® Methylated DNA Quantification Kit

DNA samples which were extracted from lentiviral and retroviral infected cells were quantified using the Nanodrop spectrophotometer. DNA samples were then diluted using DNA binding solution to achieve a concentration of 50ng in 30µl. Standard control samples consisted of a negative blank and a positive DNA sample (uninfected and standard methylated DNA samples). The negative controls and methylated DNA were also diluted in DNA binding solution. All dilutions were mixed by brief centrifugation at 12,000 x g and 30µl of each sample was added to an ELISA plate. To ensure that each well was coated the plate was gently tilted from side to side. The plate was covered with optical adhesive film and incubated at 37°C for 1hr. 10x wash buffer was thawed on ice. Following incubation 150µl of blocking buffer solution was added directly to each well to coat samples and reduce non-specific DNA binding. The plate wells were covered and incubated at 37°C for 30 minutes. The reaction mixtures were removed from each well by inverting plate. Each well was washed by adding 150µl of 1x wash buffer followed by inversion of the plate to remove the contents. This step was repeated 3 times. Methylated DNA capture involved the use of a capture antibody specific to methylated CpG dinucleotides. A 1X wash buffer was prepared in a sterile

bottle using 11ml of 10x wash buffer and 99ml of ddH2O. Capture antibody was diluted in a 1:1000 ratio using 1x wash buffer. 50µL of diluted Capture antibody was then added to each well. The plate was then covered and incubated at room temperature for 1hr. The capture antibody was removed from each well by inverting the plate. Each well was washed 4 times with 150µl of 1x wash buffer. The detection antibody was diluted to a 1 in 1000 ratio using 1x wash buffer. 50µl of diluted detection antibody was added to each well. The plate was covered and incubated at room temperature for 30 minutes. The detection antibody was removed from each well and the reaction wells were washed 5 times with 150µl of 1x wash buffer. For the detection of methylated DNA 100µl of developing solution was added to each well. The plate was covered and incubated at room temperature away from light for 1-10 minutes. The reaction mixtures were monitored for colour change to ensure the formation of a blue solution. 50µl of stop solution was added to each well which yielded a yellow solution. The absorbance values correspond to the level of CpG methylation. Absorbance (Abs) values were measured at 450nm on a plate reader (Biotex Instruments). To calculate the relative methylation levels for each DNA sample. Firstly replicate absorbance values for all DNA and blank samples were averaged. The average blank value was then subtracted from the average absorbance values for each DNA sample to give value A. Next the average blank value was subtracted from the average absorbance value taken from the positive control sample to give value B. Value A was divided by value B and multiplied by 100. This calculated percentage value represents a global methylation level that is a percentage of the positive control DNA sample.

$$\text{Calculation for global methylation: } \frac{(\text{Abs 450 sample} - \text{Abs 450 Blank})}{(\text{Abs 450 Methylation Control DNA} - \text{Abs 450 Blank})} \times 100$$

2.2.9 RNA extraction from cultured cells

Cell monolayers at 90-95% confluency were washed with 10ml PBS twice. 2-3ml trizol reagent was added and left for 2 minutes at room temperature. Lysate was retropipetted and placed in a sterile 15ml tube. The homogenized sample was then incubated at room temperature for 5 minutes. 200µl of chloroform per 1ml trizol reagent was added and

the reaction mixture was mixed vigorously by hand for 15 seconds and incubated for 2-3 minutes at room temperature. The samples were then centrifuged at 12,000 *g* for 15 minutes at 4°C in a sigma centrifuge (model GK10). Following centrifugation the reaction mixture was separated into 3 layers representing RNA solution (clear aqueous phase), proteins (white phase) and DNA (pink phase) respectively. The clear aqueous phase was transferred to a sterile epindorph tube and 500µl of isopropanol (2-propan-1-ol) per 1ml of trizol reagent was added. The mixture was mixed by inverting the tubes gently several times and left to incubate at room temperature for 10 minutes. The reaction tubes were re-centrifuged at 12, 000 *g* for 10minutes at 4°C. The supernatant was removed using a pipette and the pellet re- suspended in 1ml of 75% ice cold ethanol to wash. The reaction mixture was vortexed followed by centrifugation at 7,500 g for 5 minutes at 4°C. This washing step was repeated once. The supernatant was removed and the tubes left to air dry for 5-10 minutes. The RNA pellet was then re-suspended in 50µl of nuclease free water.

2.2.9.1 *DNase I* Treatment

A *DNase I* reaction mixture was prepared using the reagents and quantities listed in Table 16.

Reagent	Final Concentration	Working volume x1 (µl)
RNA sample	-	50
Reaction buffer	1x	5
Amplification Grade *DNaseI*	1U/ µl	5

Table 16. Preparation of one reaction mixture for *DNase* I treatment.

DNase I was used to digest DNA present in RNA samples into oligo and mononucleotides prior to cDNA synthesis. The reaction mixture was left to incubate at room temperature for 15 minutes. *DNase* is then inactivated by addition of 5µl of Stop *DNase* I (50mM EDTA) solution and mixed by brief centrifugation followed by a 10 minute incubation on a 70°C heating block. The reaction tubes were then cooled in ice.

RNA purification

Total RNA samples were extracted and RNA was purified using the Absolute Total RNA & mRNA Purification Kit (Agilent technologies, Stratagene Cat # 400806). 1.75µl of β-ME was added to total RNA samples. 250µl of lysis buffer and 250µl of 70% ethanol was added to each reaction mixture and mixed by centrifugation 12,000 x *g*. The reaction mixture was transferred to an RNA binding spin cup and seated in a 2ml receptacle tube. The reaction mixture was mixed by centrifugation for 1 min. The flow through was discarded and 500µl of 1x low salt wash buffer added to the spin cup. The tube was re-centrifuged for 1 min and the flow through discarded. The addition of wash buffer followed by centrifugation and removal of flow through was repeated once with 500µl and again 300µl of wash buffer. The reaction mixture was re-centrifuged for 2 minutes. The spin cup was transferred to a sterile 1.5ml micro-centrifuge tube and 50µl of elution buffer added. The reaction mixture was incubated at room temperature for 2 min then re- centrifuged. The elution, incubation and centrifugation step was repeated once. Purified RNA samples were placed in ice and prepared for immediate cDNA synthesis.

2.2.10 cDNA synthesis for Q-PCR

cDNA was prepared from purified total RNA samples isolated from virus infected HepG2, Mcf10a and 53BP1-/- cell lines.

Quantification of RNA samples were carried out using the Nanodrop spectrophotometer. The conditions for the PCR were amplified prior to the experiment taking place. The optimised input of RNA template was 125ng in 10µl of RNA. All reverse transcription reactions were performed on ice each RNA sample using the reagents and quantities listed in Table 17.

Reagents	1 X Working volume (µl)
ddH_2O	3.2
10X RT buffer	2
10X RT Random Primers	2
25X dNTP mix (100mM)	0.8
MultiScribe™, Reverse *Transcriptase*, 50 U/µl	1
RNase inhibitor	1

Table 17. General reagents used for cDNA synthesis of total RNA for QPCR reactions.

10µl of RNA sample was added to each reverse transcription reaction and briefly mixed by centrifugation. The reaction mixtures were transferred to the thermal cycler and reverse transcription performed using the parameters listed in Table 18.

Step	Temperature (°C)	Time (min)
Primer extension	25	10
cDNA synthesis	37	120
Reaction termination	85	5
Pause	4	-

Table 18. PCR parameters used for cDNA synthesis using the MultiScribe reaction kit.

2.2.10.1 Q-PCR for gene expression analysis

A real time PCR reaction master mix was prepared on ice using the reagents and quantities listed in table 19. The reaction mixtures were then alliquoted into a 96 well plate and 2µl of cDNA was added to each reaction master mix. The amount of DNA required for gene expression analysis of virus-inserted genes was 125ng of cDNA. The reaction plates were sealed with a MicroAmp® 96 optical adhesive film to prevent evaporation and loss of samples during PCR reactions.

Reagents	Working volume (µl)
ddH_2O	7
2X TaqMan Universal PCR Master Mix	10
20X TaqMan gene expression assay	1

Table 19. Reagents used for preparation of TaqMan PCR mastermix for amplifications

The reaction mixtures were transferred to a 7900HT real time PCR thermal cycler (Applied Biosystems). PCR amplifications were run in the absolute quantification blank template format. The parameters for all amplification reactions are listed in Table 20.

Step	Temperature (°C)	Time	No. Cycles
…	50	2 minutes	1 x
Denaturation	95	10 minutes	…
Denaturation	95	15 seconds	40 x
Annealing	60	1 minute	
Extension	72	90 seconds	

Table 20. PCR parameters required for Q-PCR.

Validation experiments for PCR efficiency and optimal template concentration required were calculated quantitatively. Raw data for each reaction plate consisted of CT values. CT values were manually transferred from the thermal cycler to a CD for data analysis. All reactions were performed in quadruplets and the reactions repeated on two occasions. All genes were normalised using the house keeping gene (18sRNA) and normal un- infected samples. The relative expression level of each gene was manually calculated from CT values using the delta delta CT (ΔΔCT) method.

1. The average CT for each gene was subtracted from the average housekeeping CT value to produce a ΔCT value.

2. ΔCT values from each sample was subtracted from the reference sample to yield a ΔΔCT value (ΔΔCT = ΔCTsample – ΔCTnormal liver).
3. Relative gene expression values $2^{(-\log \text{fold value})}$ were calculated using the following equation - $2^{-\Delta\Delta CT}$.

Statistical analysis including 95% confidence intervals, standard error of the mean (SEM) and student T testing was performed on CT values to validate gene expression data between normal and infected samples.

2.2.11 Microarray

RNA was extracted from cell monolayers, DNase treated and purified. Microarrays are only performed using good quality RNA. All RNA was assessed for quantity and purity using the Nanodrop and for integrity on the BioAnylzer. Concentration of RNA was measured using the Nanodrop. RNA should ideally have a 260/280 ratio of 1.9 to 2.1. Two microarray slides were done per experiment to reduce any errors.

2.2.11.1 cDNA synthesis from RNA

cDNA sysntheis was performed using the superscript III enzyme kit (Invitrogen).
In a sterile epindorph tube the RNA-RT Primer Mix (1.0 pmole/µl) was prepared by the addition of 2µg of RNA in 5µl being added to 1µl of the relevant RT primer (Cy3 or Cy5) as indicated in table 21.

CH1=Cy3 label (532)		CH2=Cy5 label (635)		
Sample	**~ RNA**	**Sample**	**~ RNA**	**Slide barcode**
Empty vector (1)	2ug/5ul	NC	2ug/5ul	19710929
MLV(1)	2ug/5ul	NC	2ug/5ul	19710927
EIAV(1)	2ug/5 ul	NC	2ug/5ul	19710928
NC	2ug/5ul	Empty vector (2)	2ug/5ul	19710930
NC	2ug/5ul	MLV(2)	2ug/5ul	19710931
NC	2ug/5ul	EIAV(2)	2ug/5ul	19710932
Empty vector (3)	2ug/5ul	NC	2ug/5ul	19710933
MLV(3)	2ug/5ul	NC	2ug/5ul	19710934
EIAV(3)	2ug/5ul	NC	2ug/5ul	19710935

Table 21. Samples used for the reaction master mix of cDNA synthesis.

The solution was mixed, briefly centrifuged and heated on a pre-set 80°C PCR machine for 5 minutes to denature RNA secondary structures. Tubes were immediately placed on ice for 3 minutes, quickly spun down and replaced on ice.

A Reaction Master Mix was prepared in sterile epindorph tubes using the reagents and quantities listed in table 22. The reaction master mix was formulated to a final volume dependent on the number of cDNA synthesis set up simultaneously. The specificity of labelling is determined for each channel by the primers used. Thus the master mix is the same for each channel, therefore 2 reaction amounts are for the two channel labelling of RNA samples that will be hybridized onto one slide

Reagents	Working Volumes X2 (µl)
5X SuperScript III First strand buffer	4
0.1 M DTT	2
SuperaseIn	1
dNTP mix	1
SuperScript Enzyme	1

Table 22. Reagents used for reaction master mix for cDNA synthesis.

The reaction master mix was gently mixed and briefly centrifuged. 4.5µl of the reaction master mix was added to the 6µl of RNA-RT primer mix to give a total volume of 10.5µl.

Tubes were gently mixed, briefly centrifuged and incubated at 42°C in a pre-set PCR machine for 3 hours.

2.2.11.2 Degradation of RNA

RT reaction tubes were removed from the PCR machine after 3 hours and the reactions stopped by the addition of 1µl of 1M NaOH/ 100mM EDTA solution. The tubes were then incubated at 65°C for 10 minutes in the PCR machine to denature the cDNA/ RNA hybrids and degrade the template RNA. The reaction was then neutralized by adding 1.2µl of 2M Tris-HCL, pH 7.5 for a final volume of 12.7µl.

2.2.11.3 Pre-slide scanning and Wash

Op Human Ready Array (microarrays Inc, USA) slides were handled with clean powder free gloved hands. All slides were pre-scanned before to ensure their print quality using the InnoScan (700A scanner) and Mapic software (version 3.1.0, Innoqsys, France).

2.2.11.4 Pre-hybridisation of slides

These slides were then pre-washed prior to use and scanned again to ensure that they were clean and properly blocked.

Pre-hybridisation solution was prepared in a coplin jar using the reagents and quantities in table…

Reagents	Working volume x1
BSA solution (100mg/ml)	5ml
10% SDS	500µl
20x SSC	8.75ml
MilliQ water	35.75ml
Total	50ml

Table 23. Reagents used to make pre-hybridisation solution for Microarray.

The coplin jar was then placed in a 65°C hybridisation oven for 30 minutes. Array slides were placed in the solution in the coplin jar and placed back in the 65°C oven for 20 minutes.

Slides were removed from the coplin jar and secured into a black staining rack. This was immediately immersed in a washing trough filled with MilliQ water and rinsed for 1 minute. The black staining rack was then immersed into a washing trough filled with isopropanol and rinse for 1 minute. The slides were then completely dried using the slide centrifuge.

Slides were then scanned again to check there are no smears / streaks from pre-hybridisation and kept clean and dry by placing them in a slide holder container until ready for use.

2.2.11.5 Preparation of Slidebooster

3 minutes before the end of the RT reaction the SlideBooster was prepared. 70% ethanol was used to clean the SlideBooster, making sure no liquid is left next to the bar. 500µl of hydration solution was added to each of the two hydration wells and 15µl of coupling solution was added onto each of the three transducer connections. The slide was placed over the tranducers and checked for any bubbles. LifterSlip was then placed over the slide. 60µl of coupling solution was then placed into the thumb hole at the base of the slide so that it makes contact with the solutions under the slide. The chamber protocol was then set to 55°C for 16 hours. The hybridisation chamber is then closed and left to heat up to 55°C.

2.2.11.6 cDNA hybridisation

2X SDS-based hybridisation buffer was thawed and resuspended by heating to 70°C for 10 minutes and then vortexed to make sure that components were resuspended evenly. For each array using a 22x60 LifterSlip, the following cDNA Hybridisation Mix as shown in Table 24 was used.

Reagents	X1 working Volume (µl)
cDNA synthesis reaction 1 (Cy3)	12.7
cDNA synthesis reaction 1 (Cy5)	12.7
LNA dT blocker	2
2X SDS-based hybridisation buffer	37
Nuclease free water	9.6
TOTAL	74

Table 24. Reagents used for cDNA hybridisation for Microarray.

After addition of all components the cDNA Hybridisation mix was vortexed, briefly spun down and incubated at 80°C for 10 minutes to denature secondary structures and then cooled to 60°C.

When the slide in the slide booster is warmed to 55°C, the cDNA hybridisation mix is pipetted to the microarray slide and hybridized overnight (16 hours) (mix power:27, pulse power: 3/7).

2.2.11.7 Post cDNA hybridisation wash

The slide was removed from the slide booster and quickly placed into a pre warmed trough with pre warmed (55°C) 2x SSC, 0.2% SDS wash buffer. The LifterSlip was carefully floated off the slide in the wash solution in the trough. The slide was then inserted into the submerged rack. After the following washes took place:

Wash 1: Slide was washed for 10 minutes in the pre warmed 2x SSC, 0.2% SDS wash buffer at an orbital rotation (150rpm) in the incubator at 55°C.

Wash 2: Side was washed for 10 minutes in 2x SSC wash buffer at an orbital rotation (150rpm) at room temperature.

Wash 3: Side was washed for 10 minutes in 0.2x SSC wash buffer at an orbital rotation (150rpm) at room temperature.

The slide is immediately dried using the slide centrifuge.

2.2.11.8 Hybridisation of the fluorescently labelled 3DNA to the Microarray Slide

The 3DNA capture reagents (Cy3 and Cy5) were pre-prepared for the 3DNA hybridisation by firstly placing both vials in a light proof container in the dark as these capture reagents contain fluorophores thus, light sensitive. These vials were then left at room temperature for 20 minutes. After which they were incubated at 55°C for 10 minutes in the heat block (covering the block with foil). The capture reagents were then vortexed briefly and spun down. The tubes were checked for any aggregates, as aggregates will prevent the array from labelling properly.

2X SDS-based hybridisation buffer was thawed and re suspended by heating to 70°C for 10 minutes and then vortexed to make sure that components were re suspended evenly.

For each array a 3DNA hybridisation mix relevant for use on 22x60 LifterSlip, was made according to Table 25.

Reagents	X1 working Volume (µl)
3DNA capture reagent- Cy3	2.5
3DNA capture reagent- Cy5	2.5
2X SDS-based hybridisation buffer	37
Nuclease free water	32
TOTAL	74

Table 25. Reagents used for 3DNA hybridisation mix for 1 slide for Microarray.

After addition of all components the 3DNA Hybridisation mix was vortexed, briefly spun down and incubated at 80°C for 10 minutes and then cooled to 55°C.
During these 10 minutes the array and LifterSlip was placed in the Slide Booster (with contact solution and correct hydration solution as before) and pre-warmed to 50°C. The 3DNA hybridisation mix is pipetted to the microarray slide and hybridized for 4 hours (mix power: 27, pulse power: 3/7).

2.2.11.9 Post 3DNA hybridisation wash

The slide was removed from the slide booster and quickly placed into a pre warmed trough with pre warmed (50°C) 2x SSC, 0.2% SDS wash buffer. The LifterSlip was carefully floated off the slide in the wash solution in the trough. The slide was then inserted into the submerged rack. After the following washes took place:
Wash 1: Slide was washed for 10 minutes in the pre warmed 2x SSC, 0.2% SDS wash buffer at an orbital rotation (150rpm) in the incubator at 55°C.
Wash 2: Side was washed for 10 minutes in 2x SSC wash buffer at an orbital rotation (150rpm) at room temperature.
Wash 3: Side was washed for 10 minutes in 0.2x SSC wash buffer at an orbital rotation (150rpm) at room temperature.
The slide is immediately dried using the slide centrifuge and placed in a lightproof slide holder.

2.2.11.10 Microarray image acquisition.

Microarray slides were scanned with Innoscan 700A microarray scanner/Mapix 3.1.0 software (Innopsys, France). Laser and PMT settings were manipulated to balance overall intensity between Cy3 and Cy5 channels and to avoid excess of saturated pixels in the spots.

2.2.11.11 Microarray image analysis.

Microarrays scan .tiff images were imported into and analysed by BlueFuse for Microarrays 3.2 (4484) (BlueGnome, UK). Microarray spots grid were generated from .gal file (supplied by microarrays manufacturer), and manually adjusted to the spot positions on the images. Spots were segmented and their intensities were calculated according to the software algorithms. Calculated spot intensities then were normalised by "Global Lowess" function, and spots replicates normalised intensities averaged by "fused" function.

2.2.11.12 Microarray data analysis.

Output files with both normalised spots intensities and experiment/control log2 rations were imported to the web implementations of Cyber-T (Kayala and Baldi, 2012) and Rank-Product (Laing and Smith, 2010) software to find differentially expressed genes. The cut-off for differentially expressed genes was more than 1.5 fold change and $P<0.05$.

2.2.12 mFISH

In the current project M-FISH has been performed using human paints prepared from flow-sorted human chromosomes. The 'human paint mix' has been obtained from whole chromosome paints labelled with different combinations of four fluorochromes (Cy5, Cy3.5, Cy3 and FITC) and one hapten (Biotin). In total, 24 unique combinations have been obtained, and no more than 3 fluorochromes were used for each combination.

2.2.12.1 Slide preparation and metaphase spreads

Cells were fixed with freshly prepared Carnoy's fixative (3:1 methanol/glacial acid). This metaphase cell suspension were then dropped onto clean microscope slides (sonicated at 1% decon and stored in 96% ethanol) using the water bath at 50ºC. Slides were checked under the phase contrast microscope to ensure both the cell concentration and the metaphase spreads are optimal.

2.2.12.2 Slide pre-treatment prior to hybridization

Slides were incubated in a coplin jar of 50% acetic acid (in water), at room temperature for 3 minutes and then incubated in a jar of 100% methanol, at room temperature for 3 minutes and air dried. After the slides were dry they were incubated in a coplin jar of 0.01 HCL at room temperature for 3 minutes. After which slides were thoroughly rinsed 3 times in 2X SSC for 5 minutes each and air dried. Slides were then baked at 65 ºC for an hour.

2.2.12.3 Hybridisation

Slides were denatured in a coplin jar containing 70% formamide (pre-warmed in a 72ºC waterbath) for 1 minute 30 seconds and immediately quenched in 70% ice cold ethanol for 1 minute. Slides were then dehydrated through an ethanol series (70%. 70%, 90%, 90% and 100%) for a minute each and air dried. Human M-FISH paint was vortexed, pulse microfuged and denatured at 65 ºC for 10 minutes. 10µl of human M-FISH paint probe was pipetted onto the slide and covered with a clean 22X22 coverslip and sealed with fixogum. Slides were then incubated over night at 37 ºC incubator in a humid chamber.

2.2.12.4 Post-hybridisation wash and detection

Fixogum was removed from slides and coverslips soaked off in 2X SSC at room temperature. Slides were then incubated at 50% formamide/ 2X SCC at 42ºC for 5 minutes. This was repeated again in different coplin jar containing 50% formamide/ 2X

SCC. Slides were then washed in pre-warmed 2X SSC twice at 42ºC. slides were drained and 150µl of anti-biotin Cy5.5 (1:200 dilution in 4X SSCT) was added to each slide and allowed to incubate at 37 ºC for 15-20 minutes. Slides were then washed thrice in 4X SSCT, 5 minutes each at 42ºC. Each slide was drained and approximately 15-20µl of DAPI counterstain was added, overlayed with a 22X50 mm coverslip and finally, sealed with nail varnish. Slides were then ready for imaging.

2.2.12.5 mFISH Imaging

Multicolour FISH'd metaphase images are captured and processed using the SmartCapture® (Digital Scientific, UK) digital imaging system that consists of a epifluorescent Zeiss microscope (Axioplan2 Imaging or AxioImager DI) fitted with a cooled charge coupled device (CCD) camera (Hamamatsu Orca ER), equipped with narrow band pass filters for Cy5.5, Cy5, Cy3, Cy3.5, FITC (fluorescein isothiocyanate) and DAPI (4',6-diamidino-2-phenylindole) fluorescence and an iMAC computer (Apple). Metaphase images are then karyotyped using the Digital Scientific, UK, Smattype software.

In the current study 40 images from each cell line was imaged, karyotyped and analysed.

3.1 Background

Retrovirus gene therapy vectors can deliver therapeutic genes to mammalian cells in a permanent manner by integrating their genome into host chromosomes and therefore provide the potential for long-term therapeutic gene expression. However, this is contrasted by their ability to cause mutagenesis upon integration. This insertion appears to be semi-random by integration into actively transcribed regions of the genome with target site selectivity near promoter regions. Already known is that these insertions can result in up-regulation or down-regulation of neighbouring gene expression by provirus LTR promoters or enhancers or by splicing of virus sequences together with host genes. Where the host genes are oncogenes or tumour suppressor genes IM can lead to oncogenesis.

Lentiviruses (LV) are a subgroup of retroviruses that have similar characteristics to their retrovirus counterparts, however, their integration target site selection appears to be the gene transcription unit rather than promoter regions. These vectors have been designed with SIN properties and therefore lack promoter sequences that switch on host gene expression unless internal promoter read-through takes place. Little is known, however, about their potential for IM.

The observation of HCC in mice treated by LV vectors described by Dr Themis's group in 2005 and more recently in 2013 (Appendix 1) highlights the potential for genotoxicity by these vectors and how IS profiles differ **between** primate and non primate vectors. Microarray characterization of these HCCs coupled with LAM PCR revealed gene ontologies (GO's) of genes with insertions involved in oxidative reduction and DNA damage and repair and several were known oncogenes involved in cancer and particularly HCC. Because, cancer development usually requires multiple genetic events beginning with cell immortalisation then progression to malignancy, the original hypothesis that IM caused oncogenesis alone is difficult to reconcile. The work of this thesis was, therefore, directed at investigating whether virus infection and integration could cause genotoxicity by an alternative route(s) than IM. One important route based on the microarray data (Nowrouzi *et al*., 2012) is the possibility that virus infection is associated with genome instability and this could be also contributing to the cancer phenotype identified. This hypothesis is supported by a previously published

report by the Themis group (2003) that showed high level infection of cells *in vitro* leads to the *hprt* –ve phenotype coupled to instability at this locus (Themis *et al*., 2003). To begin this work, mouse liver tissues were investigated for genome instability using the method of Comparative Genome Hybridization (CGH) in collaboration with Dr Nathalie Conte of the Wellcome Trust. CGH enables chromosome amplification and deletions to be examined using mouse chromosome specific probes. Hence CGH is a molecular cytogenetic method for the analysis of copy number variations (CNV) (gains or losses) in the DNA content of tumour cells compared with normal livers. In this process, kidney genomic DNA was used to prove normal livers had similar CNV.

3.2 Investigation of mouse tumour DNA compared to non-tumour liver using CGH

For CGH analysis, tumours that developed from mice treated with EIAV and HIV vectors and a spontaneous tumour were used. These were compared with normal livers and kidney samples for each respective liver tumour to control for normal liver CNV.

EIAV induced liver tumours vs. normal liver (n=6 each)

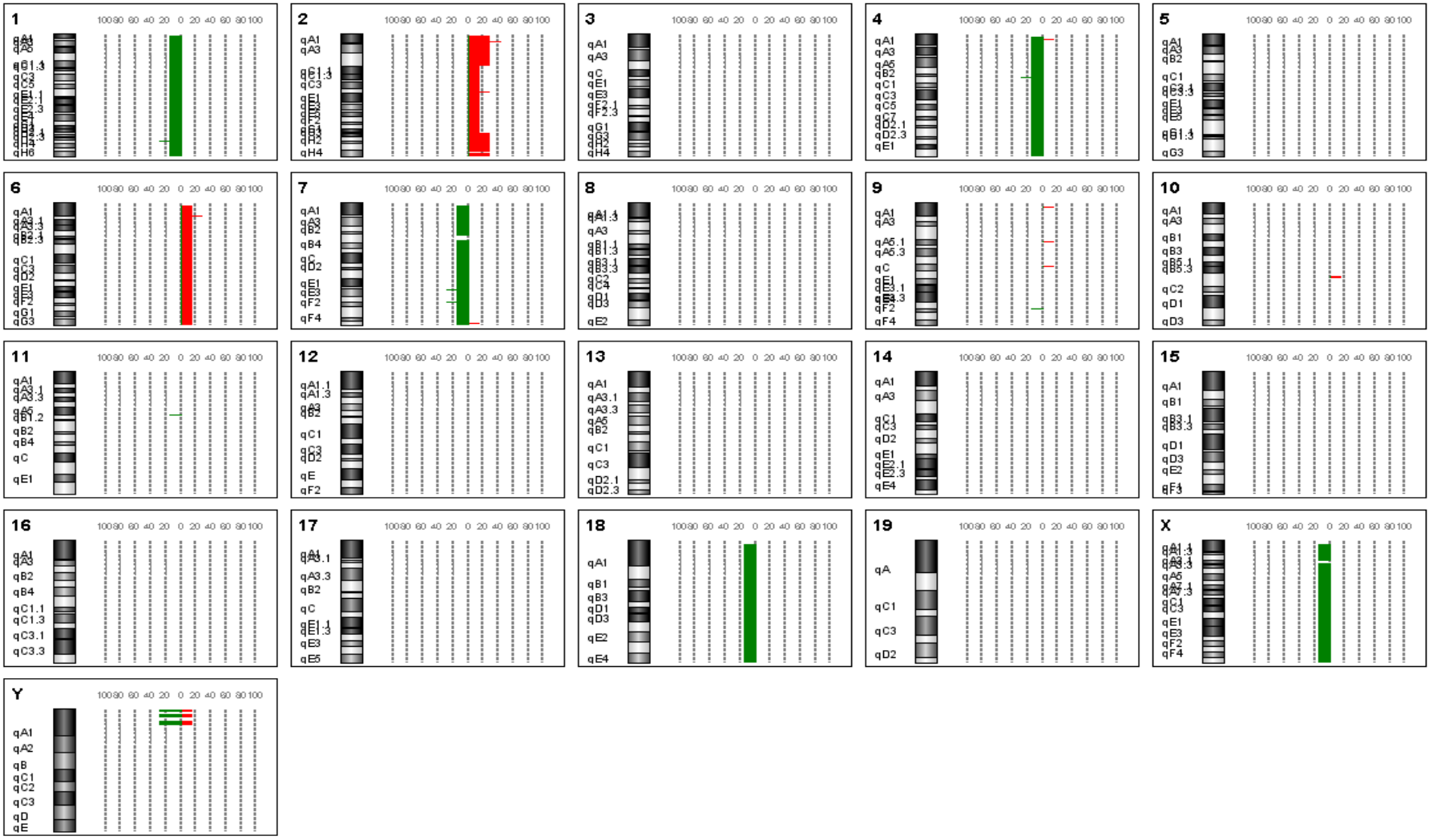

HIV induced liver tumours vs. Normal liver (n=3 each)

Spontaneous tumour vs. Kidney

Figure 7. CGH Ideograms representing pooled CNV of tumours.

Ideograms are shown of sample DNAs derived from mice treated with EIAV vector vs. respective normals (n=6), tumours that derived from animals treated with the HIV vector (n=3) and a spontaneous liver tumour. DNA from respective kidneys of each mouse was compared with normal livers first (data not shown) before comparisons between normal livers and tumours to ensure non-tumour liver DNA contained normal CNV to the kidney. The spontaneous liver tumour (without infection) was compared directly to the kidney of this animal. Chromosomes 1-19, X and Y are shown. CNV are represented as: Green bars = deletions; red bars = amplification.

The CGH shown in figure 7 represents CNV between mouse tumour DNAs compared with non-tumour livers infected with the EIAV vector. In these samples CNV representing deletions in chromosome 1, 4, 7, 18 and whole loss of chromosome X were observed. Amplifications were observed in chromosomes 2 and 6.

In the 3 HIV vector associated tumours small regions of amplifications and deletions were found. These were observed in commonly known regions that are believed unstable and found in independent CGH screens on several murine cell types at the Wellcome Trust (personal communication with Dr Nathalie Conte). Hence, these were believed unlikely to be caused by the HIV vector.

For the spontaneous tumour (not carrying a virus insertion) CNV were detected only in the Y chromosome which is also known to be unstable and common in spontaneous tumours (personal communication with Dr Nathalie Conte).

Because CNV were identified mainly in EIAV derived tumours more detailed examination of the regions carrying these CNV was made.

EIAV Tumour 2- Liver tumour vs. Normal liver and normal kidney- Chromosome 2

4559357- *Hnf4α*

147876573- *Foxa2*

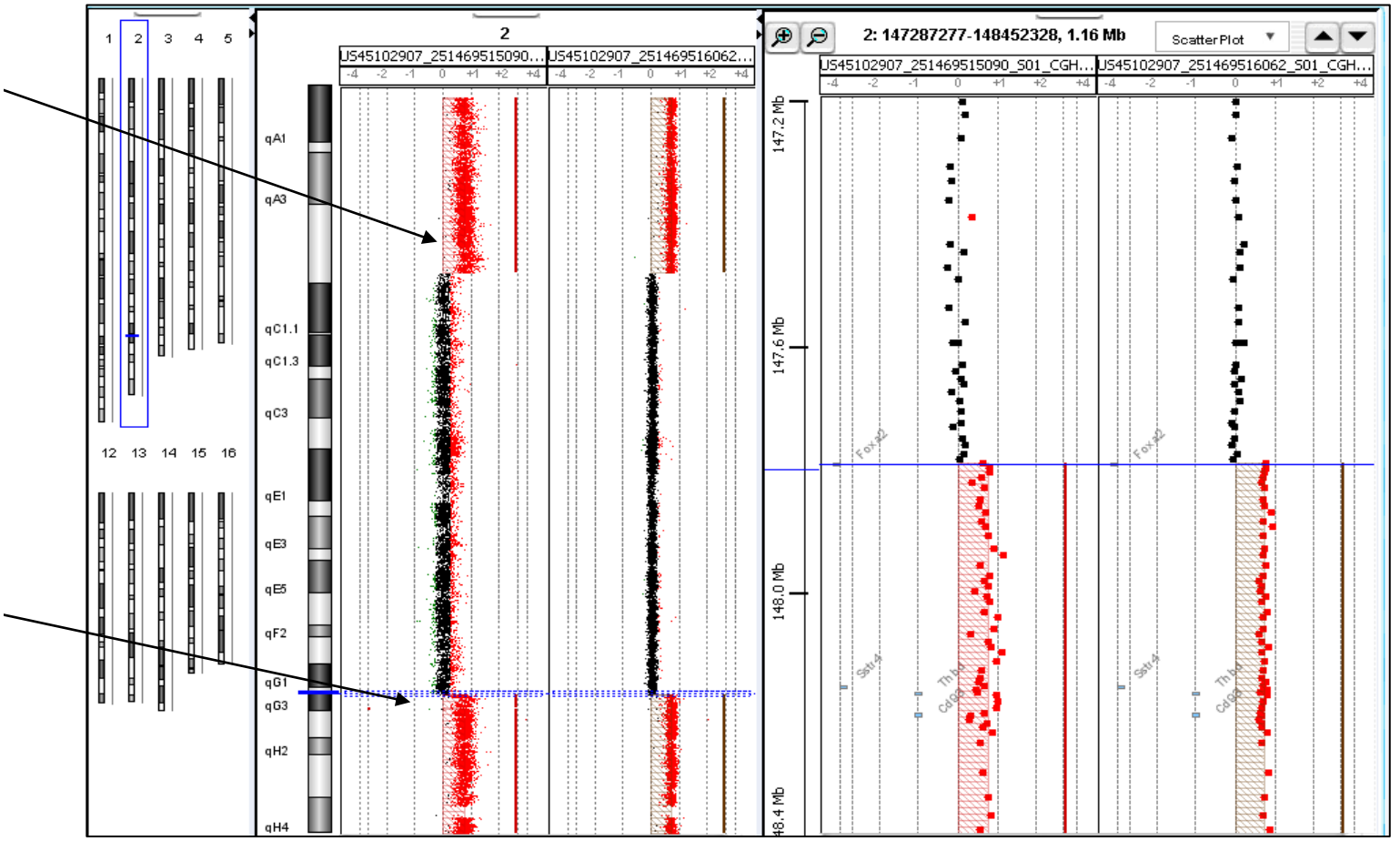

EIAV Tumour 2- Liver tumour vs. Normal liver and normal kidney- Chromosome 6

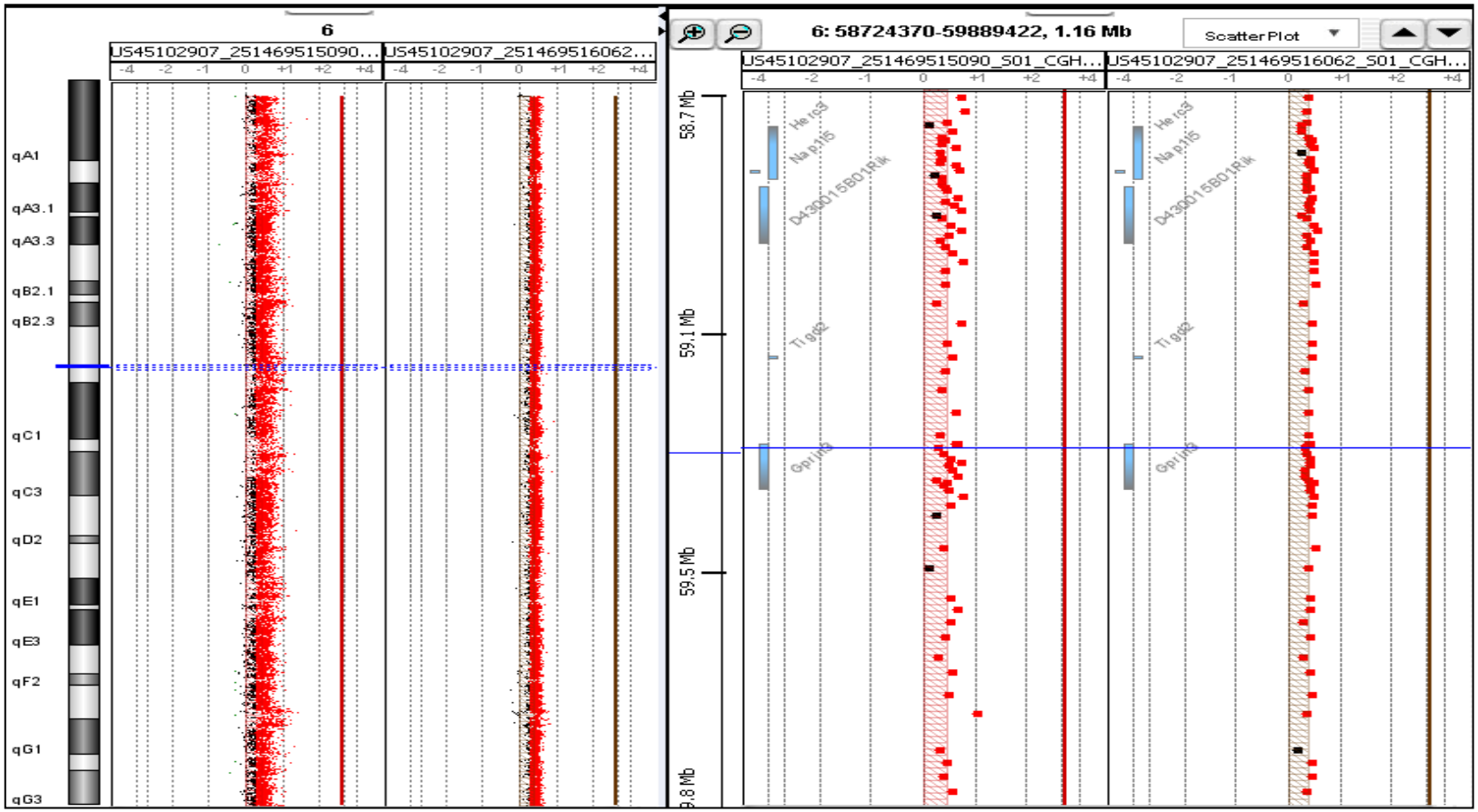

EIAV Tumour 2- Liver tumour vs. Normal liver and normal kidney- Monosomy X

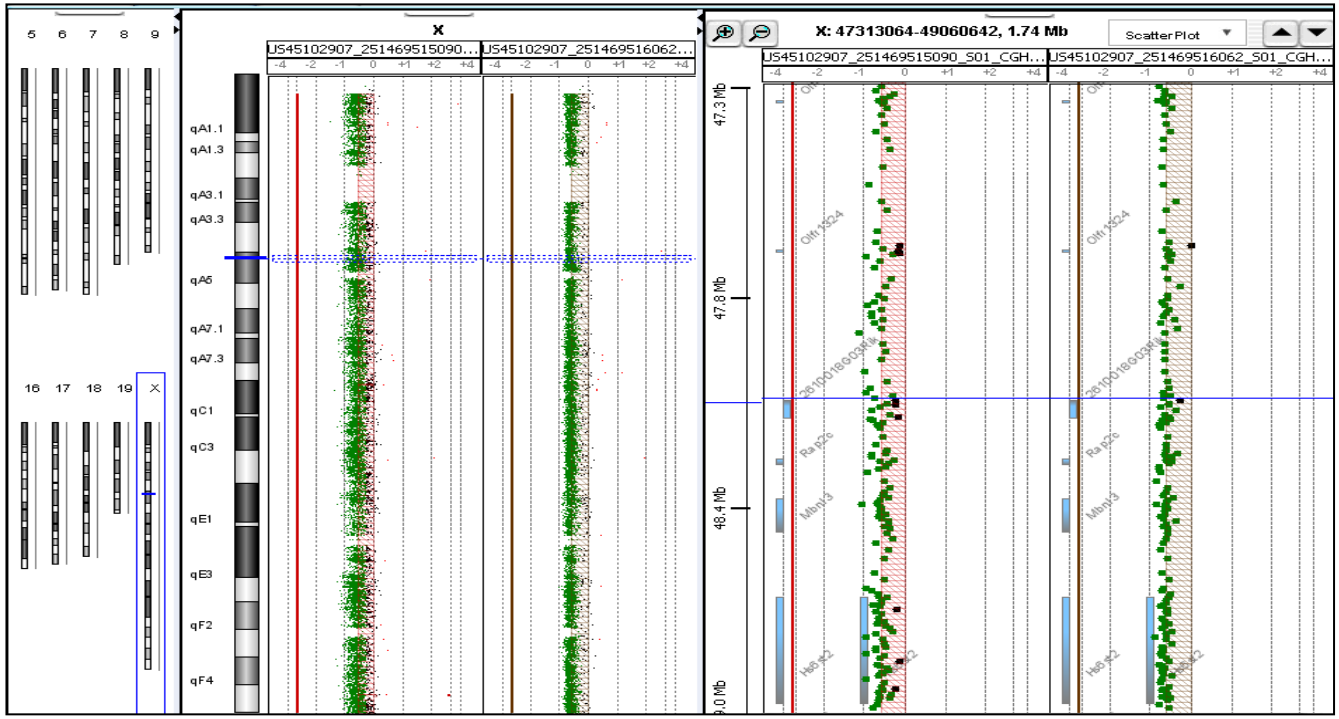

Figure 8. CGH Ideograms representing CNV in EIAV Tumour 2. The ideograms show the regions carrying CNV. This information was used for BLAST searches using NCBI (http://blast.ncbi.nlm.nih.gov/Blast.cgi) to identify the genes in the regions of CNV. In chromosome 2 a specific region between 4559357 and 147876573 was amplified. Also complete amplification was observed in, chromosome 6 and entire loss of the X chromosome.

EIAV Tumour 1- Liver tumour vs. kidney- Chromosome 2

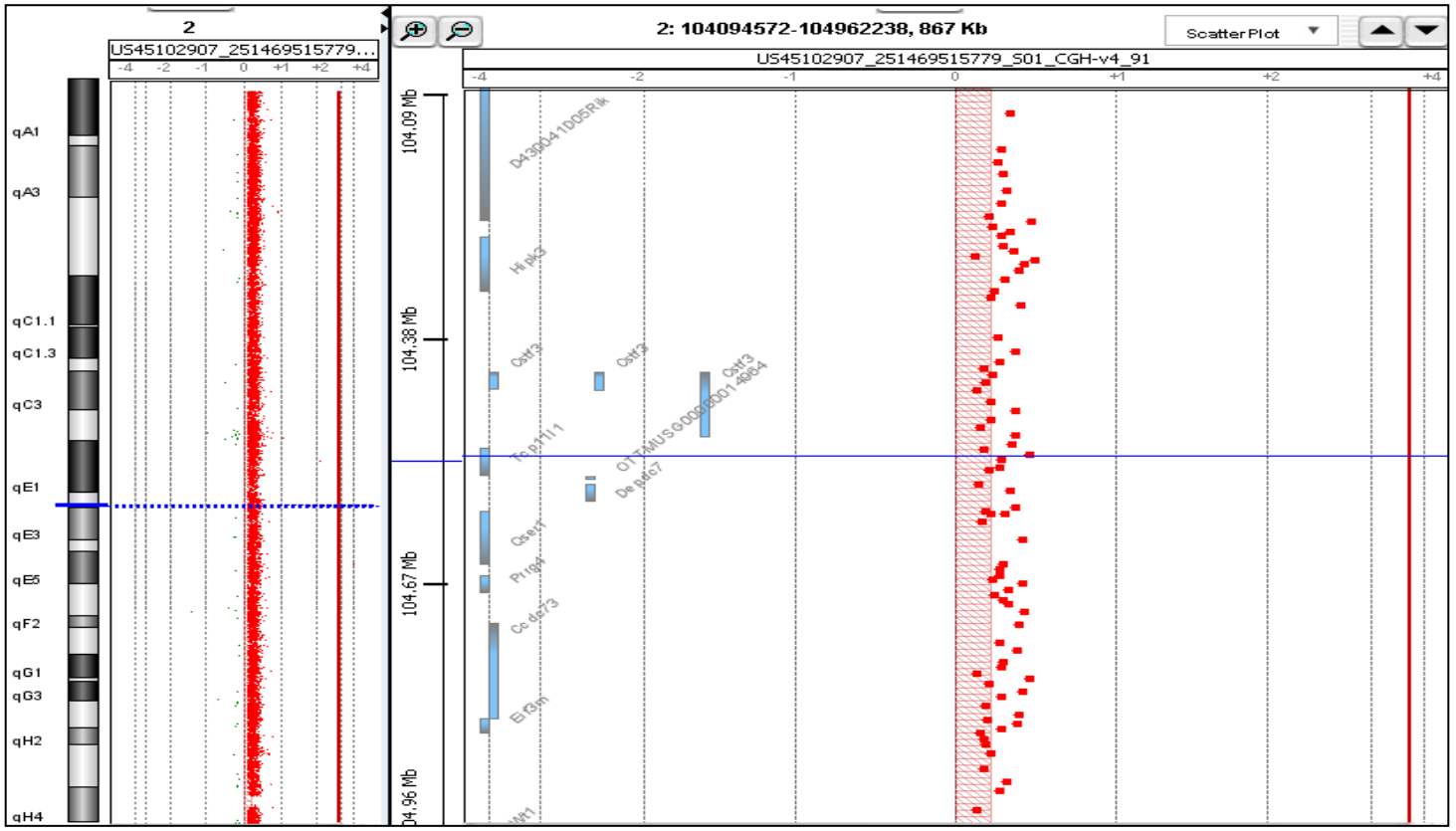

Figure 9. CGH Ideogram representing amplification of part of chromosome 2 in EIAV derived Tumour 1.

CNV are shown with the BLAST search (http://blast.ncbi.nlm.nih.gov/Blast.cgi) for the genes contained in the region of CNV.

Of the 6 EIAV derived tumours analysed tumour 1 showed amplification of the whole of chromosome 2. Common to Tumour 1 and Tumour 2 was amplification of a large region of this chromosome.

Region of amplification of chromosome 2 common to EIAV derived Tumour 1 and 2

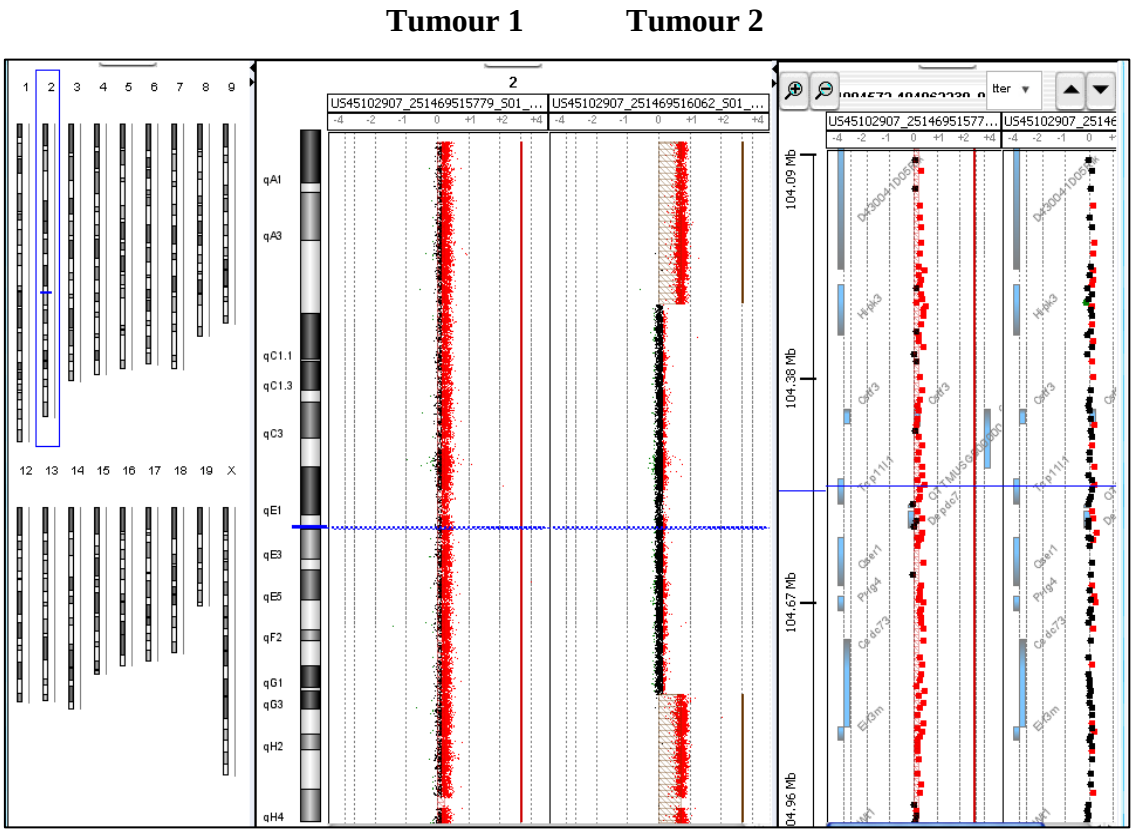

Figure 10. Ideogram comparing Tumours 1 and 2 CNV in chromosome 2
The figure shows the region of CNV found in both tumours and genes contained in this region after BLAST search.

The region of chromosome 2 shown for these tumours was investigated for genes which may have been disrupted by the amplification and possibly important to HCC. In this breakpoint region *Hnf4α* and *Foxa2* were identified after BLAST (Fig 10). These genes were then investigated further for differential expression in the microarray of these tumours.

For *Hnf4α,* microarray data showed a 1.5 ($p>0.05$) fold decrease in expression of this gene, whereas no change in expression was identified for the *Foxa2* gene.

Interestingly, in Tumour 1 microarray showed *Tgm2* expression increased by 4.5 fold ($p<0.05$). *Tgm2* is in the same region as the breakpoint region found in Tumour 2, and this gene which codes for a transglutaminase has been shown to be differentially expressed in HCC (Sun et al., 2008). To examine more accurately the changes in gene expression observed by microarray, RT-PCR using primer/probes for each gene was performed.

Table 26. Real time PCR relative change in gene expression of *Hnf4α, Hnf1α and Foxa2* in Tumour 1 and 2.

Gene name	*Relative change in gene expression (log2)*	*Relative change in gene expression (log2)*
	Tumour 1 (+/-SD)	*Tumour 2 (+/-SD)*
Foxa2	*1.57 (0.41)*	*-0.75 (0.08)*
Hnf1α	*-0.55 (0.15)*	*-0.20 (0.05)*
Hnf4α	*-0.62 (0.04)*	*-0.18 (0.04)*

RT PCR was used to measure levels of *Hnf4α, Hnf1α and Foxa2* gene expression. These were decreased in both Tumour 1 and 2 except in Tumour 1 *Foxa2* gene expression was increased compared with normal liver tumour samples. All levels of expression are given as log 2 fold changes that were normalised to 18S RNA gene expression that was set at 1. SD= standard deviation.

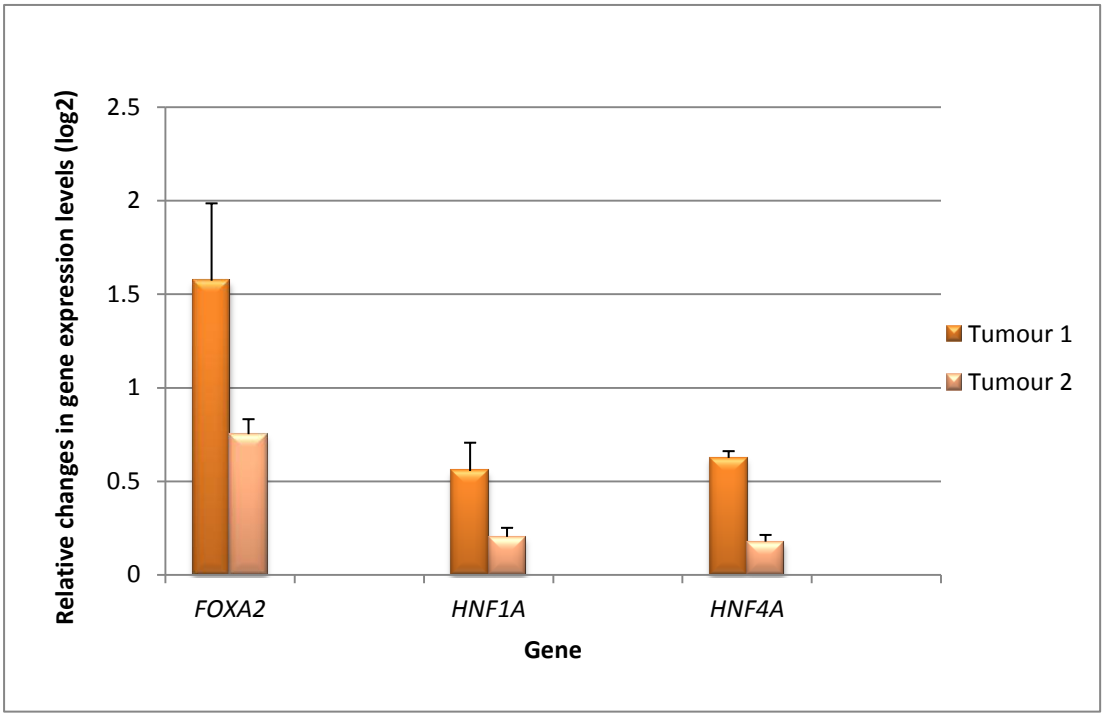

Figure 11. RT-PCR of *Hnf4α, Hnf1α and Foxa2* genes in Tumours 1 and Tumour 2.

RT-PCR was performed on mRNA isolated from Tumour 1 and 2. Gene expression (ΔΔCT) were calculated for each gene and compared to normal liver samples. Values were shown are those with changes that were statistically significant. All experiments were performed in quadruplets and repeated on different occasions. The conditions for all amplification reactions were optimised and a validation efficiency test performed. 18sRNA expression was used to normalise gene expression. Statistical analysis using the Student T test at 95% confidence interval testing was performed on all Q-PCR data ($P<0.05$).

As shown in Table 26 and Figure 11 *Hnf4α* expression levels was reduced in Tumours 1 and 2 compared with normal livers for these tumours. *Hnf1α* was also reduced in both tumours. These genes are known to be repressed during liver oncogenesis and HCC. *Foxa2* had increased expression levels in RT-PCR of Tumour 1 and increased expression in Tumour 2.

To investigate the potential cause of oncogenesis in Tumour 2, *Hnf4α, Hnf1α and Foxa2* genes found by CGH and *Pah* and *Acvr2α* genes found with EIAV vector insertions and described by Themis *et al* 2013 (Nowrouzi *et al*., 2012) were investigated together for pathways common to these genes using the STRING

(http;//string-db.org/) database. This database identifies predicted protein interactions that include direct (physical) and indirect (functional) associations. Four of the five genes were found in related pathways (Fig 12). The *Pah* gene was found to be associated with *Hnf1a,* H*nf4a* and *Foxa2* which are all associated with HCC. *Foxa2*, *Hnf1a* and H*nf4a* are closely related transcription factors which are critical to the development and function of the mouse liver. *Acvr2a* and *Tgm2* were not found to be linked.

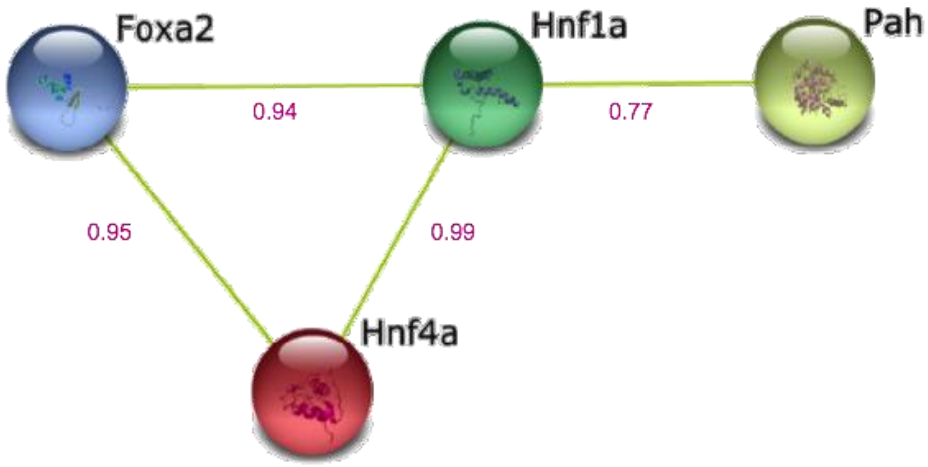

Figure 12. Analysis of the relationship between genes found by CGH and IM of tumour 2

Foxa2, Hnf1α, H*nf4α* and *Tgm2* identified using CGH of Tumour 2 and *Pah* and *Acvr2a* genes found with EIAV vector insertions were imputed into the STRING (http;//string-db.org/) database. The *Pah* gene was found to be associated with *Hnf1a,* H*nf4a*. No association was found for these genes with *Acvr2a* and *Tgm2*, however, all 6 genes are known to be associated with liver disease and specifically to HCC. Confidence levels are provided from the STRING database for gene interactions.

The results obtained by CGH suggest genome instability. However, because the tumours identified in the mice treated with EIAV were as a result of clonal evolution, the CNV observed could not be strictly assigned to being caused by the EIAV vector. The work carried out in this thesis, therefore, concerns the use of alternative assays to investigate genotoxicity independent of IM. The work investigates the possible

connection between retroviral infection and genome instability and the host innate response to infection in the form of epigenetic changes.

4.1 Investigation of vector associated genotoxicity in cells following *in vitro* delivery of RV and LV

Evidence of genome instability following RV infection has been provided by the laboratory of Frederick Bushman who showed that virus integration causes double strand breaks (DSB) (Bushman *et al*., 2001). To examine this process further, the relationship between DSB and mutagenesis was investigated here using *in-vitro* assays.
To begin this study, genome instability was measured following infection. This was initially performed to confirm the findings of Bushman *et al* (2001). To do this, different gene therapy vectors were applied to cell lines either capable or incapable of DNA damage repair pathways. Throughout this study Mcf10a cells, with an intact DNA repair pathway were used as an *in vitro* model cell line. This cell line has previously been used in genotoxic studies. It lacks the ability to grow as anchorage-independent and is one step away from being metastatic (Yang *et al*., 2006).

4.1.1 Cell infectibility

Before the investigation of genome instability could commence, the level of infection of cell lines required for this study was established. In addition to using Mcf10a cells that have active pathways to DNA damage repair (DDR), the Mrc5 cell line was included because it is also known to display normal DDR kinetics (Bourton *et al*., 2012). At5biva and Xp14br cells that have been shown previously to be repair deficient without intact pathways of DSB repair (Bourton *et al*., 2012) were also used to demonstrate DSB.

MCF10A

Un-Infected

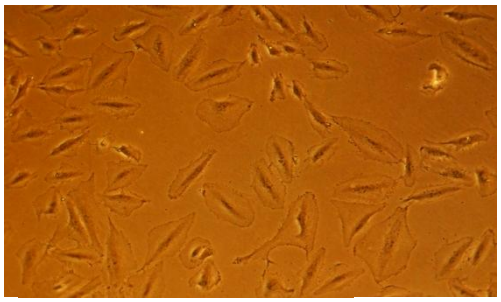

MLV- High MOI

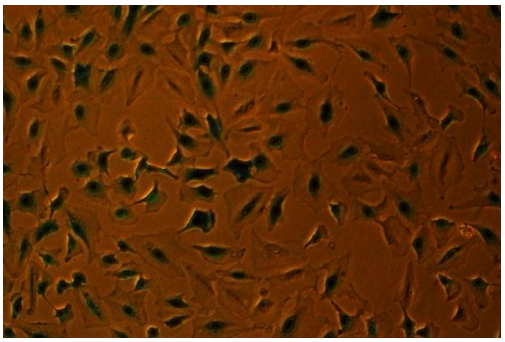

MLV- Low MOI

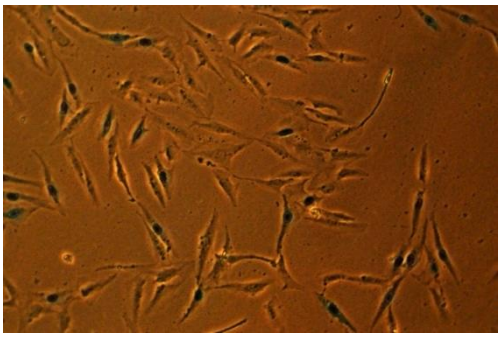

HIV- High MOI

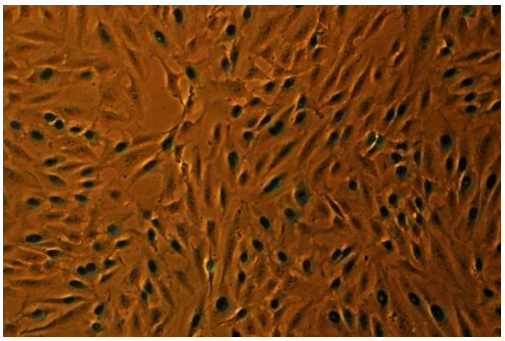

HIV- Low MOI

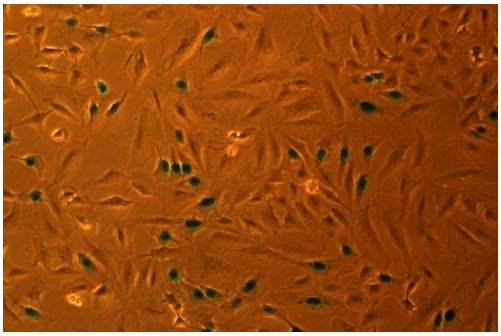

EIAV- High MOI

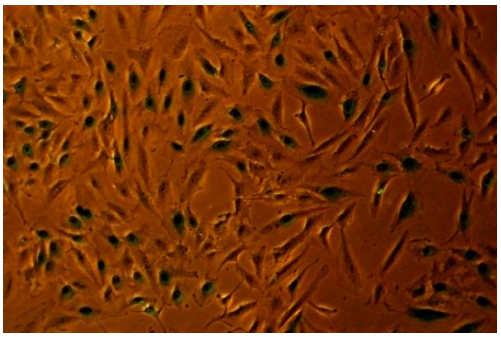

EIAV- Low MOI

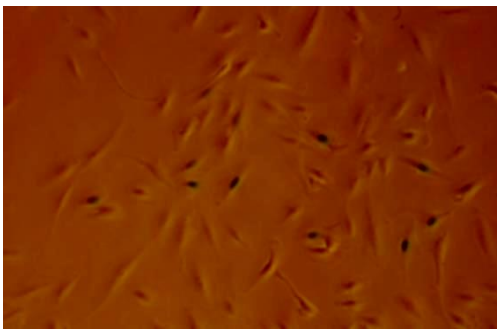

Figure 13. Mcf10a cells infected with RV and LV vectors. Infection was performed using MLV, HIV and EIAV at high and low MOI. Level of infection was measured using β-galactosidase staining of cells and counting the percentage of blue cells. Images were taken at X100 magnification using the Zeiss Axiovert 25 microscope.

MRC5

Un-Infected

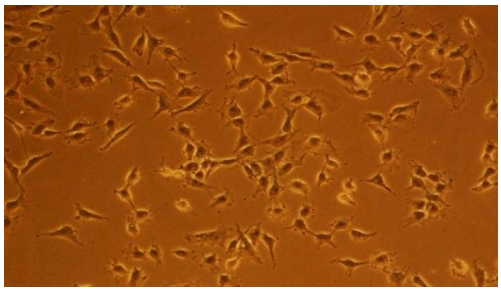

MLV- High MOI

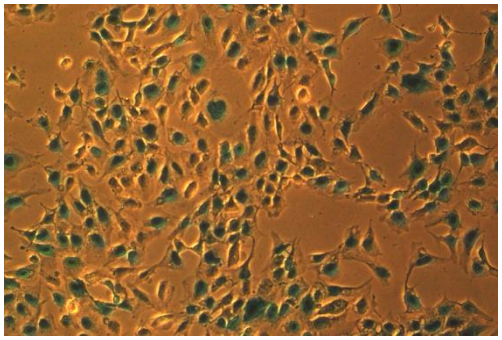

MLV- Low MOI

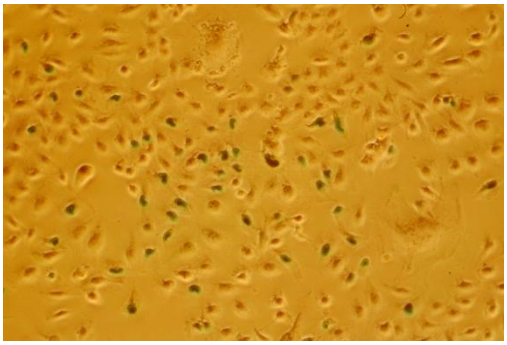

HIV- High MOI

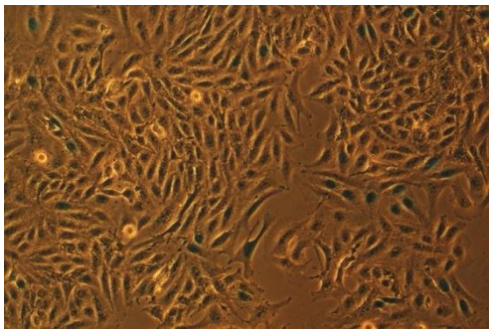

HIV- Low MOI

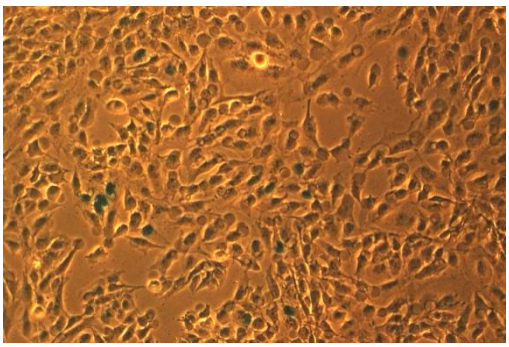

EIAV- High MOI

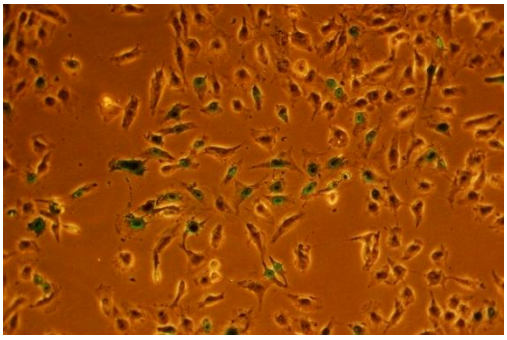

EIAV- Low MOI

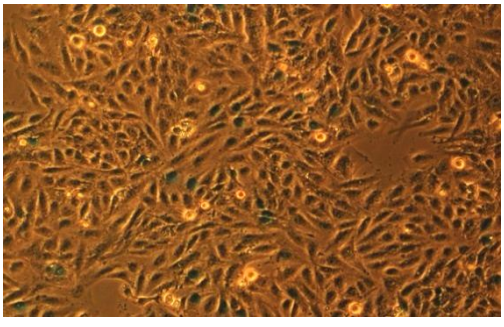

Figure 14. Mrc5 cells infected with RV and LV vectors. Infection was performed using MLV, HIV and EIAV at high and low MOI. Level of infection was measured using β-galactosidase staining of cells and counting the percentage of blue cells. Images were taken at X100 magnification using the Zeiss Axiovert 25 microscope.

AT5BIVA

Un-Infected

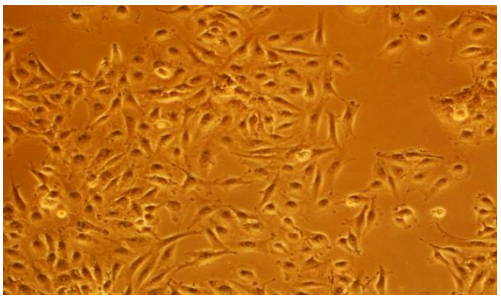

MLV- High MOI

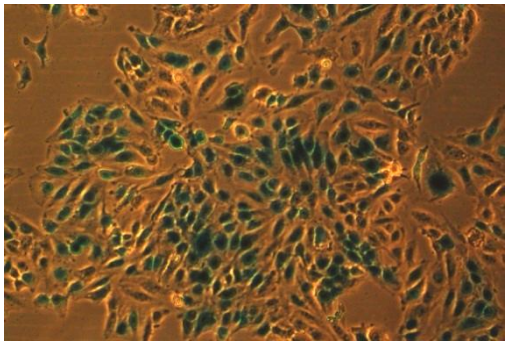

MLV- Low MOI

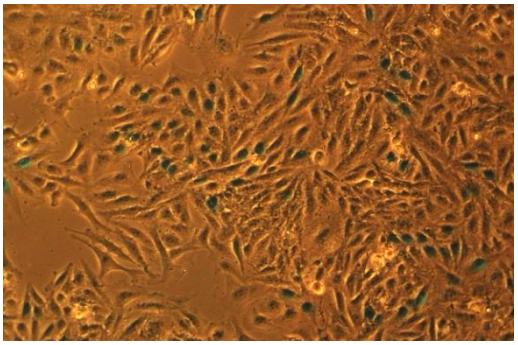

HIV- High MOI

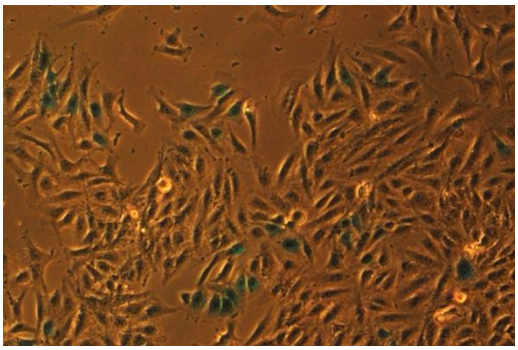

HIV- Low MOI

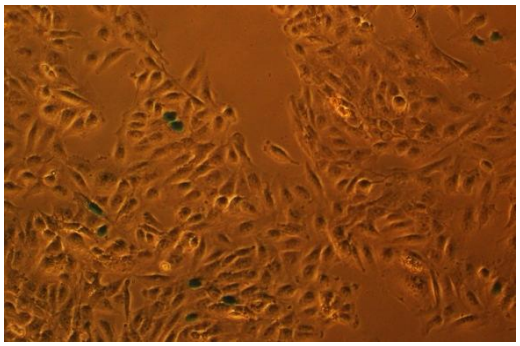

EIAV- High MOI

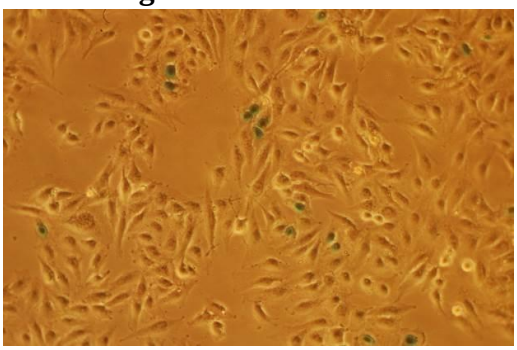

EIAV- Low MOI

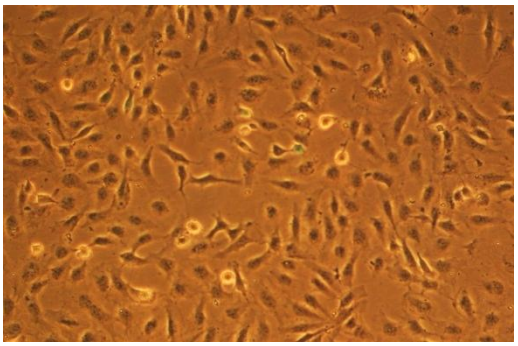

Figure 15. At5biva cells infected with RV and LV vectors. Infection was performed using MLV, HIV and EIAV at high and low MOI. Level of infection was measured using β-galactosidase staining of cells and counting the percentage of blue cells. Images were taken at X100 magnification using the Zeiss Axiovert 25 microscope.

XP14BR

Un-Infected

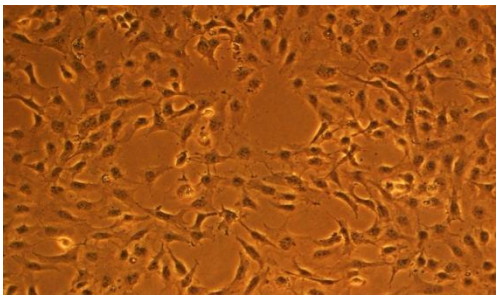

MLV- High MOI

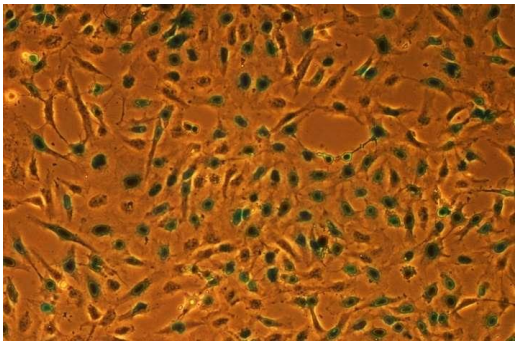

MLV- Low MOI

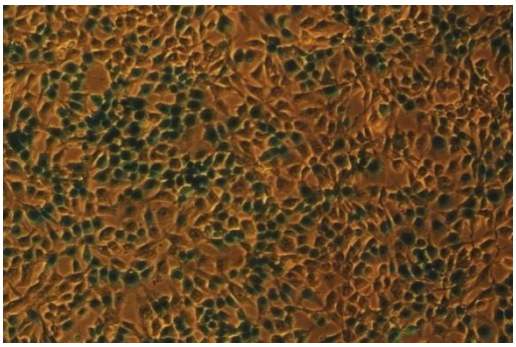

HIV- High MOI

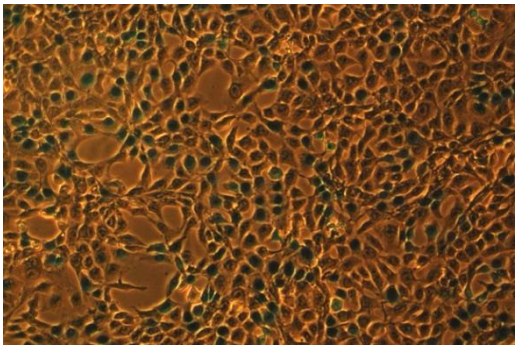

HIV- Low MOI

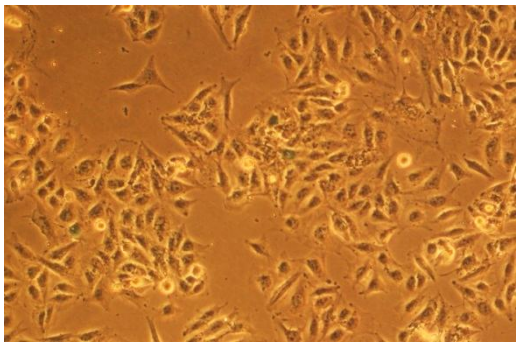

EIAV- High MOI

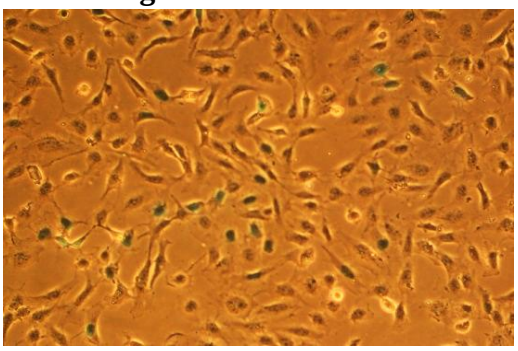

EIAV- Low MOI

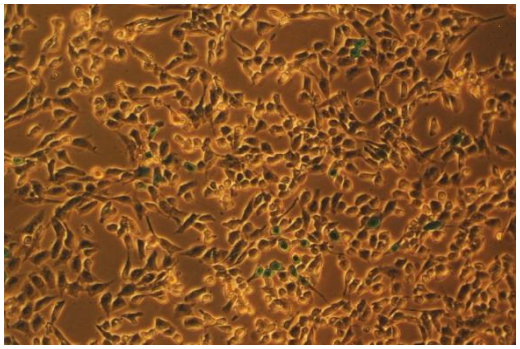

Figure 16. Xp14br cells infected with RV and LV vectors. Infection was performed using MLV, HIV and EIAV at high and low MOI. Level of infection was measured using β-galactosidase staining of cells and counting the percentage of blue cells. Images were taken at X100 magnification using the Zeiss Axiovert 25 microscope.

IN-

MCF10A- High MOI

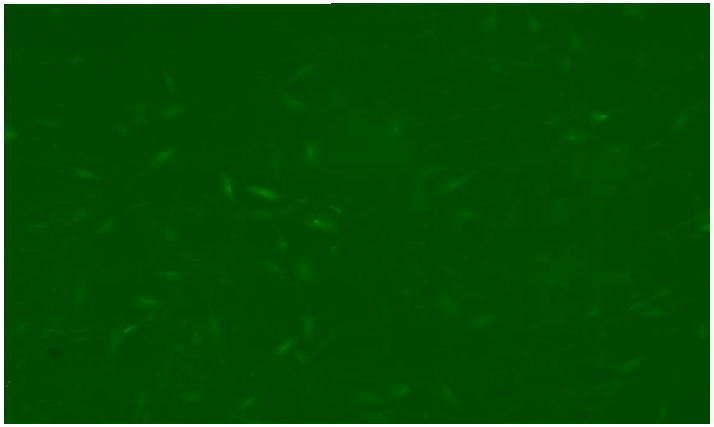

MCF10A- Low MOI

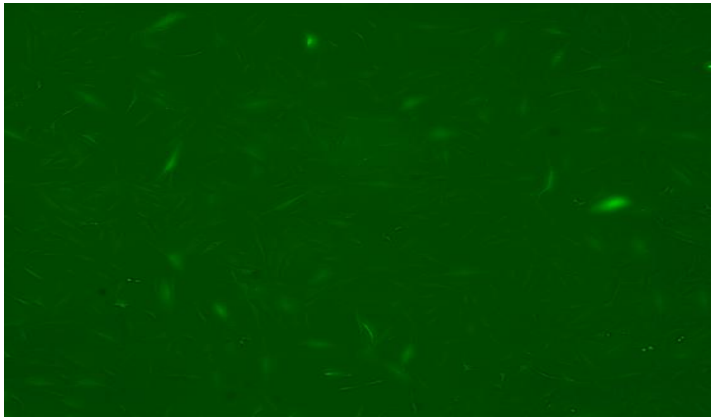

MRC5- High MOI

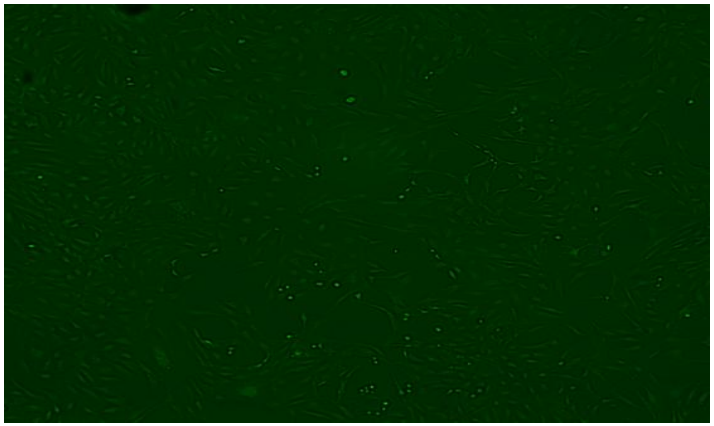

MRC5- Low MOI

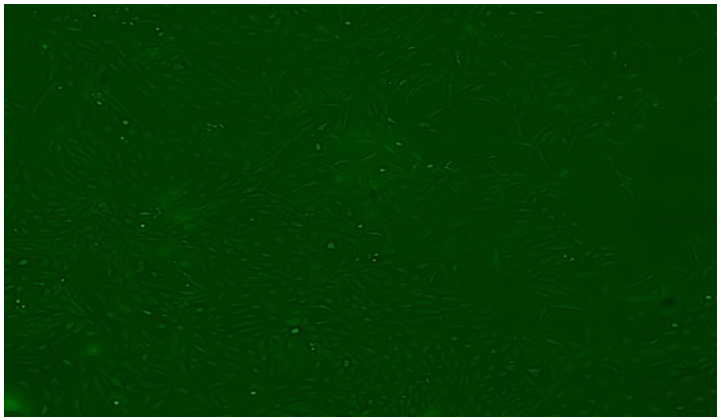

AT5BIVA- High MOI

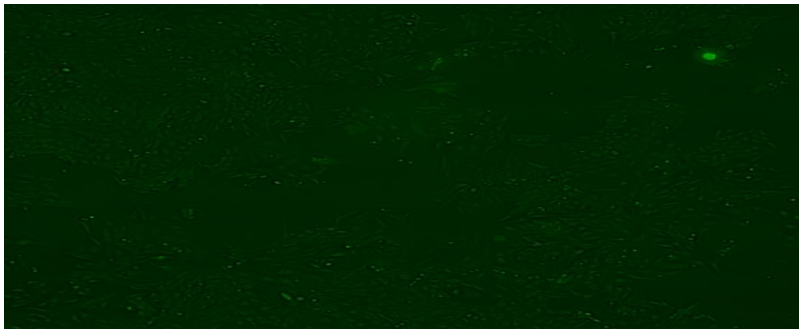

AT5BIVA- Low MOI

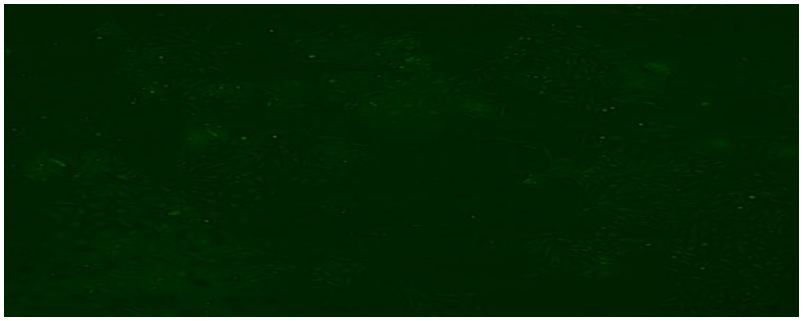

XP14BR- High MOI

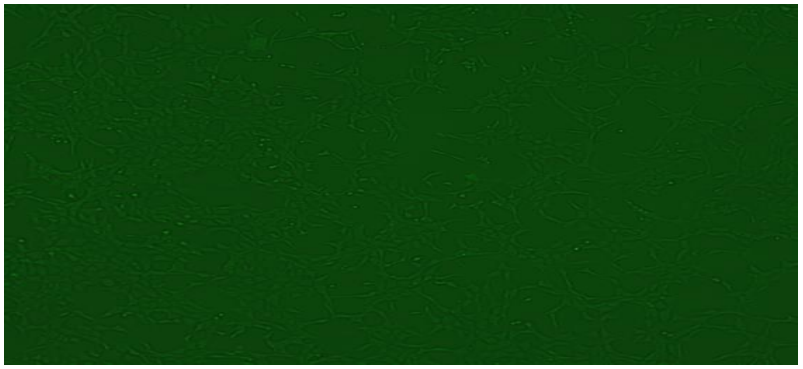

XP14BR- Low MOI

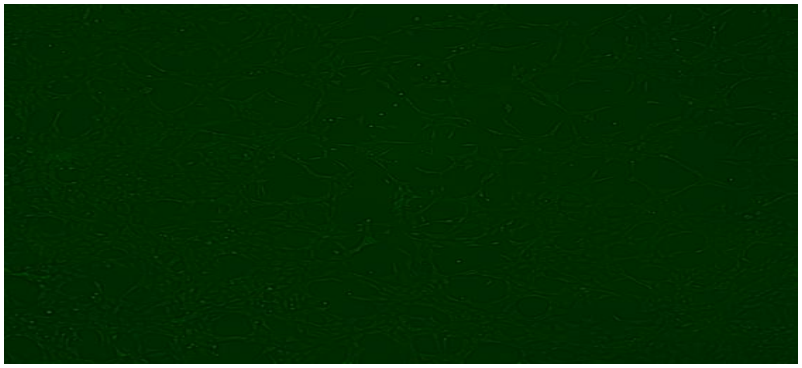

Figure 17. Mcf10a, Mrc5, At5biva and Xp154br cells were infected with an HIV derived integrase negative (IN-ve) vector at high MOI (22) and low MOI (10). The IN- vector carries the GFP marker gene. Green cells were counted using the JuLI smart fluorescent cell analyzer at X40 3 days post-infection. Mcf10a cells showed high levels of infection. Mrc5, At5biva and Xp14br cells showed low levels of infection. Un-infected cells did not show any green immunofluorescence (data not shown).

Table 27. Percentage level of infection in Mcf10a, Mrc5, At5biva and Xp14br cells

Cell Line	MOI	Percentage infection (+/- SEM)			
		MLV	HIV	EIAV	IN-
MCF10A	H	99 (1)	62 (8)	68 (4)	72 (3)
	L	75 (5)	22 (5)	12 (4)	64 (4)
MRC5	H	100 (0)	21 (5)	43 (6)	22 (3)
	L	37 (2)	8 (3)	14 (2)	15 (3)
AT5BIVA	H	98 (2)	31 (2)	9 (5)	10 (5)
	L	28 (5)	7 (0)	3 (3)	4 (7)
XP14BR	H	98 (2)	44 (4)	27 (3)	5 (7)
	L	88 (4)	8 (4)	11 (3)	2 (6)

Cells were infected with RV and LV vectors. Level of infection of cells was measured using β-galactosidase staining of cells and percentages of blue cells were counted and calculated. Negative controls were cultured in an identical manner to virally infected cells and mock infected in the presence of 5µg/ml DEAE dextran. All infections used DEAE dextran at 5µg/ml. 24 hours after infection cells were re-fed with complete medium and 24 hours later infection levels were calculated. Upon infection with LV or RV all cell lines showed positive infection. Levels of infection are greater when a high MOI was used. Un-infected cells showed no positively blue cells. Due to differences in titres between viruses that could be generated, high and low MOIs, respectively, were not identical. Mcf10a, Mrc5, At5biva and Xp14br cells were infected with **MLV** (High MOI:200, Low MOI:10), **HIV** (High MOI:50, Low MOI:10), **EIAV** (High MOI:20, Low MOI:10), **IN-** (High MOI:22, Low MOI:10). **Un-Infected**=negative control; **MLV**=Moloney murine leukaemia virus; **HIV**=Human immunodeficiency virus; **EIAV**=Equine infectious anaemia virus; **IN-**, Human immunodeficiency virus vector with mutated integrase=**IN-** This vector had a GFP marker gene. SEM's are derived from triplicate readings. High MOI=H, Low MOI=L

Highest level infection for each vector was achieved at high MOI. 100% infection was found on Mrc5 cells with the MLV vector at an MOI of 200 (Fig 14) in contrast to negative controls. Mcf10a cells were infected at the highest level (99% +/-1) with MLV. Lowest level of infection was found using the EIAV vector (12% +/-4) for this cell line (Fig 13). Mrc5 level reached 8% (+/-3) using the HIV vector (Table 27). At5biva and Xp14br cell lines showed highest levels of infection with the MLV vector at 98% (+/-2) (Table 27).

Levels of infection using high or low MOI of the IN- vector were low for Mrc5, Atbiva and Xp14br, however, levels of infection for Mcf10a cells infected with high MOI IN- vector was 72% (+/-3) and 64% (+/- 4) with low MOI IN- vector.

The results obtained suggest the cell lines could be infected with RV and LV vectors and that the highest infection was achieved using Mcf10a and Mrc5 cell lines. Next, cell viability was tested on each cell line to determine the effects of virus infection on cell survival.

4.1.2 Survival of cells following infection

Following infection cell survival assays were performed using the trypan blue assay. Trypan blue staining of cells distinguishes between cells that are alive or dead. Cells that are viable exclude the dye whereas dead cells do not and can be viewed by microscopy. Cell viability assays were carried out on Mcf10a, Mrc5, At5biva and Xp14br cell lines. Cells were infected with a range of retroviral vectors at high and low MOI and percentages of viable cells were counted 0-5 days post infection.

Graphs showing percentage cell survival after infection with RV and LV at high MOI

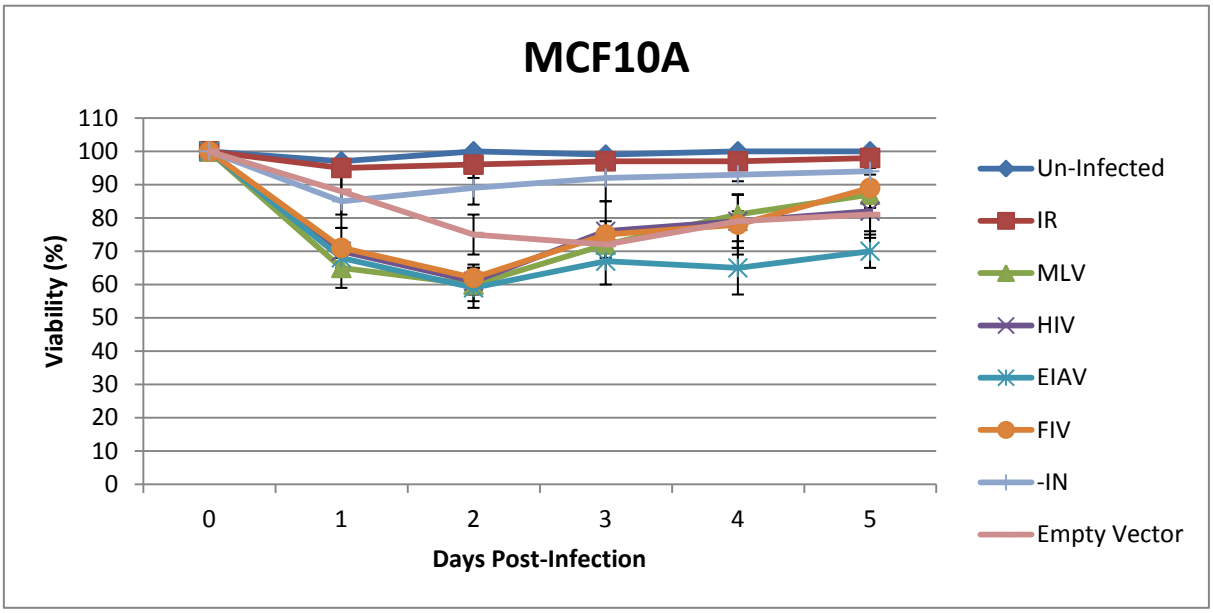

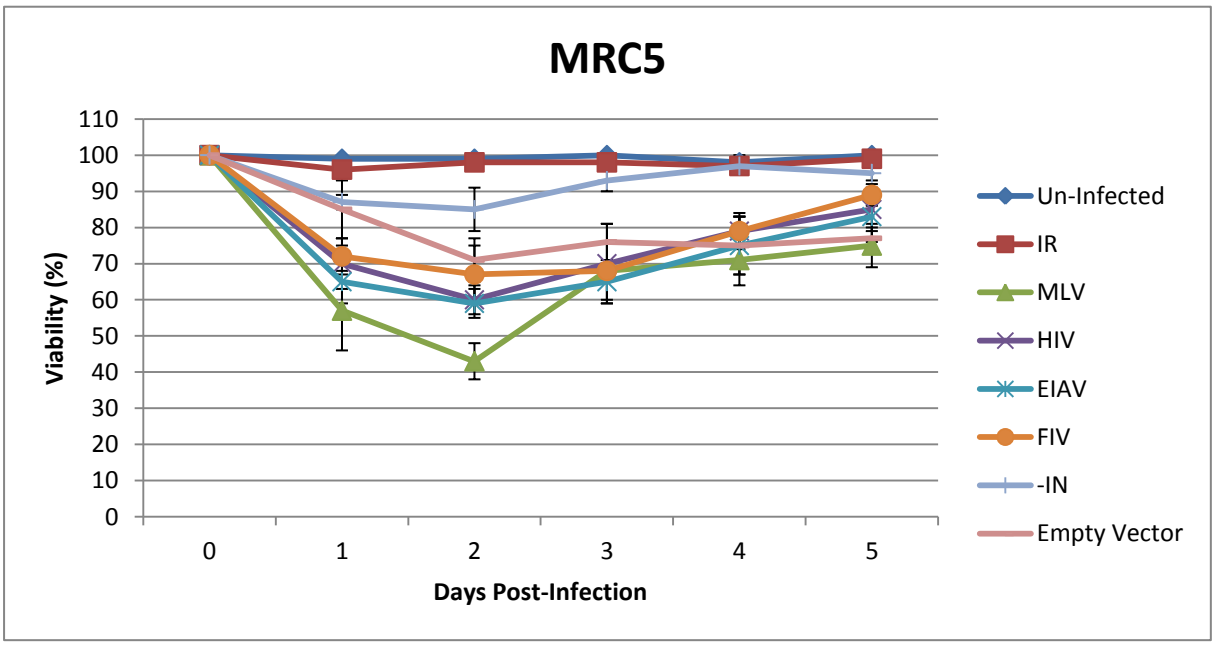

Figure 18. Mcf10a and Mrc5 percentage cell survival following infection with RV and LV at high MOI. Mcf10a cells that were either un-infected or irradiated show cell survival levels between 95-100% over the 5-day period following infection. After infection with MLV, HIV, EIAV, FIV and the MLV vector without the virus genome, cell viability decreased 24 to 48 hours post infection and then increased thereafter. Mrc5 cells showed similar survival to Mcf10a cells post infection, however cells infection by the MLV vector 24 hours post infection showed low cell viability (43%+/-5).

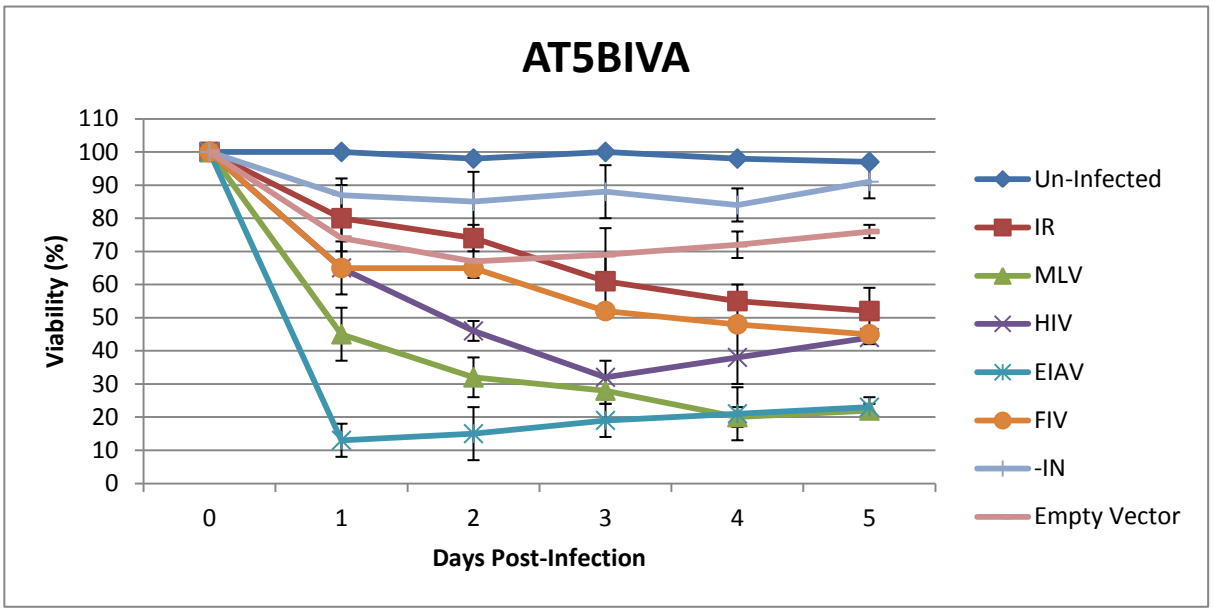

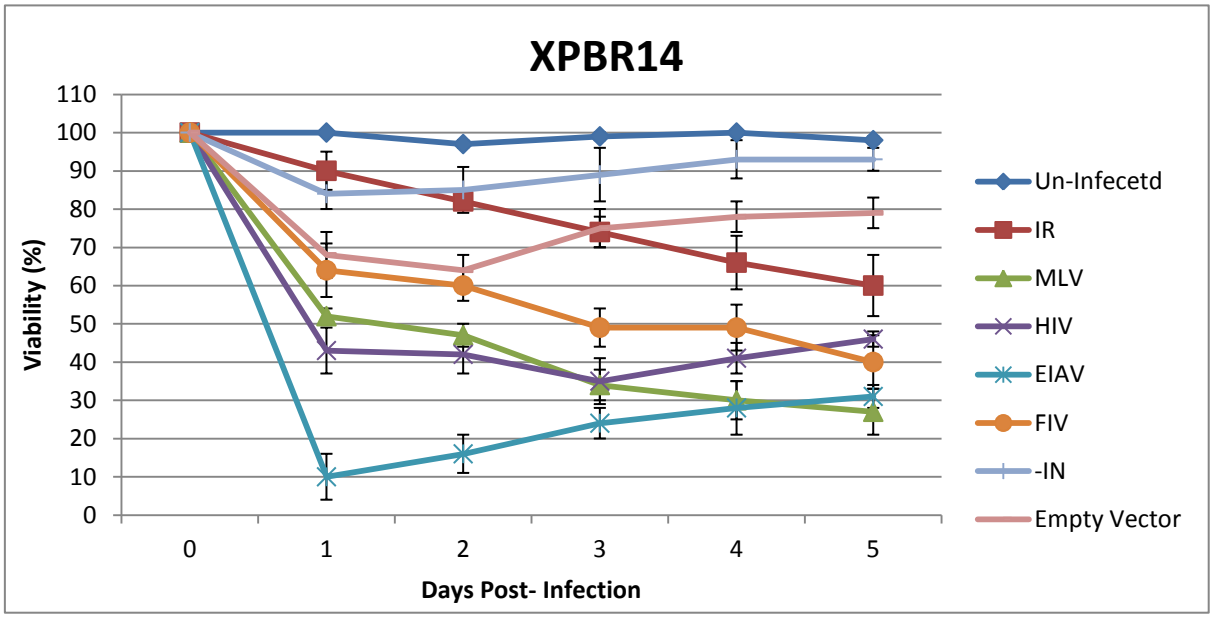

Figure 19. At5biva and Xp14br percentage cell survival on infection with RV and LV at high MOI. At5biva and Xp14br exhibit least survival with the EIAV vector, shown 1 day post infection with cell viability reduced to 10%. Un-infected cells remained with 97-100% cell viability throughout. Irradiated cells had decreased cell viability 0-5 days post irradiation.

Graphs showing percentage cell survival after infection with RV and LV at low MOI

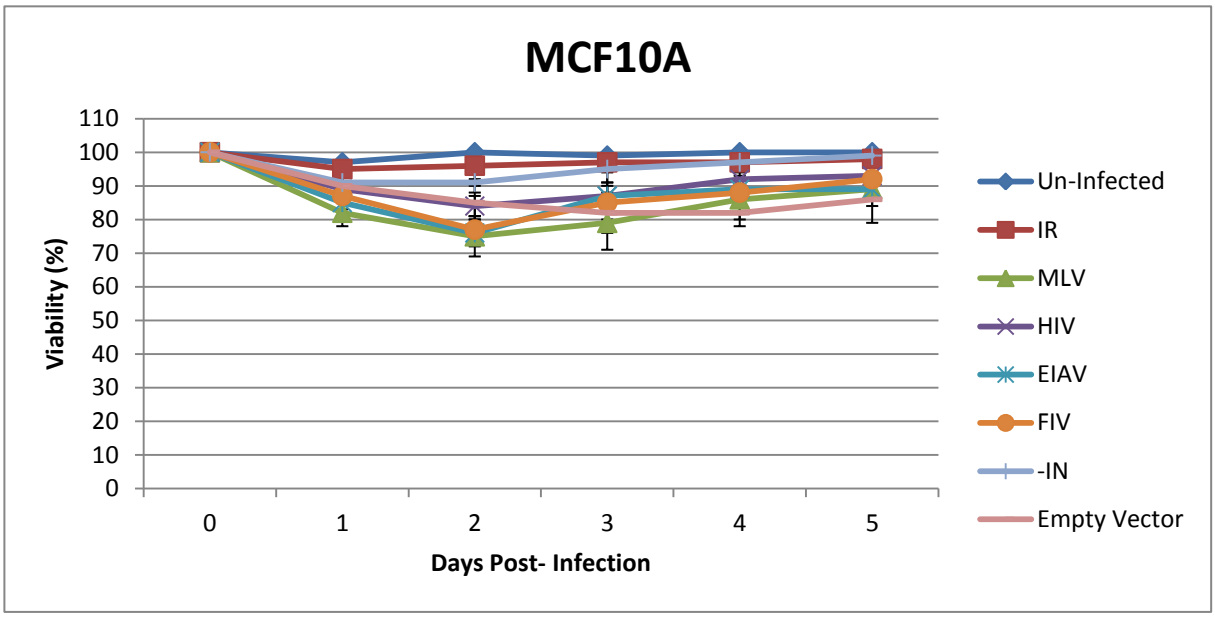

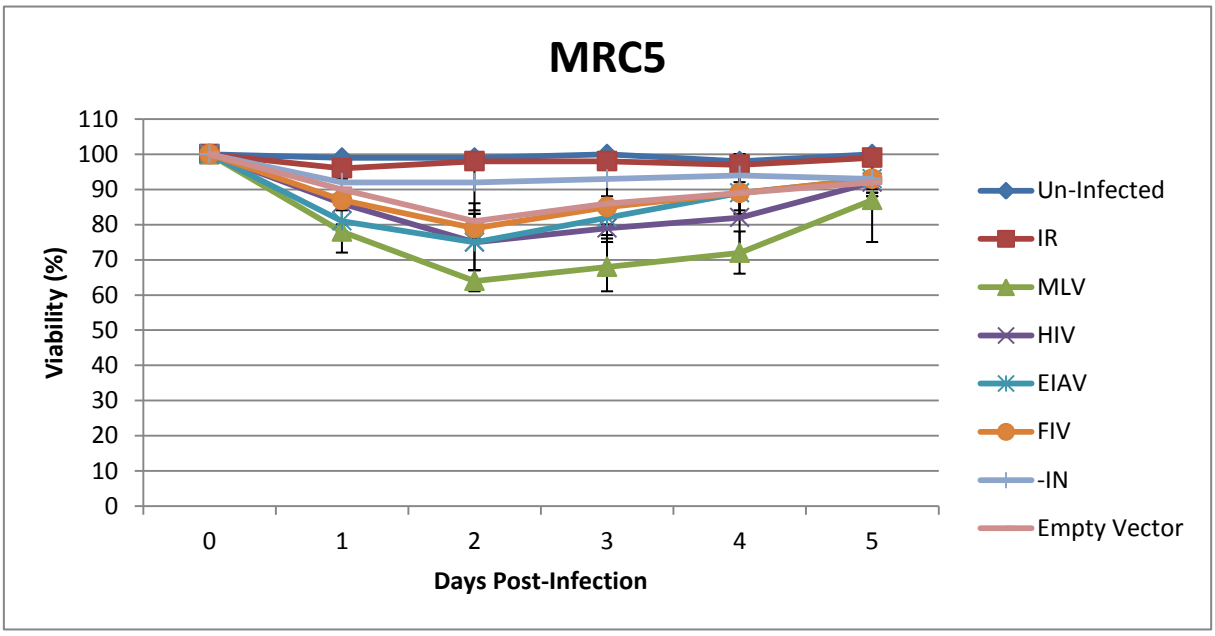

Figure 20. Mcf10a and Mrc5 percentage cell survival after infection with RV and LV at low MOI. Mcf10a and Mrc5 cells infected with MLV shows the lowest rate of cell viability 2 days post infection at 75% (+/-6) and 64% (+/-3), respectively. Cell viability increases after 2 days post infection with each vector.

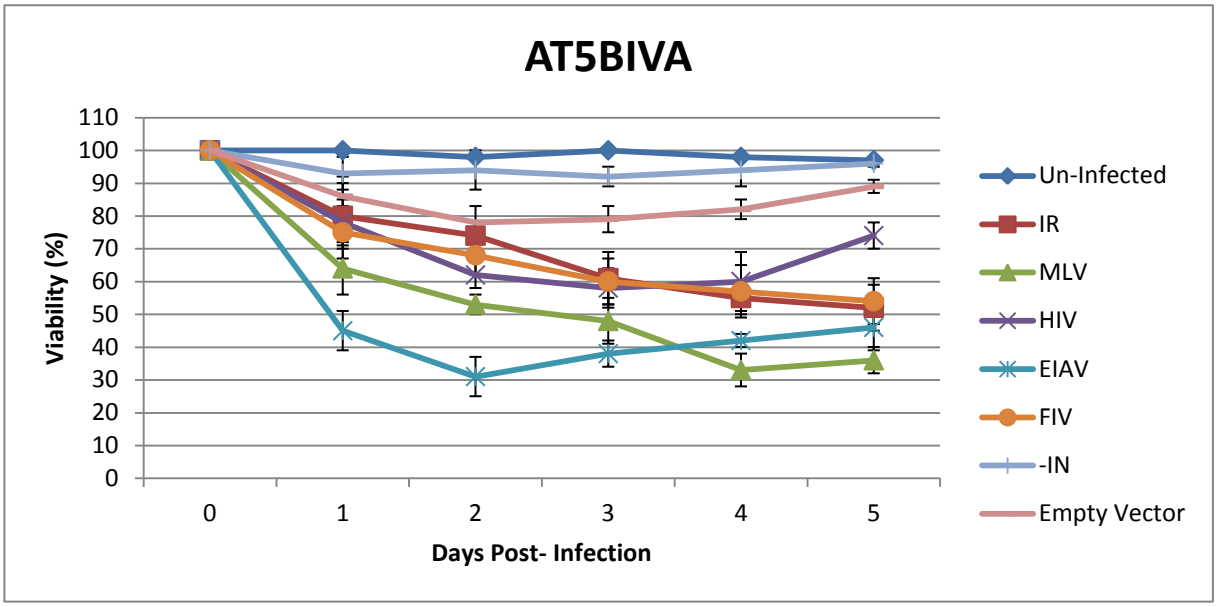

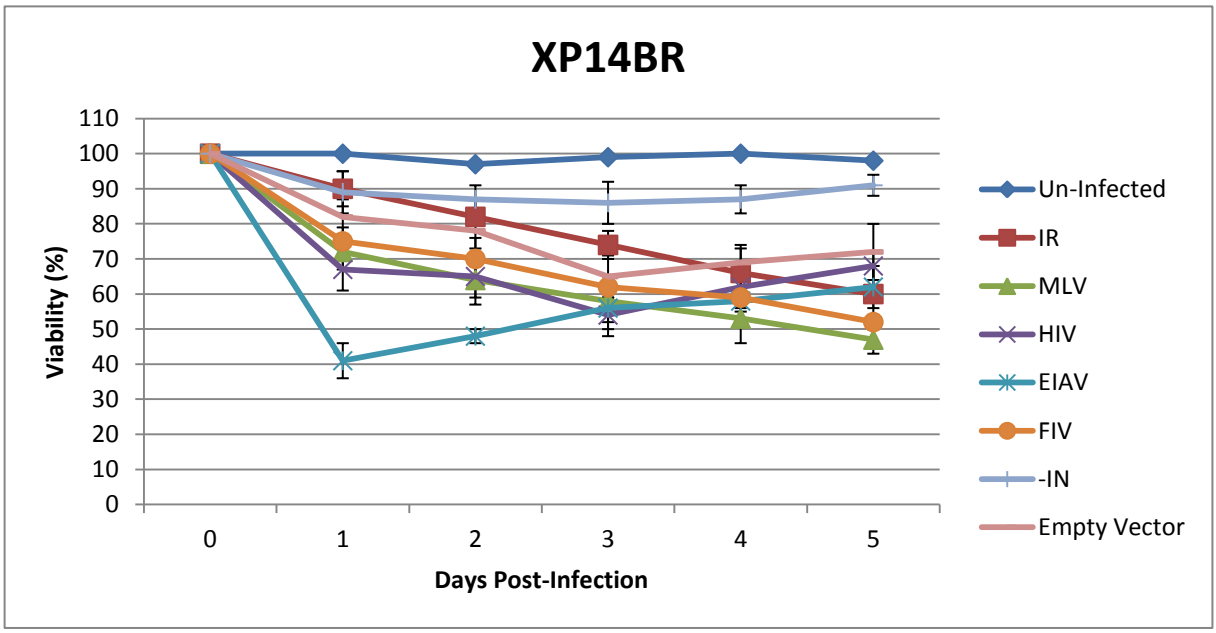

Figure 21. At5biva and Xp14br percentage cell survival after infection with RV and LV at Low MOI. At5biva and Xp14br infected with EIAV have a drastically reduced cell survival 1 day post infection with cell viability falling to 45% (+/-6) and 41% (+/-5), respectively.

Table 28. Percentage of viable cells on infection with High MOI RV and LV vectors

CELL LINE	Vector	DAYS POST-INFECTION Percentage infection (+/-SEM)					
		0	1	2	3	4	5
MCF01A	Un-Infected	100 (0)	97 (1)	100 (0)	99 (0)	100 (0)	100 (0)
	IR	100 (0)	95 (1)	96 (4)	97 (0)	97 (2)	98 (2)
	MLV	100 (0)	65 (6)	60 (5)	72 (4)	81 (1)	87 (6)
	HIV	100 (0)	70 (2)	61 (4)	76 (9)	79 (8)	82 (6)
	EIAV	100 (0)	68 (5)	59 (6)	67 (7)	65 (8)	70 (5)
	FIV	100 (0)	71 (6)	62 (4)	75 (4)	78 (9)	89 (6)
	IN-	100 (0)	85 (8)	89 (5)	92 (7)	93 (2)	94 (5)
	Empty Vector	100 (0)	88 (7)	75 (6)	72 (2)	79 (8)	81 (7)
MRC5	Un-Infected	100 (0)	99 (1)	99 (1)	100 (0)	98 (2)	100 (0)
	IR	100 (0)	96 (3)	98 (2)	98 (0)	97 (1)	99 (1)
	MLV	100 (0)	57 (11)	43 (5)	68 (8)	71 (7)	75 (6)
	HIV	100 (0)	70 (7)	60 (4)	70 (11)	79 (5)	85 (6)
	EIAV	100 (0)	65 (6)	59 (4)	65 (6)	7 (8)	83 (7)
	FIV	100 (0)	72 (5)	67 (8)	68 (2)	79 (4)	89 (3)
	IN-	100 (0)	87 (2)	85 (6)	93 (3)	97 (1)	95 (2)
	Empty Vector	100 (0)	85 (10)	71 (6)	76 (5)	75 (8)	77 (3)
AT5BIVA	Un-Infected	100 (0)	100 (0)	98 (1)	100 (0)	98 (1)	97 (1)
	IR	100 (0)	80 (10)	74 (4)	61 (8)	55 (5)	52 (7)
	MLV	100 (0)	45 (8)	32 (6)	28 (4)	20 (3)	22 (2)
	HIV	100 (0)	65 (8)	46 (3)	32 (5)	38 (8)	44 (2)
	EIAV	100 (0)	13 (5)	15 (8)	19 (5)	21 (8)	23 (3)
	FIV	100 (0)	65 (2)	65 (6)	52 (7)	48 (8)	45 (3)
	IN-	100 (0)	87 5)	85 (9)	88 (8)	84 (5)	91 (5)
	Empty Vector	100 (0)	74 (7)	67 (5)	69 (8)	72 (4)	76 (2)
XP14BR	Un-Infected	100 (0)	100 (0)	97 (1)	99 (1)	100 (0)	98 (1)
	IR	100 (0)	90 (5)	82 (2)	74 (4)	66 (7)	60 (8)
	MLV	100 (0)	52 (2)	47 (3)	34 (4)	30 (5)	27 (6)
	HIV	100 (0)	43 (6)	42 (5)	35 (6)	41 (4)	46 (2)
	EIAV	100 (0)	10 (6)	16 (5)	24 (4)	28 (7)	31 (3)
	FIV	100 (0)	64 (7)	60 (4)	49 (5)	49 (6)	40 (7)
	IN-	100 (0)	84 (4)	85 (6)	89 7)	93 (5)	93 (3)
	Empty Vector	100 (0)	68 (6)	64 (4)	75 (5)	78 (4)	79 (4)

Mcf10a, Mrc5, At5biva and Xp14br were infected with RV and LV at a low MOI of 10 and cell survival was measured using the trypan blue assay. Percentage cell survival was calculated after counting cells using the Invitrogen Countess Automated cell counter 0-5 days post

infection. Negative controls were cultured in an identical manner to virus infected cells and mock infected in the presence of 5µg/ml DEAE dextran. All infections used DEAE dextran at 5µg/ml. 24 hours after infection cells were re-fed with complete medium. All cell lines showed 100% cell viability 0 days post infection. 24 hours post infection cell viability was significantly reduced.

Mcf10a, Mrc5, At5biva and Xp14br cells were infected at the maximum MOI allowed by virus titre (high MOI). **MLV** (MOI 100), **HIV** (MOI 100), **EIAV** (MOI 100), **IN-** (MOI 22), **FIV** (MOI 100) and empty Vector (MOI estimated at 100). Un-Infected cells were treated as negative control; **IR**=Irradiated (1Gy); **MLV**=Moloney murine leukaemia virus; **HIV**=Human immunodeficiency virus; **EIAV**=Equine infectious anaemia virus; **IN-**=Human immunodeficiency virus with mutated integrase; **FIV**=Feline immunodeficiency virus; **Empty Vector**=MLV without viral genome.

Table 29. Percentage of viable cells following infection with RV and LV at low MOI

CELL LINE	Vector	DAYS POST-INFECTION Percentage Survival (SEM +/-) post infection					
		0	1	2	3	4	5
MCF01A	MLV	100 (0)	82 (4)	75 (6)	79 (8)	86 (6)	89 (2)
	HIV	100 (0)	89 (6)	84 (3)	87 (3)	92 (6)	93 (5)
	EIAV	100 (0)	85 (4)	76 (4)	87 (7)	89 (4)	89 (3)
	FIV	100 (0)	87 (6)	77 (4)	85 (6)	88 (2)	92 (8)
	IN-	100 (0)	91 (5)	91 (3)	95 (4)	97 (3)	99 (1)
	Empty Vector	100 (0)	90 (3)	85 (5)	82 (6)	82 (4)	86 (7)
MRC5	MLV	100 (0)	78 (6)	64 (3)	68 (7)	72 (6)	87 (12)
	HIV	100 (0)	86 (6)	75 (8)	79 (3)	82 (10)	92 (3)
	EIAV	100 (0)	81 (5)	75 (8)	82 (2)	89 (6)	93 (4)
	FIV	100 (0)	87 (9)	79 (2)	85 (8)	89 (7)	93 (5)
	IN-	100 (0)	92 (3)	92 (8)	93 (5)	94 (5)	93 (5)
	Empty Vector	100 (0)	90 (4)	81 (5)	86 (11)	89 (5)	92 (2)
AT5BIVA	MLV	100 (0)	64 (8)	53 (3)	48 (7)	33 (5)	36 (4)
	HIV	100 (0)	78 (7)	62 (4)	58 (6)	60 (9)	74 (4)
	EIAV	100 (0)	45 (6)	31 (6)	38 (4)	42 (2)	46 (7)
	FIV	100 (0)	75 (8)	68 (6)	60 (7)	57 (8)	54 (7)
	IN-	100 (0)	93 (5)	94 (6)	92 (3)	94 (5)	96 (1)
	Empty Vector	100 (0)	86 (6)	78 (5)	79 (4)	82 (3)	89 (2)
XP14BR	MLV	100 (0)	72 (5)	64 (5)	58 (6)	53 (7)	47 (4)
	HIV	100 (0)	67 (6)	65 (8)	54 (4)	62 (7)	68 (4)
	EIAV	100 (0)	41 (5)	48 (2)	56 (8)	58 (7)	62 (6)
	FIV	100 (0)	75 (4)	70 (6)	62 (3)	59 (3)	52 (2)
	IN-	100 (0)	89 6)	87 (4)	86 (6)	87 (4)	91 (3)
	Empty Vector	100 (0)	82 (5)	78 (9)	65 (6)	69 (5)	72 (8)

Mcf10a, Mrc5, At5biva and Xp14br cells were infected with RV and LV at a low MOI of 10 and the percentage cell survival was measured using the trypan blue assay followed by counting using an Invitrogen Countess Automated cell counter at 0-5 days post infection. Negative controls were cultured in an identical manner to virally infected cells and mock infected in the presence of 5µg/ml DEAE dextran. All infections were performed with DEAE dextran at 5µg/ml. 24 hours after infection cells were re-fed with complete medium. All cell lines showed 100% cell viability at day 0 post infection. 24 hours post infection cell viability appeared reduced.

Un-infected Mcf10a and Mrc5 cells survival throughout the 5 day duration of cell culturing was 97-100%. Irradiated (1Gy) Mcf10a and Mrc5 cell viability did not show a large change in cell survival, however, the percentage of viable cells decreased slightly after 24 hours post infection after which time cells appeared to recover possibly as a result of DNA damage repair as cell viability increased to 98% (SEM +/- 2) and 99% (+/-1) by day 5, respectively. Mcf10a and Mrc5 cells infected with MLV showed the lowest rate of cell viability at 2 days post infection of 60% (+/-5) and 43% (+/-5), respectively. Interestingly, cell infected with the HIV vector containing a mutated integrase showed a similar pattern to that of the irradiated cell lines although the percentage viable cells were slightly lower than the irradiated cells.

Irradiated (1Gy) At5biva and Xp14br cell viability decreased initially to 80% (+/-10) and 90% (+/-5), respectively, then further decreased to 52% (+/-7) and 60% (+/-8), respectively, 5 days post irradiation. Using the EIAV vector at high MOI to infect At5biva and Xp14br the lowest level of viable cells was observed at 13% (+/-5) and 10% (+/-6), respectively.

The results obtained show percentage cells with intact DNA repair pathways have decreased cell survival upon infection with RV and LV vectors 2 days post infection after which cells appear to recover possibly due to DNA repair. Atbiva and Xp14br cells without DNA repair pathways intact showed cell viability to decrease throughout the 5 days.

Following the findings described, cells were next investigated to identify DSB in their genomes following infection by each vector to attempt to correlate cell survival with DNA damage.

4.1.3 The effect of infection by RV and LV on DNA DSB

DNA damage is known to cause chromosomal instability that can lead to tumour induction. The extent of DSB caused by integrating RV and LV is not clearly defined. It was necessary, therefore to investigate this for each vector and demonstrate proviral integration as a major assault on the genome of the cell and whether this varies between different vectors. DNA damage on the cell has already been shown following irradiation or by the use of genotoxic drugs. DNA damage has been shown following integration by the laboratory of F. Bushman using HIV-1 derived LV. The Bushman group demonstrated a rapid DDR was measurable using γH2AX immunofluorescence to identify DSB foci at the sites of DNA damage (Bushman *et al*., 2001). In the following work, to measure the extent of DNA damage on the genome by several RV and LV, cells were infected and immunofluorescence of the DNA damage/repair protein 53BP1 was used for measuring induction of foci representing DSB. 53BP1 was used as an alternative to gH2AX because this protein is important in signalling pathways of DNA repair as well as apoptosis. For this purpose, a number of cell lines were tested with and without intact repair pathways followed by 53BP1 immunofluorescence.

Figure 22 a

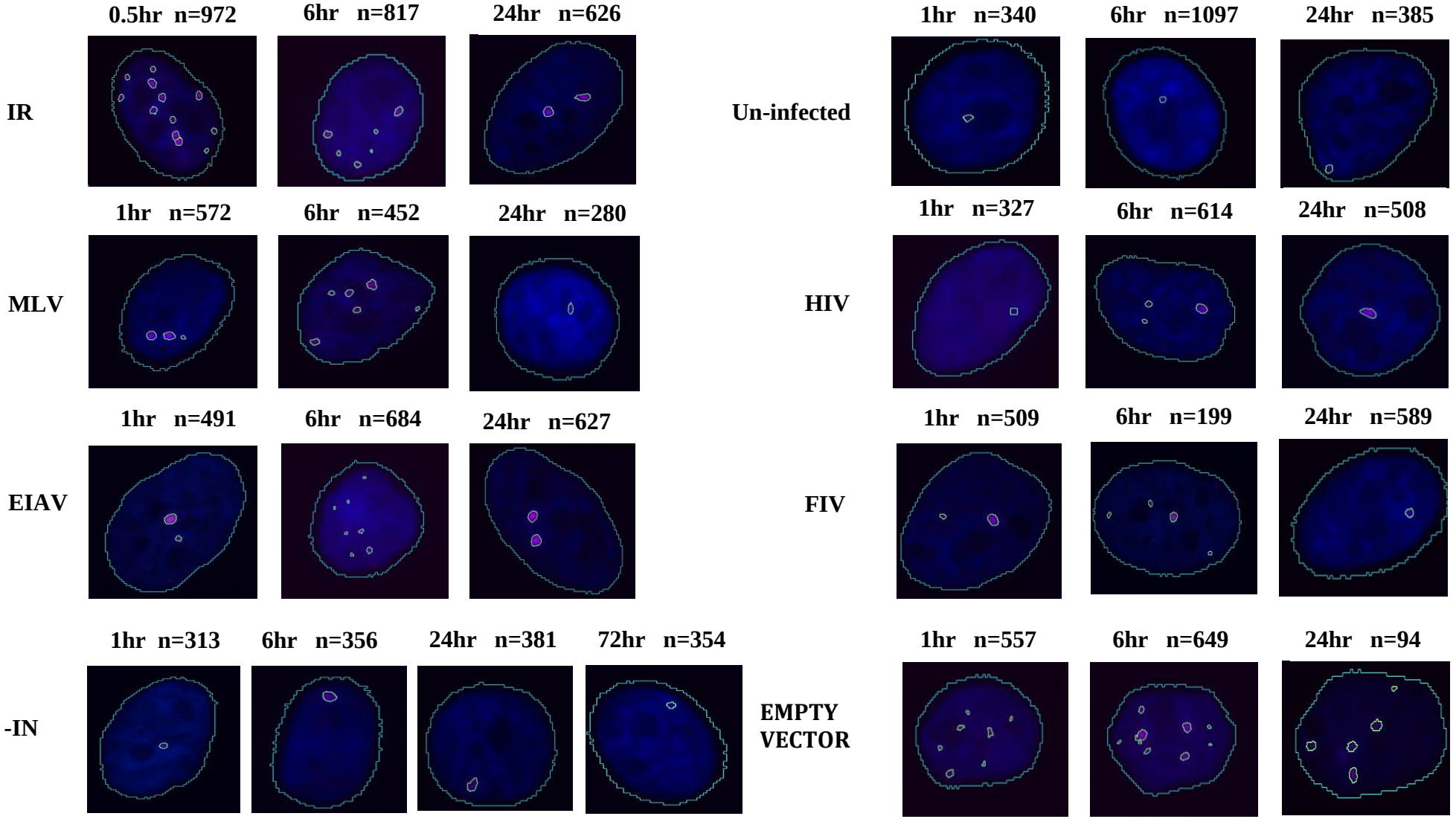
0.5hr n=972
6hr n=817
24hr n=626
IR
1hr n=340
6hr n=1097
24hr n=385
Un-infected
1hr n=572
6hr n=452
24hr n=280
MLV
1hr n=327
6hr n=614
24hr n=508
HIV
1hr n=491
6hr n=684
24hr n=627
EIAV
1hr n=509
6hr n=199
24hr n=589
FIV
1hr n=313
6hr n=356
24hr n=381
72hr n=354
-IN
1hr n=557
6hr n=649
24hr n=94
EMPTY VECTOR

Figure 22 b

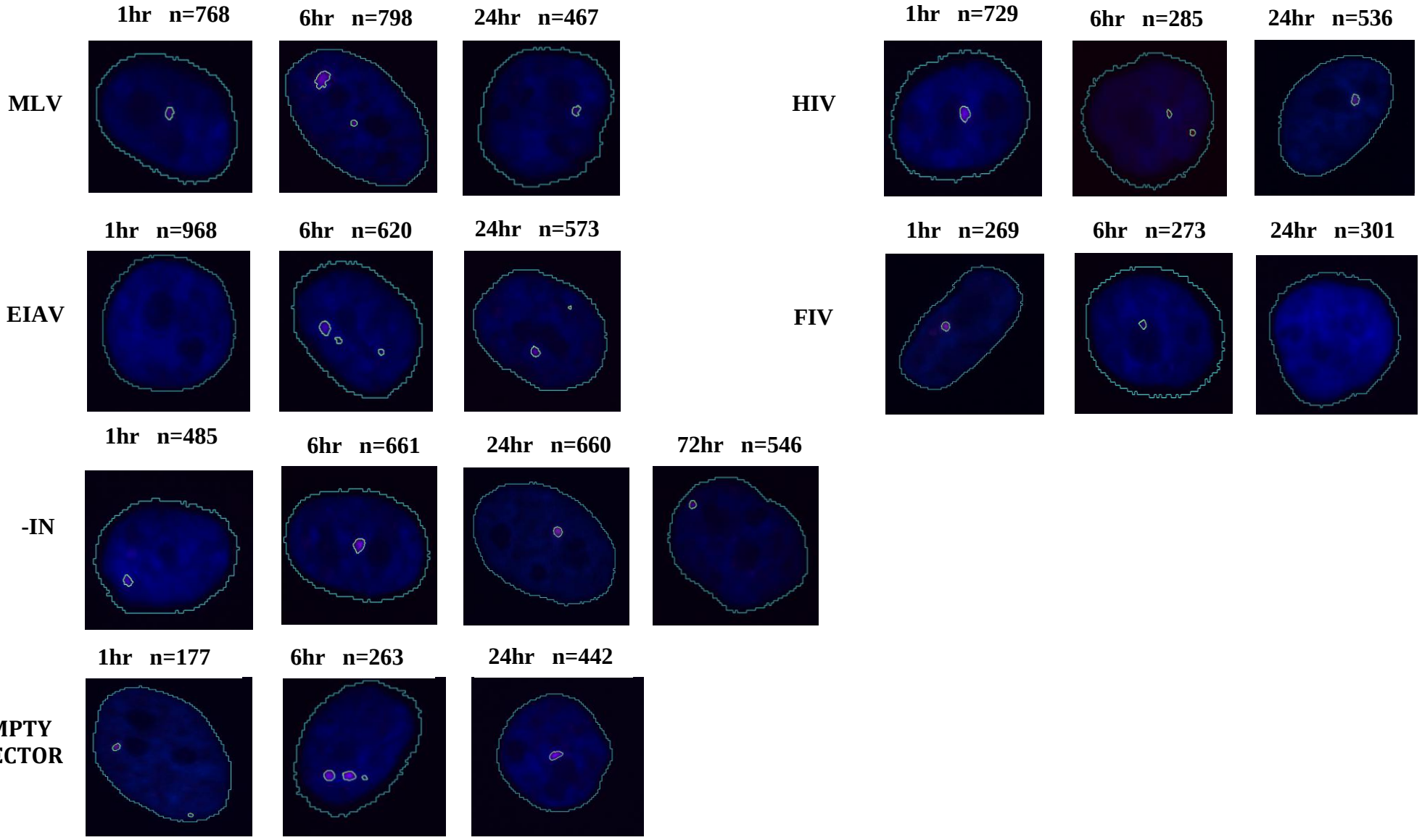
1hr n=768
6hr n=798
24hr n=467
MLV
1hr n=729
6hr n=285
24hr n=536
HIV
1hr n=968
6hr n=620
24hr n=573
EIAV
1hr n=269
6hr n=273
24hr n=301
FIV
1hr n=485
6hr n=661
24hr n=660
72hr n=546
-IN
1hr n=177
6hr n=263
24hr n=442
EMPTY VECTOR

Figure 22a and b. Photomicrographs of immunofluorescence of 53BP1 in MCF10a cells infected by RV and LV at high and low MOI. A DNA damage response (DDR) is evident for each vector tested. Control positive cells were irradiated at 1Gy. Negative controls were cultured in an identical manner to virus infected cells and mock infected in the presence of 5µg/ml DEAE dextran. All infections used DEAE dextran at 5µg/ml. Following irradiation the DDR increases followed by repair over a 6 hour period. RV and LV infection generates foci over a 6 hour period believed to be the time required for infection and integration to occur. This is then followed by DDR. Where no viral integrase (-IN) is present no DDR appears, however where the vector is present but no genome DDR occurs and shown by the presence of 53BP1 foci. The number of nuclei counted is indicated.

IR=irradiated; **NC**=negative control; **MLV**=Moloney murine leukaemia virus; **HIV**=Human immunodeficiency virus; **-IN**=Human immunodeficiency virus with mutated integrase; **EIAV**=Equine infectious anaemia virus; **FIV**=Feline immunodeficiency virus; **Empty Vector**=MLV without viral genome. Photomicrographs are shown for Mcf10a cells infected with **MLV** at high MOI of 200 and low MOI of 10, **HIV** high MOI of 50 and low MOI of 10, **EIAV** at high MOI of 20 and low MOI of 10, **IN-** at high MOI of 22 and low MOI of 10, **FIV** at high MOI of 10 and low MOI of 10, **Empty Vector** at high MOI of 200 and low MOI of 10, **IR** was performed using 1Gy. Images were viewed using the Zeiss Axioplan 2 Imaging microscope and images were captured using the Metafer4 software. Images were then processed using the Definiens programme.

Figure 23a. Mcf10a

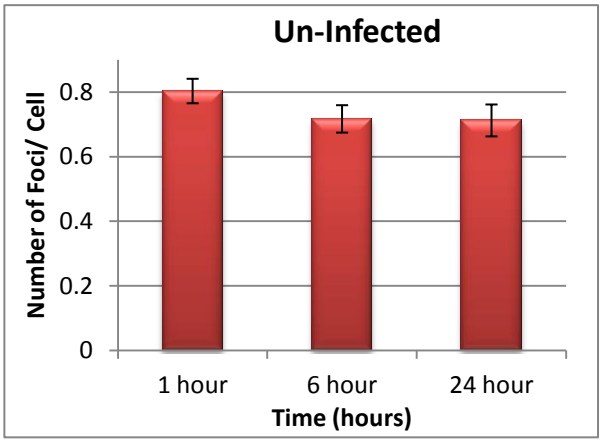

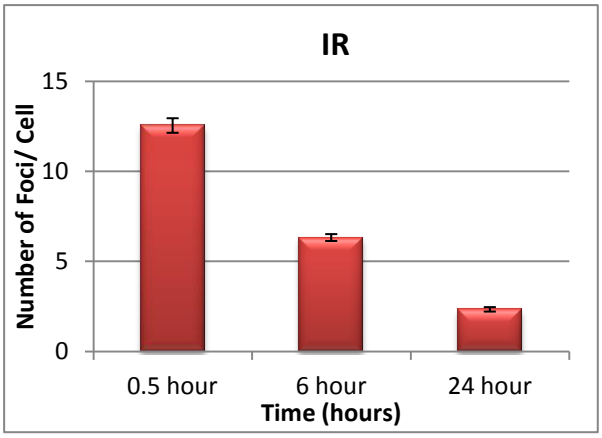

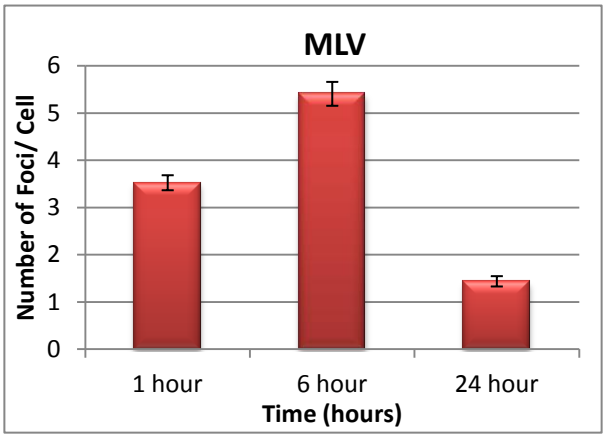

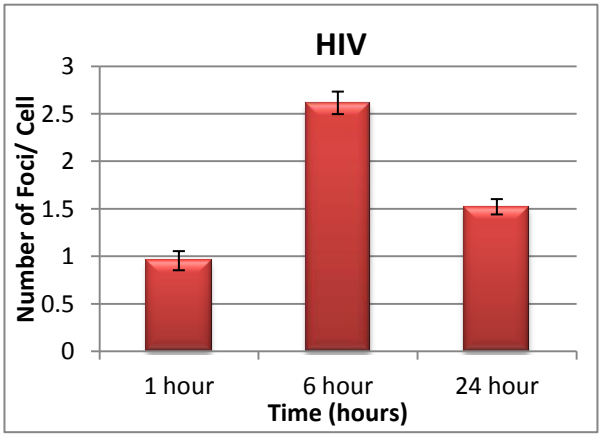

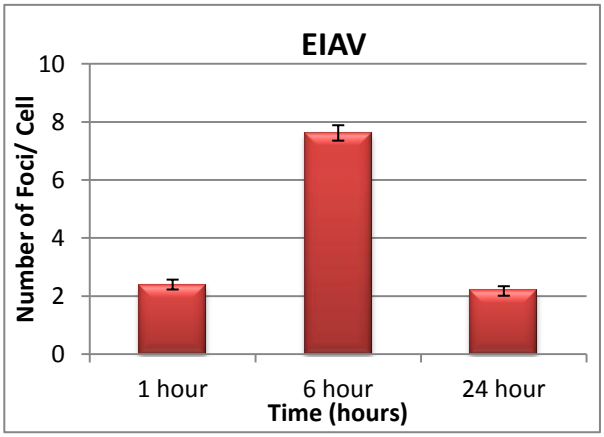

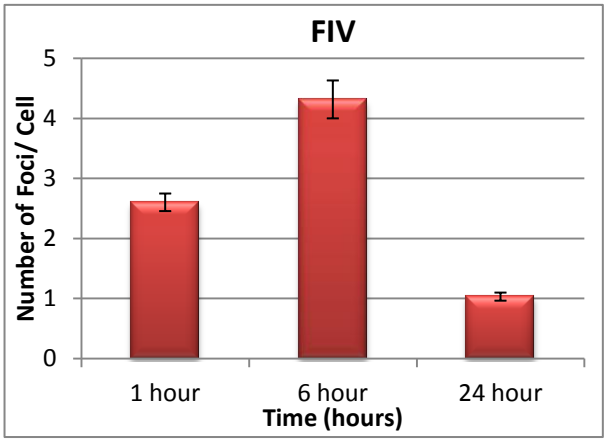

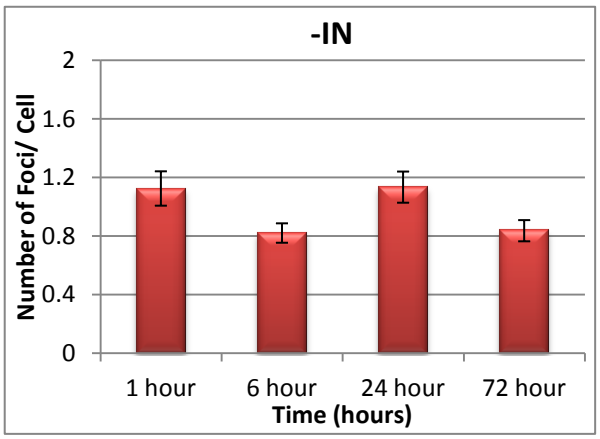

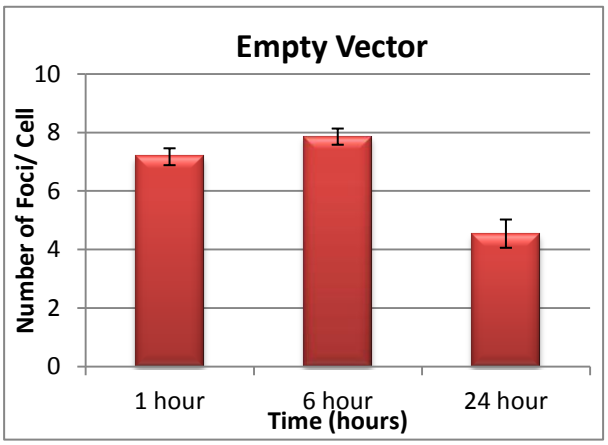

Figure 23b. Mcf10a cells

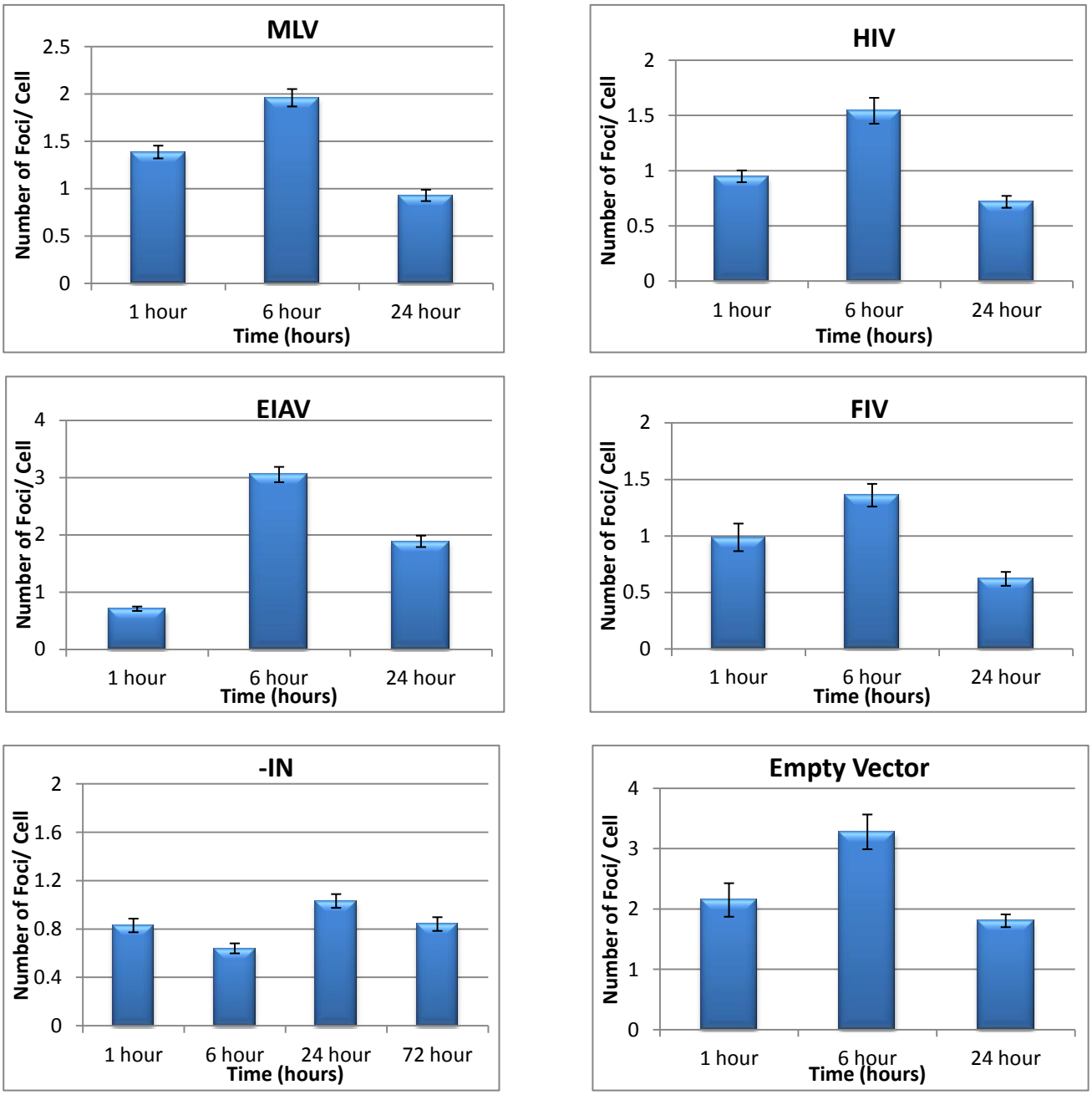

Histograms of the mean number of 53BP1 foci in MCF10a cells infected at high and low MOI

Figure 23a and b represent values of the means and standard errors of Mcf10a 53BP1 foci counted and calculated after each treatment. Infections were performed with RV and LV at high (red) and low (blue) MOI. Un-infected Mcf10a cells have a mean of 0.7-0.8 foci per nuclei. IR cells show a peak at 30minutes of 12.54 foci per nuclei that gradually decreases over a 24 hour period. Cells treated with the empty vector at high MOI vector generated highest average number of foci at 6 hours post infection with a mean of 7.86, compared to virus vectors with genomes. Cells infected with the HIV –IN vector generated similar average of foci as un-infected cells.

Table 30a. Mean number of DSB foci in Mcf10a nuclei at high MOI

Treatment		Time (hours)			
		1	6	24	72
Un-infected	MEAN (+/- SEM)	0.80 (0.04)	0.72 (0.04)	0.71 (0.05)	
	p-value		0.15	0.06	
	No of nuclei	972	817	626	
IR	MEAN (+/- SEM)	12.54 (0.40)	6.32 (0.19)	2.34 (0.12)	
	p-value		6.52E-10	8.80E-38	
	No of nuclei	340	1092	385	
MLV	MEAN (+/- SEM)	3.52 (0.16)	5.40 (0.25)	1.44 (0.11)	
	p-value		1.61E-08	7.75E-27	
	No of nuclei	572	452	280	
HIV	MEAN (+/- SEM)	0.95 (0.10)	2.62 (0.12)	1.52 (0.08)	
	p-value		4.09E-13	4.31E-12	
	No of nuclei	327	614	508	
EIAV	MEAN (+/- SEM)	2.40 (0.17)	7.62 (0.27)	2.17 (0.16)	
	p-value		3.63E-46	4.12E-57	
	No of nuclei	491	684	627	
FIV	MEAN (+/- SEM)	2.60 (0.15)	4.32 (0.32)	1.03 (0.07)	
	p-value		4.42E-08	6.98E-16	
	No of nuclei	509	199	589	
IN-	MEAN (+/- SEM)	1.12 (0.12)	0.82 (0.07)	1.13 (0.11)	0.84 (0.07)
	p-value		0.03	0.01	0.03
	No of nuclei	313	356	381	354
Empty Vector	MEAN (+/- SEM)	7.17 (0.29)	7.86 (0.28)	4.54 (0.48)	
	p-value		0.01	5.80E-05	
	No of nuclei	557	649	94	

Table 30b. Mean number of DSB foci in Mcf10a nuclei at low MOI

Treatment		Time (hours)			
		1	6	24	72
MLV	MEAN (+/- SEM)	1.39 (0.07)	1.96 (0.09)	0.93 (0.06)	
	p-value		2.16E-05	1.37E-09	
	No of nuclei	768	798	467	
HIV	MEAN (+/- SEM)	0.95 (0.05)	1.54 (0.12)	0.72 (0.05)	
	p-value		5.75E-09	2.33E-08	
	No of nuclei	729	285	536	
EIAV	MEAN (+/- SEM)	0.71 (0.04)	3.05 (0.13)	1.88 (0.10)	
	p-value		7.42E-50	2.08E-09	
	No of nuclei	968	620	573	
FIV	MEAN (+/- SEM)	0.99 (0.12)	1.36 (0.10)	0.62 (0.06)	
	p-value		0.01	3.41E-09	
	No of nuclei	269	273	301	
IN-	MEAN (+/- SEM)	0.83 (0.06)	0.64 (0.04)	1.03 (0.06)	0.84 (0.06)
	p-value		0.00	4.01E-08	0.00
	No of nuclei	485	661	660	546
Empty Vector	MEAN (+/- SEM)	2.15 (0.28)	3.28 (0.29)	1.81 (0.11)	
	p-value		0.03	1.19E-05	
	No of nuclei	177	263	442	

MCF10a cells exposed to RV and LV vectors at high and low MOI are shown in table 30a and b above. The DNA damage response (DDR) was measured using 53BP1 immunoflourescence. Control positive cells were irradiated at 1Gy. Negative controls were cultured in an identical manner to virus infected cells and mock infected in the presence of 5µg/ml DEAE dextran. All infections used DEAE dextran at 5µg/ml. Following irradiation the DDR increases followed by repair over a 6 hour period. RV and LV infection appeared to occur over an approximate 6 hour period where a peak in the mean number of 53bp1 foci was observed. This is then followed by a reduction in foci believed due to DDR. All infected cells appear to show DDR. Where no viral integrase is present no DDR appears, however where the MLV vector is present with no genome DDR occurs. Calculated mean values, p-values obtained from standard t-test and no of nuclei counted are shown in the table.

Figure 24a. Mrc5 cells

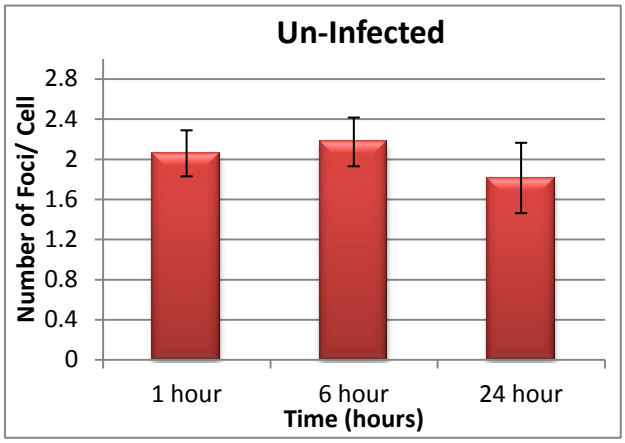

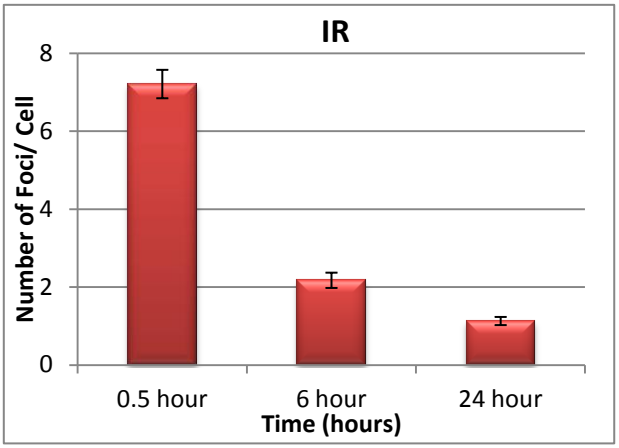

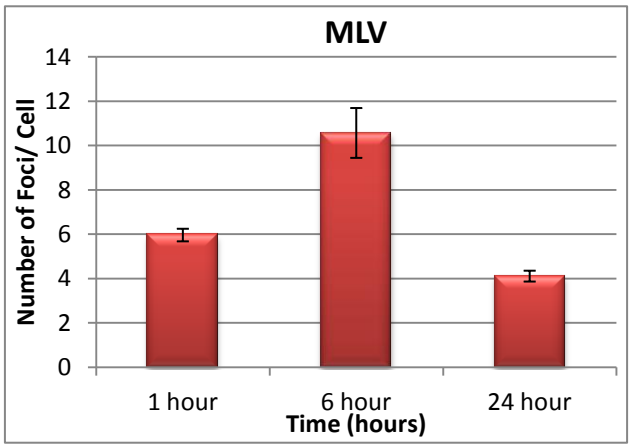

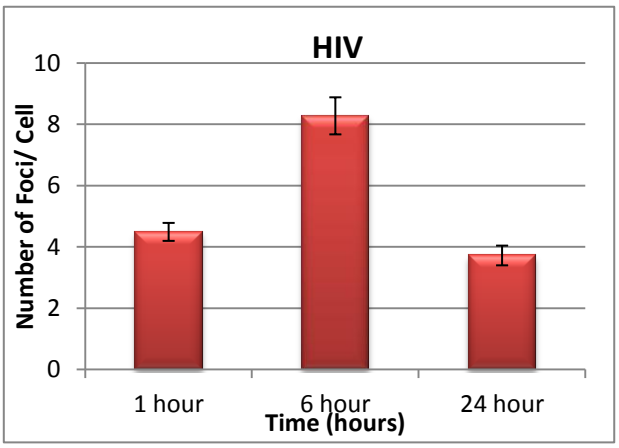

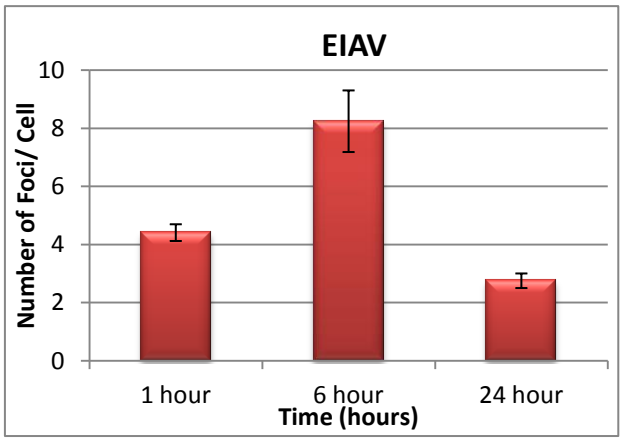

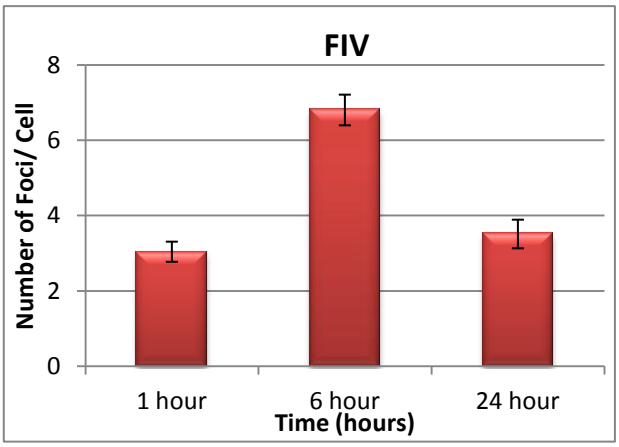

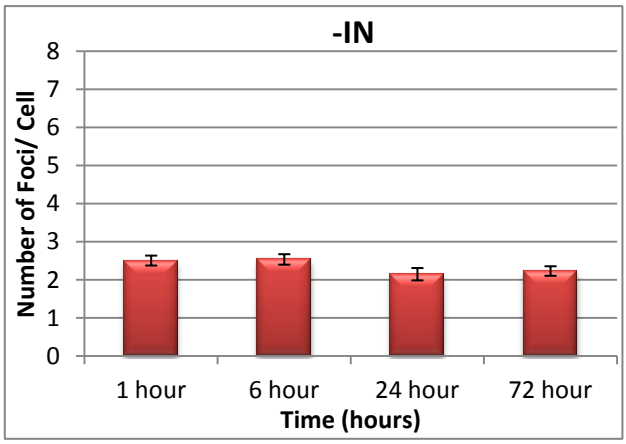

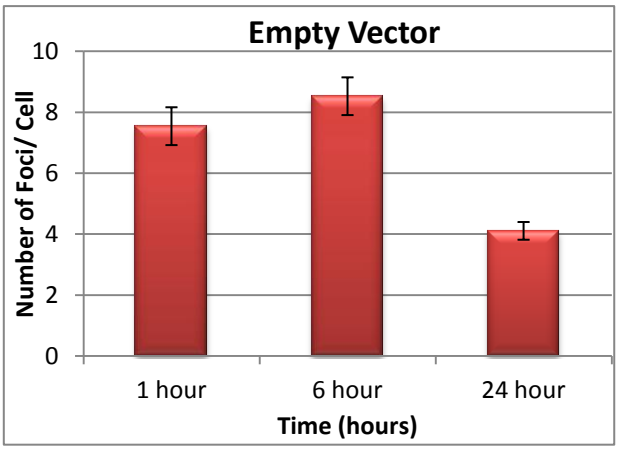

Figure 24b. Mrc5 cells

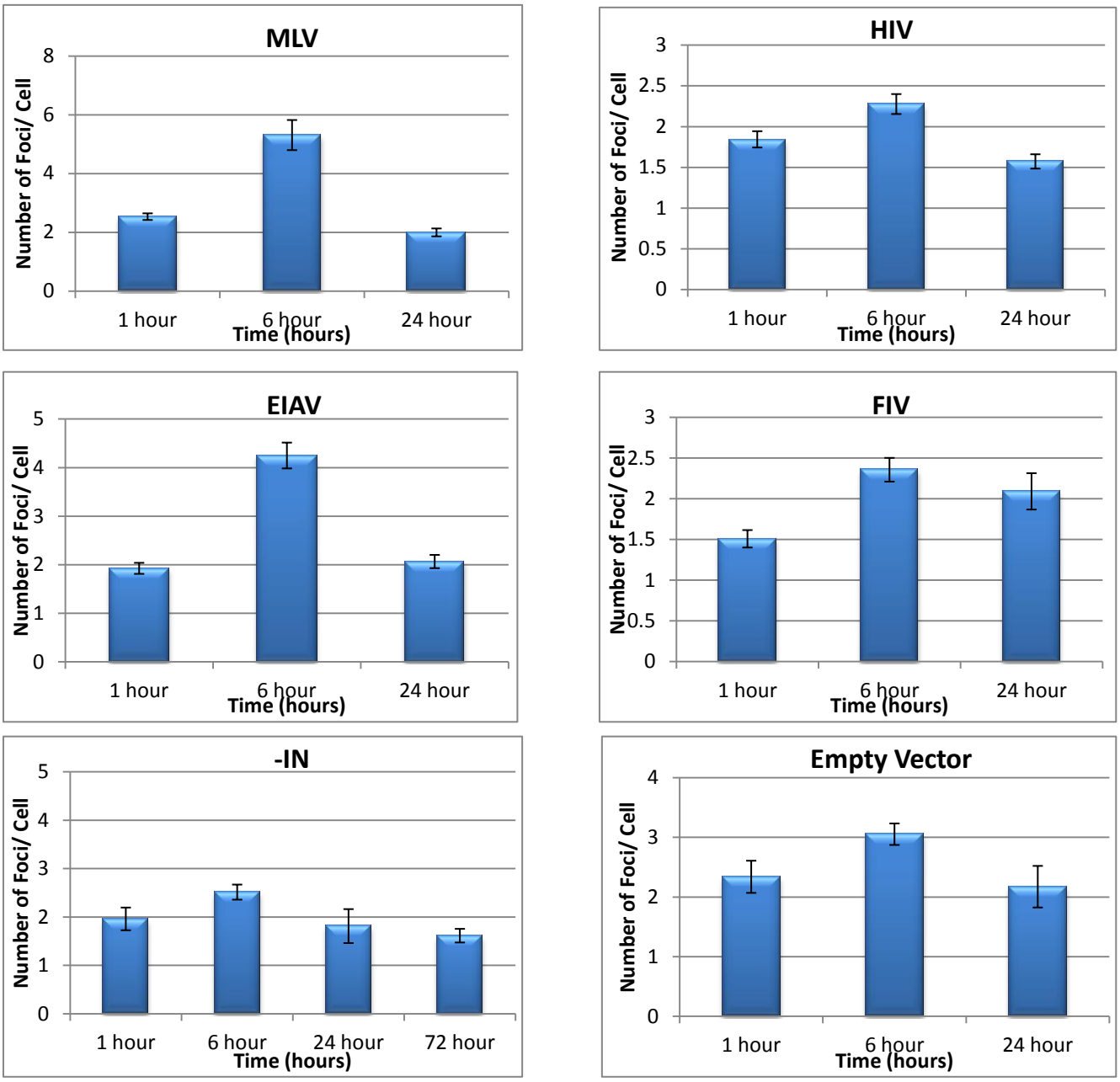

Histograms of the mean number of 53BP1 foci in MRC 5 cells infected at high and low MOI

Figures 24 a and b. represent values of the means and standard errors of Mrc5 53bp1 foci observed for each treatment. Infection was performed with RV and LV vectors at high (red) and low (blue) MOI. Un-infected Mrc5 cells have a mean of 1.81-2.17 foci per nuclei. IR cells at 30minutes have a peak foci number of 7.21 per nuclei that gradually decreases over a 24 hour period. Cells infected with the MLV vector at high MOI vector had the highest mean number of foci at 6 hours post infection with a mean of 10.57, compared with cells treated with other vectors. Cells infected with HIV mutated integrase vector showed similar mean foci patterns as the un-infected cells with a very slight peak at 6 hours.

Table 31a. Mean number of DSB foci in MRC5 nuclei at high MOI

Treatment		Time (hours)			
		1	6	24	72
Un-infected	MEAN (+/- SEM)	2.06 (0.23)	2.17 (0.24)	1.81 (0.35)	
	p-value		0.64	0.54	
	no of nuclei	139	146	85	
IR	MEAN (+/- SEM)	7.21 (0.36)	2.17 (0.20)	1.12 (0.10)	
	p-value		2.25E-12	1.25E-10	
	no of nuclei	457	183	425	
MLV	MEAN (+/- SEM)	5.96 (0.28)	10.57 (1.12)	4.11 (0.24)	
	p-value		0.00	1.82E-07	
	no of nuclei	368	128	329	
HIV	MEAN (+/- SEM)	4.49 (0.29)	8.28 (0.60)	3.72 (0.32)	
	p-value		4.06E-09	2.85E-09	
	no of nuclei	344	190	165	
EIAV	MEAN (+/- SEM)	4.41 (0.29)	8.25 (1.06)	2.75 (0.25)	
	p-value		0.00	1.51E-06	
	no of nuclei	387	102	269	
FIV	MEAN (+/- SEM)	3.04 (0.27)	6.81 (0.41)	3.51 (0.38)	
	p-value		6.28E-11	1.68E-07	
	no of nuclei	168	252	123	
IN-	MEAN (+/- SEM)	2.50 (0.13)	2.53 (0.14)	2.14 (0.16)	2.23 (0.13)
	p-value		0.92	0.38	0.96
	no of nuclei	369	372	226	409
Empty Vector	MEAN (+/- SEM)	7.54 (0.62)	8.53 (0.62)	4.11 (0.29)	
	p-value		0.16	1.40E-10	
	no of nuclei	214	195	197	

Table 31b. Mean number of DSB foci in MRC5 nuclei at low MOI

Treatment		Time (hours)			
		1	6	24	72
MLV	MEAN (+/- SEM)	2.53 (0.11)	5.30 (0.51)	1.99 (0.13)	
	p-value		2.64E-07	4.09E-09	
	no of nuclei	605	347	373	
HIV	MEAN (+/- SEM)	1.84 (0.10)	2.27 (0.12)	1.57 (0.09)	
	p-value		0.05	3.49E-06	
	no of nuclei	549	513	531	
EIAV	MEAN (+/- SEM)	1.92 (0.11)	4.25 (0.27)	2.06 (0.14)	
	p-value		1.04E-14	1.83E-12	
	no of nuclei	578	434	543	
FIV	MEAN (+/- SEM)	1.51 (0.11)	2.36 (0.15)	2.09 (0.22)	
	p-value		0.01	0.03	
	no of nuclei	458	580	212	
IN-	MEAN (+/- SEM)	1.96 (0.23)	2.51 (0.16)	1.81 (0.35)	1.61 (0.14)
	p-value		0.01	0.01	0.20
	no of nuclei	75	335	85	323
Empty Vector	MEAN (+/- SEM)	2.34 (0.27)	3.05 (0.18)	2.17 (0.35)	
	p-value		0.00	0.00	
	no of nuclei	177	297	104	

Mrc5 cells exposed to RV and LV vectors at high and low MOI are shown in table 31a and b.The DNA damage response (DDR) was measured using 53BP1 immuno-flourescence. Control positive cells were irradiated at 1Gy. Negative controls were cultured in an identical manner to virally infected cells and mock infected in the presence of 5µg/ml DEAE dextran. All infections used DEAE dextran at 5µg/ml. Following irradiation the DDR increases followed by repair over a 6 hour period. RV and LV infection appeared to occur over an approximate 6 hour period where a peak in the mean number of 53bp1 foci was observed. This is then followed by a reduction in foci believed due to DDR. All infected cells appear to show DDR. Where no viral integrase is present no DDR appears, however where the MLV vector is present with no genome DDR occurs. Calculated mean values, p-values obtained from standard t-test and number of nuclei counted are shown in the table.

Figure 25a. At5biva cells

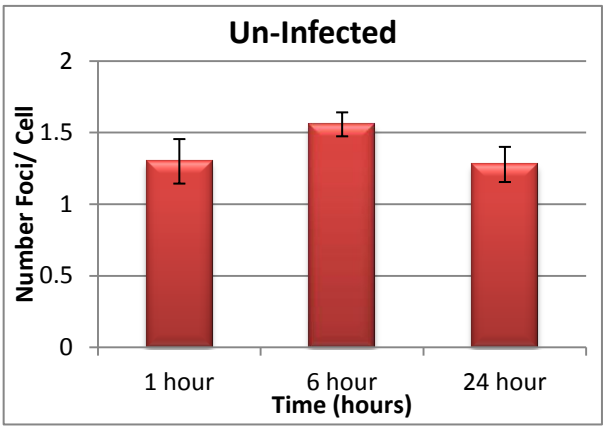

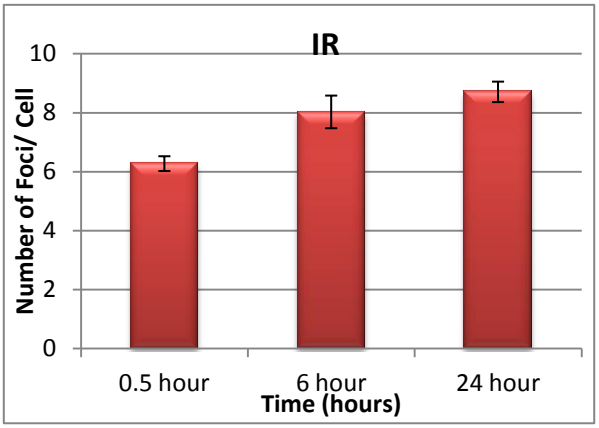

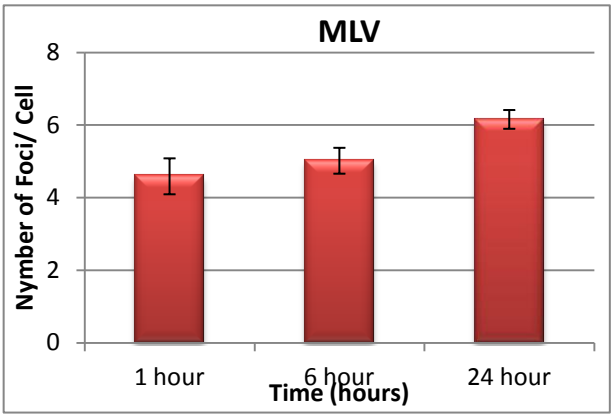

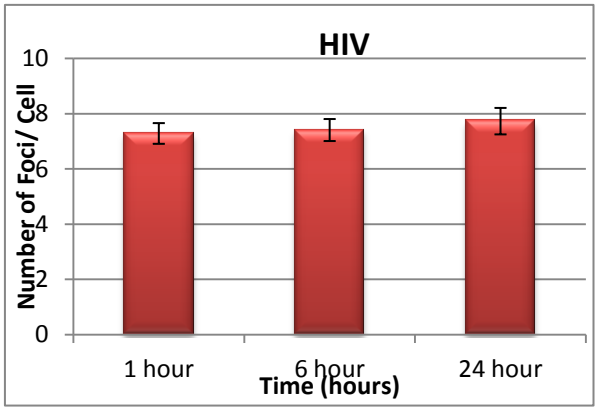

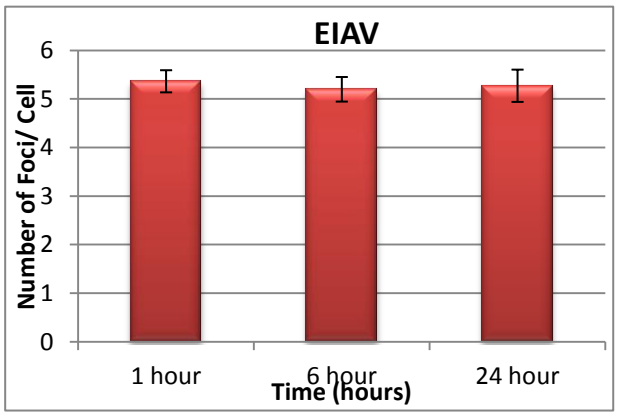

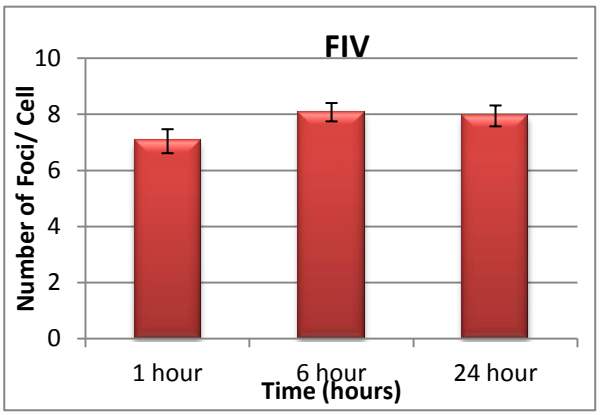

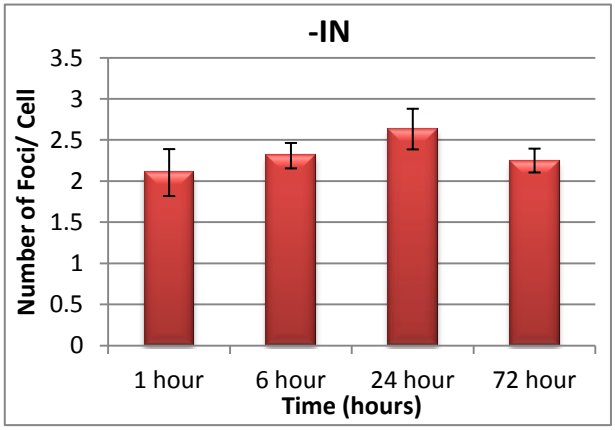

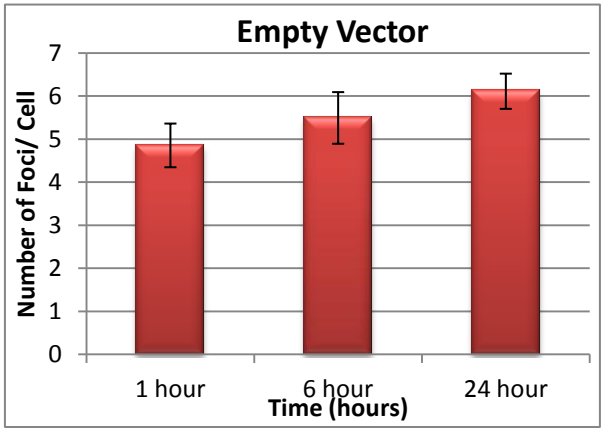

Figure 25b. At5biva cells

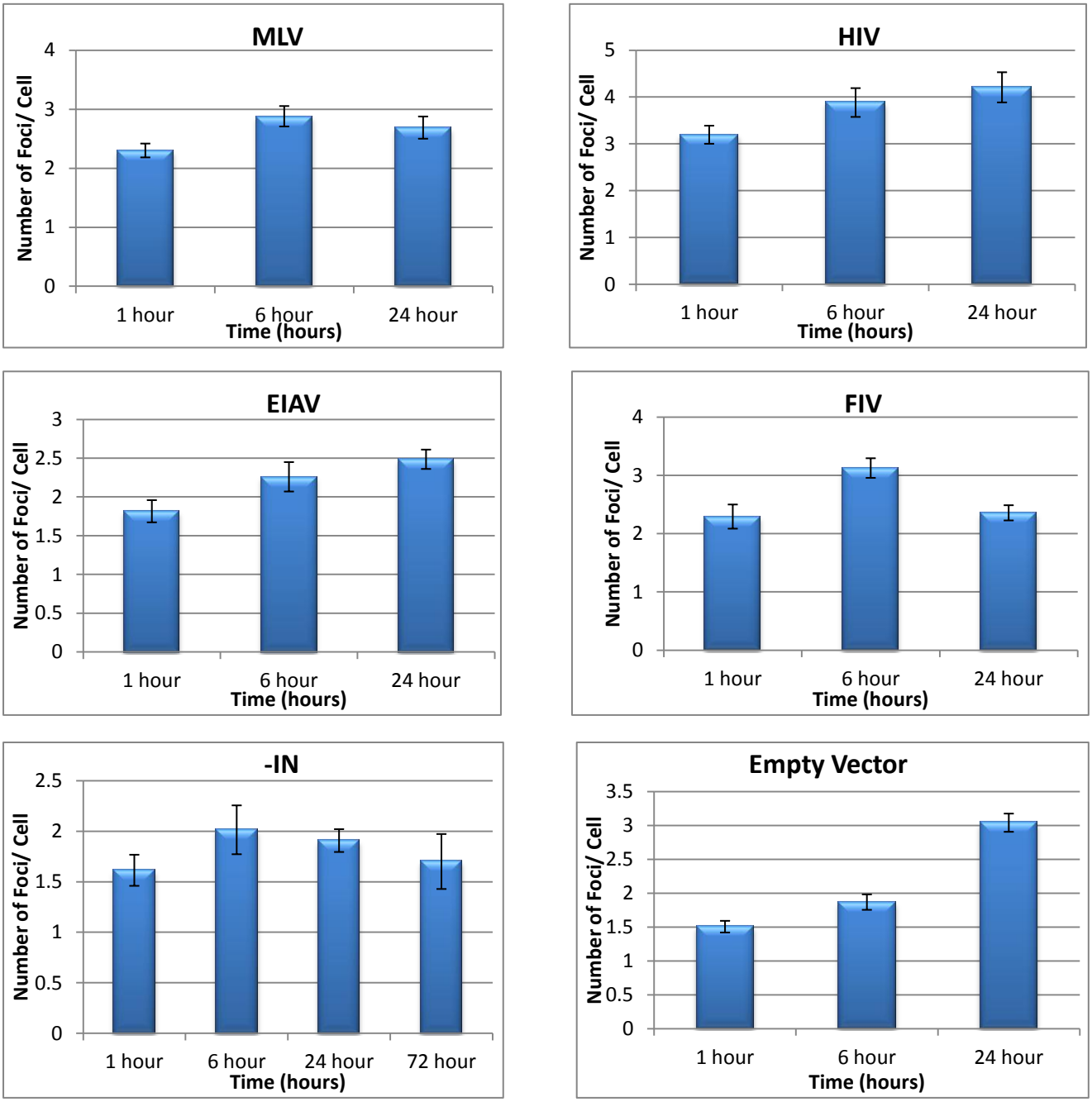

Histograms of the mean number of 53BP1 foci in At5biva cells infected at high and low MOI

Figures 25a and b represent values of the means and standard errors of At5biva 53bp1 foci observed for each treatment. Infection was performed with RV and LV vectors at high (red) and low (blue) MOI's. This cell line is repair deficient. Un-infected cells show a mean number of foci of 1.28-1.56 per nuclei. IR cells show foci number that increases up to the 24 hour period of measurement at 8.70 foci per nucleus.

Table 32a. Mean number of DSB foci in AT5BIVA nuclei at high MOI

Treatment		Time (hours)			
		1	6	24	72
Un-infected	MEAN (+/- SEM)	1.30 (0.16)	1.56 (0.08)	1.28 (0.12)	
	p-value		0.16	0.35	
	no of nuclei	459	483	300	
IR	MEAN (+/- SEM)	6.27 (0.25)	8.02 (0.55)	8.70 (0.35)	
	p-value		0.04	0.03	
	no of nuclei	496	179	440	
MLV	MEAN (+/- SEM)	4.58 (0.50)	5.01 (0.36)	6.15 (0.26)	
	p-value		0.39	0.02	
	no of nuclei	91	360	464	
HIV	MEAN (+/- SEM)	7.28 (0.38)	7.41 (0.40)	7.73 (0.48)	
	p-value		0.02	0.01	
	no of nuclei	303	478	185	
EIAV	MEAN (+/- SEM)	5.36 (0.23)	5.20 (0.25)	5.27 (0.33)	
	p-value		0.80	0.98	
	no of nuclei	558	377	280	
FIV	MEAN (+/- SEM)	7.04 (0.43)	8.08 (0.33)	7.94 (0.37)	
	p-value		0.03	0.69	
	no of nuclei	314	425	364	
IN-	MEAN (+/- SEM)	2.11 (0.29)	2.31 (0.15)	2.63 (0.25)	2.25 (0.14)
	p-value		0.70	0.22	0.43
	no of nuclei	133	277	183	251
Empty Vector	MEAN (+/- SEM)	4.86 (0.51)	5.50 (0.60)	6.12 (0.41)	
	p-value		0.80	0.04	
	no of nuclei	141	288	163	

Table 32b. Mean number of DSB foci in AT5BIVA nuclei at low MOI

Treatment		Time (hours)			
		1	6	24	72
MLV	MEAN (+/- SEM)	2.30 (0.12)	2.88 (0.17)	2.69 (0.19)	
	p-value		0.01	0.89	
	no of nuclei	398	407	274	
HIV	MEAN (+/- SEM)	3.19 (0.19)	3.88 (0.31)	4.21 (0.32)	
	p-value		0.14	0.19	
	no of nuclei	272	255	222	
EIAV	MEAN (+/- SEM)	1.82 (0.14)	2.26 (0.19)	2.49 (0.12)	
	p-value		0.03	0.15	
	no of nuclei	299	288	450	
FIV	MEAN (+/- SEM)	2.29 (0.21)	3.13 (0.17)	2.36 (0.13)	
	p-value		0.00	0.00	
	no of nuclei	221	348	399	
IN-	MEAN (+/- SEM)	1.61 (0.15)	2.01 (0.24)	1.91 (0.11)	1.7 (0.27)
	p-value		0.57	0.37	0.54
	no of nuclei	243	72	442	250
Empty Vector	MEAN (+/- SEM)	1.51 (0.09)	1.89 (0.11)	3.04 (0.13)	
	p-value		0.02	1.30E-05	
	no of nuclei	435	440	611	

At5biva cells exposed to RV and LV vectors at high and low MOI are shown in table 32a and b. The DNA damage response (DDR) was measured using 53BP1 immunoflourescence. Control positive cells were irradiated at 1Gy. Negative controls were cultured in an identical manner to virally infected cells and mock infected in the presence of 5µg/ml DEAE dextran. All infections used DEAE dextran at 5µg/ml. At5biva are deficient in DDR thus following irradiation instead of eventually decreasing in DSB (foci) the level increases. This is also found for the virus infected cells. Mean, p-values obtained from standard t-test and number of nuclei counted are all shown in the table.

Figure 26a.Xp14br cells

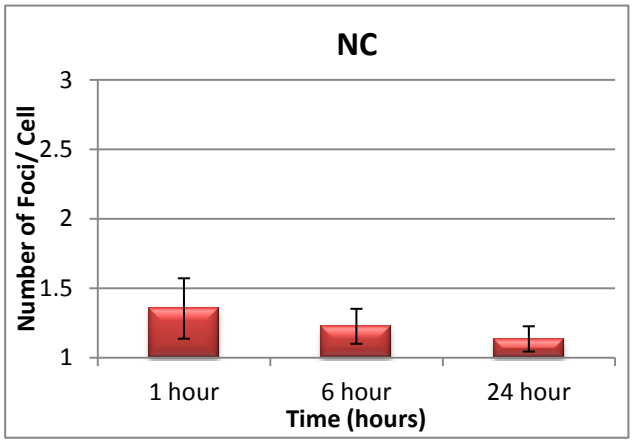

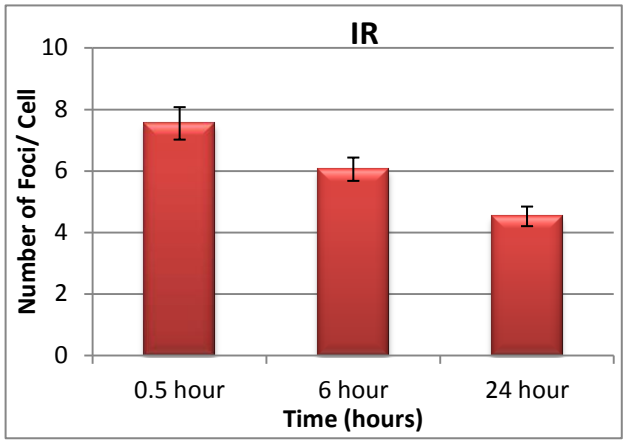

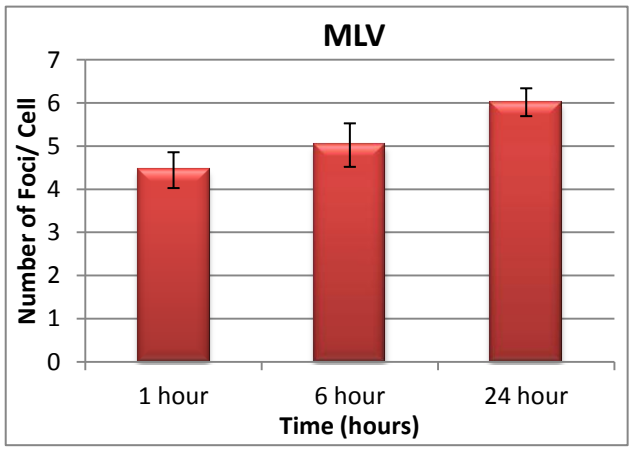

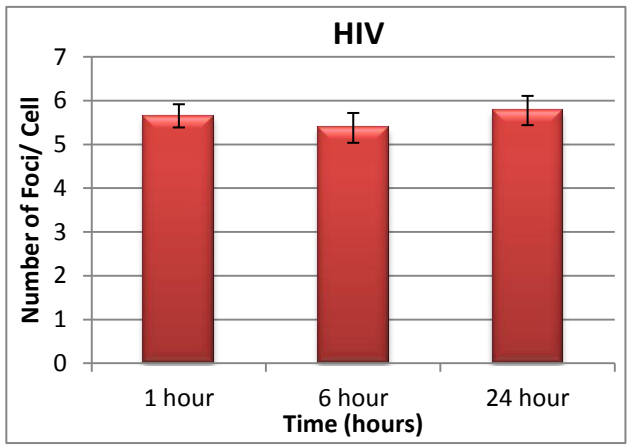

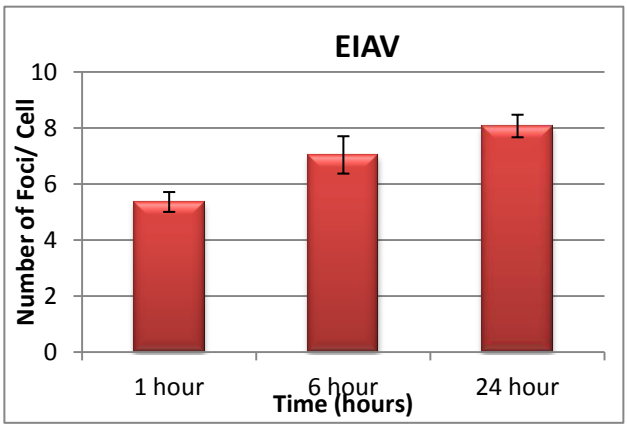

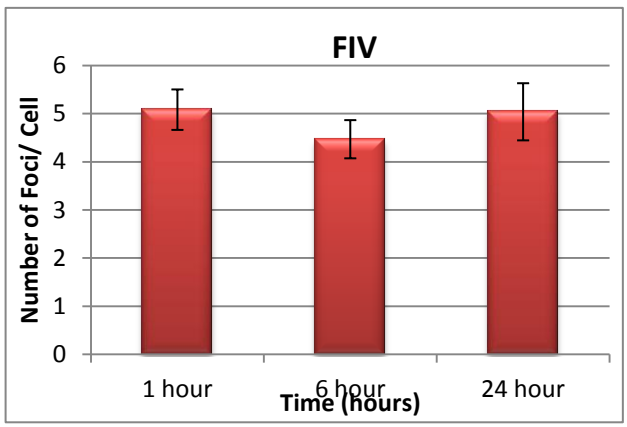

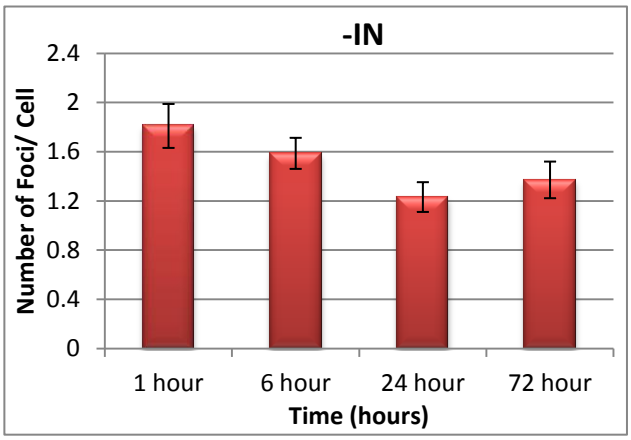

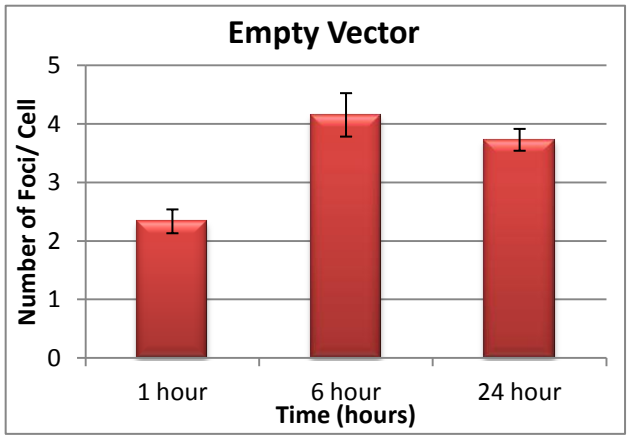

Figure 26b. Xp14br cells

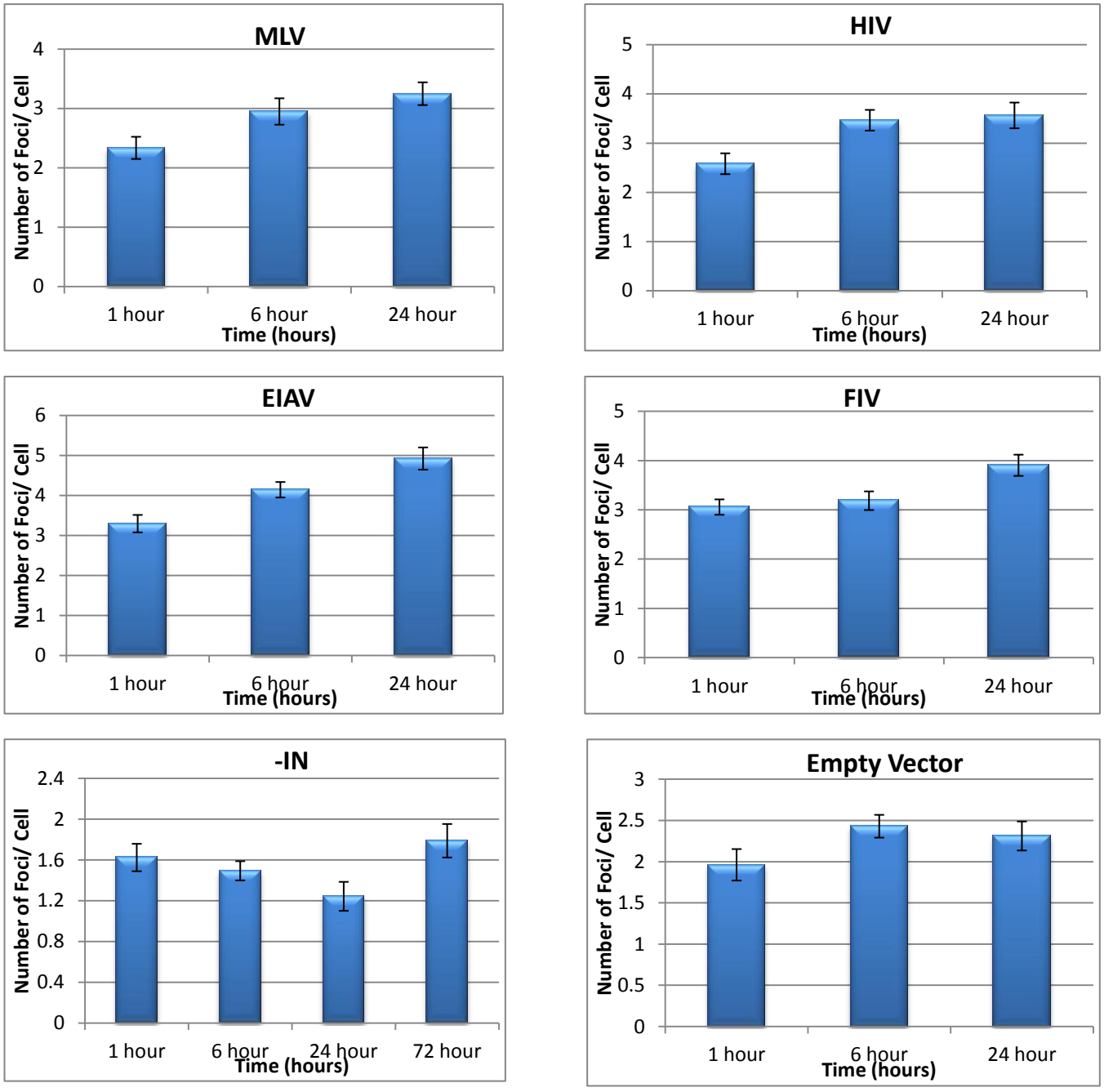

Histograms of the mean number of 53BP1 foci in Xp14br cells infected at high and low MOI

Figures 26a and b represent values of the means and standard errors of Xp14br 53bp1 foci observed for each treatment. Infection was performed with RV and LV vectors at high (red) and low (blue). DDR does not take place in these cells in contrast to cells with intact DDR pathways such as Mcf10a OR Mrc5.

Table 33a. Mean number of DSB foci in XP14BR nuclei at high MOI

Treatment		Time (hours)			
		1	6	24	72
Un-infected	MEAN (+/- SEM)	1.35 (0.22)	1.23 (0.13)	1.13 (0.09)	
	p-value		0.63	0.49	
	no of nuclei	297	293	424	
IR	MEAN (+/- SEM)	7.54 (0.53)	6.05 (0.38)	4.52 (0.32)	
	p-value		0.01	0.00	
	no of nuclei	246	252	226	
MLV	MEAN (+/- SEM)	4.44 (0.42)	5.02 (0.50)	6.02 (0.32)	
	p-value		0.44	0.34	
	no of nuclei	327	168	513	
HIV	MEAN (+/- SEM)	5.65 (0.27)	5.38 (0.34)	5.78 (0.33)	
	p-value		0.40	0.28	
	no of nuclei	519	291	30	
EIAV	MEAN (+/- SEM)	5.36 (0.35)	7.04 (0.67)	8.07 (0.40)	
	p-value		0.01	0.52	
	no of nuclei	201	182	297	
FIV	MEAN (+/- SEM)	5.08 (0.42)	4.47 (0.40)	5.04 (0.59)	
	p-value		0.34	0.91	
	no of nuclei	171	265	79	
IN-	MEAN (+/- SEM)	1.81 (0.18)	1.59 (0.13)	1.23 (0.12)	1.37 (0.15)
	p-value		2.54E-05	0.88	0.53
	no of nuclei	219	340	300	295
Empty Vector	MEAN (+/- SEM)	2.33 (0.20)	4.15 (0.37)	3.73 (0.19)	
	p-value		1.68E-05	0.77	
	no of nuclei	488	182	448	

Table 33b. Mean number of DSB foci in XP14BR nuclei at low MOI

Treatment		Time (hours)			
		1	6	24	72
MLV	MEAN (+/- SEM)	2.33 (0.19)	2.95 (0.22)	3.25 (0.19)	
	p-value		0.00	1.76E-05	
	no of nuclei	628	424	326	
HIV	MEAN (+/- SEM)	2.58 (0.21)	3.46 (0.21)	3.56 (0.26)	
	p-value		0.01	0.81	
	no of nuclei	338	328	256	
EIAV	MEAN (+/- SEM)	3.30 (0.22)	4.14 (0.19)	4.92 (0.28)	
	p-value		0.08	0.00	
	no of nuclei	273	444	343	
FIV	MEAN (+/- SEM)	3.06 (0.16)	3.19 (0.19)	3.91 (0.22)	
	p-value		0.72	0.06	
	no of nuclei	383	419	510	
IN-	MEAN (+/- SEM)	1.62 (0.13)	1.49 (0.09)	1.24 (0.14)	1.79 (0.16)
	p-value		0.55	0.77	0.09
	no of nuclei	276	351	194	198
Empty Vector	MEAN (+/- SEM)	1.96 (0.19)	2.43 (0.14)	2.31 (0.18)	
	p-value		0.09	0.70	
	no of nuclei	237	393	465	

Xp14br cells exposed to RV and LV vectors at high and low MOI are shown in table 33a and b. The DNA damage response (DDR) was measured using 53BP1 immuno-flourescence. Control positive cells were irradiated at 1Gy. Negative controls were cultured in an identical manner to virally infected cells and mock infected in the presence of 5µg/ml DEAE dextran. All infections used DEAE dextran at 5µg/ml. Xp14br are deficient in DDR thus following irradiation instead of eventually decreasing in DSB (foci) the level increases. This is also found for the virus infected cells. Mean, p-values obtained from standard t-test and number of nuclei counted are all shown in the table.

By infecting Mcf10a and Mrc5 cells it was demonstrated that the expected normal repair of DSB occurs 6 hours post infection whereas for Xp14br and At5biva cells without intact pathways for DSB DBR did not take place. Instead, DSB foci remain constant as visualized by the presence of 53BP1 immuno staining up to the 24 hour time point where measurements ceased.

The highest number of foci recorded at 6 hours post infection in the Mcf10a cell line was induced by the MLV genome free vector. For the Mrc5 cell line this occurred with the MLV vector carrying a genome. The HIV integrase mutated vector (IN-) induced similar numbers of nuclei with foci to the un-infected Mcf10a and Mrc5 cells. At5biva and Xp14br infected cell lines demonstrated genotoxicity to their genomes after infection where DBR does not take place.

To measure the extent of DSB and the possible genotoxicity caused by integrative vectors on cell genomes, the frequency of DSB were compared between vectors.

Frequency of foci in MCF10A nuclei at high MOI 6 hours post infection

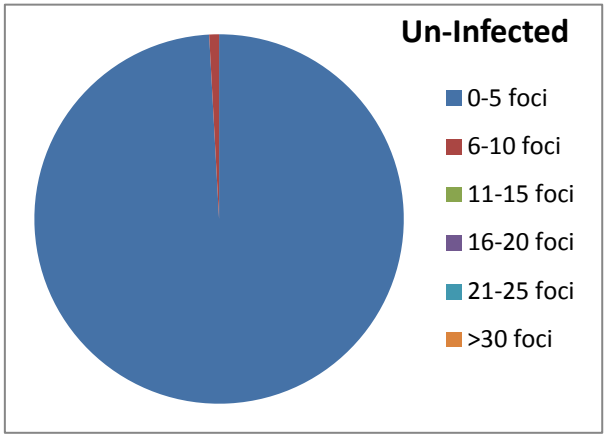

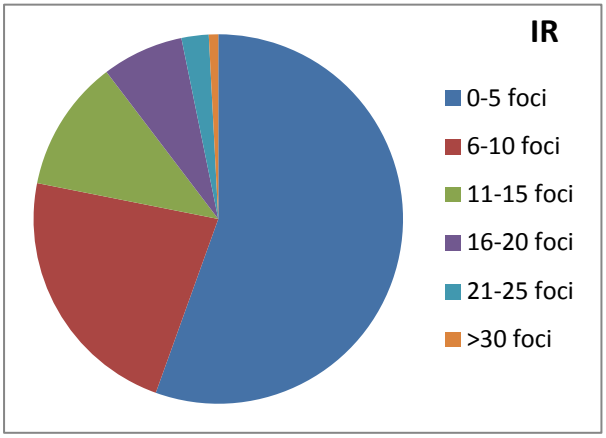

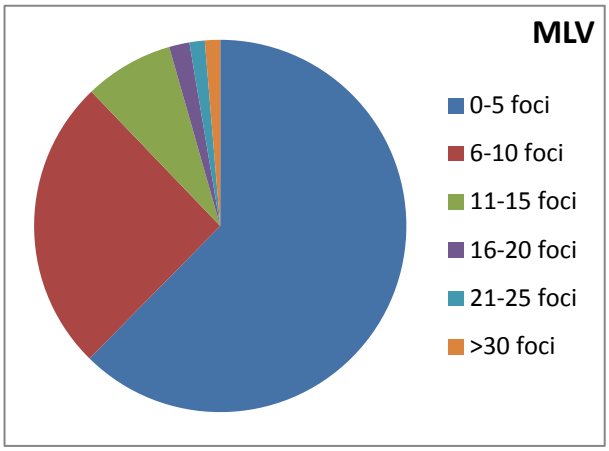

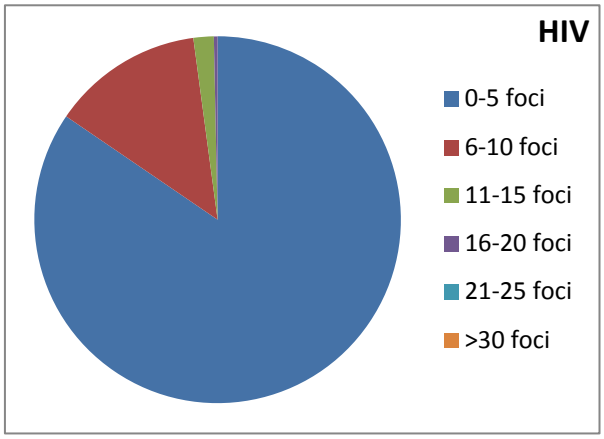

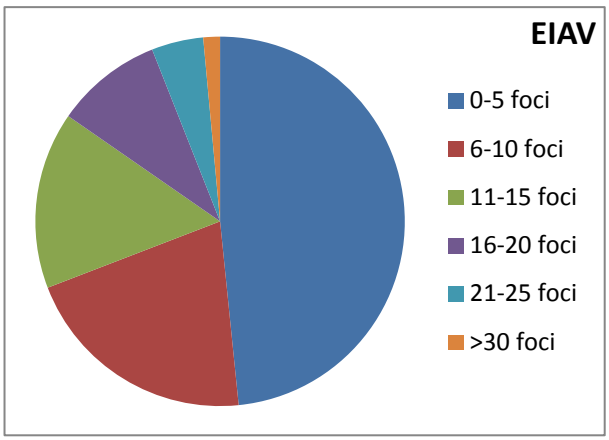

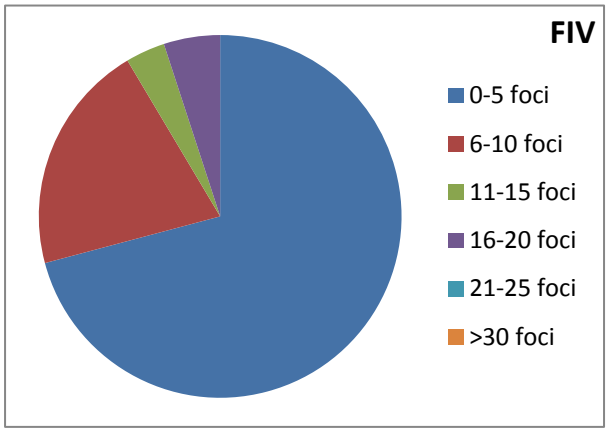

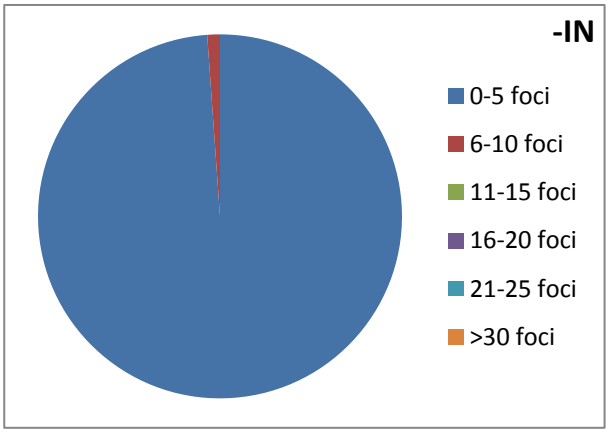

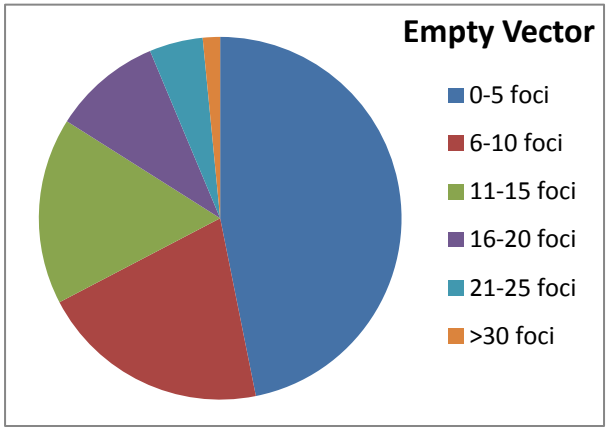

Frequency of foci in MCF10A nuclei at low MOI 6 hours post infection

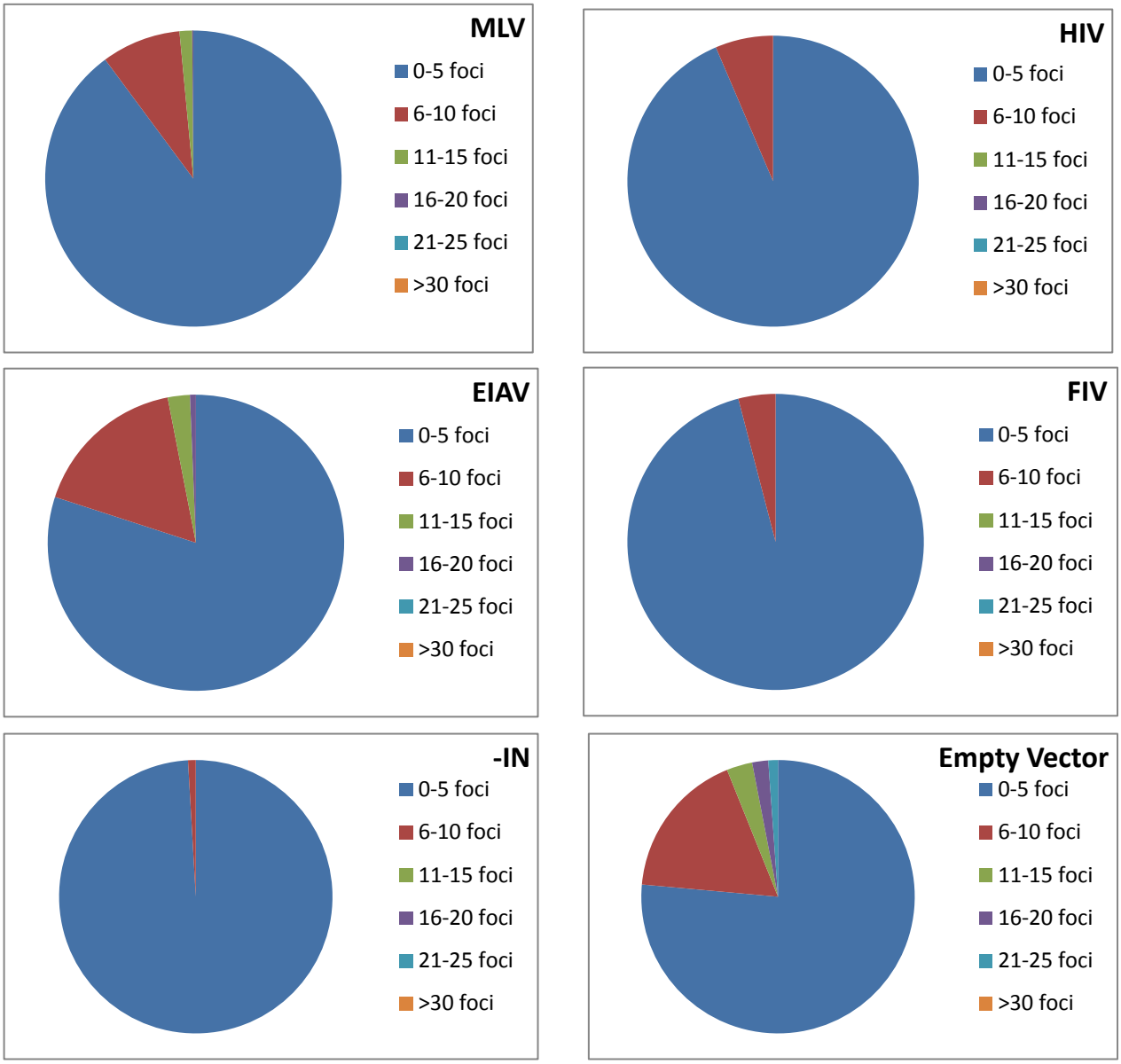

Figure 27. Pie charts representing the frequency of 53BP1 foci in Mcf10a nuclei at 6 hours post treatment with IR, MLV, HIV, EIAV, FIV, IN- and MLV without genome.

MLV and EIAV have similar profiles with regards to nuclei with 6-10 foci but on the whole EIAV appears to have nuclei with higher numbers of foci. FIV, which like EIAV is a non-primate LV, shows a similar profile to EIAV but without nuclei with high numbers of foci. Of all the vectors tested the HIV vector appears to have nuclei mainly very low numbers of foci. Interestingly, however, cells infected with the MLV vector without a genome (empty vector) appeared with nuclei the highest number of foci ranging from 0-5 up to more than 30 per nucleus. Also un-infected cells appeared with a similar range of nuclei to cells infected with integrase negative vector (IN-). Cells infected with vectors at low MOI followed a similar trend to those treated with vectors at high MOI albeit with fewer foci per nucleus.

Frequency of foci in MRC5 nuclei at high MOI 6 hours post infection

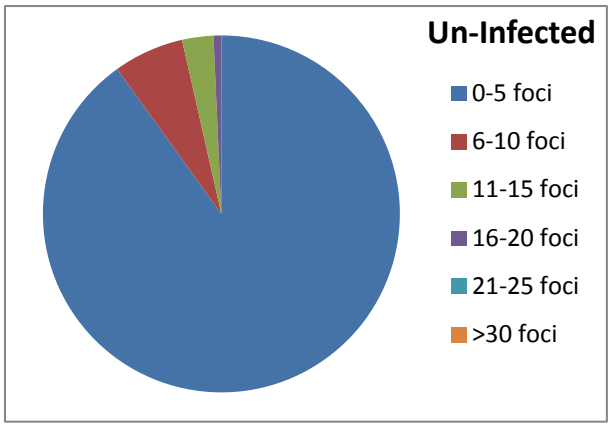

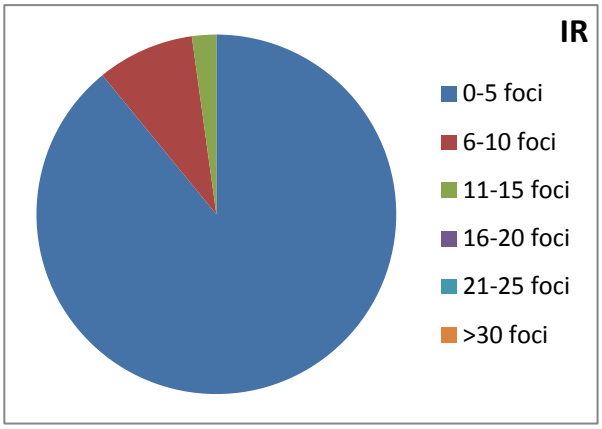

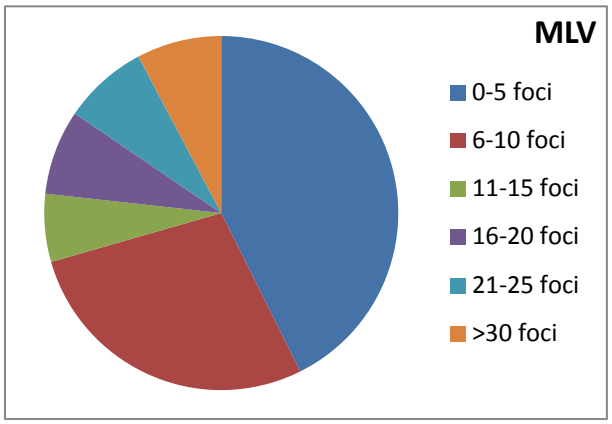

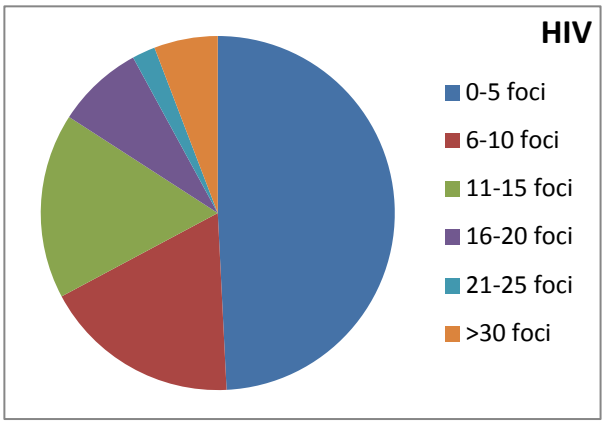

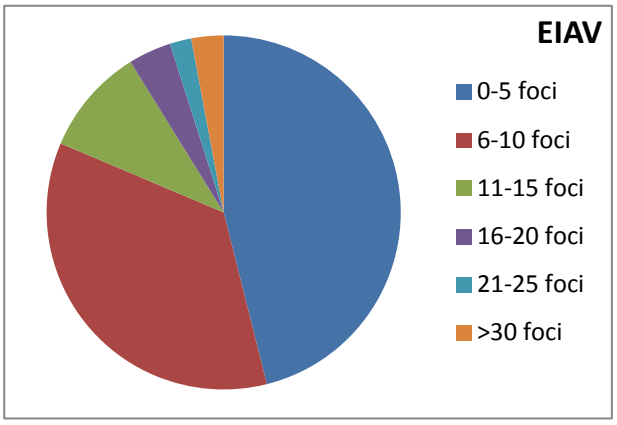

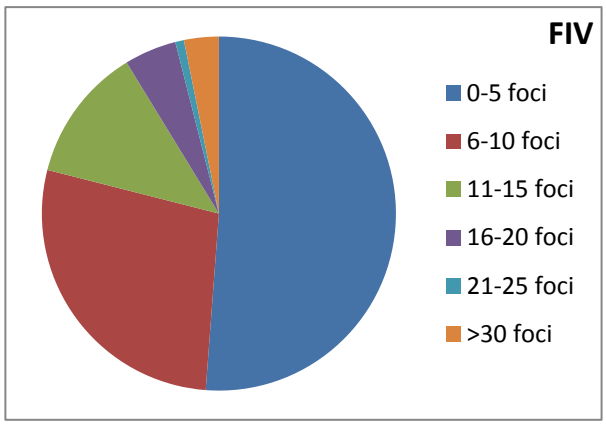

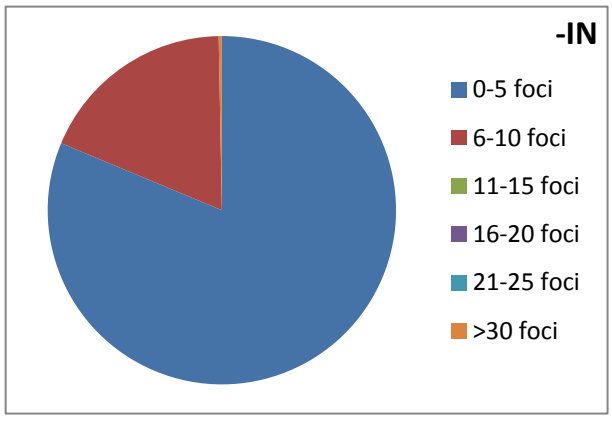

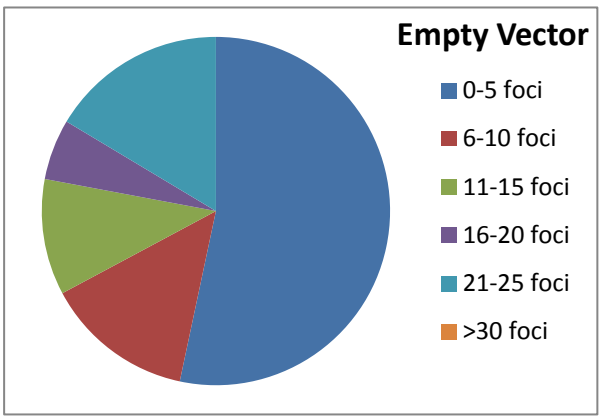

Frequency of foci in MRC5 nuclei at low MOI 6 hours post infection

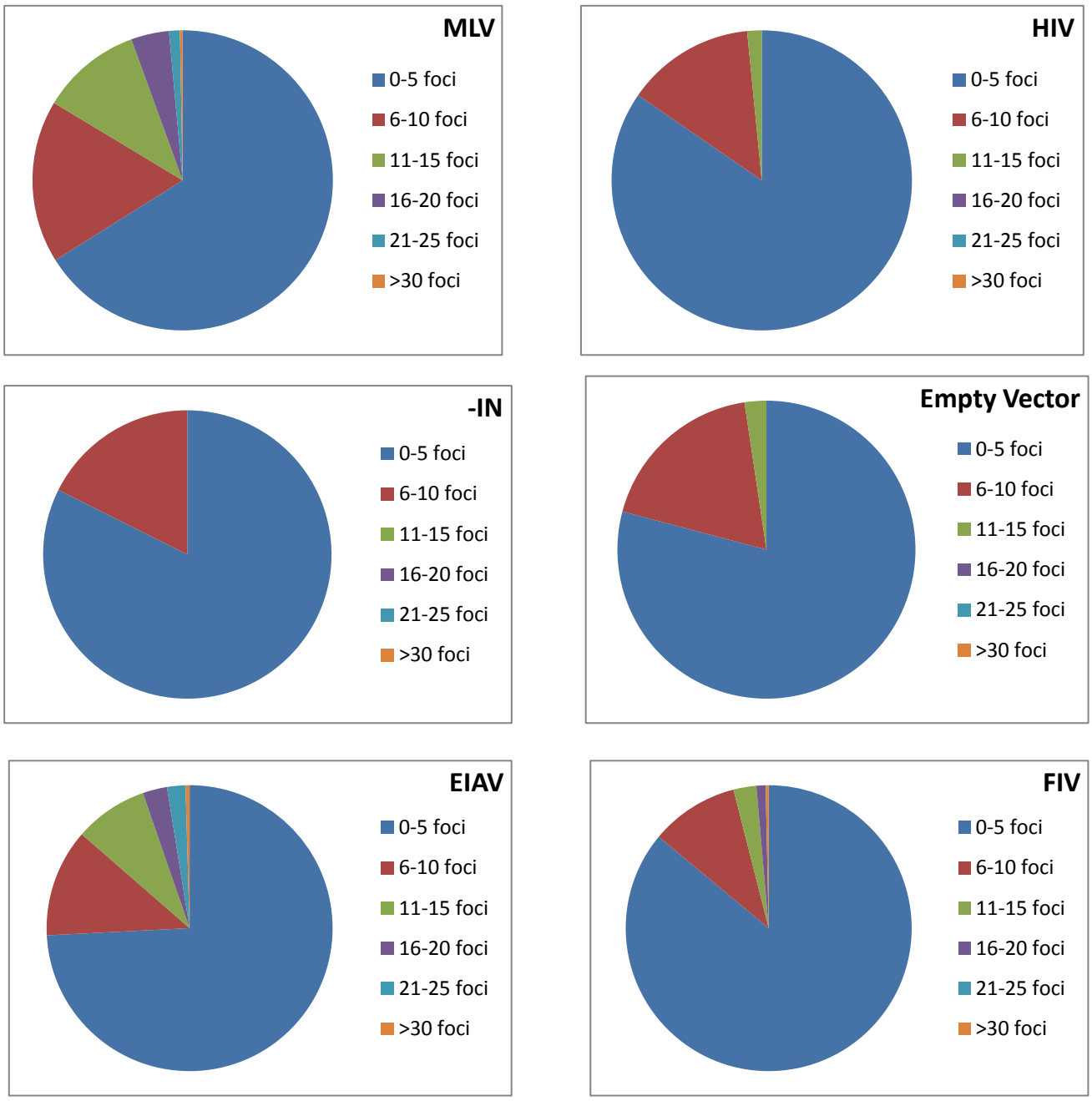

Figure 28. Pie charts representing the frequency of 53BP1 foci in Mrc5 nuclei at 6 hours post treatment with IR, MLV, HIV, EIAV, FIV, IN- and MLV without genome.

Cells infected with IN- and un-infected cells have similar profiles of 6-10 nuclei with foci. EIAV and FIV have very similar foci number in their nuclei. Interestingly, however, the MLV vector without a genome (empty vector) appeared with a more evenly distributed range of nuclei with foci from 6-10 up to more than 30. Vectors at low MOI followed a similar trend to the high MOI vectors however they had lower numbers of nuclei with foci.

Frequency of foci in AT5BIVA nuclei at high MOI 6 hours post infection

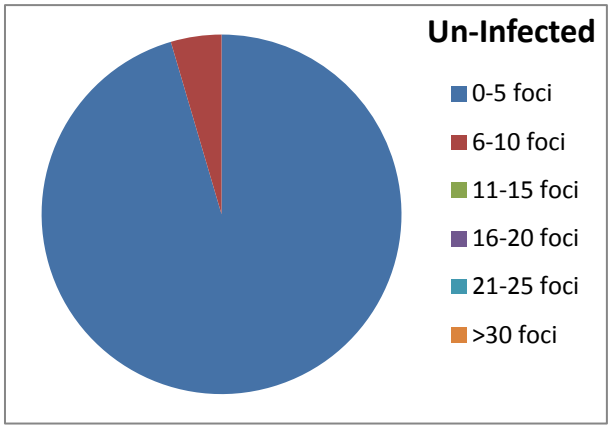

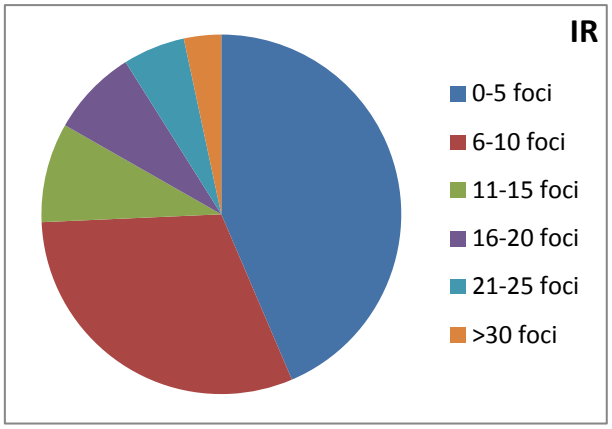

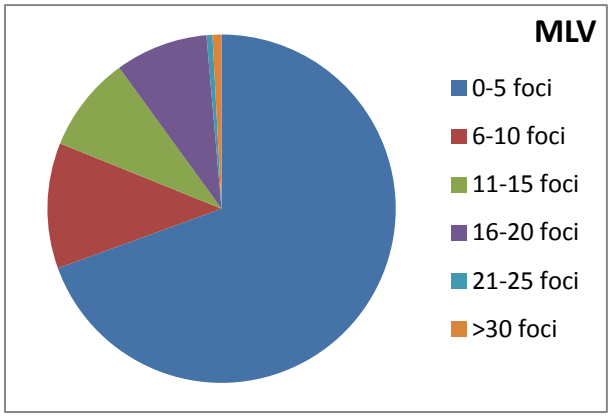

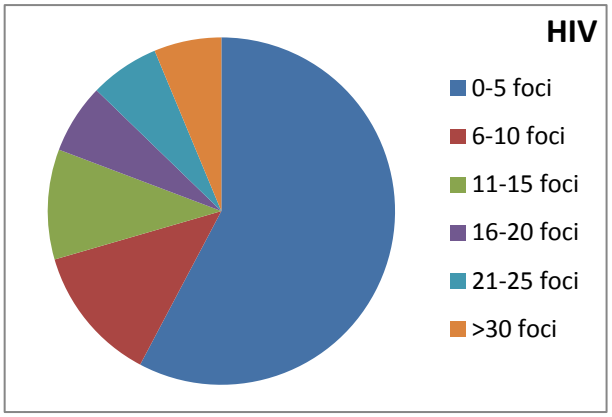

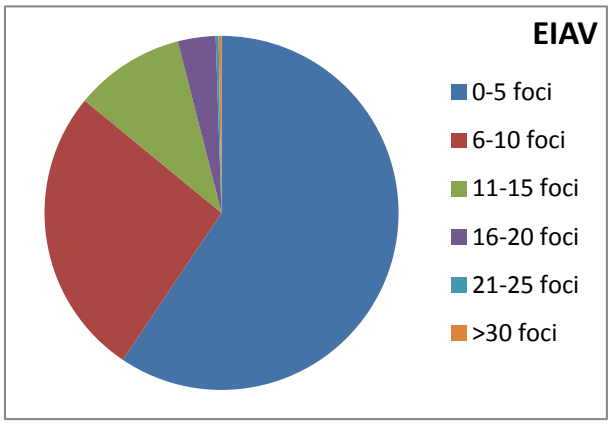

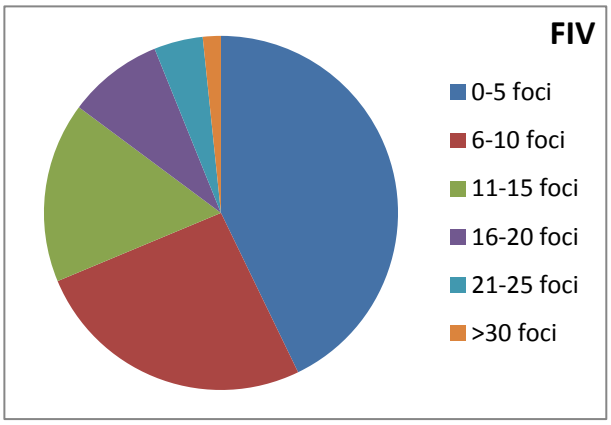

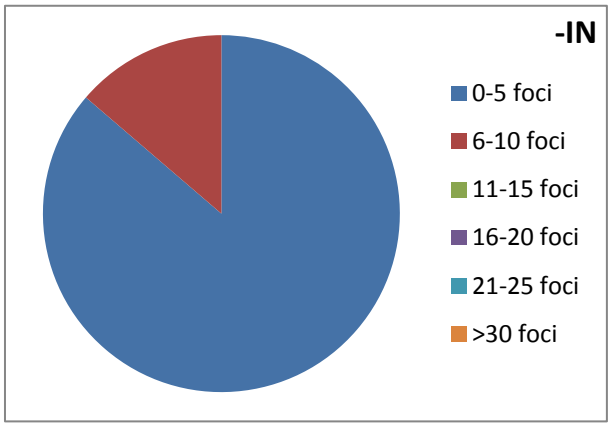

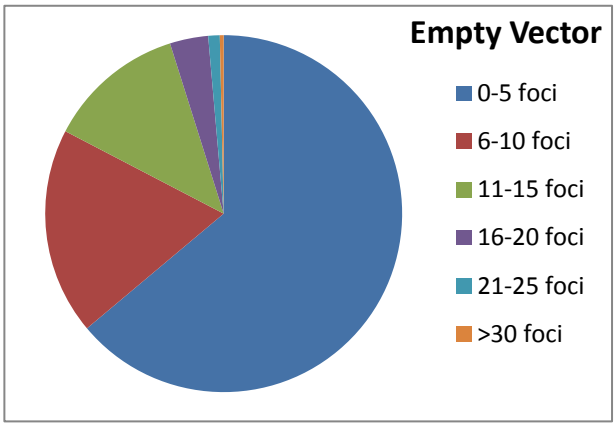

Frequency of foci in AT5BIVA nuclei at low MOI 6 hours post infection

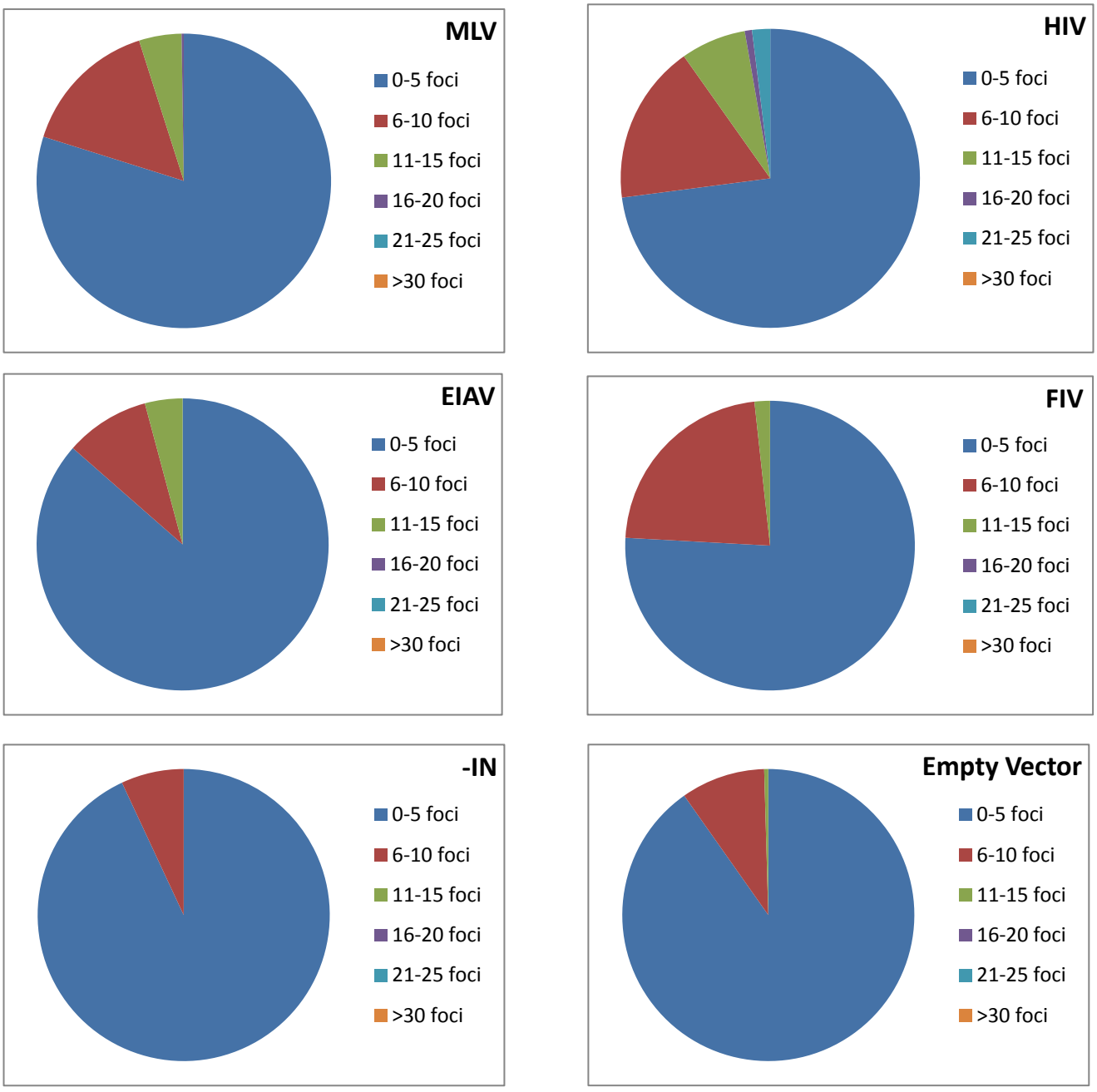

Figure 29. Pie charts representing the frequency of 53BP1 foci in At5biva nuclei at 6 hours post treatment with IR, MLV, HIV, EIAV, FIV, IN- and MLV without genome.

Cells either un-infected or infected with IN- vector showed the similar profiles of nuclei with foci. IR and MLV treated cells also follow a similar pattern to each other in regards to nuclei with foci from 0-5 to more than 30. Interestingly, FIV treated cells have a similar trend to cell infected with the MLV vector without a genome (empty vector). Vectors at low MOI followed similar trends to cells infected at high MOI vectors, however, with lower foci numbers.

Frequency of foci in XP14BR nuclei at high MOI 6 hours post infection

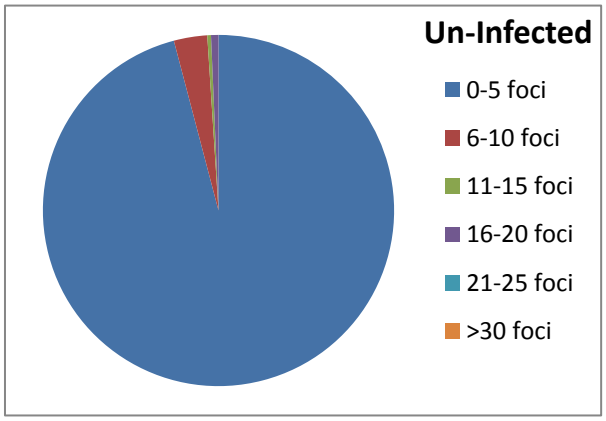

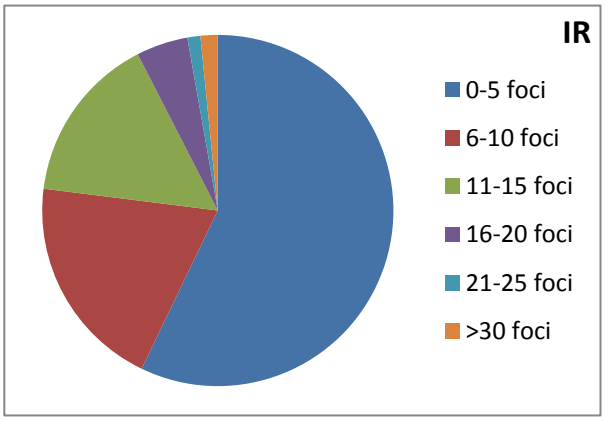

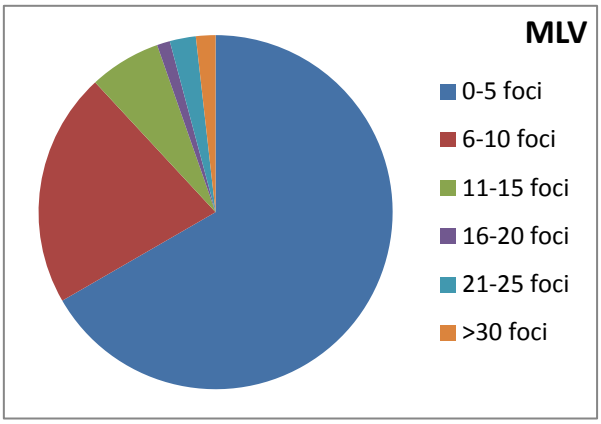

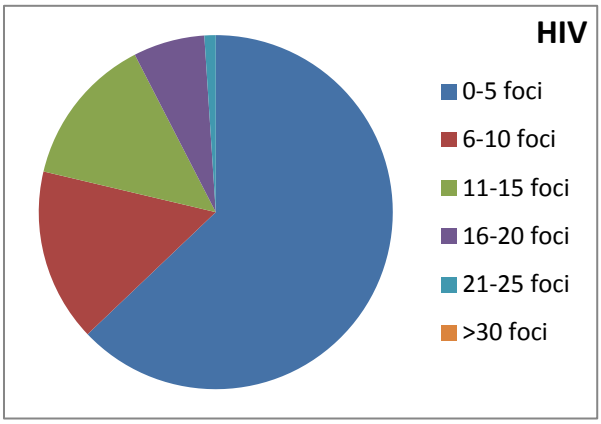

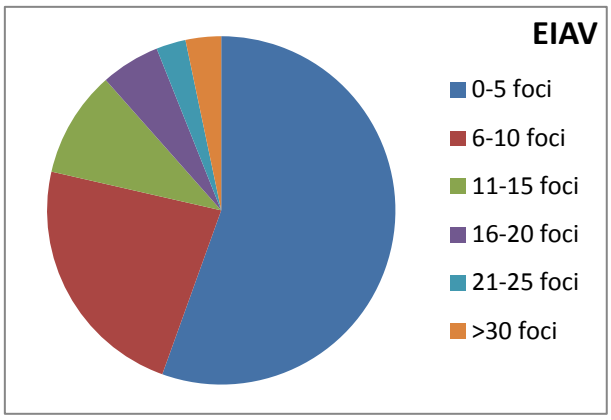

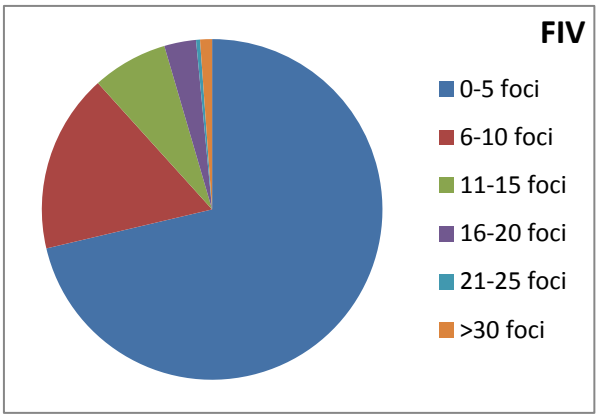

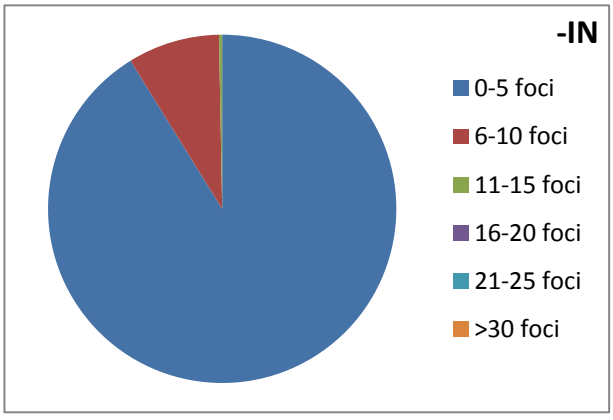

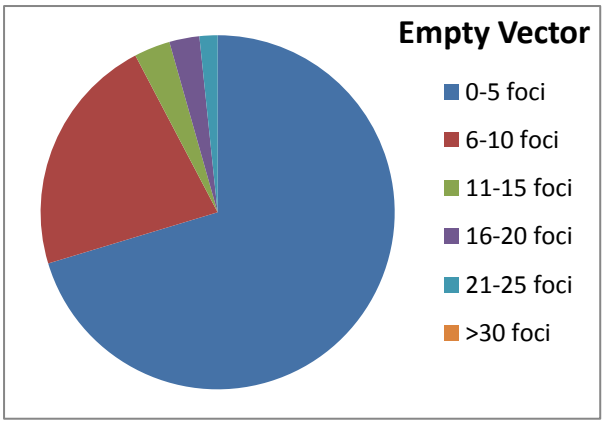

Frequency of foci in XP14BR nuclei at low MOI 6 hours post infection

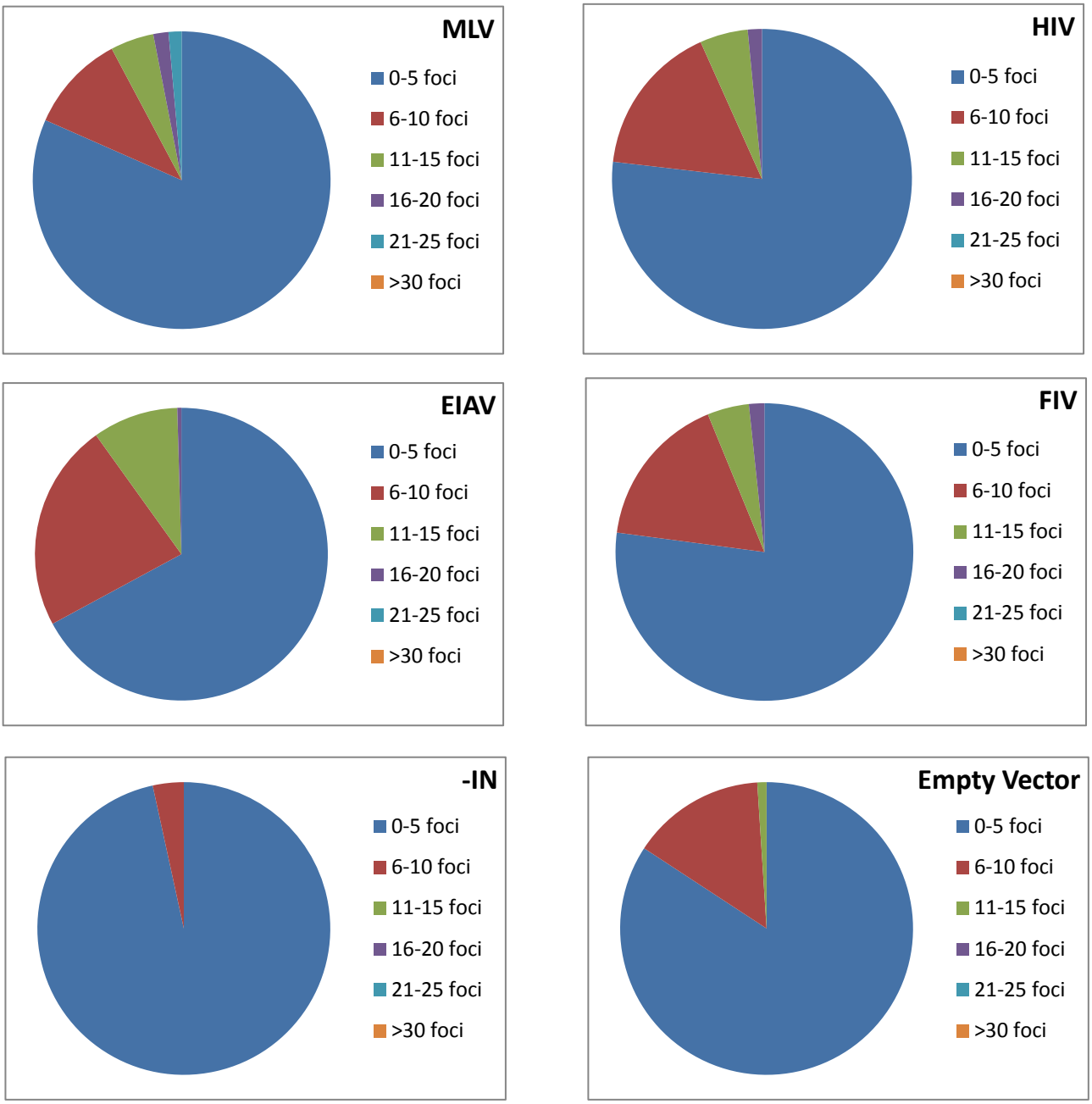

Figure 30. Pie charts representing the frequency of 53BP1 foci in Xp14br nuclei at 6 hours post treatment with IR, MLV, HIV, EIAV, FIV, IN- and MLV without genome.

Un-infected cells and cells infected with the IN- vector show similar trends with regards to nuclei that have mainly 0-5 foci. Cells treated by IR or with MLV, HIV, EIAV, FIV and the MLV vector without a genome show similar patterns in regards to the frequency of nuclei with foci. Cell infected with vectors at low MOI followed a similar trend to those treated with vector at high MOI, however, with nuclei with lower foci number.

The frequency pie charts show the number of nuclei in Mcf10a cells with 53BP1 positive foci to be similar to Mcf10a cells infected with the IN- HIV based vector and uninfected cells. This was also the case in Mrc5 cells. Mrc5 also appeared to show this trend, however, this cell line appears to be a more sensitive cell line to DNA damage with nuclei containing higher numbers of foci (6-10) than Mcf10a. The MLV vector containing no genome (empty vector) showed similar patterns to cells treated with the other vectors (excluding IN-). At5biva and Xp14br, which are cell lines that are repair deficient again showed similar trends to each other.

To determine whether DSB are repaired following infection of Mcf10a cell that contain intact DSB repair pathways whole chromosome analysis using muticolour fluorescent *in situ* hybridisation (mFISH) and G-banding chromosomes was then performed. This was to determine whether chromosome rearrangement occurs as a result of genome instability caused by infection.

4.2 An investigation of chromosome integrity using multicolour fluorescent *in situ* hybridisation (mFISH) and G-banding following infection

In the previous chapters 3 to 4 that described investigations of CGH for chromosome CNV in mouse tumours obtained by the *in vivo* study of the Themis group (Nowrouzi *et al*., 2012) and the occurrence of DSB and DBR after infection of cells *in vitro* with RV and LV, the next step was to examine the integrity of chromosomes in infected cells.

In collaboration with Dr Ruby Banerjee of the Wellcome trust the method of multicolour fluorescent *in situ* hybridisation (mFISH) and G-banding of chromosomes was used to analyze infected cells. To begin with, uninfected Mcf10a cells were characterized for their karyotype. This was followed by examination of these cells infected with MLV, EIAV and HIV vectors for chromosome aberrations. Cells for each treatment were given 2 weeks post infection before analysis to allow for any rearrangements to occur.

mFISH of Mcf10a cell without infection

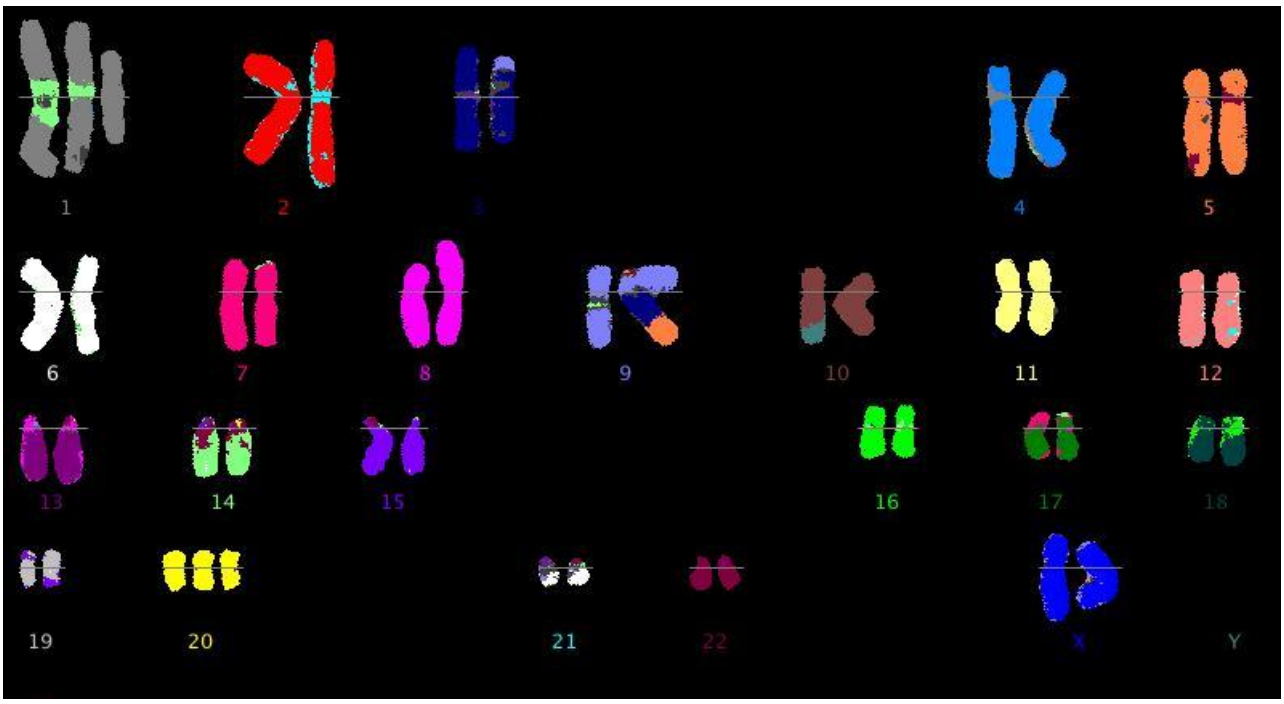

Pseudo G-banding of Mcf10a without infection

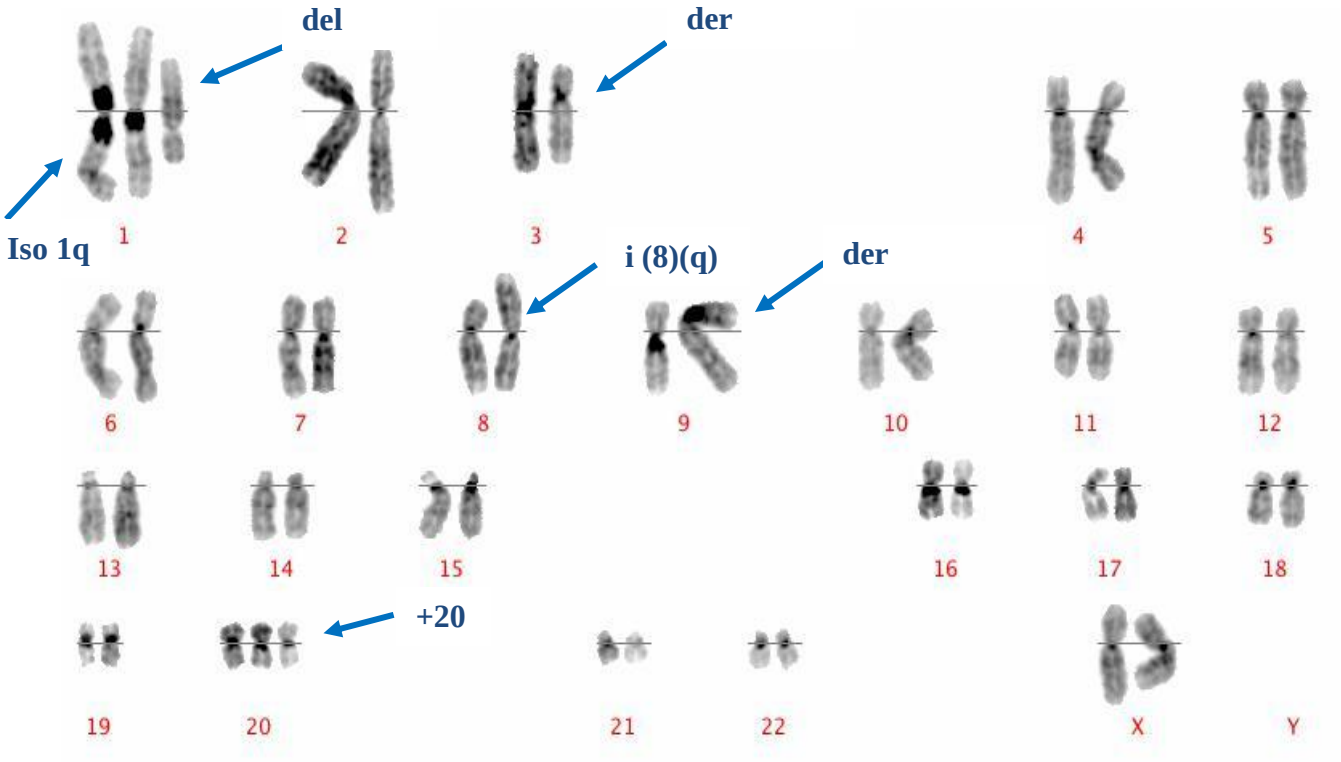

48 chromsomes, XX, i(1)(q)+del91)(q), der(3)t(3;9), i(8)(q), der(9)t(3;5;9)+20

Figure 31. mFISH and pseudo G-Banding of un-infected Mcf10a.

Structural aberrations (100%): chromosome 1- **i (1)(q) and del (1)(q)** showed an isochromosome on chromosome 1 involving q arm and partial deletion on 1q. Chromosome 3- **der (3)t(3;9)** showed a derivative chromosome 3 and translocation involving chromosome 3 and 9. Chromosome 8- **i (8)(q)** showed isochromosome on chromosome 8 involving q arm. Chromosome 9- **der (3)t(3;5;9)** Complex rearrangement involving chromosome 3,5 and 9. 40 metaphases were analysed. Numerical aberrations (100%) Chromosome 20- **(+20)** extra copy of chromosome 20.

The karyotype identified for the Mcf10a cell line appears to be identical to that reported by Cowell *et al* (2005) and therefore, these cells have not undergone any gross chromosomal changes during culturing in the laboratory (Cowell *et al.*, 2005). This provided a good basis to begin exploring the effects on these cells of virus infection. Mcf10a cells were infected with MLV at MOI of 200, EIAV at MOI of 20 and HIV at MOI of 50. Uninfected cells were treated in the same manner as infected cells except for exposure to RV and LV then grown for 2 weeks after which mFISH and G-banding was carried out.

mFISH of EIAV infected Mcf10a

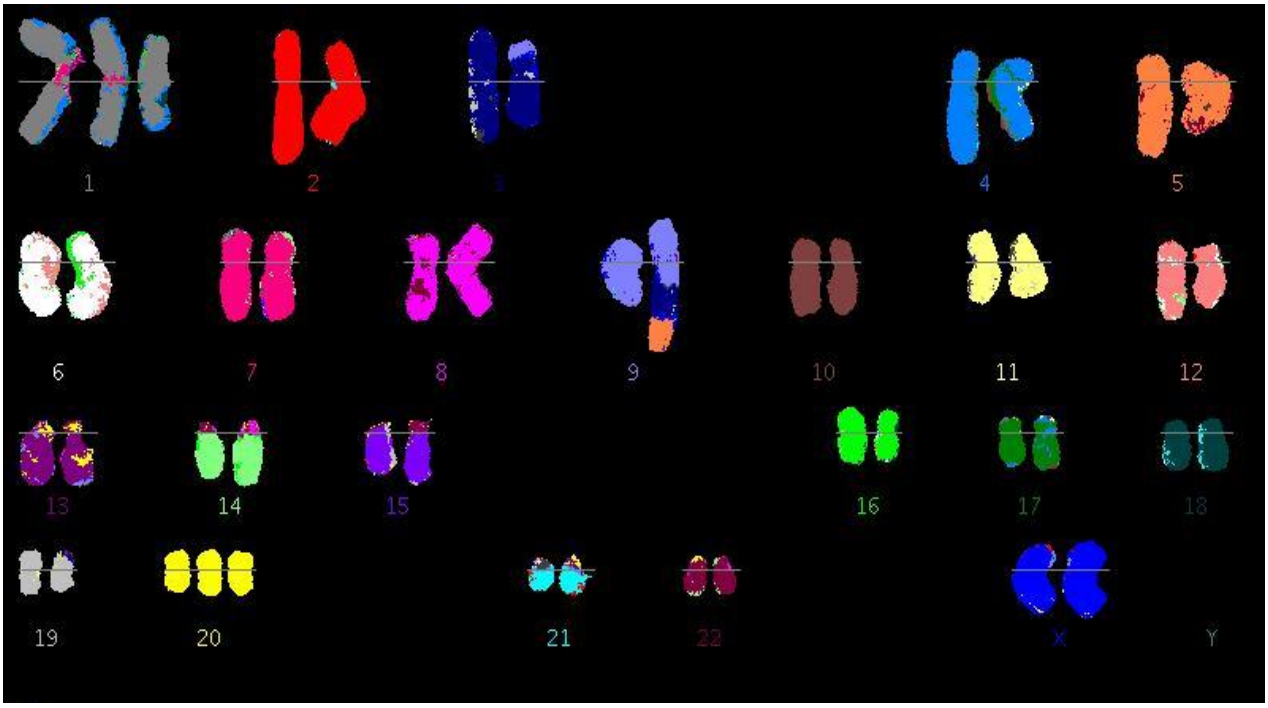

Pseudo G-banding of EIAV infected Mcf10a

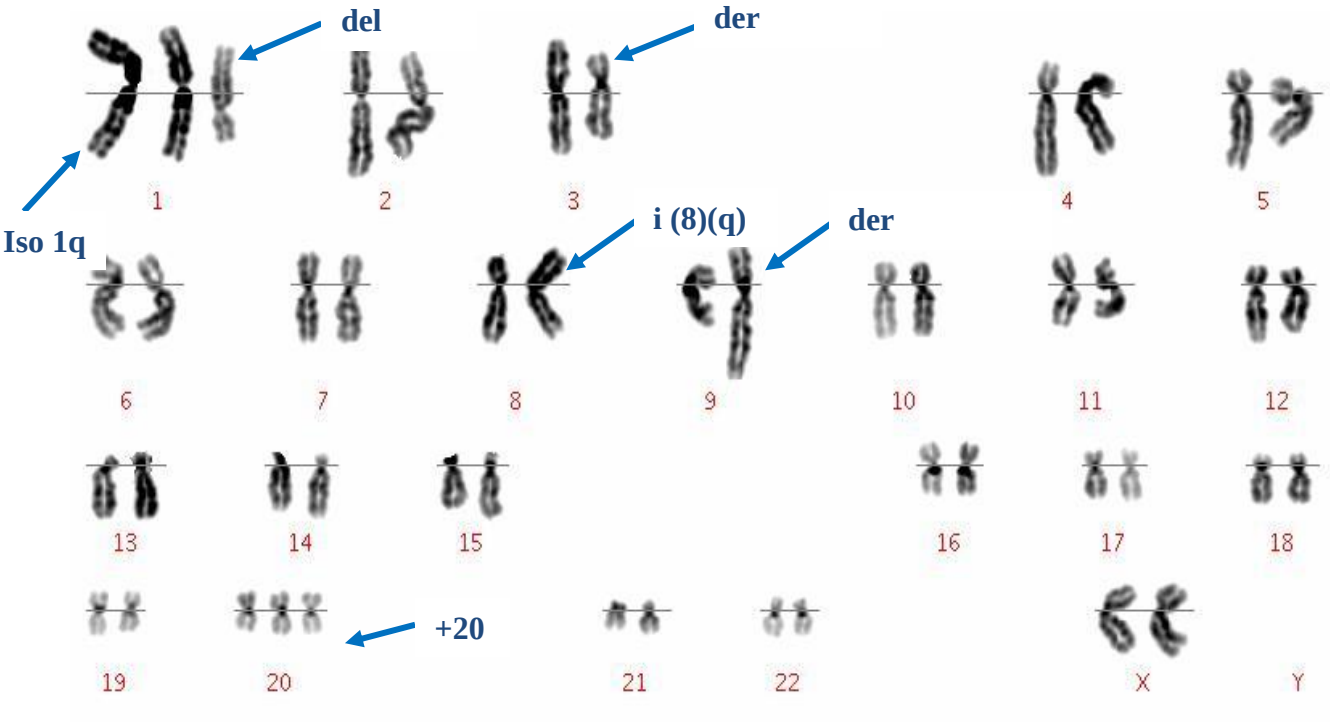

48 chromsomes, XX, i(1)(q)+del91)(q), der(3)t(3;9), i(8)(q), der(9)t(3;5;9)+20

mFISH of HIV infected Mcf10a

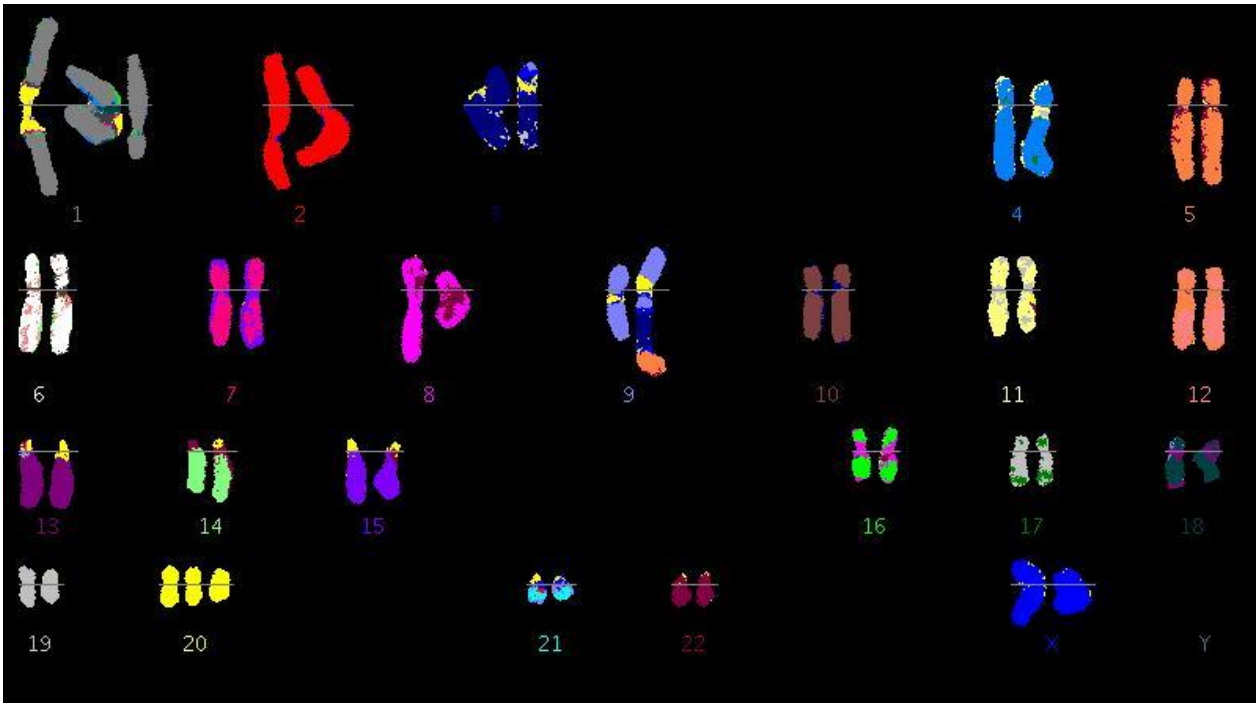

Pseudo G-banding of HIV infected Mcf10a

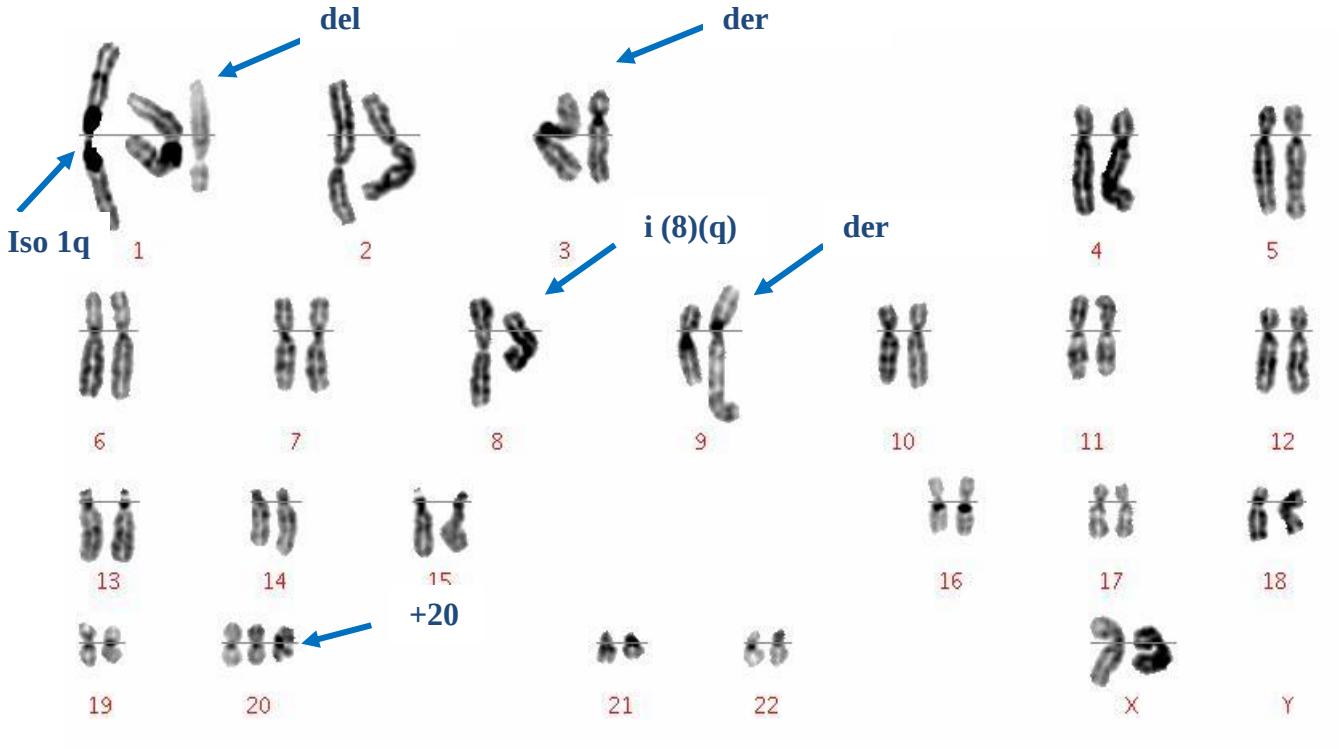

48 chromsomes, XX, i(1)(q)+del91)(q), der(3)t(3;9), i(8)(q), der(9)t(3;5;9)+20

mFISH of MLV infected Mcf10a

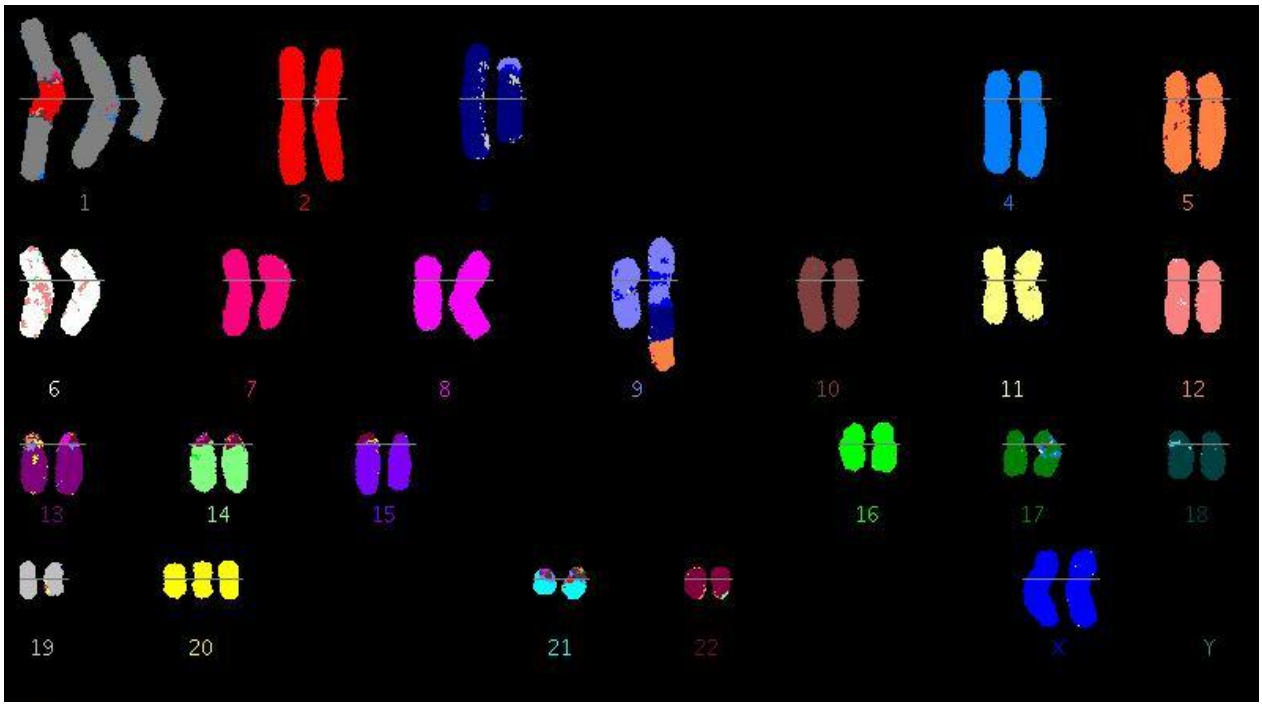

Pseudo G-banding of MLV infected Mcf10a

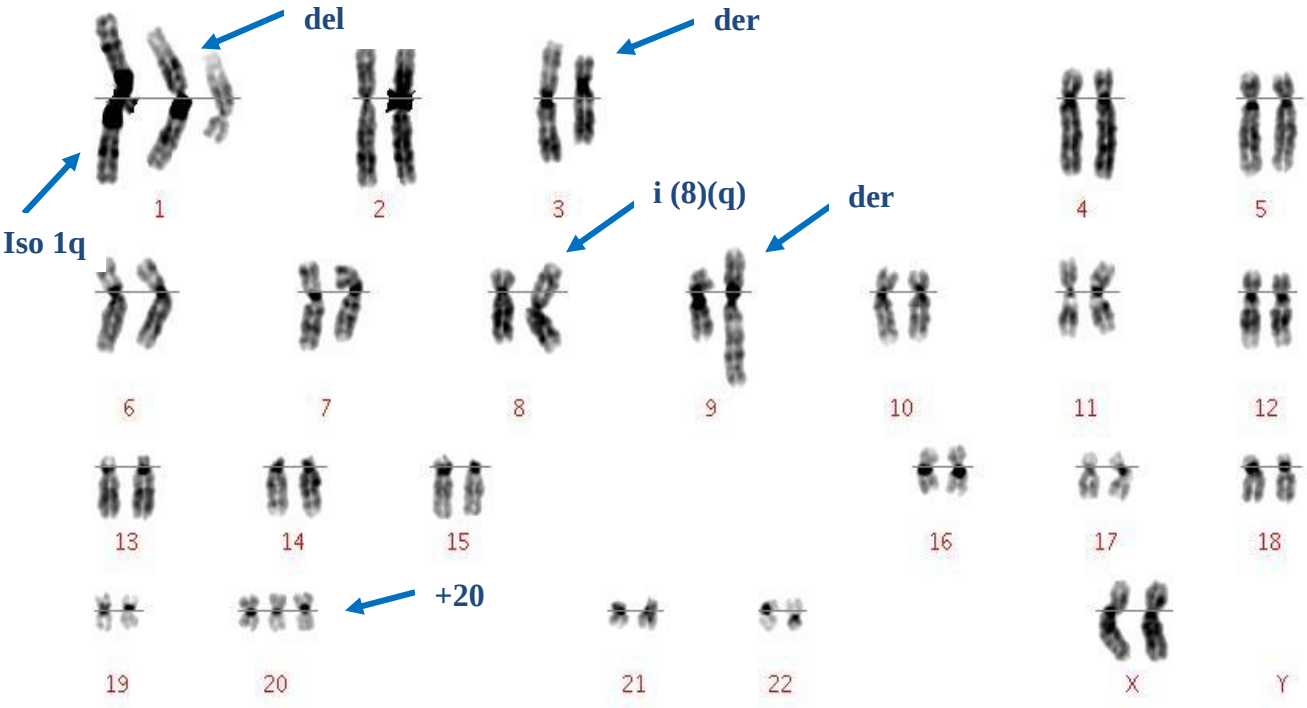

48 chromsomes, XX, i(1)(q)+del91)(q), der(3)t(3;9), i(8)(q), der(9)t(3;5;9)+20

Figure 32. mFISH and pseudo G-Banding of EIAV, HIV and MLV infected Mcf10a cells.

Structural aberrations (100%): chromosome 1- **i (1)(q) and del (1)(q)** showed an isochromosome on chromosome 1 involving q arm and partial deletion on 1q. Chromosome 3- **der (3)t(3;9)** showed a derivative chromosome 3 and translocation involving chromosome 3 and 9. Chromosome 8- **i (8)(q)** showed isochromosome on chromosome 8 involving q arm. Chromosome 9- **der (3)t(3;5;9)** Complex rearrangement involving chromosome 3,5 and 9. 40 metaphases analysed. Numerical aberrations (100%) Chromosome 20- **(+20)** extra copy of chromosome 20.

The karyotypes of Mcf10a infected with EIAV, HIV and MLV vectors were identical to that of uninfected cells demonstrating that 2 weeks after infection no gross chromosomal changes can be attributed to infection by RV or LV.

5.1 Epigenetic modification and E2F regulation of host genes following RV and LV vector delivery

5.1.1 The effects of RV and LV infection on host epigenetics via methylation

In previously published findings the group of Fang *et al* (2001) demonstrated a DNA damage response following LV infection to be linked to global methylation changes in lymphoblastoid cells. This was attributed to an immune response by cells via epigenetic changes to protect the host cell from infection (Fang *et al*., 2001). Epigenetic changes involve DNA methylation using DNA methyltransferases DNMT 1, 3a and 3b, where DNMT 3a and b are involved in establishing new methylation of DNA in cells and DNMT1 maintains methylation changes during division. In this chapter, the link between RV and LV infection and host methylation is further examined.

To investigate whether the response by cells to RV and LV infection is not specific to lymphoblastoid cells only, Mcf10a, HepG2 were infected with each of the MLV, HIV, EIAV, FIV vectors. DNA methylation response was measured at 3 time points (6 hours, 24 hours and 3 days) after infection. Analysis of global methylation changes and DNMT 1, 3a and 3b gene expression levels were performed. To determine whether methylation changes could be found related to the DDR, a 53BP1-/- cell line was also infected in the same manner as for M cf10a and HepG2 cells and the epigenetic response investigated. These cell lines were also infected with MLV, HIV, EIAV, FIV and MLV virus without genome vectors and examined at the same 3 time points (6 hours, 24 hours and 3 days) mentioned above post infection. To determine whether methylation changes were due to virus integration, cells were also infected with the integrase negative HIV vector.

Table 34. Measurement of global methylation in Mcf10a cells infected with RV and LV vectors

Sample	Time (hours)	Relative methylated levels (%) SEM
Un-infected	**6**	100 (0.01)
	24	100 (0.02)
	72	100 (0.02)
HIV	**6**	286.57 (0.03)
	24	121.21 (0.03)
	72	414.71 (0.08)
IN-	**6**	143.28 (0.01)
	24	154.55 (0.05)
	72	150.33 (0.02)
MLV	**6**	143.28 (0.01)
	24	272.73 (0.04)
	72	255.23 (0.01)
EIAV	**6**	205.97 (0.01)
	24	96.97 (0.00)
	72	33.33 (0.02)
Empty Vector	**6**	4423.88 (0.15)
	24	1262.63 (0.12)
	72	712.25 (0.07)

The experimental samples represent Mcf10a infected with the following vectors: MLV, HIV, IN- (HIV with mutated integrase), EIAV and Empty Vector (MLV without viral genome).

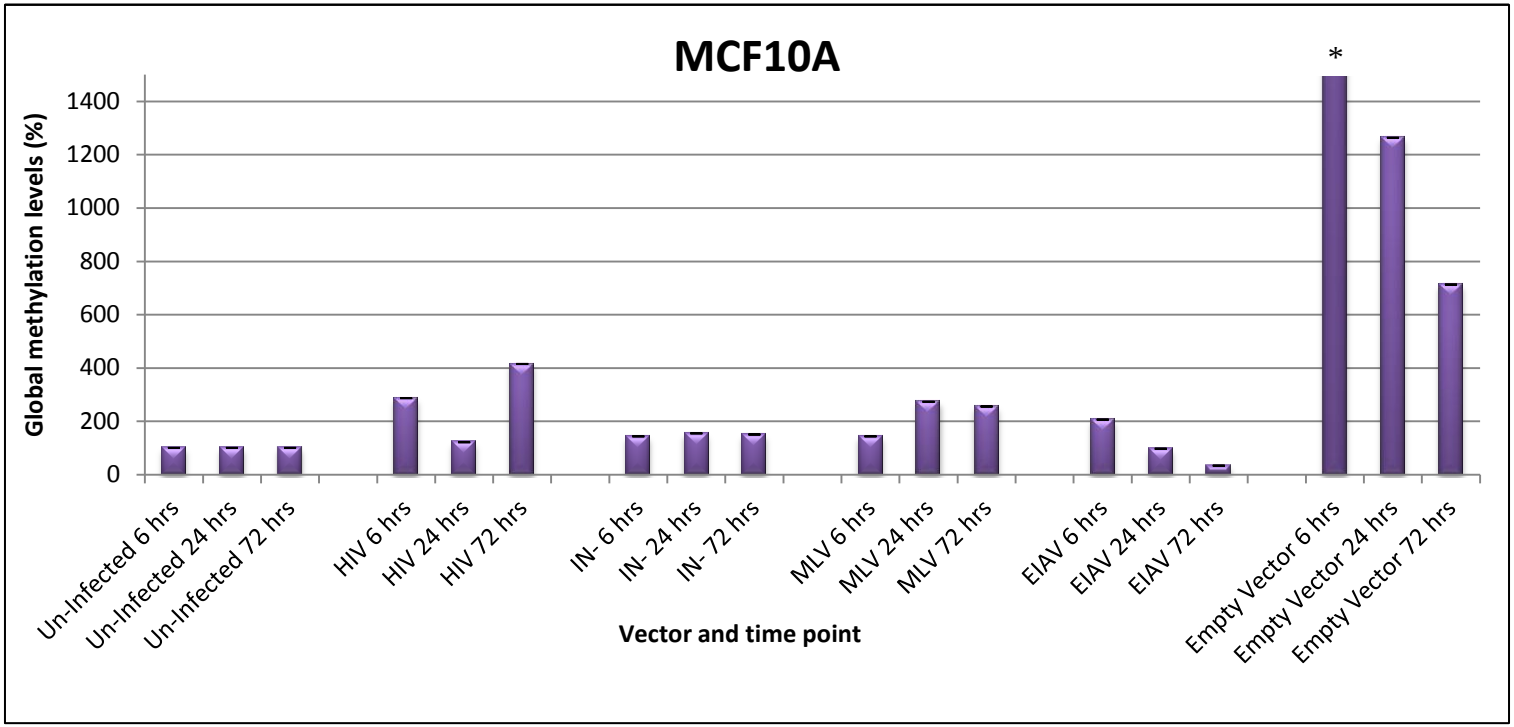

Figure 33. Global methylation levels in RV and LV infected Mcf10a cells.

Global methylation was measured in control, uninfected cells (NC) and compared with cells infected with HIV, IN-, MLV, EIAV, FIV and MLV without genomes (empty vector). Percentage methylation levels were calculated using average spectrophotometric absorbance measured at 450nm. Elevated global methylation was observed in all infected samples. Standards errors of the means of 3 readings = SEM are represented as error bars. *Denotes the methylation level that exceeded the y-axis chart value measured at 4423.88%.

Table 35. Measurement of global methylation in HepG2 cells infected with RV and LV vectors

Treatment	Time (hours)	Relative methylated levels (%) SEM
Un-infected	**6**	100 (0.30)
	24	100 (0.06)
	72	100 (0.00)
HIV	**6**	2.41 (0.09)
	24	138.34 (0.15)
	72	0 (0.09)
IN-	**6**	0 (0.10)
	24	207.25 (0.34)
	72	266 (0.03)
MLV	**6**	47.81 (0.04)
	24	39.01 (0.01)
	72	341 (0.03)
EIAV	**6**	199.57 (0.11)
	24	24.99 (0.16)
	72	204 (0.07)
Empty Vector	**6**	387.4 (0.01)
	24	208.03 (0.14)
	72	69.09 (0.21)
FIV	**6**	23.42 (0.12)
	24	425.27 (0.11)
	72	914 (0.30)

The experimental samples represent HepG2 cells infected with the following vectors: MLV, HIV, IN- (HIV with mutated integrase), EIAV, FIV and Empty Vector (MLV without viral genome).

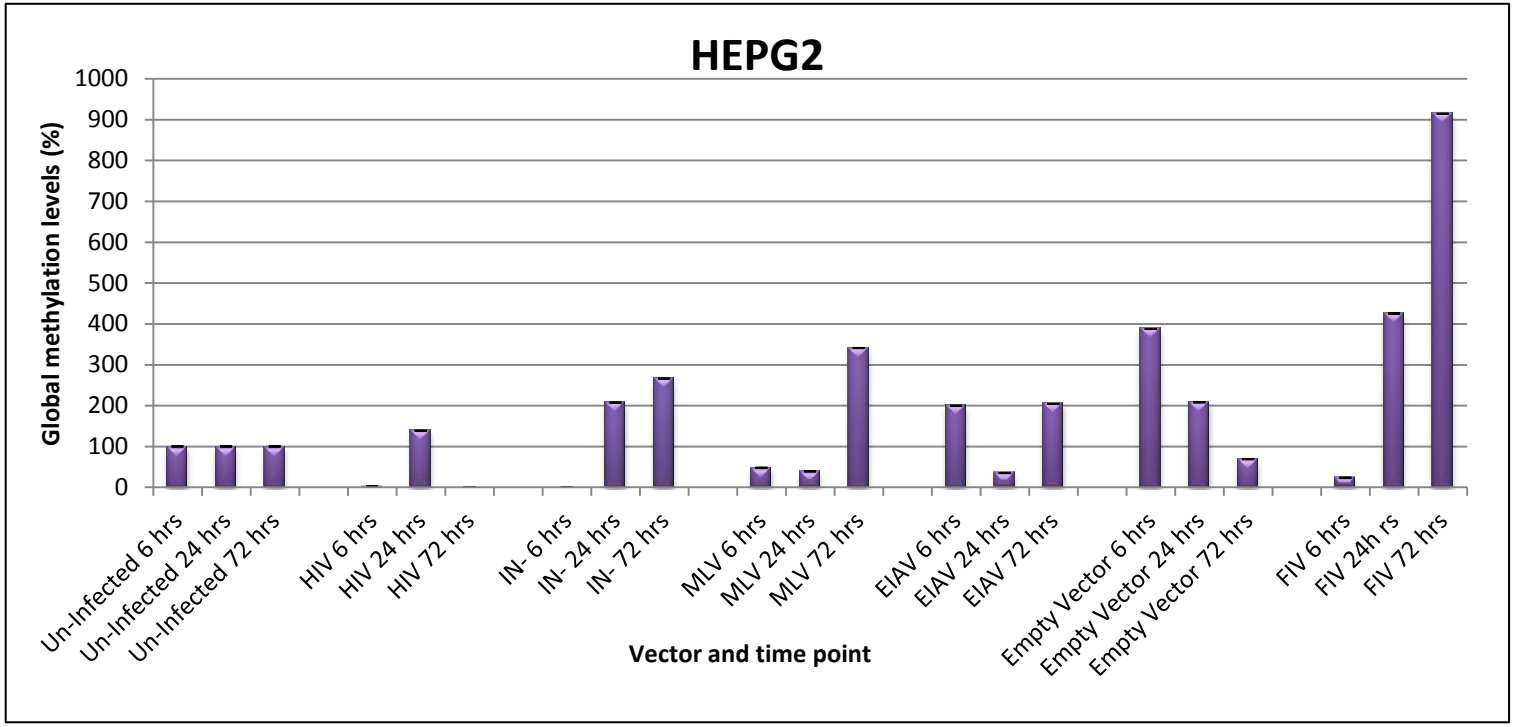

Figure 34. Global methylation levels in RV and LV infected HEPG2 cells.

Global methylation was measured in control, uninfected cells (NC) and compared with cells infected with HIV, IN-, MLV, EIAV, FIV and MLV without genomes (empty vector). Percentage methylation levels were calculated using average spectrophotometric absorbance measured at 450nm. Elevated global methylation was observed in all infected samples. Standards errors of the means of 3 readings = SEM are represented as error bars

Table 36. Measurement of global methylation in 53BP1 -/- cells infected with RV and LV vectors

Treatment	Time (hours)	Relative methylated levels (%) SEM
Un-infected	**6**	100 (0.08)
	24	100 (0.00)
	72	100 (0.15)
HIV	**6**	0 (0.01)
	24	0 (0.02)
	72	30.90 (0.01)
IN-	**6**	0 (0.01)
	24	105.37 (0.02)
	72	0 (0.16)
MLV	**6**	0 (0.02)
	24	0 (0.01)
	72	10.39 (0.00)
EIAV	**6**	135.45 (0.01)
	24	0 (0.12)
	72	0 (0.03)
Empty Vector	**6**	99.01 (0.12)
	24	101.91 (0.12)
	72	100.66 (0.04)
FIV	**6**	111.19 (0.07)
	24	56.87 (0.22)
	72	0 (0.31)

The experimental samples represent 53BP1 -/- cells infected with the following vectors: MLV, HIV, IN- (HIV with mutated integrase), FIV, EIAV and Empty Vector (MLV without viral genome).

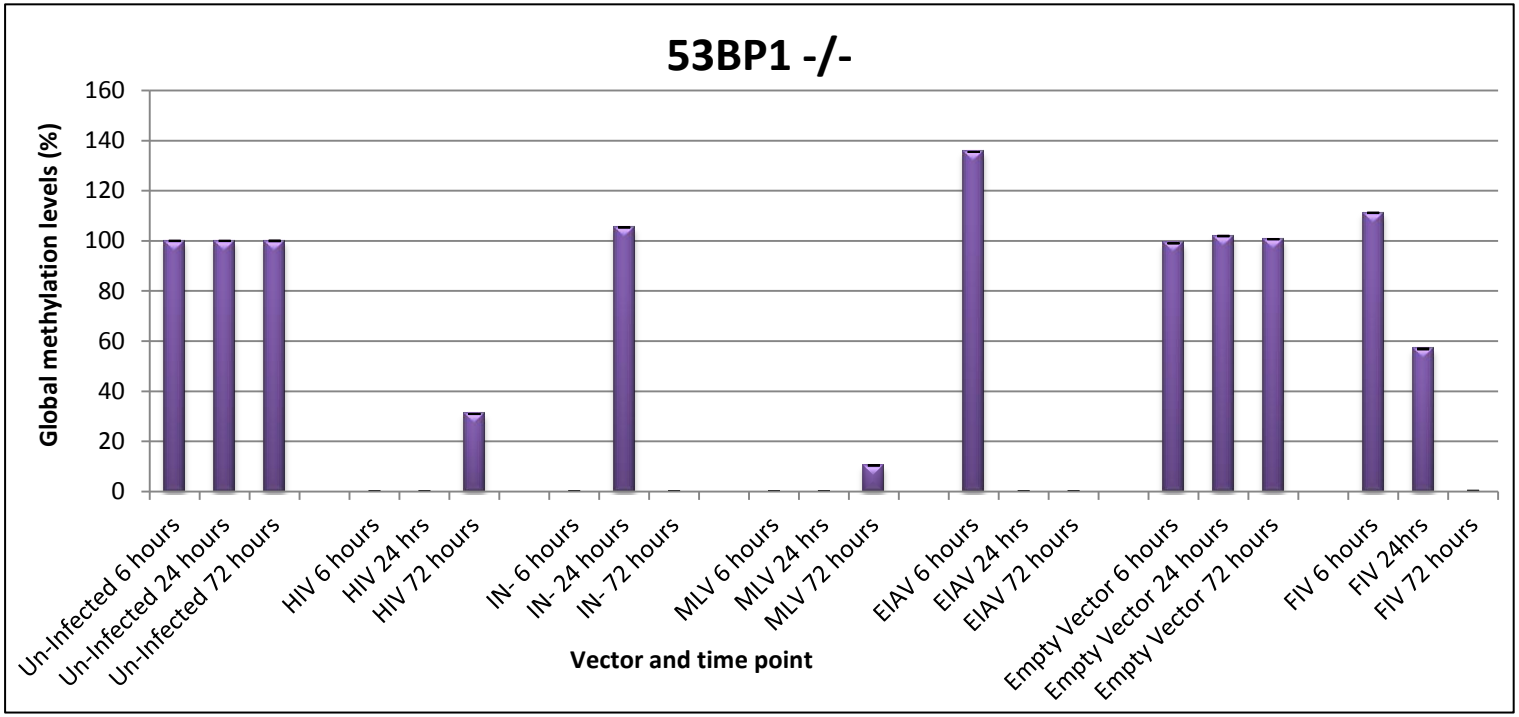

Figure 35. Global methylation levels in RV and LV infected 53BP1-/- cells.

Global methylation was measured in control, uninfected cells (NC) and compared with cells infected with HIV, IN-, MLV, EIAV, FIV and MLV without genomes (empty vector). Percentage methylation levels were calculated using average spectrophotometric absorbance measured at 450nm. Elevated global methylation was observed in all infected samples. Standards errors of the means of 3 reading = SEM are represented as error bars

Global methylation assays performed on the Mcf10a cell line showed a significant increase ($P < 0.05$) in methylation levels at virtually all time points by all vectors (excluding EIAV 24 and 72 hours). Global methylation levels in cells infected with HIV, IN, MLV, EIAV, MLV without genomes were 4.14 (+/- 0.08), 1.54 (+/- 0.05), 2.72 (+/- 0.04), 2.05 (+/- 0.01) and 44.23 (+/- 0.15) fold greater, respectively, than untreated cells. The highest increase in global methylation levels was associated with MLV without genomes. Global methylation however decreased between 6 hours and 3 days for each treatment.

To test this observation in an alternative cell line, mouse liver cells (HepG2) were chosen and the study was repeated. HepG2 cells showed similar results to that of Mcf10a. Global methylation levels increased significantly ($P < 0.5$) above control untreated cells (excluding MLV). Interestingly, the highest global methylation increases were observed in FIV samples which reached a maximum of 4.25 (+/- 0.11) fold greater than untreated cells.

The 53BP1-/- mouse embryonic fibroblast cell line lacks the NHEJ DNA damage repair pathway and is, therefore, useful to investigate whether the DDR pathway may be associated with genome methylation. Cells infected with each vector showed very little change in global methylation. Interestingly, only a small change in global methylation levels was seen in cells infected by the EIAV vector 6 hours post infection ($P < 0.5$). Hence, this preliminary work suggests the DNA damage response may be associated with genome methylation and to possible influence gene expression in infected cells.

Alongside this investigation DNMT expression was examined as the possible cause of elevated global methylation levels.

Table 37. DNA methyltransferase gene expression in Mcf10a cells following RV and LV infection.

Sample	Time (hours)	DNMT1 (+/- SEM)	DNMT3a (+/- SEM)	DNMT3b (+/- SEM)
Un-infected	**6**	1 (0.06)	1 (0.06)	1 (0.03)
	24	1 (0.05)	1 (0.11)	1 (0.19)
HIV	**6**	0.03 (0.26)	1.3 (0.14)	0 (0.0)
	24	0.20 (0.04)	0.28 (0.25)	0 (0.0)
IN-	**6**	0.29 (0.43)	0.78 (0.12)	0.18 (0.09)
	24	0.99 (0.09)	1.94 (0.43)	0.43 (0.15)
MLV	**6**	0.14 (0.01)	0.11 (0.06)	0.09 (0.13)
	24	1.43 (0.09)	1.74 (0.18)	2.11 (0.05)
EIAV	**6**	0.25 (0.09)	0.19 (0.08)	0.36 (0.12)
	24	0.39 (0.06)	0.24 (0.06)	1.36 (0.23)
Empty Vector	**6**	0.47 (0.27)	3.48 (1.73)	2.74 (0.39)
	24	0.59 (0.04)	1.62 (0.15)	0.54 (0.64)

DNMT 1, 3a and 3b expression levels were measured in MCF10a cells infected with MLV, HIV, IN-, EIAV, and MLV without genome vectors. RNA was extracted 6 hours and 24hours post infection. Expression levels shown represent $2^{-\Delta\Delta CT}$ values. All final $2^{-\Delta\Delta CT}$ values were normalised against the values obtained for the untreated cells. Standard errors of the means were calculated from quadruplet readings.

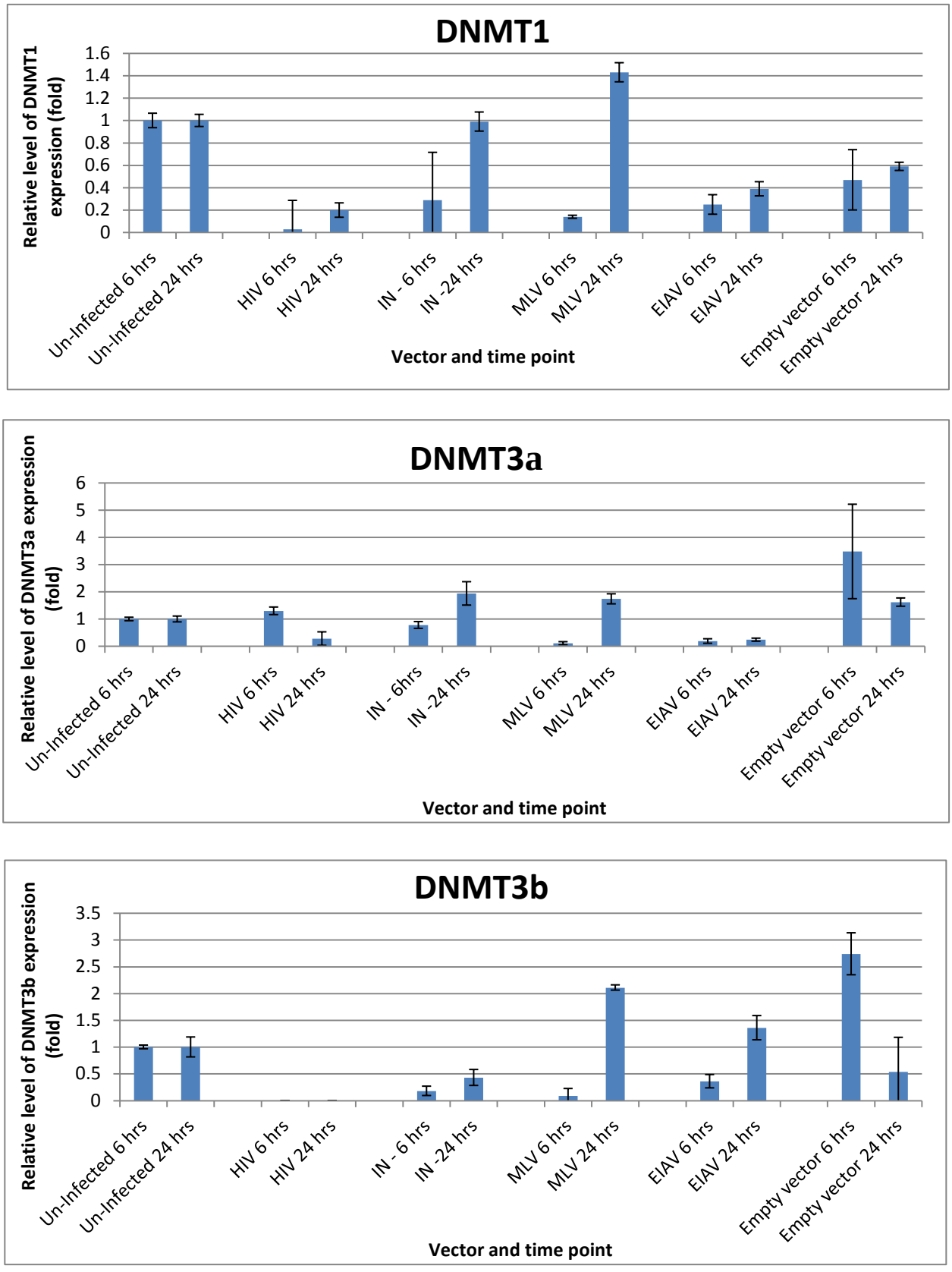

Figure 36. DNMT 1 3a and 3b expression in Mcf10a cells following RV and LV infection.

Q-RT-PCR was performed using DNMT1, 3a and 3b specific primer probes on untreated cells and cells infected with HIV, IN-, MLV, EIAV, and MLV without genome vectors.

To calculate RQ levels in experimental samples several steps were carried out:

DNMT values were normalized against 18sRNA CT values. All samples were measured in triplicate. ΔCT values were used for calculations. ΔCT values from experimental samples were subtracted from ΔCT values produced from controls samples. Each bar represents the relative gene expression levels (RQ) - $2^{-\Delta\Delta CT}$ calculated for each sample. The RQ levels for controls were set a value of 1. Error bars, depict the standard error of the means taken from quadruplet readings. P.values was derived using replicate CT values for T-tests.

Table 38. DNA methyltransferase gene expression in HepG2 cells following RV and LV infection.

Sample	Time (hours)	DNMT1 (+/- SEM)	DNMT3a (+/- SEM)	DNMT3b (+/- SEM)
Un-infected	**6**	1 (0.46)	1 (0.08)	1 (0.04)
	24	1 (0.50)	1 (0.05)	1 (0.26)
IN-	**6**	0 (0.11)	0 (0.03)	0 (0.07)
	24	0.09 (0.06)	0.11 (0.16)	0 (0.06)
MLV	**6**	0.1 (0.15)	0.13 (0.05)	0.18 (0.15)
	24	0.05 (0.14)	0.02 (0.09)	0.03 (0.07)
EIAV	**6**	0.74 (0.33)	0.22 (0.05)	0.17 (0.12)
	24	0.17 (0.25)	0.07 (0.13)	0.8 (0.15)
Empty Vector	**6**	0 (0.08)	0.01 (0.03)	0.01 (0.06)
	24	0.69 (0.06)	1.52 (0.01)	0.19 (0.02)
FIV	**6**	0.05 (0.11)	0.6 (0.10)	0.12 (0.01)
	24	0.77 (0.04)	33.13 (0.21)	8.22 (0.10)

DNMT 1, 3a and 3b expression levels were measured in HepG2 cells infected with MLV, IN-, EIAV, FIV and MLV without genome vectors. RNA was extracted 6 hours and 24hours post infection. Expression levels shown represent $2^{-\Delta\Delta CT}$ values. All final $2^{-\Delta\Delta CT}$ values were normalised against the values obtained for the untreated cells. Standard errors of the means were calculated from quadruplet readings.

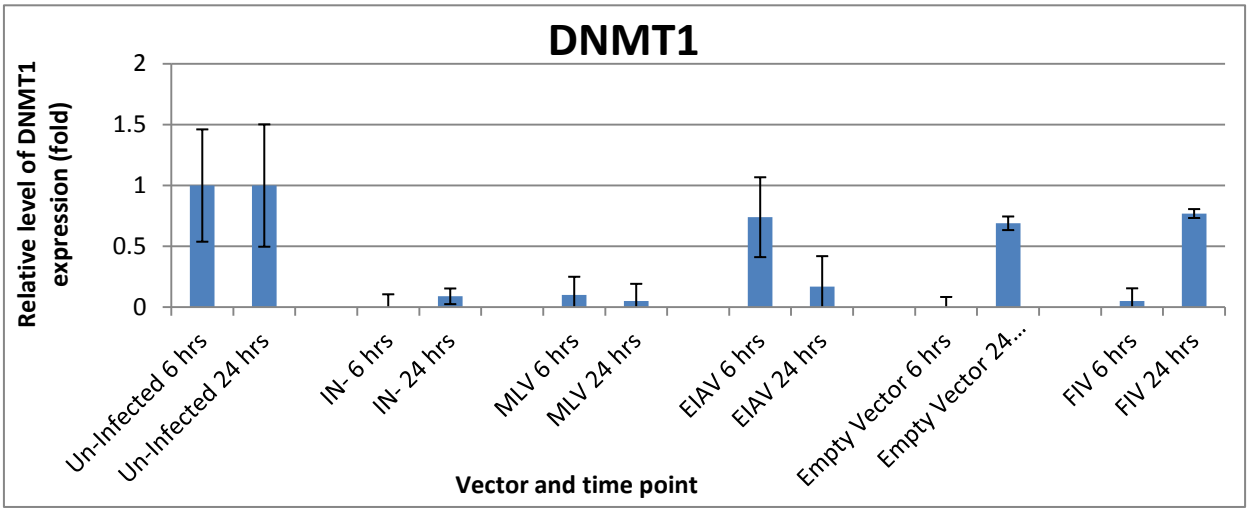

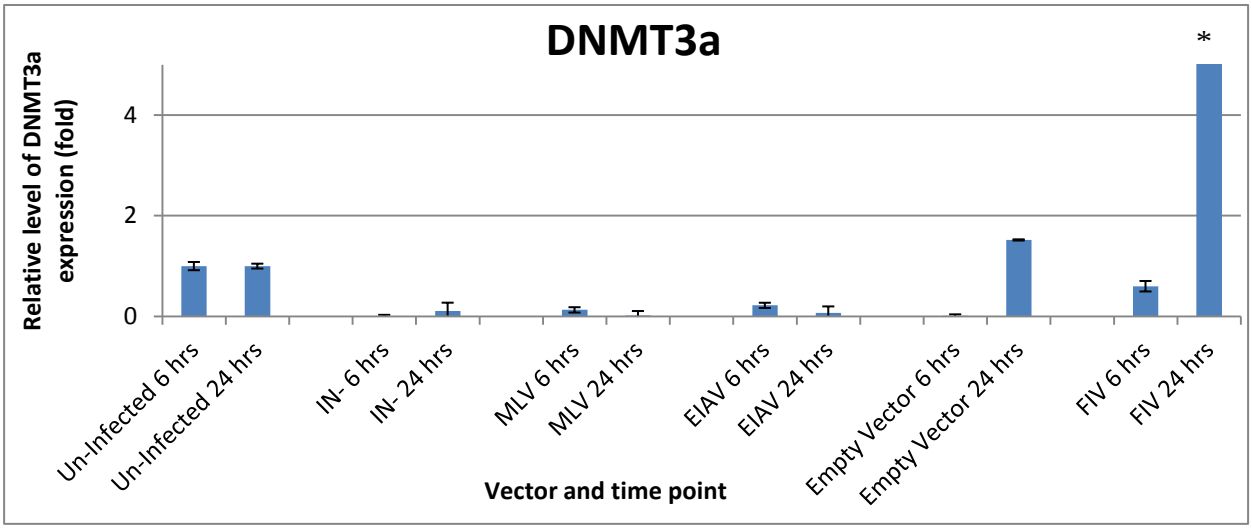

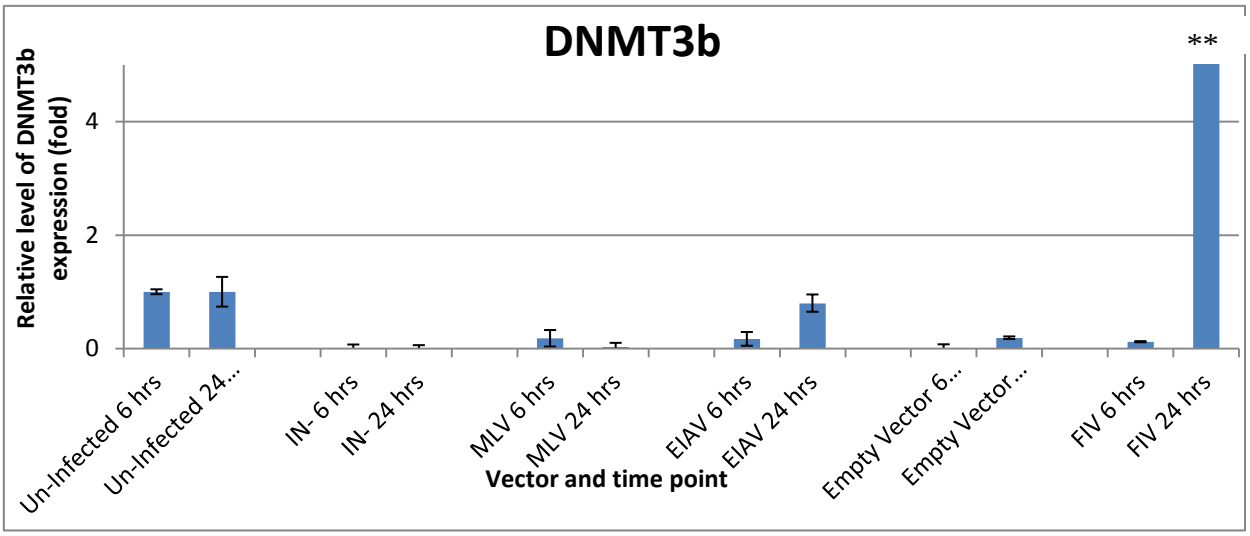

Figure 37. DNMT 1 3a and 3b expression in HepG2 cells following RV and LV infection.

Q-RT-PCR was performed using DNMT1, 3a and 3b specific primer probes on untreated cells and cells infected with FIV, IN-, MLV, EIAV, and MLV without genome vectors.

To calculate RQ levels in experimental samples several steps were carried out:

DNMT values were normalized against 18sRNA CT values. All samples were measured in triplicate. ΔCT values were used for calculations. ΔCT values from experimental samples were subtracted from ΔCT values produced from controls samples. Each bar represents the relative gene expression levels (RQ) - $2^{-\Delta\Delta CT}$ calculated for each sample. The RQ levels for controls were set a value of 1. Error bars, depict the standard error of the means taken from quadruplet readings. P.values was derived using replicate CT values for T-tests.

*Denotes the DNMT3a level that exceeded the y-axis chart value measured at 33.13 fold greater.

** Denotes the DNMT3b level that exceeded the y-axis chart value measured at 8.22 fold greater.

Table 39. DNA methyltransferase gene expression in 53BP1-/- cells following RV and LV infection.

Sample	Time (hours)	*Dnmt1* (+/- SEM)	*Dnmt3a* (+/- SEM)
Un-infected	**6**	1 (0.46)	1 (0.48)
	24	1 (0.17)	1 (0.13)
HIV	**6**	4.18 (0.07)	3.1 (0.44)
	24	0 (0.00)	0.04 (0.16)
IN-	**6**	0.96 (0.25)	0.88 (0.18)
	24	0.79 (0.38)	0.83 (0.20)
MLV	**6**	0.9 (0.42)	1.48 (0.38)
	24	1.24 (0.10)	0.42 (0.29)
EIAV	**6**	0.65 (0.05)	0.77 (0.21)
	24	0.7 (0.25)	0.47 (0.11)
Empty Vector	**6**	1.59 (0.10)	1.08 (0.03)
	24	0.62 (0.09)	0.16 (0.16)

Dnmt 1 and *3a* expression levels were measured in 53Bp1 -/- cells infected with MLV, IN-, EIAV, HIV and MLV without genome vectors. RNA was extracted 6 hours and 24hours post infection. Expression levels shown represent $2^{-\Delta\Delta CT}$ values. All final $2^{-\Delta\Delta CT}$ values were normalised against the values obtained for the untreated cells. Standard errors of the means were calculated from quadruplet readings.

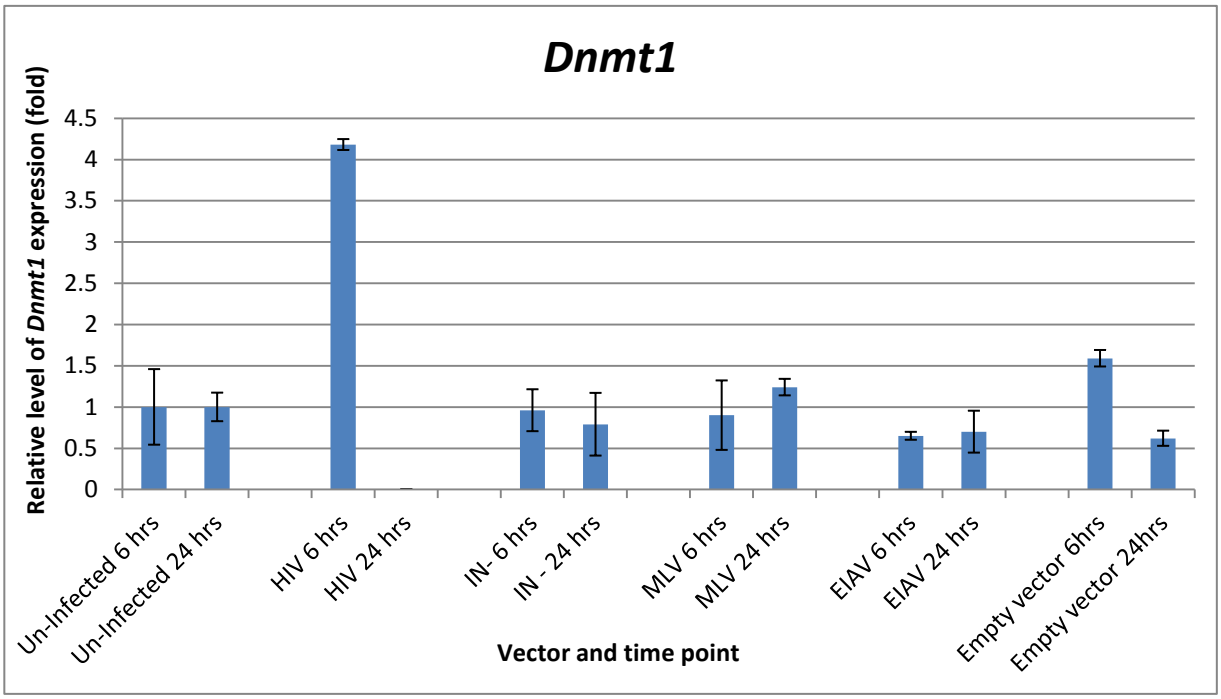

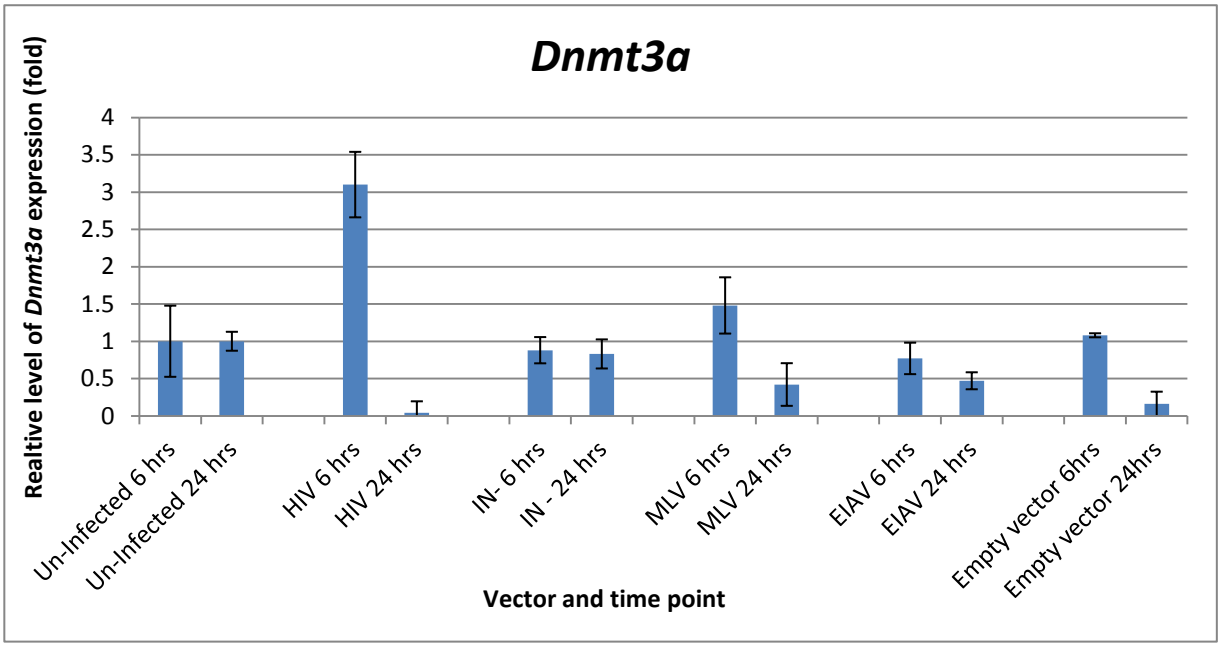

Figure 38. *Dnmt 1 and 3a* expression in 53BP1-/- cells following RV and LV infection

Q-RT-PCR was performed using *Dnmt1* and *3a* specific primer probes on untreated cells and cells infected with IN-, MLV, EIAV, HIV and MLV without genome vectors.

To calculate RQ levels in experimental samples several steps were carried out:

DNMT values were normalized against 18sRNA CT values. All samples were measured in triplicate. ΔCT values were used for calculations. ΔCT values from experimental samples were subtracted from ΔCT values produced from controls

samples. Each bar represents the relative gene expression levels (RQ) - $2^{-\Delta\Delta CT}$ calculated for each sample. The RQ levels for controls were set a value of 1. Error bars, depict the standard error of the means taken from quadruplet readings. P.values was derived using replicate CT values for T-tests.

Results showed DNMT1 expression levels to be low in Mcf10a cells infected with HIV, IN- vector, MLV, EIAV and MLV without genome (empty vector). The only elevated levels of DNMT1 expression was at 24 hour post infection with MLV (1.43, SEM +/- 0.09, $p<0.01$). DNMT3a expression levels were elevated for HIV 6 hours, HIV integrase negative 24 hours and MLV 24 hours. Interestingly, MLV without a genome showed increased levels of DNMT3a expression at both 6 hours and 24 hours (3.48, +/- 1.73 and 1.62, +/-0.15 respectively, $p<0.05$). DNMT3b expression was elevated in just HIV integrase negative, MLV 24 hours and EIAV 24 hours. Elevated expression levels for DNMT1, 3a and 3b were seen in MLV infected Mcf10a cells at 24 hours.

Q-PCR showed low levels of DNMT1, 3a and 3b expression in HepG2 cells infected with the IN- vector, MLV, EIAV, MLV without genome and FIV. Interestingly, the elevated levels of expression were shown in DNMT3a and 3b in HepG2 cells on infection with the FIV vector at 24 hours (33.13, +/- 0.21 and 8.22, +/-0.10 respectively, $p<0.01$). These results were compared with to data obtained from un-infected HepG2 cells. MLV vector containing no genome showed elevated DNMT3a levels at 24 hours (1.52, +/-0.01, $p<0.01$).

Q-PCR results for 53BP1-/- cells showed elevated expression levels for both *Dnmt1* and 3a in HIV at 6 hours (4.18, +/-0.07 and 3.1, +/-0.44 respectively, $p<0.01$) Interestingly MLV without genome showed elevated levels in both *Dnmt1* and *3a* at 6 hours (1.59, +/-0.10) and 1.08, +/- 0.03 respectively, $p<0.01$). *Dnmt1* levels rose for MLV at 6 hours and 24 hours with *Dnmt3a*.

Microarray analysis of cells infected with RV and LV vectors

In Chapters 4 and 5 on DNA damage and elevated methylation associated with RV and LV infection were investigated. This suggested these processes linked where comparisons were made in cells with or without 53BP1 related, DDR pathways. To examine in detail pathways relating to DDR following infection, comparison was made between infected and uninfected cells for differential gene expression. Significantly differentially expressed genes ($p<0.05$) were then assigned to gene networks to associate RV and LV infection with genes in pathways of DDR and methylation.

For this, Mcf10a cells were infected with MLV, EIAV and MLV without viral genome vectors that provided the most obvious DDR and altered methylation status. Total RNA was collected 6 hours post infection for cDNA synthesis and subsequent microarray analysis. Gene expression analysis involved measurement of gene expression in infected Mcf10a cells compared to normal uninfected Mcf10a cells.

Genes with gene ontology (GO) terms of “DNA repair”, “DNA damage” and “DNA methylation” were selected from the microarray data. Then from these lists, genes with differential expression of 1.2 fold or more were divided into sets that were up and down regulated to create 6 sublists of genes for each of the 3 vectors.

Table 40. Genes up-regulated by 1.2 following infection of Mcf10a cells by MLV, EIAV and MLV without viral genome vectors.

Sample	DNA Repair	DNA Damage	DNA Methylation
MLV	CDT-2526A2.1 Eya3 Rpain Upf1 Xrcc4 Cdc14b Men1	Hipk1 Hmox1 Cdc14b Men1	Trmt11
EIAV	Apex2 Fgf10 Pole Atrx	Bcl6 Hmox1 Nipbl Pml Psma8 Sgk1 Vav3	Tdrd9 Atrx
MLV without genomes	Apex2 Eya2	Hmox1	

The genes indicated are those whose ontologies belong to pathways involved in DNA damage, repair and methylation. Genes highlighted in red indicate co-membership of pathways. Fold changes in expression were calculated and those with statistically significant fold changes in expression (Log2 1.5, with $P<0.05$) compared to control untreated cells are shown.

Table 41 Genes down-regulated by 1.2 following infection of Mcf10a cells by MLV, EIAV and MLV without viral genome vectors.

Sample	DNA Repair	DNA Damage	DNA Methylation
MLV	Clorf124 Eme1 Pcna pttg1 Pttg3p Rad51ap1 Tyms Znf319 Rpa3	Ccna2 Cdk1 Psma8 Rpa3	Tdrd9
EIAV	Ac091565.1 Herc2 Herc2p3 Herc2p9 Pttg1 Pttg3p Rp11-959f10.4	Bcl6 Ccna2 Cdk1 Ctla4 Foxn3 Foxo1 Rp5-1100e15.2 Zmat3	Tdrd1
MLV without genomes	Amac1 Amac1l1 Amac1l3 Cdkn2d Chaf1a Fanci Lig1 Pttg1 Pttg3p rad51ap1 Rp11-959f10.4 Tyms Ube2t Ac010894.4 Apitd1 Apitd1-cort Brca1 Cdc14b Fancd2 Rpa3 Top2a Usp28	Brip1 Ccna2 Cdk1 Gtse1 Map2k6 Plk1 Timeless Ac010894.4 Apitd1 Apitd1-cort Brca1 Cdc14b Fancd2 Rpa3 Top2a Usp28	Dnmt1 Hells Tdrd1

The genes indicated are those whose ontologies belong to pathways involved in DNA damage, repair and methylation. Genes in red indicate co-membership of pathways. Fold changes in expression were calculated and those with statistically significant fold changes in expression (Log2 1.5, with P<0.05) compared to control untreated cells are shown.

Analysis of differential expression of target genes associated with the E2F transcription factor

The E2F transcription factor has been found to be closely associated with oncogenesis and is also known to control the expression of several genes in this process. E2F control of its targets is also known to be closely controlled by methylation. Hence, the microarray data generated in this study was also examined for differential expression of E2F and its target genes. All genes differentially expression by Log2 1.2 fold or more (up or down) with GO terms relating to pathways associated with DNA damage, repair and methylation were analysed, using Opossum software http://opossum.cisreg.ca/oPOSSUM3/ to carry predicted binding sites for the E2F family of transcription factors. These genes are listed in Table 42. From the human genome the number of genes that bind E2F was calculated to be 32.77%. From the microarray the number of genes identified differentially expressed and binding E2F was 59%, which is significantly above the background.

Table 42 Genes associated with E2F binding from virus treated Mcf10a cells

Name	Function	EIAV		MLV		MLV without genomes	
		P-value	Differential expression	P-value	Differential expression	P-value	Differential expression
C1orf124	DNA repair	0.593754	0.166	0.464841	0.198	0.819603	0.055
BRCA1	DNA repair, DNA damage	0.679369	0.400	0.901237	0.103	0.679565	-0.272
FOXN3	DNA damage	0.197869	-0.497	0.273247	-0.374	0.821102	-0.058
EYA2	DNA repair	0.673374	0.324	0.851833	0.430	0.429063	1.179
FGF10	DNA repair	0.123058	1.692	0.943362	-0.050	0.229637	1.038
ATRX	DNA methylation	0.020665	1.171	0.210453	0.442	0.407759	0.511
TDRD1	DNA methylation	0.361696	-1.388	0.680574	-0.467	0.296241	-2.252
LIG1	DNA repair	0.750754	-0.102	0.027018	-1.046	0.00024	-1.814
MAP2K6	DNA damage	0.078655	-0.955	0.156164	-0.604	0.007363	-1.165
RAD51AP1	DNA repair	0.4863	-0.265	0.027787	-0.586	0.009958	0.027
TIMELESS	DNA damage	0.159691	-0.763	0.057118	-0.940	0.000786	-1.639
BCL6	DNA damage	0.004255	1.278	0.052734	0.255	0.960462	-0.009
HELLS	DNA methylation	0.227824	-0.645	0.245671	-0.328	0.004707	-1.026
CDKN2D	DNA repair	0.528424	-0.285	0.064288	-0.735	0.003066	-1.178
DNMT1	DNA methylation	0.700485	-0.170	0.056385	-0.922	0.002446	-1.385
PCNA	DNA repair	0.090303	-0.948	0.022073	-1.353	0.016983	-0.992
VAV3	DNA damage	0.568429	1.667	0.263471	0.548	0.973223	0.323
BRIP1	DNA damage	0.331419	0.547	0.602064	0.291	0.011866	-1.806
FANCD2	DNA repair, DNA damage	0.247943	-0.589	0.966359	0.017	0.001998	-1.348
FOXO1	DNA damage	0.000345	-1.772	0.117376	-0.474	0.475278	-0.203
EME1	DNA repair	0.364587	-0.478	0.058038	-1.204	0.070106	-0.717
TDRD9	DNA methylation	0.920135	1.877	0.993967	0.003	0.198465	0.461
EYA3	DNA repair	0.707922	0.904	0.271913	1.953	0.658206	0.608

HIPK1	DNA damage	0.006986	0.930	0.001852	1.194	0.007403	1.063
CTLA4	DNA damage	0.409349	-0.325	0.954332	0.099	0.549172	0.932
NIPBL	DNA damage	0.406258	1.984	0.556546	-0.265	0.929151	0.027
CHAF1A	DNA repair	0.326786	0.269	0.805402	0.077	0.072468	-1.031
APEX2	DNA repair	0.032328	1.229	0.113473	0.845	0.006691	1.272
CDK1	DNA damage	0.058512	-1.553	0.022671	-2.118	0.015603	-1.892
ZMAT3	DNA damage	0.096393	-0.520	0.486877	0.235	0.816517	0.401
APITD1	DNA repair, DNA damage	0.294114	0.583	0.339019	-0.423	0.071054	-0.594
POLE	DNA repair, DNA damage	0.889581	1.866	0.87434	0.443	0.905337	0.956
HERC2P3	DNA repair	0.062007	-1.657	0.24794	-0.346	0.822555	-0.077

Table 42. Genes associated with E2F binding from virus treated cells. The number of genes, with any of the 3 GO terms, predicted to bind E2F transcription factors was determined using OPossum software http://opossum.cisreg.ca/oPOSSUM3/ single site analysis using the default parameters for human gene analysis. The analysis was carried out using sequence 5000bp up and downstream of the annotated start and stop positions of the genes. In humans the number of background genes predicted to bind E2F transcription factors is 8113 out of 24752 genes or 32.77%. In our list of aberrantly regulated genes 33 out of 56 or 59% are predicted to bind. This is a significant increase above background. Genes highlighted in green are those with P values<0.05.

Those genes identified (highlighted in green) as binding E2F and associated with DNA repair, damage and methylation appeared, in the main to be down regulated. Very few genes were identified up regulated.

6.1 Discussion

RV and LV gene therapy vectors deliver therapeutic genes to mammalian cells by integrating their genome into host chromosome to provide the potential for permanent therapeutic gene expression. However, this integration can be oncogenic as shown by RV transduction of haematopoietic stem cells that led to leukaemia in animal models and in several patients in gene therapy trials for the correction of X-SCID (Cavazzana-Calvo, M. and Hacein-Bey-Abina, S., 2001; Cavazzana-Calvo *et al.*, 2000) and caused myelodysplasia in patients treated for chronic granulomatous disease (CGD) (Stein *et al.*, 2010; Malech *et al.*, 1997; Bjorgvinsdottir *et al.*, 1997). LV with SIN configuration has been used successfully in the clinic for metachromic leukodystrophy and Wiskott-Aldrich syndrome, however clonal dominance has been identified in patients following transplantation of bone marrow in a patient with β-thalassemia (Cavazzana-Calvo, M. and Hacein-Bey-Abina, S., 2010). In animal studies used to develop models for genotoxicity, tumours have been associated with RV and LV delivery in a tumour prone mouse and following non-primate LV administration *in utero* and neonatally to outbred immune-competent mice. Transformation *in vitro* has also been documented in murine stem cells. In the gene therapy trials for X-SCID performed by M. Cavazzana-Calvo in France and A. Thrasher in the UK, the *ex-vivo* gene transfer protocol using MLV transduction of hematopoietic stem cells (HSC) and re-infusion back to patients led to intense research into the cause of the leukaemias in 5 patients from these trials. This work enabled identification of RV integration into the LMO-2 gene and that this gene, which is already known involved in childhood leukaemia, was dysregulated due to active promoters and enhancers in the vector LTR(Cavazzana-Calvo et al, 2000; Hacein-Bey-Abina et al, 2002; Gaspar and Thrasher, 2009).

The phenomenon of insertional mutagenesis (IM) has been studied for several years and it is not entirely surprising this occurred in the gene therapy trials using RV vectors. IM is clearly a genotoxic risk to the host as genes that are considered cancer associated are potential targets for dysregulation. Down regulated gene expression has been demonstrated following retrovirus insertion within genes and gene control regions or by chromatin remodelling effects (Lazo and Tsichlis, 1988). This has resulted in tumour suppressor gene inactivation (Ben-David *et al.*, 1990). The genotoxic effects can occur at some distance from the affected locus and furthermore, provirus can undergo

homologous recombination to elicit chromosomal rearrangements that could lead to tumour development (Lazo and Tsichlis, 1988).

As a result of the findings of IM in gene therapy clinical trials, several groups including that of Dr Michael Themis developed the highly sensitive *in utero* model to test the safety of LV. In this genotoxicity model, lentiviral vectors were shown associated, at high frequency, with the development of clonal liver tumours that have been characterized as hepatocellular carcinoma (HCC). Both in adult KO mice for factor IX (FIX) with haemophilia B and wild-type outbred, fully MF-1 immune-competent adult mice, tumours were found to develop following administration of the EIAV (SMART2) non-primate vector at day 16 gestation. Conversely, no tumours developed in mice treated with primate HIV (HR'SIN-cPPT-S-FIX-W) vector carrying the human FIX gene that enabled correction of the KO mouse model (Themis *et al.,* 2005). These findings were the origin of the fetal genotoxicity model and led to the proposal that gene transfer *in utero* could be used as a valuable tool to evaluate LV genotoxicity and discover genes involved in liver oncogenesis.

The development of liver tumours in mice treated with LV is suspected most likely due to IM. However, tumour development varied with age in this model and some of the clonal tumours had single virus insertions making difficult the assignment of oncogenesis due only to IM but possibly due to alternative events supporting clonal evolution either influenced and initiated by IM or completely independent to IM that are synergistic to oncogenesis. Hence, oncogenesis may be due to provirus insertions within or near to cancer genes on genes related to pathways of cancer and/or alternatively events associated with virus infection.

6.1.1 Investigation of mouse tumour DNA compared to non-tumour liver using CGH

Recently, Themis *et al* (2013) published two sets of findings using the *in utero* model. In the first study they showed LV insertion is highly influenced by gene density and the level of gene transcription, which they showed to be high in the foetal mouse. Also these phenomena appear dependant on the vector where non-primate LV appears to prefer highly transcribed genes whereas primate vector integration is less influenced by this (Nowrouzi *et al.,* 2012). In the second study, the group, in collaboration with Eithan

Galun at Haddassah Hospital, Jerusalem showed that genome instability is associated with LV integration. This was demonstrated using comparative genome hybridisation (CGH) that found amplifications and deletions of chromosomes following foetal infection of mice and in cells *in vitro* with an alternative non-primate feline leukaemia virus vector (Condiotti *et al*., 2013). Hence, in the work presented in this thesis CGH was applied to 3 tumours isolated from the EIAV and HIV *in utero* treated mice of the Themis model. Fortuitously, a spontaneous liver tumour that developed in an MF-1 mouse was also available for CGH. The CGH work out that was carried out in collaboration with Dr Nathalie Conte of the Wellcome Trust indeed showed amplifications and deletions in the non-primate treated tumours. Interestingly, in Tumour 1 the entire chromosome 2 was amplified. In Tumour 2, a specific region between 4559357 and 147876573 was amplified also and hence, further investigation of this region was performed. Interestingly, in the region of amplification in Tumour 2, near to the breakpoint, were the transcription factors *Hnf4α* and *Foxa2*. *Foxa2* and *Hnf4a* are closely related transcription factors and *Hnf4a* is also known to control *Hnf1a*. *Hnf4a* and *Hnf1a* are known to be critical to the development and function of the mouse liver (Wederell *et al*., 2008) and *Foxa2* expression is also critical for hepatocyte function (Wederell *et al*., 2008) . To test whether these genes were dysregulated RT-PCR was applied to Tumour 1 and Tumour 2 compared with the normal livers of each respective mouse.

In Tumour 1, *Hnf4α* and *Hnf1α* levels were found reduced by 0.62 $\log^2$ and 0.55 $\log^2$ fold respectively ($p<0.05$) and *Foxa2* was found increased in expression by 1.57 $\log^2$ fold ($p<0.05$). In Tumour 2, *Hnf4α* and *Hnf1α* and *Foxa2* levels of expression were all reduced by 0.18, 0.20 and 0.75 $\log^2$ fold ($p<0.05$), respectively. Hence, the CGH data correlated with changes in gene expression. To further explore the possibility that oncogenesis could involve IM and the genes identified by CGH of chromosome 2 in Tumours 1 and 2, the provirus inserted genes in Tumour 2, described by Themis *et al* (2005), were examined with *Hnf4α* and *Hnf1α* and *Foxa2* for involvement in common pathways relating to HCC.

Proviral insertions sites were retrieved from Tumour 2 mouse samples using LAM-PCR retrieval. This resulted in the identification of insertions in the *Pah* and *Acvr2a* genes. *Acvr2a* has not been found associated with HCC, however, the *Pah* gene that codes for the enzyme phenylalanine hydroxylase has been found down-regulated when mutated in

individuals with phenylketonuria (PKU) who cannot process pheylalanine effectively (Konecki and Lichter-Konecki, 1991) and has also been found down-regulated in HCC (Lazarevich and Fleishman, 2008). As a result of this change in expression amino acids build up to toxic levels in the blood and tissues. In Tumour 2, RT-PCR showed *Pah* gene expression down regulated by 65.3%. To find a relationship between *Pah* and its associated genes, *Pah* was investigated using the STRING (http;//string-db.org/) database that finds predicted protein interactions that are directly (physical) and/or indirectly (functional) associated in pathways between genes. From this analysis *Pah* was found linked to *Hnf4α* and *Hnf1α* and *Foxa2* along with several other genes that were found differentially expressed in the microarray of Tumour 2. Unfortunately, the microarray did not appear to show differential expression of *Hnf1α* and *Foxa2* or *Pah* but did identify reduced expression of *Hnf4α.*

Pah expression is linked to reduced expression of *Hnf4α* and *Hnf4α,* a master regulator of hepatocyte transcription and as mentioned is linked to HCC. A study by Jixuan Li *et al* showed that steady state levels of *Pah* could be seen in *Hnf4α* +/+ embryonic stem cells derived from mouse livers and in the absence of *Pah* expression*, Hnf4α expression* was found to be almost undetectable (Li *et al*., 2000).

Pcbd1 is known to be the stimulator of *Pah* in the phenylalanine hydroxylation pathway with its co-factor hepatocyte nuclear factor (*Hnf1α*) a ubiquitous gene promoter activator (Lockwood *et al*., 2003). It was therefore not surprising that *Pcbd1* levels were increased (0.343 $\log^{-2}$, p-value 0.01) in Tumour 2. However, as *Hnf4α,* which is known to activate *Hnf1α* was reduced in expression this may be the reason why it was not possible to identify increased levels of *Hnf1α* in the microarray of this tumour. Indeed, RT-PCR revealed *Hnf1α* levels reduced by 0.2 $\log^{2}$. In addition, reduced levels of *Pah* is also linked to a reduced expression of *Hnf1α.* Disruption of the *Hnf1α* transcription factor causes methylaton of the *Pah* promoter region, blocking hepatic chromatin remodelling of the *Pah* locus and thereby results in undetectable levels of *Pah* gene (Pontoglio *et al.*, 1997). *Hnf1α* is also known to bind to *Slc01α4* (Lockwood *et al*., 2003) and since *Hnf1α* expression was reduced it therefore was not surprising that a reduction in *Slc01α4* expression was also identified (-0.113 $\log^{-2}$, p=0.017).

The gene expression changes in Tumour 2 of the closely related transcription factors *Foxa2, Hnf1a* and *Hnf4a* that are critical to the development and function of the mouse liver appear to coincide with that expected for development of liver cancer (Wederell *et*

al., 2008). These changes also appear in line with altered *Pah* expression believed caused by IM. This is also the case in Tumour 1 except for *Foxa2*, which was found increased in expression by RT-PCR.

In conclusion, from these analyses, possible pathways to tumour development were identified and the related genes that were found associated with genes identified using CGH or by IM in the STRING data base support future research into mechanisms of liver cell oncogenesis. However, it is well known that pathways to HCC are complex and several pathways may exist for solid tumour development. Hence, the CGH and IM data must be considered highly speculative before more detailed studies are applied to the tumours found by the *in utero* genotoxicity model. What was evident from this work was that vectors with the potential for genotoxicity exist and they differ in their genotoxic potential.

Further study using Ingenuity Pathway analysis (IPA) of the microarray and RT-PCR of these tumours revealed gene ontologies of genes in pathways of oxidative reduction and DNA damage and repair (Nowrouzi *et al.*, 2012). As already mentioned, cancer development usually requires multiple genetic events beginning with cell immortalization then progressing to malignancy and the hypothesis that IM alone cause oncogenesis is hard to reconcile. Therefore, although the initial work using CGH and IM inserted genes was useful, this study was directed towards investigating alternative routes other than IM that contribute to oncogenesis. One such route was to investigate in more detail the role of virus infection on genome instability. This choice of study was based on the findings of genome instability by the Bushman laboratory that showed virus integration to causes double strand breaks (Bushman *et al*., 2001). As this was difficult to perform using the *in utero* model, assays to determine genome instability involved the development of a cell culture model.

6.1.2 Investigation of vector associated genotoxicity in cells following *in vitro* delivery of RV and LV

Four cell lines were used in the study. Two of which exhibited normal DNA repair (Mcf10a and Mrc5) and two that are known to be repair deficient (At5biva and Xp14br).

Most importantly, the level of infection of each cell line was first established. Each of the four cell lines was found to be infectable albeit at different levels with RV and LV vectors. At high titre, infection by MLV appeared highest for each cell line (98-100%) followed by HIV (21-62%), EIAV (9-68%) and IN- (5-72%). These levels of infection were assessed 24 hours post infection and the variation observed would also be expected due to the survival of cells just after infection. Indeed, RV and LV DNA integration is already known to cause damage to the host cell chromosome with DSB being known to be highly pro-apoptotic, with as little as one DNA DSB sufficient to arrest the cell cycle in G_1 that then leads to cell death.

High concentrations of un integrated virus DNA which have free ends, may be sensed as irreparable DNA damage in the cell, hence, the NHEJ pathway suppresses an apoptotic response by joining ends to form circles. Where un-integrated viral DNA accumulates cell death may occur. Indeed, At5biva and Xp14br cells showed low cell survival after infection again suggesting virus infection causes cell death where DNA damage repair is not present or inefficient. Interestingly, cell survival appeared lowest in these cells compared to Mcf10a and Mrc5 cells when infected by most vectors, even more so than when these cells were subject to 1Gy irradiation. Irradiation appeared to cause little cell death in Mcf10a and Mrc5 cells compared to infection by virus vectors suggesting the DNA damage caused by infection if not repaired is greater than when cells are subjected to 1Gy irradiation. Levels of infection by the IN- vector were measured after 72 hours using microscopy for GFP gene expression. Why this vector infected cells to a greater level in cells with intact DNA repair pathways again points to the requirement for DNA damage repair of RT converted virus genomes to circles before gene expression can take place which is at a low level in At5biva and Xp14br cells. Thus, high concentrations of unintegrated DNA may be toxic to cells as suggested by Temim *et al* (1980) who showed un-integrated RV cDNA in infected cell correlates with extent of the cytopathic effect observed after RV infection (Joy and Temin., 1980).

RV integration is catalyzed by the viral integrase protein which is required for the insertion of virus DNA into the chromatin of host cells. Insertion of a 3-10kb vector into the host DNA is likely to be sensed as a major assault on the genomic integrity of the cell. Recruitment of DNA damage signaling and repair proteins to integration sites is known to be essential for survival of the host cell and of the virus. In this respect attenuated virus act in a similar manner to wild type replication competent virus. A

stable integrated provirus need not generally cause deleterious effects in the host cell, however, if the DNA damage caused by the virus integrase in the host chromosome is repaired and that unintegrated linear viral DNA is somehow protected so it is not recognized by the DNA repair mechanism. The IN- vector showed a small decrease in cell viability in all cell lines infected, however, it was far less so than the integrase competent RV and LV. Therefore, if the IN- vector did induce apoptosis it was at low levels. The fact that much lower cell survival was associated with the integrase competent vector, especially in At5biva and Xp14br cells suggests that NHEJ activity may be required for repair of DSB and possibly DNA gaps in integration intermediates for cell survival. The requirement for cells to complete repair of DNA damage was also demonstrated following irradiation of cells. The conclusion from these data is, therefore that RV and LV infection is a DNA damage event that must be repaired for cell survival. What is not known is how much repair is not completed and whether incomplete repair leaves cell with mutations. Importantly, the fact that MLV without genomes causes the highest DNA damage response suggests that vector production should aim to reduce the number of active integrase enzyme molecules carried in virus particles for gene transfer to reduce potential cell death or mutagenesis.

To quantify the DNA damage response to DSB in Mcf10a and Mrc5 that have been previously shown with intact DNA repair pathways and Xp14br and At5biva cells which do not have these pathways immunoflourescence of the DNA damage protein 53BP1 was used at 3 time points post infection or irradiation.

In Mcf10a and Mrc5 cells a typical, rapid recognition of DSB by 53BP1 was observed and predictable induction of foci detected at 30 minutes post irradiation and at 6 hours post RV and LV infection which was followed by repair of the DSB and reduction DSB positive foci. The identification of DSB 6 hours post infection suggests this is the time taken for the virus integrase to reach the nucleus and generate DSB. DSB is also known to occur during DNA replication and cell division and also believed due to endogenous agents such a reactive oxygen species from cellular metabolism within cells reactions resulting in 1-2 foci being observable as ‘background’ DSB. This was observed in this study as 53BP1 positive foci in the uninfected control cells. Positive controls for 53BP1 foci were irradiated cells (at 1Gy). The emergence of 53BP1 positive foci in the irradiated cells were at a maximum level 30 minutes after irradiation where 13 foci per nucleus was observed compared to 1-2 foci in the un-infected cells. Although not

examined for in this study, DSB are known to develop after 5 minutes following irradiation (Schultz *et al.,* 2000). Conversely, as mentioned, the number of DSB peaked 6 hours following infection as RV and LV need to cross the cell plasma membrane, traverse the cytoplasm, penetrate the nuclear membrane and reach the genome for insertion.

In the At5biva cell line derived from a classical ataxia telangiectasia patient, there was a predictable induction of DSB. However due to the defect in the ATM gene which results in a defective DSB repair there is a persistence of 53BP1 positive foci in the cells 24 hour post irradiation and infection. In the Xp14br cells exposed to irradiation and infection gave a similar observation. However, these cells have been shown previously to be able to partially repair DSB following irradiation (Bourton *et al.*, 2012). This is believed due to the splicing defect in the DNA-Pkcs gene not eradicating all active DNA-PKcs molecules enabling the remaining functional DNA-PKcs to support the NHEJ repair pathway (Bourton *et al.*, 2012). In the infected Xp14br cells, unlike irradiation, infection may continue and cause further DSB. This was clearly observed by the increase in DSB 6 hours post infection.

By using an IN- HIV derived defective vector, unlike the integrase positive vector a similar number of 53BP1 positive foci to uninfected cells was found. Although the extent of mutagenesis or lack of repair was not quantified in this study following infection of cells, this would suggest once again the difference in the potential to cause genotoxicity by each vector. This could be further tested using IN- and IN positive vectors in the *in utero* mouse model where IN- would be expected not to be associated with induction of HCC. Most importantly and as previously mentioned, the fact that the vector not carrying genome caused such a high DSB response suggests this vector may induce HCC in the *in utero* model if DSB induction is indeed involved in oncogenesis.

The study of virus integration being associated with DSB presented in this work suggests a relationship between vector-related features and cell-intrinsic properties that may be involved in oncogenesis. The outcome of infection and DSB repair is unknown. One possible outcome is chromosomal instability and, therefore, it is tempting to hypothesize that viral integration may induce tumour formation by this process acting independently or synergistically with IM. DSB induced by treatment with irradiation or genotoxic drugs has been suggested as a considerable pathway to oncogenesis previously (Skalka and Katz 2005). By showing this also to be the cause during virus

infection, albeit at a lower level, suggests this mechanism of oncogenesis to be feasible and should not be overlooked when infecting cells at high titre as is often performed during *ex-vivo* gene therapy.

Several genes involved in cell division, growth and differentiation that are also known involved in tumour development once mutated and classed as oncogenes or tumour suppressor genes are potential targets for integration. If these genes are being 'hit' by the virus integration leading to DSB and then repair, then any mistakes in this repair will lead to mutagenesis. How much virus that recruits the DNA repair pathway machinery is unknown. This could in turn reduce the ability of the cell to repair DSB especially where infection involved high titre virus. Clearly, further examination of this potential is required.

It is also natural to question whether the DSB breaks observed *in vitro* following infection was the cause of genome instability leading to amplifications and deletions identified by the CGH assay of the tumours harvested from the mice treated *in utero* by EIAV LV. It would not be possible to determine this from the mouse tumours because these evolved over several month's time making it impossible to associate virus infection and integration changes in DNA structure.

6.1.3 Investigation of chromosome integrity using mFISH and G-banding following infection

To assign genome instability to virus integration, *in vitro* analysis of Mcf10a cells for karyotypic chromosome changes was performed in collaboration with Ruby Banerjee at the Welcome Trust, Hinxton, UK. This work involved multi-colour fluorescence *in situ* hybridisation (mFISH). Mcf10a cells were infected with each of the MLV, HIV and EIAV vectors and 2 weeks later cells were compared karyotypically with un-infected Mcf10a cells. Because no rearrangements were observed in the infected cells no gross chromosomal changes could be assigned to infection. However, it would be interesting to perform this in a time course from 2 weeks to 6 weeks in case instability takes time to manifest itself. Also, although not performed in this study, CGH of infected cells versus uninfected controls would highlight amplifications or deletions that could have occurred that would not be identified by mFISH.

Incoming retrovirus-like elements to the cell genome have been closely associated with the innate immune response of the cell. This response, in the form of methylation has evolved to protect the host genome from invasion by switching off gene expression from the incoming invading element. This element can be bacterial or a virus and is well documented for endogenous retrovirus particles and intracisternal A-type particles (Rowe *et al*., 2013). DNA damage has been also been associated with the enzymes involved in methylation and DNMT1 has also recently been found associated with DNA repair (Palii *et al*., 2008). DNMT1 deficient MESCs were found to have a 10 fold increase in *de novo* mutation of the *hrpt* locus (Chen *et al.*, 1998) suggesting the increase in the rate of mutation to be linked to a role by DNMT1 in the DNA repair pathway. (Armstrong *et al.*, 2012). DNMT1 is also known to be involved in maintaining genome integrity as it has been shown to accumulate at sites of DNA damage. Cells deficient in DNMT1 showed severe defects in the activation of key DSB responses such as lack of gH2AX induction and reduced phosphorylation of p53 and CHK1 (Palii *et al.*, 2008).

6.1.4 Epigenetic modifications and E2F regulation of host genes following RV and LV vector delivery

Therefore this study also investigated the effects of RV and LV infection on global methylation in Mcf10a, and HepG2 cells. MEF 53BP1 -/- cells were also used in this analysis to determine whether a block in the repair of DSB restricts an increase in methylation levels as opposed to that found in Mcf10a and HepG2 cells that have intact DNA repair pathways. Also, to determine whether methylation changes were associated only with integration, the IN- defective vector was used. A MLV vector containing no genome (empty vector) was also used to identify whether infection alone without the virus genome initiates methylation.

Global methylation levels in Mcf10a, HepG2 and MEF 53BP1 -/- cell genomes were investigated to indicate whether host methylation had occurred following infection. In Mcf10a cells global methylation levels increased significantly ($P<0.05$) at virtually all time points for each vector (excluding the EIAV LV at 24 and 72 hours). Although these increases were not consistent for all time points, the general trend was that methylation increased following infection. This was found even more pronounced following infection with the MLV empty vector and only partially with the IN- vector

that was consistent for each time point post infection. This observation appeared repeated for HepG2 cells except that for these cells IN- at 24 and 72 hours, MLV at 72 hours and the alternative non-primate FIV vector all showed levels of global methylation increase. Interestingly, the FIV vector that also were shown by the Themis group in collaboration with the research group of Dr Eithan Galun at Haddassah university, Jerusalem, to be associated with high frequency HCC (Condiotti *et al*., 2013) caused the greatest increase of global methylation 4.25 (+/- 0.11) fold greater than un-infected HeG2 samples. Interestingly, the IN- vector in this cells line appeared more strongly associated with increased methylation suggesting that integration may add to the cell's methylation response to the incoming virus and that the presence of non-integrating genomes can independently initiate a host innate immune response. Importantly, though MLV empty particles induce a larger response in both Mcf10a and HepG2 cells than IN- vector.

To associate the methylation response by cells to DNA damage, global methylation was then measured in the MEF 53BP1-/- cell line. Only the EIAV vector appeared to increase global methylation in these cells. As the rest of the vectors used on MEF 53BP1-/- cells did not cause elevated global methylation levels the EIAV observation may be an anomaly and warrants repeating. Most importantly, very little or no increase in methylation was found in this cell line following infection by the remaining RV and LV strongly indicating DNA damage to be associated with the innate cells methylation response. This is consistent with studies by Palii *et al* in 2008 that showed cells deficient in DNMT1 resulted in defects in the activation of key DSB responses (Palii *et al.*, 2008).

DNA methyl transferase (DNMTs) contributes to the maintenance (DNMT1) of methylation patterns in the mammalian genome and plays a key role in *de novo* methylation (DNMT 3a and 3b). A number of studies have highlighted the role of viral infection on stimulating the cellular methylation machinery. Leonard *et al* (2011) showed an up regulation of DNMT3a and a down regulation of DNMT3b and DNMT1 following EBV infection of B cells (Leonard *et al.*, 2011). Thus it was of significance to show that the observed changes in the in global methylation found in RV and LV infected cells correlated with changes in DNMT expression. Q-PCR analysis was used

to measure the expression of DNMT1, 3a and 3b in Mcf10a, HepG2 and 53BP1 -/- cell types.

Analysis of DSB in Mcf10a cells infected with the MLV vector identified levels of 53BP1 foci increase at 6 hours and subsequently decrease at 24 hours, presumably due to DNA repair. At this time point global methylation levels increased albeit slightly (1.4 fold) and then further at 24 hours (2.72 fold) and remained similar to this level after 72 hours. This follows the DNMT1 expression levels observed which although found decreased at 6 hours (0.14 fold) increased at 24 hours (1.43 fold).

The MEF 53BP1-/-cell line that is NHEJ deficient showed no increases in DNA global methylation at 6 and 24 hours post infection with MLV vectors suggesting 53BP1 may be involved in initiation of host methylation. This appears accompanied by levels of DNMT1 decreasing at 6 hours post infection with MLV followed by a very slight increase at 24 hours (1.24 fold). For the cell lines that have DNA repair pathways, DSB appear at 6 hours followed by repair at 24 hours onwards after infection except At5biva and Xp14br cell lines where DSB continue to increase at 24 hours as no repair in taking place. It would be interesting to measure global methylation and DNMT1 levels in At5biva and Xp14br cell lines following infection to determine whether induction of DNMT1 occurs and if this is truly dependent on the 53BP1 protein alone. Collectively, these data suggests that DNA methylation may require DNMT1 for DNA repair.

Mcf10a cells infected with MLV vector containing no genome had a more pronounced increase in numbers of 53BP1 foci at 6 hours post infection followed by repair at 24 hours shown by the decrease in 53BP1 foci at this time point. Global methylation levels for this vector increased to the highest level compared to any of the other vectors used (44.23 fold) at 6 hours. Once again, global methylation then decreased after 24 hours and further at 72 hours (12.62 and 7.12 fold, respectively). However, DNMT1 expression levels were found decreased at 6 and 24 hours post infection. This was also supported by microarray of Mcf10a cells with a decrease in DNMT1 levels at 6 hours post infection for cells infected with the MLV without genome. This suggests methylation does not require DNMT1. Also, where there is MLV genome but no integrase (IN-) there is increasing global methylation and levels of DNMT1 increase. It is impossible to reconcile this data because the IN- vector is HIV based and different genomes or integrase molecules may have different effects on the host response to these factors as found by the variation in DSB levels, global meathylation and DNMT levels

between treated cells. What is clearly evident is that lack of DNMT 1 coincides with absence of global methylation. Ideally, focussing on MLV vectors alone with and without genomes and with IN- would be beneficial to understanding the relationship between DNA damage and methylation.

HIV vector infection of Mcf10a is followed by an increase in global methylation levels at 6 hours (2.86 fold) then a decrease (1.21 fold) followed by an increase at 72 hours (4.14 fold). DNMT1 levels were found to decrease at 6 hours (0.03 fold) and 24 hours (0.20 fold) post infection. These results are inconsistent with the findings of Fang *et al* (2000) (Fang *et al.*, 2001) where cells infected with attenuated HIV vectors show an increase in DNMT1 expression. Their DNMT1 measurements were, however, performed at 3-5 days post infection and levels of DNMT1 in this study may have increased in line with the increase in global methylation identified if measurements of DNMT1 were taken at this time point. Surprisingly, DNMT1 rose markedly in MEF 53BP-/- cells infected with the HIV vector at 6 hours and slightly for EIAV.

Increases in DNMT 3a and 3b (the DNA methyltransferases required to establish DNA methylation) levels in cells increased in Mcf10 cells for most vectors except IN- suggesting the integrase is required to induce these methyltransferases. The requirement for the vector genome to induce DNMT 3a and b expression is questionable since infection with the MLV vector without genome appeared to be associated with the highest DNMT 3a and b level increase. In HepG2 cells, no such increase in DNMT 3a and b was observed except for when FIV vector was used, however, global methylation increases did occur in these cells when infected by all vectors. This made the results obtained in HepG2 difficult to explain and this work requires repeating.

It is obvious from the study presented here that different vectors appear to be associated with different responses by the host. Not only were these differences found for MLV and HIV vectors but even the FIV vector which is an alternative non-primate vector to EIAV showed a markedly different host global methylation response to infection in HepG2 cells. Indeed, *in vivo* the HIV vector was not associated with oncogenesis but the EIAV and FIV vectors were. Although, analysis of DNMTs was not performed in cells infected with the FIV vector, the lack of global methylation increase in MEF 53BP1-/- cells infected with this vector agrees with this finding for each of the other vectors used in this study.

Our results from our methylation assay suggested infection to be related to DNA damage and elevated methylation levels. To examine this is detail differential gene expression in pathways for DNA damage, DNA repair and DNA methylation were studied in Mcf10a cells. Gene expression was measured in all infected samples and compared to normal un-infected Mcf10a samples. Mcf10a samples were infected with the EIAV, MLV and MLV vector without genome (empty vector). Genes with gene ontology terms of "DNA repair", "DNA damage" and "DNA methylation" were selected from the microarray data. Genes with 1.2 fold or more increase or decrease difference were selected. Out of the 61 genes found to be up-regulated 62.3% were found to be associated with the DNA damage pathway, 46% involved in the DNA repair pathway and 8.2% in the DNA methylation pathway. 25 genes were found down regulated. Out of these genes 52% were associated with DNA repair, 48% involved in the DNA repair pathway and 12% in the DNA methylation pathway.

E2F control of its target genes is known to be controlled by methylation of CpG regions of target gene promoters. It was suspected that the increased global methylation could potentially lead to changes in the expression of these transcription factor target genes some of which are oncogenes or tumour suppressor genes and known to be involved in several cancers. E2F target genes are also genes involved in DNA damage and repair mechanisms. This was shown by Polager *et al* (2002) who demonstrated E2F1 and E2F3 actively up regulates DNA repair gene expression (Polager *et al.,* 2002). Frame *et al* (2006) also showed that following dysregulation of E2F1 that the MRN complex, which is required NHEJ DNA repair cannot localise 53BP1 and γH2AX to sites of DNA damage (Frame *et al.,* 2006). Hence E2F transcription factors are closely linked to DNA damage and this process is controlled by methylation which if altered could have a role in cancer development.

Using Opossum software http://opossum.cisreg.ca/oPOSSUM3/, the number of genes in the human genome with predicted motifs for E2F binding and are thus potential E2F targets equates to 32.7%. The number of genes that have E2F binding motifs found deregulated by microarray analysis ($p<0.05$) after infection of Mcf10a cells with EIAV, MLV and MLV without genome was 59%. Hence, there were significant changes in E2F targets differentially expressed in infected cells compared with un-infected cells. Of the E2F target genes analysed 28.6% was found to be involved in DNA damage,

28.6% were known to be involved in DNA repair and 9% were found to be involved in DNA methylation. Interestingly of the 56 genes found aberrantly expressed the number of genes most significantly changed in expression levels ($p<0.05$) were in cells infected by the MLV vector without genome and the majority of these genes are involved in the DDR pathway. This also agrees with the DSB identified by 53BP1 immunofluorescence in nuclei of Mcf10a cells infected with this vector.

6.1 Conclusion

The findings described in this thesis although preliminary suggest an alternative pathway of genotoxicity related to virus infection whereby infection followed by integration leads to DNA damage. This then provokes the host innate immune system to methylate its own genome and this leads to changes in E2F target gene expression. As these targets are known involved in cell proliferation, division, differentiation, control of homeostasis and have a role in cancer, this suggests such changes in expression would be detrimental to cells. We can hypothesize that this may be linked or independent to insertional mutagenesis and may potentially be mechanistic to the HCC found in mice treated with EIAV and FIV vectors. Although it was not shown here *in vitro* that genome instability occurred after incomplete DNA damage repair this should be further investigated.

Abbaszadeh, F., Clingen, P.H., Arlett, C.F., Plowman, P.N., Bourton, E.C., Themis, M., Makarov, E.M., Newbold, R.F., Green, M.H. and Parris, C.N. (2010) "A novel splice variant of the DNA-PKcs gene is associated with clinical and cellular radiosensitivity in a patient with xeroderma pigmentosum ", *Journal of medical genetics*, vol. 47, no. 3, pp. 176-181.

Aiuti, A., Slavin, S., Aker, M., Ficara, F., Deola, S., Mortellaro, A., Morecki, S., Andolfi, G., Tabucchi, A., Carlucci, F., Marinello, E., Cattaneo, F., Vai, S., Servida, P., Miniero, R., Roncarolo, M.G. and Bordignon, C. (2002) "Correction of ADA-SCID by stem cell gene therapy combined with nonmyeloablative conditioning ", *Science (New York, N.Y.)*, vol. 296, no. 5577, pp. 2410-2413.

Akagi, K., Suzuki, T., Stephens, R.M., Jenkins, N.A. and Copeland, N.G. (2004) "RTCGD: retroviral tagged cancer gene database ", *Nucleic acids research*, vol. 32, no. Database issue, pp. D523-7.

Albanese, A., Arosio, D., Terreni, M. and Cereseto, A. (2008) "HIV-1 pre-integration complexes selectively target decondensed chromatin in the nuclear periphery ", *PloS one*, vol. 3, no. 6, pp. e2413.

Amsterdam, A., Burgess, S., Golling, G., Chen, W., Sun, Z., Townsend, K., Farrington, S., Haldi, M. and Hopkins, N. (1999) "A large-scale insertional mutagenesis screen in zebrafish ", *Genes & development*, vol. 13, no. 20, pp. 2713-2724.

Arlett, C.F., Green, M.H., Priestley, A., Harcourt, S.A. and Mayne, L.V. (1988) "Comparative human cellular radiosensitivity: I. The effect of SV40 transformation and immortalisation on the gamma-irradiation survival of skin derived fibroblasts from normal individuals and from ataxia-telangiectasia patients and heterozygotes ", *International journal of radiation biology*, vol. 54, no. 6, pp. 911-928.

Armstrong, C.A., Jones, G.D., Anderson, R., Iyer, P., Narayanan, D., Sandhu, J., Singh, R., Talbot, C.J. and Tufarelli, C. (2012) "DNMTs are required for delayed genome instability caused by radiation ", *Epigenetics : official journal of the DNA Methylation Society*, vol. 7, no. 8, pp. 892-902.

Astrakhan, A., Sather, B.D., Ryu, B.Y., Khim, S., Singh, S., Humblet-Baron, S., Ochs, H.D., Miao, C.H. and Rawlings, D.J. (2012) "Ubiquitous high-level gene expression in hematopoietic lineages provides effective lentiviral gene therapy of murine Wiskott-Aldrich syndrome ", *Blood*, vol. 119, no. 19, pp. 4395-4407.

Barnes, D.E. (2001) "Non-homologous end joining as a mechanism of DNA repair ", *Current biology : CB*, vol. 11, no. 12, pp. R455-7.

Barraza, R.A. and Poeschla, E.M. (2008) "Human gene therapy vectors derived from feline lentiviruses", *Veterinary immunology and immunopathology*, vol. 123, no. 1-2, pp. 23-31.

Bassing, C.H. and Alt, F.W. (2004) "The cellular response to general and programmed DNA double strand breaks ", *DNA repair*, vol. 3, no. 8-9, pp. 781-796.

Bassing, C.H., Suh, H., Ferguson, D.O., Chua, K.F., Manis, J., Eckersdorff, M., Gleason, M., Bronson, R., Lee, C. and Alt, F.W. (2003) "Histone H2AX: a dosage-dependent suppressor of oncogenic translocations and tumors ", *Cell*, vol. 114, no. 3, pp. 359-370.

Bassing, C.H., Swat, W. and Alt, F.W. (2002) "The mechanism and regulation of chromosomal V(D)J recombination ", *Cell*, vol. 109 Suppl, pp. S45-55.

Baum, C., Dullmann, J., Li, Z., Fehse, B., Meyer, J., Williams, D.A. and von Kalle, C. (2003) "Side effects of retroviral gene transfer into hematopoietic stem cells ", *Blood*, vol. 101, no. 6, pp. 2099-2114.

Baum, C., Kustikova, O., Modlich, U., Li, Z. and Fehse, B. (2006) "Mutagenesis and oncogenesis by chromosomal insertion of gene transfer vectors", *Human Gene Therapy*, vol. 17, no. 3, pp. 253-263.

Baum, C., von Kalle, C., Staal, F.J., Li, Z., Fehse, B., Schmidt, M., Weerkamp, F., Karlsson, S., Wagemaker, G. and Williams, D.A. (2004) "Chance or necessity? Insertional mutagenesis in gene therapy and its consequences ", *Molecular therapy : the journal of the American Society of Gene Therapy*, vol. 9, no. 1, pp. 5-13.

Baylin, S.B. and Herman, J.G. (2000) "DNA hypermethylation in tumorigenesis: epigenetics joins genetics ", *Trends in genetics : TIG*, vol. 16, no. 4, pp. 168-174.

Ben-David, Y., Lavigueur, A., Cheong, G.Y. and Bernstein, A. (1990) "Insertional inactivation of the p53 gene during friend leukemia: a new strategy for identifying tumor suppressor genes ", *The New biologist*, vol. 2, no. 11, pp. 1015-1023.

Bendich, A. (1961) "Nucleic Acids and the Genesis of Cancer ", *Bulletin of the New York Academy of Medicine*, vol. 37, no. 10, pp. 661-674.

Benit, L., Dessen, P. and Heidmann, T. (2001) "Identification, phylogeny, and evolution of retroviral elements based on their envelope genes ", *Journal of virology*, vol. 75, no. 23, pp. 11709-11719.

Bestor, T., Laudano, A., Mattaliano, R. and Ingram, V. (1988) "Cloning and sequencing of a cDNA encoding DNA methyltransferase of mouse cells. The carboxyl-terminal domain of the mammalian enzymes is related to bacterial restriction methyltransferases ", *Journal of Molecular Biology*, vol. 203, no. 4, pp. 971-983.

Bjorgvinsdottir, H., Ding, C., Pech, N., Gifford, M.A., Li, L.L. and Dinauer, M.C. (1997) "Retroviral-mediated gene transfer of gp91phox into bone marrow cells rescues defect in host defense against Aspergillus fumigatus in murine X-linked chronic granulomatous disease ", *Blood*, vol. 89, no. 1, pp. 41-48.

Blackburn, M.R., Datta, S.K., Wakamiya, M., Vartabedian, B.S. and Kellems, R.E. (1996) "Metabolic and immunologic consequences of limited adenosine deaminase expression in mice ", *The Journal of biological chemistry*, vol. 271, no. 25, pp. 15203-15210.

Blaese, R.M., Culver, K.W., Miller, A.D., Carter, C.S., Fleisher, T., Clerici, M., Shearer, G., Chang, L., Chiang, Y., Tolstoshev, P., Greenblatt, J.J., Rosenberg, S.A., Klein, H., Berger, M., Mullen, C.A., Ramsey, W.J., Muul, L., Morgan, R.A. and Anderson, W.F. (1995) "T lymphocyte-directed gene therapy for ADA- SCID: initial trial results after 4 years ", *Science (New York, N.Y.)*, vol. 270, no. 5235, pp. 475-480.

Borenfreund, E. and Bendich, A. (1961) "A Study of the Penetration of Mammalian Cells by Deoxyribonucleic Acids ", *The Journal of biophysical and biochemical cytology*, vol. 9, no. 1, pp. 81-91.

Bouard, D., Alazard-Dany, D. and Cosset, F.L. (2009) "Viral vectors: from virology to transgene expression ", *British journal of pharmacology*, vol. 157, no. 2, pp. 153-165.

Bourton, E.C., Plowman, P.N., Zahir, S.A., Senguloglu, G.U., Serrai, H., Bottley, G. and Parris, C.N. (2012) "Multispectral imaging flow cytometry reveals distinct frequencies of gamma-H2AX foci induction in DNA double strand break repair defective human cell lines ", *Cytometry.Part A : the journal of the International Society for Analytical Cytology*, vol. 81, no. 2, pp. 130-137.

Boveri, T. (2008) "Concerning the origin of malignant tumours by Theodor Boveri. Translated and annotated by Henry Harris ", *Journal of cell science*, vol. 121 Suppl 1, pp. 1-84.

Brown, K.D. and Robertson, K.D. (2007) "DNMT1 knockout delivers a strong blow to genome stability and cell viability ", *Nature genetics*, vol. 39, no. 3, pp. 289-290.

Brügger, B., Krautkrämer, E., Tibroni, N., Munte, C.E., Rauch, S., Leibrecht, I., Glass, B., Breuer, S., Geyer, M., Kräusslich, H., Kalbitzer, H., Wieland, F.T. and Fackler, O.T. (2007) "Human Immunodeficiency Virus Type 1 Nef protein modulates the lipid composition of virions and host cell membrane microdomains ", *Retrovirology*, vol. 4, no. 1, pp. 70.

Buchschacher, G.L.,Jr and Wong-Staal, F. (2000) "Development of lentiviral vectors for gene therapy for human diseases ", *Blood*, vol. 95, no. 8, pp. 2499-2504.

Bukrinsky, M.I., Sharova, N., McDonald, T.L., Pushkarskaya, T., Tarpley, W.G. and Stevenson, M. (1993) "Association of integrase, matrix, and reverse transcriptase

antigens of human immunodeficiency virus type 1 with viral nucleic acids following acute infection ", *Proceedings of the National Academy of Sciences of the United States of America,* vol. 90, no. 13, pp. 6125-6129.

Burns J C, Friedmann T and Driever W, Burrascano M, and Yee J K. (1993) "Vesicular stomatitis virus G glycoprotein pseudotyped retroviral vectors: concentration to very high titer and efficient gene transfer into mammalian and nonmammalian cells", *PNAS,* Vol. 90, no 17, pp.8033-8037

Bushman, F., Lewinski, M., Ciuffi, A., Barr, S., Leipzig, J., Hannenhalli, S. and Hoffmann, C. (2005) "Genome-wide analysis of retroviral DNA integration", *Nature reviews.Microbiology,* vol. 3, no. 11, pp. 848-858.

Bushman, F.D. (2007) "Retroviral integration and human gene therapy ", *The Journal of clinical investigation,* vol. 117, no. 8, pp. 2083-2086.

Cardone, G., Purdy, J.G., Cheng, N., Craven, R.C. and Steven, A.C. (2009) "Visualization of a missing link in retrovirus capsid assembly ", *Nature,* vol. 457, no. 7230, pp. 694-698.

Cattoglio, C., Maruggi, G., Bartholomae, C., Malani, N., Pellin, D., Cocchiarella, F., Magnani, Z., Ciceri, F., Ambrosi, A., von Kalle, C., Bushman, F.D., Bonini, C., Schmidt, M., Mavilio, F. and Recchia, A. (2010) "High-definition mapping of retroviral integration sites defines the fate of allogeneic T cells after donor lymphocyte infusion ", *PloS one,* vol. 5, no. 12, pp. e15688.

Cavazzana-Calvo, M. and Hacein-Bey-Abina, S. (2001) "Correction of genetic blood defects by gene transfer", *Current opinion in hematology,* vol. 8, no. 6, pp. 360-367.

Cavazzana-Calvo, M., Hacein-Bey, S., de Saint Basile, G., Gross, F., Yvon, E., Nusbaum, P., Selz, F., Hue, C., Certain, S., Casanova, J.L., Bousso, P., Deist, F.L. and Fischer, A. (2000) "Gene therapy of human severe combined immunodeficiency (SCID)-X1 disease ", *Science (New York, N.Y.),* vol. 288, no. 5466, pp. 669-672.

Celeste, A., Petersen, S., Romanienko, P.J., Fernandez-Capetillo, O., Chen, H.T., Sedelnikova, O.A., Reina-San-Martin, B., Coppola, V., Meffre, E., Difilippantonio, M.J., Redon, C., Pilch, D.R., Olaru, A., Eckhaus, M., Camerini-Otero, R.D., Tessarollo, L., Livak, F., Manova, K., Bonner, W.M., Nussenzweig, M.C. and Nussenzweig, A. (2002) "Genomic instability in mice lacking histone H2AX ", *Science (New York, N.Y.),* vol. 296, no. 5569, pp. 922-927.

Chang, L.J., Liu, X. and He, J. (2005) "Lentiviral siRNAs targeting multiple highly conserved RNA sequences of human immunodeficiency virus type 1 ", *Gene therapy,* vol. 12, no. 14, pp. 1133-1144.

Check, E. (2002) "A tragic setback", *Nature,* vol. 420, no. 6912, pp. 116-118.

Chellappan, S.P., Hiebert, S., Mudryj, M., Horowitz, J.M. and Nevins, J.R. (1991) "The E2F transcription factor is a cellular target for the RB protein ", *Cell,* vol. 65, no. 6, pp. 1053-1061.

Chen, R.Z., Pettersson, U., Beard, C., Jackson-Grusby, L. and Jaenisch, R. (1998) "DNA hypomethylation leads to elevated mutation rates ", *Nature,* vol. 395, no. 6697, pp. 89-93.

Chen, S.T., Iida, A., Guo, L., Friedmann, T. and Yee, J.K. (1996) "Generation of packaging cell lines for pseudotyped retroviral vectors of the G protein of vesicular stomatitis virus by using a modified tetracycline inducible system ", *Proceedings of the National Academy of Sciences of the United States of America,* vol. 93, no. 19, pp. 10057-10062.

Cherepanov, P. (2007) "LEDGF/p75 interacts with divergent lentiviral integrases and modulates their enzymatic activity in vitro ", *Nucleic acids research,* vol. 35, no. 1, pp. 113-124.

Cleaver, J.E. (1968) "Defective repair replication of DNA in xeroderma pigmentosum ", *Nature,* vol. 218, no. 5142, pp. 652-656.

Coffin, J.M. (1996) "Retroviridae: the viruses and their replication.", *Fields Virology,* , pp. 1767-848.

Condiotti R, Goldenberg D, Giladi H, Schnitzer-Perlman T, Waddington S, Buckley SM, Heim D, Cheung W, Themis M, Charles C, Simerzin A, Osejindu E, Wege H, Themis M, Galun E. (2013) "Transduction of fetal mice with a feline lentiviral vector induces liver tumors which exhibit an E2F activation signature.", *Mol.Ther.,* [Online], . [9/25/2013].

Cosset, F.L., Takeuchi, Y., Battini, J.L., Weiss, R.A. and Collins, M.K. (1995) "High-titer packaging cells producing recombinant retroviruses resistant to human serum ", *Journal of virology,* vol. 69, no. 12, pp. 7430-7436.

Coutelle, C., Themis, M., Waddington, S., Gregory, L., Nivsarkar, M., Buckley, S., Cook, T., Rodeck, C., Peebles, D. and David, A. (2003) "The hopes and fears of in utero gene therapy for genetic disease--a review ", *Placenta,* vol. 24 Suppl B, pp. S114-21.

Coutelle, C., Themis, M., Waddington, S.N., Buckley, S.M., Gregory, L.G., Nivsarkar, M.S., David, A.L., Peebles, D., Weisz, B. and Rodeck, C. (2005) "Gene therapy progress and prospects: fetal gene therapy--first proofs of concept--some adverse effects ", *Gene therapy,* vol. 12, no. 22, pp. 1601-1607.

Cowell, J.K., LaDuca, J., Rossi, M.R., Burkhardt, T., Nowak, N.J. and Matsui, S. (2005) "Molecular characterization of the t(3;9) associated with immortalization in the MCF10A cell line ", *Cancer genetics and cytogenetics,* vol. 163, no. 1, pp. 23-29.

Cronin, J., Zhang, X.Y. and Reiser, J. (2005) "Altering the tropism of lentiviral vectors through pseudotyping ", *Current gene therapy*, vol. 5, no. 4, pp. 387-398.

Culver, K.W., Osborne, W.R., Miller, A.D., Fleisher, T.A., Berger, M., Anderson, W.F. and Blaese, R.M. (1991) "Correction of ADA deficiency in human T lymphocytes using retroviral-mediated gene transfer ", *Transplantation proceedings*, vol. 23, no. 1 Pt 1, pp. 170-171.

Cuozzo, C., Porcellini, A., Angrisano, T., Morano, A., Lee, B., Di Pardo, A., Messina, S., Iuliano, R., Fusco, A., Santillo, M.R., Muller, M.T., Chiariotti, L., Gottesman, M.E. and Avvedimento, E.V. (2007) "DNA damage, homology-directed repair, and DNA methylation ", *PLoS genetics*, vol. 3, no. 7, pp. e110.

Damico, R. and Bates, P. (2000) "Soluble receptor-induced retroviral infection of receptor-deficient cells ", *Journal of virology*, vol. 74, no. 14, pp. 6469-6475.

Daniel, R., Greger, J.G., Katz, R.A., Taganov, K.D., Wu, X., Kappes, J.C. and Skalka, A.M. (2004) "Evidence that stable retroviral transduction and cell survival following DNA integration depend on components of the nonhomologous end joining repair pathway ", *Journal of virology*, vol. 78, no. 16, pp. 8573-8581.

Daniel, R., Katz, R.A. and Skalka, A.M. (1999) "A role for DNA-PK in retroviral DNA integration ", *Science (New York, N.Y.)*, vol. 284, no. 5414, pp. 644-647.

Danos, O. and Mulligan, R.C. (1988) "Safe and efficient generation of recombinant retroviruses with amphotropic and ecotropic host ranges", *Proceedings of the National Academy of Sciences of the United States of America*, vol. 85, no. 17, pp. 6460-6464.

Das, S.R. and Jameel, S. (2005) "Biology of the HIV Nef protein ", *The Indian journal of medical research*, vol. 121, no. 4, pp. 315-332.

Dave, U.P., Akagi, K., Tripathi, R., Cleveland, S.M., Thompson, M.A., Yi, M., Stephens, R., Downing, J.R., Jenkins, N.A. and Copeland, N.G. (2009) "Murine leukemias with retroviral insertions at Lmo2 are predictive of the leukemias induced in SCID-X1 patients following retroviral gene therapy ", *PLoS genetics*, vol. 5, no. 5, pp. e1000491.

DeGregori, J., Leone, G., Miron, A., Jakoi, L. and Nevins, J.R. (1997) "Distinct roles for E2F proteins in cell growth control and apoptosis ", *Proceedings of the National Academy of Sciences of the United States of America*, vol. 94, no. 14, pp. 7245-7250.

del Pozo-Rodriguez, A., Delgado, D., Solinis, M.A., Gascon, A.R. and Pedraz, J.L. (2008) "Solid lipid nanoparticles for retinal gene therapy: transfection and intracellular trafficking in RPE cells ", *International journal of pharmaceutics*, vol. 360, no. 1-2, pp. 177-183.

Delassus, S., Cheynier, R. and Wain-Hobson, S. (1991) "Evolution of human immunodeficiency virus type 1 nef and long terminal repeat sequences over 4 years in vivo and in vitro ", *Journal of virology*, vol. 65, no. 1, pp. 225-231.

Delviks-Frankenberry, K., Galli, A., Nikolaitchik, O., Mens, H., Pathak, V.K. and Hu, W.S. (2011) "Mechanisms and factors that influence high frequency retroviral recombination ", *Viruses*, vol. 3, no. 9, pp. 1650-1680.

Devaskar, S.U. & Raychaudhuri, S. (2007) "Epigenetics--a science of heritable biological adaptation.", *Pediatric research*, vol. 5, no1R-4R

Dinauer, M.C., Gifford, M.A., Pech, N., Li, L.L. and Emshwiller, P. (2001) "Variable correction of host defense following gene transfer and bone marrow transplantation in murine X-linked chronic granulomatous disease ", *Blood*, vol. 97, no. 12, pp. 3738-3745.

Dolinoy, D.C., Weidman, J.R. and Jirtle, R.L. (2007) "Epigenetic gene regulation: linking early developmental environment to adult disease ", *Reproductive toxicology (Elmsford, N.Y.)*, vol. 23, no. 3, pp. 297-307.

Douar, A., Themis, M. and Coutelle, C. (1996) "Fetal somatic gene therapy ", *Molecular human reproduction*, vol. 2, no. 9, pp. 633 <last_page> 641.

DS, G. (2005) "The molecular perspective: double-stranded DNA breaks", *stem cells*, vol. 23, no. 7, pp. 1021-2.

Dull, T., Zufferey, R., Kelly, M., Mandel, R.J., Nguyen, M., Trono, D. and Naldini, L. (1998) "A third-generation lentivirus vector with a conditional packaging system ", *Journal of virology*, vol. 72, no. 11, pp. 8463-8471.

Dyson, N. (1998) "The regulation of E2F by pRB-family proteins ", *Genes & development*, vol. 12, no. 15, pp. 2245-2262.

Edelstein, M.L., Abedi, M.R. and Wixon, J. (2007) "Gene therapy clinical trials worldwide to 2007--an update ", *The journal of gene medicine*, vol. 9, no. 10, pp. 833-842.

Erlwein, O., Bieniasz, P.D. and McClure, M.O. (1998) "Sequences in pol are required for transfer of human foamy virus-based vectors ", *Journal of virology*, vol. 72, no. 7, pp. 5510-5516.

Essers, J., van Steeg, H., de Wit, J., Swagemakers, S.M., Vermeij, M., Hoeijmakers, J.H. and Kanaar, R. (2000) "Homologous and non-homologous recombination differentially affect DNA damage repair in mice ", *The EMBO journal*, vol. 19, no. 7, pp. 1703-1710.

Fang, J.Y., Mikovits, J.A., Bagni, R., Petrow-Sadowski, C.L. and Ruscetti, F.W. (2001) "Infection of lymphoid cells by integration-defective human immunodeficiency virus type 1 increases de novo methylation ", *Journal of virology*, vol. 75, no. 20, pp. 9753-9761.

Fehse, B. and Roeder, I. (2008) "Insertional mutagenesis and clonal dominance: biological and statistical considerations ", *Gene therapy*, vol. 15, no. 2, pp. 143-153.

Fernandez-Capetillo, O., Chen, H.T., Celeste, A., Ward, I., Romanienko, P.J., Morales, J.C., Naka, K., Xia, Z., Camerini-Otero, R.D., Motoyama, N., Carpenter, P.B., Bonner, W.M., Chen, J. and Nussenzweig, A. (2002) "DNA damage-induced G2-M checkpoint activation by histone H2AX and 53BP1 ", *Nature cell biology*, vol. 4, no. 12, pp. 993-997.

Finer, M.H., Dull, T.J., Qin, L., Farson, D. and Roberts, M.R. (1994) "kat: a high-efficiency retroviral transduction system for primary human T lymphocytes", *Blood*, vol. 83, no. 1, pp. 43-50.

FitzGerald, J.E., Grenon, M. and Lowndes, N.F. (2009) "53BP1: function and mechanisms of focal recruitment ", *Biochemical Society transactions*, vol. 37, no. Pt 4, pp. 897-904.

Follenzi, A., Ailles, L.E., Bakovic, S., Geuna, M. and Naldini, L. (2000) "Gene transfer by lentiviral vectors is limited by nuclear translocation and rescued by HIV-1 pol sequences", *Nature genetics*, vol. 25, no. 2, pp. 217-222.

Fouchier, R.A. and Malim, M.H. (1999) "Nuclear import of human immunodeficiency virus type-1 preintegration complexes ", *Advances in Virus Research*, vol. 52, pp. 275-299.

Fouty, B. and Solodushko; Chapter 4, V. (2011) "Viral Gene Therapy; The Glucocorticoid Receptor in Retroviral Infection"

Frame, F.M., Rogoff, H.A., Pickering, M.T., Cress, W.D. and Kowalik, T.F. (2006) "E2F1 induces MRN foci formation and a cell cycle checkpoint response in human fibroblasts ", *Oncogene*, vol. 25, no. 23, pp. 3258-3266.

Friedberg, E.C. (2002) "The intersection between the birth of molecular biology and the DNA repair and mutagenesis field", *DNA Repair (Amst)*, vol. 1, pp. 855-867.

Friedmann, T. and Roblin, R. (1972) "Gene therapy for human genetic disease? ", *Science (New York, N.Y.)*, vol. 175, no. 4025, pp. 949-955.

Ganser-Pornillos, B.K., Yeager, M. and Sundquist, W.I. (2008) "The structural biology of HIV assembly ", *Current opinion in structural biology*, vol. 18, no. 2, pp. 203-217.

Gartler, S.M., Goldstein, L., Tyler-Freer, S.E. and Hansen, R.S. (1999) "The timing of XIST replication: dominance of the domain ", *Human molecular genetics,* vol. 8, no. 6, pp. 1085-1089.

Gaspar, H.B., Parsley, K.L., Howe, S., King, D., Gilmour, K.C., Sinclair, J., Brouns, G., Schmidt, M., Von Kalle, C., Barington, T., Jakobsen, M.A., Christensen, H.O., Al Ghonaium, A., White, H.N., Smith, J.L., Levinsky, R.J., Ali, R.R., Kinnon, C. and Thrasher, A.J. (2004) "Gene therapy of X-linked severe combined immunodeficiency by use of a pseudotyped gammaretroviral vector", *Lancet,* vol. 364, no. 9452, pp. 2181-2187.

Gaspar, H.B., Parsley, K.L., Howe, S., King, D., Gilmour, K.C., Sinclair, J., Brouns, G., Schmidt, M., Von Kalle, C., Barington, T., Jakobsen, M.A., Christensen, H.O., Al Ghonaium, A., White, H.N., Smith, J.L., Levinsky, R.J., Ali, R.R., Kinnon, C. and Thrasher, A.J. (2004) "Gene therapy of X-linked severe combined immunodeficiency by use of a pseudotyped gammaretroviral vector ", *Lancet,* vol. 364, no. 9452, pp. 2181-2187.

Gilbert, P.B., McKeague, I.W., Eisen, G., Mullins, C., Gueye-NDiaye, A., Mboup, S. and Kanki, P.J. (2003) "Comparison of HIV-1 and HIV-2 infectivity from a prospective cohort study in Senegal ", *Statistics in medicine,* vol. 22, no. 4, pp. 573-593.

Goff, S.P. (2001) "Intracellular trafficking of retroviral genomes during the early phase of infection: viral exploitation of cellular pathways ", *The journal of gene medicine,* vol. 3, no. 6, pp. 517-528.

Goff, S.P. (1987) "Gene isolation by retroviral tagging ", *Methods in enzymology,* vol. 152, pp. 469-481.

Goverdhana, S., Puntel, M., Xiong, W., Zirger, J.M., Barcia, C., Curtin, J.F., Soffer, E.B., Mondkar, S., King, G.D., Hu, J., Sciascia, S.A., Candolfi, M., Greengold, D.S., Lowenstein, P.R. and Castro, M.G. (2005) "Regulatable gene expression systems for gene therapy applications: progress and future challenges ", *Molecular therapy : the journal of the American Society of Gene Therapy,* vol. 12, no. 2, pp. 189-211.

Guo, G., Wang, W. and Bradley, A. (2004) "Mismatch repair genes identified using genetic screens in Blm-deficient embryonic stem cells ", *Nature,* vol. 429, no. 6994, pp. 891-895.

Hacein-Bey-Abina, S., Garrigue, A., Wang, G.P., Soulier, J., Lim, A., Morillon, E., Clappier, E., Caccavelli, L., Delabesse, E., Beldjord, K., Asnafi, V., MacIntyre, E., Dal Cortivo, L., Radford, I., Brousse, N., Sigaux, F., Moshous, D., Hauer, J., Borkhardt, A., Belohradsky, B.H., Wintergerst, U., Velez, M.C., Leiva, L., Sorensen, R., Wulffraat, N., Blanche, S., Bushman, F.D., Fischer, A. and Cavazzana-Calvo, M. (2008) "Insertional oncogenesis in 4 patients after retrovirus-mediated gene therapy of SCID-X1 ", *The Journal of clinical investigation,* vol. 118, no. 9, pp. 3132-3142.

Hacein-Bey-Abina, S., Hauer, J., Lim, A., Picard, C., Wang, G.P., Berry, C.C., Martinache, C., Rieux-Laucat, F., Latour, S., Belohradsky, B.H., Leiva, L., Sorensen, R., Debre, M., Casanova, J.L., Blanche, S., Durandy, A., Bushman, F.D., Fischer, A. and Cavazzana-Calvo, M. (2010) "Efficacy of gene therapy for X-linked severe combined immunodeficiency ", *The New England journal of medicine*, vol. 363, no. 4, pp. 355-364.

Hacein-Bey-Abina, S., Von Kalle, C., Schmidt, M., McCormack, M.P., Wulffraat, N., Leboulch, P., Lim, A., Osborne, C.S., Pawliuk, R., Morillon, E., Sorensen, R., Forster, A., Fraser, P., Cohen, J.I., de Saint Basile, G., Alexander, I., Wintergerst, U., Frebourg, T., Aurias, A., Stoppa-Lyonnet, D., Romana, S., Radford-Weiss, I., Gross, F., Valensi, F., Delabesse, E., Macintyre, E., Sigaux, F., Soulier, J., Leiva, L.E., Wissler, M., Prinz, C., Rabbitts, T.H., Le Deist, F., Fischer, A. and Cavazzana-Calvo, M. (2003) "LMO2-associated clonal T cell proliferation in two patients after gene therapy for SCID-X1 ", *Science (New York, N.Y.)*, vol. 302, no. 5644, pp. 415-419.

Hacker, C.V., Vink, C.A., Wardell, T.W., Lee, S., Treasure, P., Kingsman, S.M., Mitrophanous, K.A. and Miskin, J.E. (2006) "The integration profile of EIAV-based vectors ", *Molecular therapy : the journal of the American Society of Gene Therapy*, vol. 14, no. 4, pp. 536-545.

Helleday, T., Lo, J., van Gent, D.C. and Engelward, B.P. (2007) "DNA double-strand break repair: from mechanistic understanding to cancer treatment ", *DNA repair*, vol. 6, no. 7, pp. 923-935.

Hematti, P., Hong, B.K., Ferguson, C., Adler, R., Hanawa, H., Sellers, S., Holt, I.E., Eckfeldt, C.E., Sharma, Y., Schmidt, M., von Kalle, C., Persons, D.A., Billings, E.M., Verfaillie, C.M., Nienhuis, A.W., Wolfsberg, T.G., Dunbar, C.E. and Calmels, B. (2004) "Distinct genomic integration of MLV and SIV vectors in primate hematopoietic stem and progenitor cells ", *PLoS biology*, vol. 2, no. 12, pp. e423.

Holman, A.G. and Coffin, J.M. (2005) "Symmetrical base preferences surrounding HIV-1, avian sarcoma/leukosis virus, and murine leukemia virus integration sites ", *Proceedings of the National Academy of Sciences of the United States of America*, vol. 102, no. 17, pp. 6103-6107.

Howe, S.J., Mansour, M.R., Schwarzwaelder, K., Bartholomae, C., Hubank, M., Kempski, H., Brugman, M.H., Pike-Overzet, K., Chatters, S.J., de Ridder, D., Gilmour, K.C., Adams, S., Thornhill, S.I., Parsley, K.L., Staal, F.J., Gale, R.E., Linch, D.C., Bayford, J., Brown, L., Quaye, M., Kinnon, C., Ancliff, P., Webb, D.K., Schmidt, M., von Kalle, C., Gaspar, H.B. and Thrasher, A.J. (2008) "Insertional mutagenesis combined with acquired somatic mutations causes leukemogenesis following gene therapy of SCID-X1 patients ", *The Journal of clinical investigation*, vol. 118, no. 9, pp. 3143-3150.

Huyen, Y., Zgheib, O., Ditullio, R.A.,Jr, Gorgoulis, V.G., Zacharatos, P., Petty, T.J., Sheston, E.A., Mellert, H.S., Stavridi, E.S. and Halazonetis, T.D. (2004) "Methylated lysine 79 of histone H3 targets 53BP1 to DNA double-strand breaks ", *Nature*, vol. 432, no. 7015, pp. 406-411.

Iovino, F., Lentini, L., Amato, A. and Di Leonardo, A. (2006) "RB acute loss induces centrosome amplification and aneuploidy in murine primary fibroblasts ", *Molecular cancer*, vol. 5, pp. 38.

Jackson, S.P. (2002) "Sensing and repairing DNA double-strand breaks ", *Carcinogenesis*, vol. 23, no. 5, pp. 687-696.

Jeggo, P.A. and Lobrich, M. (2007) "DNA double-strand breaks: their cellular and clinical impact? ", *Oncogene*, vol. 26, no. 56, pp. 7717-7719.

Joachims, M.L., Marble, P.A., Laurent, A.B., Pastuszko, P., Paliotta, M., Blackburn, M.R. and Thompson, L.F. (2008) "Restoration of adenosine deaminase-deficient human thymocyte development in vitro by inhibition of deoxynucleoside kinases ", *Journal of immunology (Baltimore, Md.: 1950)*, vol. 181, no. 11, pp. 8153-8161.

Jones, P.A. and Laird, P.W. (1999) "Cancer epigenetics comes of age ", *Nature genetics*, vol. 21, no. 2, pp. 163-167.

Josephson, C.D. and Abshire, T.C. (2006) "Clinical uses of plasma and plasma fractions: plasma-derived products for hemophilias A and B, and for von Willebrand disease ", *Best practice & research.Clinical haematology*, vol. 19, no. 1, pp. 35-49.

Kaiser, J. (2003) "Gene therapy. Seeking the cause of induced leukemias in X-SCID trial", *Science (New York, N.Y.)*, vol. 299, no. 5606, pp. 495.

Kanaar, R., Hoeijmakers, J.H. and van Gent, D.C. (1998) "Molecular mechanisms of DNA double strand break repair ", *Trends in cell biology*, vol. 8, no. 12, pp. 483-489.

Kang, E.M. and Malech, H.L. (2009) "Advances in treatment for chronic granulomatous disease ", *Immunologic research*, vol. 43, no. 1-3, pp. 77-84.

Kastan, M.B. and Bartek, J. (2004) "Cell-cycle checkpoints and cancer ", *Nature*, vol. 432, no. 7015, pp. 316-323.

Katen, L.J., Januszeski, M.M., Anderson, W.F., Hasenkrug, K.J. and Evans, L.H. (2001) "Infectious entry by amphotropic as well as ecotropic murine leukemia viruses occurs through an endocytic pathway ", *Journal of virology*, vol. 75, no. 11, pp. 5018-5026.

Kayala, M.A. and Baldi, P. (2012) "Cyber-T web server: differential analysis of high-throughput data ", *Nucleic acids research*, vol. 40, no. Web Server issue, pp. W553-9.

Kim, J., Daniel, J., Espejo, A., Lake, A., Krishna, M., Xia, L., Zhang, Y. and Bedford, M.T. (2006) "Tudor, MBT and chromo domains gauge the degree of lysine methylation ", *EMBO reports*, vol. 7, no. 4, pp. 397-403.

Kim, J.B. and Sharp, P.A. (2001) "Positive transcription elongation factor B phosphorylates hSPT5 and RNA polymerase II carboxyl-terminal domain independently of cyclin-dependent kinase-activating kinase ", *The Journal of biological chemistry*, vol. 276, no. 15, pp. 12317-12323.

King, W., Patel, M.D., Lobel, L.I., Goff, S.P. and Nguyen-Huu, M.C. (1985) "Insertion mutagenesis of embryonal carcinoma cells by retroviruses ", *Science (New York, N.Y.)*, vol. 228, no. 4699, pp. 554-558.

Klose, R.J. and Bird, A.P. (2006) "Genomic DNA methylation: the mark and its mediators ", *Trends in biochemical sciences*, vol. 31, no. 2, pp. 89-97.

Kohn, D.B., Mitsuya, H., Ballow, M., Selegue, J.E., Barankiewicz, J., Cohen, A., Gelfand, E., Anderson, W.F. and Blaese, R.M. (1989) "Establishment and characterization of adenosine deaminase-deficient human T cell lines ", *Journal of immunology (Baltimore, Md.: 1950)*, vol. 142, no. 11, pp. 3971-3977.

Konecki, D.S. and Lichter-Konecki, U. (1991) "The phenylketonuria locus: current knowledge about alleles and mutations of the phenylalanine hydroxylase gene in various populations ", *Human genetics*, vol. 87, no. 4, pp. 377-388.

Kustikova, O.S., Geiger, H., Li, Z., Brugman, M.H., Chambers, S.M., Shaw, C.A., Pike-Overzet, K., de Ridder, D., Staal, F.J., von Keudell, G., Cornils, K., Nattamai, K.J., Modlich, U., Wagemaker, G., Goodell, M.A., Fehse, B. and Baum, C. (2007) "Retroviral vector insertion sites associated with dominant hematopoietic clones mark "stemness" pathways ", *Blood*, vol. 109, no. 5, pp. 1897-1907.

Kustikova, O.S., Modlich, U. and Fehse, B. (2009) "Retroviral insertion site analysis in dominant haematopoietic clones ", *Methods in molecular biology (Clifton, N.J.)*, vol. 506, pp. 373-390.

Kustikova, O.S., Wahlers, A., Kuhlcke, K., Stahle, B., Zander, A.R., Baum, C. and Fehse, B. (2003) "Dose finding with retroviral vectors: correlation of retroviral vector copy numbers in single cells with gene transfer efficiency in a cell population ", *Blood*, vol. 102, no. 12, pp. 3934-3937.

Laing, E. and Smith, C.P. (2010) "RankProdIt: A web-interactive Rank Products analysis tool ", *BMC research notes*, vol. 3, pp. 221-0500-3-221.

Lazarevich, N.L. and Fleishman, D.I. (2008) "Tissue-specific transcription factors in progression of epithelial tumors ", *Biochemistry.Biokhimiia*, vol. 73, no. 5, pp. 573-591.

Lazo, P.A. and Tsichlis, P.N. (1988) "Recombination between two integrated proviruses, one of which was inserted near c-myc in a retrovirus-induced rat thymoma: implications for tumor progression ", *Journal of virology*, vol. 62, no. 3, pp. 788-794.

Lee, C., Chang, J.H., Lee, H.S. and Cho, Y. (2002) "Structural basis for the recognition of the E2F transactivation domain by the retinoblastoma tumor suppressor ", *Genes & development*, vol. 16, no. 24, pp. 3199-3212.

Lee, S., Lee, H.J., Kim, J.H., Lee, H.S., Jang, J.J. and Kang, G.H. (2003) "Aberrant CpG island hypermethylation along multistep hepatocarcinogenesis ", *The American journal of pathology*, vol. 163, no. 4, pp. 1371-1378.

Lee, Y.M., Choi, W.H., Kim, Y.B., Ha, C.S., Song, C.W., Lee, M., Joo, C.W., Hong, Y., Ho, S.H., Kim, S., Kim, J.M. and Koh, W.S. (2008) "Toxicity of repeated intravenous injection of gene therapeutics for X-CGD in mice ", *Human & experimental toxicology*, vol. 27, no. 5, pp. 401-407.

Lentini, L., Pipitone, L. and Di Leonardo, A. (2002) "Functional inactivation of pRB results in aneuploid mammalian cells after release from a mitotic block ", *Neoplasia (New York, N.Y.)*, vol. 4, no. 5, pp. 380-387.

Leonard, S., Wei, W., Anderton, J., Vockerodt, M., Rowe, M., Murray, P.G. and Woodman, C.B. (2011) "Epigenetic and transcriptional changes which follow Epstein-Barr virus infection of germinal center B cells and their relevance to the pathogenesis of Hodgkin's lymphoma ", *Journal of virology*, vol. 85, no. 18, pp. 9568-9577.

Lewinski, M.K., Yamashita, M., Emerman, M., Ciuffi, A., Marshall, H., Crawford, G., Collins, F., Shinn, P., Leipzig, J., Hannenhalli, S., Berry, C.C., Ecker, J.R. and Bushman, F.D. (2006) "Retroviral DNA integration: viral and cellular determinants of target-site selection ", *PLoS pathogens*, vol. 2, no. 6, pp. e60.

Li, E., Bestor, T.H. and Jaenisch, R. (1992) "Targeted mutation of the DNA methyltransferase gene results in embryonic lethality ", *Cell*, vol. 69, no. 6, pp. 915-926.

Li, J., Ning, G. and Duncan, S.A. (2000) "Mammalian hepatocyte differentiation requires the transcription factor HNF-4alpha ", *Genes & development*, vol. 14, no. 4, pp. 464-474.

Li, L., Olvera, J.M., Yoder, K.E., Mitchell, R.S., Butler, S.L., Lieber, M., Martin, S.L. and Bushman, F.D. (2001) "Role of the non-homologous DNA end joining pathway in the early steps of retroviral infection ", *The EMBO journal*, vol. 20, no. 12, pp. 3272-3281.

Li, Z., Dullmann, J., Schiedlmeier, B., Schmidt, M., von Kalle, C., Meyer, J., Forster, M., Stocking, C., Wahlers, A., Frank, O., Ostertag, W., Kuhlcke, K., Eckert, H.G., Fehse,

B. and Baum, C. (2002) "Murine leukemia induced by retroviral gene marking", *Science (New York, N.Y.)*, vol. 296, no. 5567, pp. 497.

Lindwasser, O.W., Chaudhuri, R. and Bonifacino, J.S. (2007) "Mechanisms of CD4 downregulation by the Nef and Vpu proteins of primate immunodeficiency viruses ", *Current Molecular Medicine*, vol. 7, no. 2, pp. 171-184.

Lo, M., Bloom, M.L., Imada, K., Berg, M., Bollenbacher, J.M., Bloom, E.T., Kelsall, B.L. and Leonard, W.J. (1999) "Restoration of lymphoid populations in a murine model of X-linked severe combined immunodeficiency by a gene-therapy approach ", *Blood*, vol. 94, no. 9, pp. 3027-3036.

Lockwood, C.R., Bingham, C. and Frayling, T.M. (2003) "In silico searching of human and mouse genome data identifies known and unknown HNF1 binding sites upstream of beta-cell genes ", *Molecular genetics and metabolism*, vol. 78, no. 2, pp. 145-151.

Lukas, J., Lukas, C. and Bartek, J. (2004) "Mammalian cell cycle checkpoints: signalling pathways and their organization in space and time ", *DNA repair*, vol. 3, no. 8-9, pp. 997-1007.

Malech, H.L., Maples, P.B., Whiting-Theobald, N., Linton, G.F., Sekhsaria, S., Vowells, S.J., Li, F., Miller, J.A., DeCarlo, E., Holland, S.M., Leitman, S.F., Carter, C.S., Butz, R.E., Read, E.J., Fleisher, T.A., Schneiderman, R.D., Van Epps, D.E., Spratt, S.K., Maack, C.A., Rokovich, J.A., Cohen, L.K. and Gallin, J.I. (1997) "Prolonged production of NADPH oxidase-corrected granulocytes after gene therapy of chronic granulomatous disease ", *Proceedings of the National Academy of Sciences of the United States of America*, vol. 94, no. 22, pp. 12133-12138.

Matouk, C.C. and Marsden, P.A. (2008) "Epigenetic regulation of vascular endothelial gene expression ", *Circulation research*, vol. 102, no. 8, pp. 873-887.

McBride, M.S. and Panganiban, A.T. (1997) "Position dependence of functional hairpins important for human immunodeficiency virus type 1 RNA encapsidation in vivo ", *Journal of virology*, vol. 71, no. 3, pp. 2050-2058.

McBride, M.S., Schwartz, M.D. and Panganiban, A.T. (1997) "Efficient encapsidation of human immunodeficiency virus type 1 vectors and further characterization of cis elements required for encapsidation ", *Journal of virology*, vol. 71, no. 6, pp. 4544-4554.

McCabe, M.T., Davis, J.N. and Day, M.L. (2005) "Regulation of DNA methyltransferase 1 by the pRb/E2F1 pathway ", *Cancer research*, vol. 65, no. 9, pp. 3624-3632.

McKinnon, P.J. and Caldecott, K.W. (2007) "DNA strand break repair and human genetic disease ", *Annual review of genomics and human genetics*, vol. 8, pp. 37-55.

Mikovits, J.A., Raziuddin, Gonda, M., Ruta, M., Lohrey, N.C., Kung, H.F. and Ruscetti, F.W. (1990) "Negative regulation of human immune deficiency virus replication in monocytes. Distinctions between restricted and latent expression in THP-1 cells ", *The Journal of experimental medicine*, vol. 171, no. 5, pp. 1705-1720.

Miller, A.D. and Buttimore, C. (1986) "Redesign of retrovirus packaging cell lines to avoid recombination leading to helper virus production", *Molecular and cellular biology*, vol. 6, no. 8, pp. 2895-2902.

Miller, M.D., Farnet, C.M. and Bushman, F.D. (1997) "Human immunodeficiency virus type 1 preintegration complexes: studies of organization and composition ", *Journal of virology*, vol. 71, no. 7, pp. 5382-5390.

Miller, M.D., Wang, B. and Bushman, F.D. (1995) "Human immunodeficiency virus type 1 preintegration complexes containing discontinuous plus strands are competent to integrate in vitro ", *Journal of virology*, vol. 69, no. 6, pp. 3938-3944.

Mills, K.D., Ferguson, D.O. and Alt, F.W. (2003) "The role of DNA breaks in genomic instability and tumorigenesis ", *Immunological reviews*, vol. 194, pp. 77-95.

Mitchell, R.S., Beitzel, B.F., Schroder, A.R., Shinn, P., Chen, H., Berry, C.C., Ecker, J.R. and Bushman, F.D. (2004) "Retroviral DNA integration: ASLV, HIV, and MLV show distinct target site preferences ", *PLoS biology*, vol. 2, no. 8, pp. E234.

Miyauchi, K., Marin, M. and Melikyan, G.B. (2011) "Visualization of retrovirus uptake and delivery into acidic endosomes ", *The Biochemical journal*, vol. 434, no. 3, pp. 559-569.

Miyoshi, H., Blomer, U., Takahashi, M., Gage, F.H. and Verma, I.M. (1998) "Development of a self-inactivating lentivirus vector ", *Journal of virology*, vol. 72, no. 10, pp. 8150-8157.

Modlich, U. and Baum, C. (2009) "Preventing and exploiting the oncogenic potential of integrating gene vectors", *The Journal of clinical investigation*, vol. 119, no. 4, pp. 755-758.

Modlich, U., Bohne, J., Schmidt, M., von Kalle, C., Knoss, S., Schambach, A. and Baum, C. (2006) "Cell-culture assays reveal the importance of retroviral vector design for insertional genotoxicity ", *Blood*, vol. 108, no. 8, pp. 2545-2553.

Modlich, U., Kustikova, O.S., Schmidt, M., Rudolph, C., Meyer, J., Li, Z., Kamino, K., von Neuhoff, N., Schlegelberger, B., Kuehlcke, K., Bunting, K.D., Schmidt, S., Deichmann, A., von Kalle, C., Fehse, B. and Baum, C. (2005) "Leukemias following retroviral transfer of multidrug resistance 1 (MDR1) are driven by combinatorial insertional mutagenesis ", *Blood*, vol. 105, no. 11, pp. 4235-4246.

Montini, E., Cesana, D., Schmidt, M., Sanvito, F., Bartholomae, C.C., Ranzani, M., Benedicenti, F., Sergi, L.S., Ambrosi, A., Ponzoni, M., Doglioni, C., Di Serio, C., von Kalle, C. and Naldini, L. (2009) "The genotoxic potential of retroviral vectors is strongly modulated by vector design and integration site selection in a mouse model of HSC gene therapy", *The Journal of clinical investigation,* vol. 119, no. 4, pp. 964-975.

Mortusewicz, O., Schermelleh, L., Walter, J., Cardoso, M.C. and Leonhardt, H. (2005) "Recruitment of DNA methyltransferase I to DNA repair sites ", *Proceedings of the National Academy of Sciences of the United States of America,* vol. 102, no. 25, pp. 8905-8909.

Moshous, D., Pannetier, C., Chasseval Rd, R., Deist Fl, F., Cavazzana-Calvo, M., Romana, S., Macintyre, E., Canioni, D., Brousse, N., Fischer, A., Casanova, J.L. and Villartay, J.P. (2003) "Partial T and B lymphocyte immunodeficiency and predisposition to lymphoma in patients with hypomorphic mutations in Artemis ", *The Journal of clinical investigation,* vol. 111, no. 3, pp. 381-387.

Mukhopadhyay, P., Rezzoug, F., Kaikaus, J., Greene, R. and Pisano, M. (2013) "Alcohol modulates expression of DNA methyltranferases and methyl CpG-/CpG domain-binding proteins in murine embryonic fibroblasts.", *Reprod Toxicol,* vol. 37, pp. 40-8.

Muller, H.J. (1927) "Artificial Transmutation of the Gene ", *Science (New York, N.Y.),* vol. 66, no. 1699, pp. 84-87.

Murnane, J.P., Fuller, L.F. and Painter, R.B. (1985) "Establishment and characterization of a permanent pSV ori--transformed ataxia-telangiectasia cell line ", *Experimental cell research,* vol. 158, no. 1, pp. 119-126.

Muthumani, K., Choo, A.Y., Zong, W.X., Madesh, M., Hwang, D.S., Premkumar, A., Thieu, K.P., Emmanuel, J., Kumar, S., Thompson, C.B. and Weiner, D.B. (2006) "The HIV-1 Vpr and glucocorticoid receptor complex is a gain-of-function interaction that prevents the nuclear localization of PARP-1 ", *Nature cell biology,* vol. 8, no. 2, pp. 170-179.

Muul, L.M., Tuschong, L.M., Soenen, S.L., Jagadeesh, G.J., Ramsey, W.J., Long, Z., Carter, C.S., Garabedian, E.K., Alleyne, M., Brown, M., Bernstein, W., Schurman, S.H., Fleisher, T.A., Leitman, S.F., Dunbar, C.E., Blaese, R.M. and Candotti, F. (2003) "Persistence and expression of the adenosine deaminase gene for 12 years and immune reaction to gene transfer components: long-term results of the first clinical gene therapy trial ", *Blood,* vol. 101, no. 7, pp. 2563-2569.

Naldini, L., Blomer, U., Gallay, P., Ory, D., Mulligan, R., Gage, F.H., Verma, I.M. and Trono, D. (1996) "In vivo gene delivery and stable transduction of nondividing cells by a lentiviral vector", *Science (New York, N.Y.),* vol. 272, no. 5259, pp. 263-267.

Nam, C.H. and Rabbitts, T.H. (2006) "The role of LMO2 in development and in T cell leukemia after chromosomal translocation or retroviral insertion ", *Molecular therapy : the journal of the American Society of Gene Therapy*, vol. 13, no. 1, pp. 15-25.

Narayan, O. and Clements, J.E. (1989) "Biology and pathogenesis of lentiviruses ", *The Journal of general virology*, vol. 70 (Pt 7), no. Pt 7, pp. 1617-1639.

Nienhuis, A.W., Dunbar, C.E. and Sorrentino, B.P. (2006) "Genotoxicity of retroviral integration in hematopoietic cells", *Molecular therapy : the journal of the American Society of Gene Therapy*, vol. 13, no. 6, pp. 1031-1049.

Nisole, S. and Saib, A. (2004) "Early steps of retrovirus replicative cycle", *Retrovirology*, vol. 1, pp. 9.

Nisole, S., Stoye, J.P. and Saib, A. (2005) "TRIM family proteins: retroviral restriction and antiviral defence ", *Nature reviews.Microbiology*, vol. 3, no. 10, pp. 799-808.

Nowrouzi, A., Cheung, W.T., Li, T., Zhang, X., Arens, A., Paruzynski, A., Waddington, S.N., Osejindu, E., Reja, S., von Kalle, C., Wang, Y., Al-Allaf, F., Gregory, L., Themis, M., Holder, M., Dighe, N., Ruthe, A., Buckley, S.M., Bigger, B., Montini, E., Thrasher, A.J., Andrews, R., Roberts, T.P., Newbold, R.F., Coutelle, C., Schmidt, M. and Themis, M. (2012) "The Fetal Mouse Is a Sensitive Genotoxicity Model That Exposes Lentiviral-associated Mutagenesis Resulting in Liver Oncogenesis", *Molecular Therapy*,vol.21, no.6, pp. 324-327

O'Driscoll, M. and Jeggo, P.A. (2006) "The role of double-strand break repair - insights from human genetics ", *Nature reviews.Genetics*, vol. 7, no. 1, pp. 45-54.

Okano, M., Bell, D.W., Haber, D.A. and Li, E. (1999) "DNA methyltransferases Dnmt3a and Dnmt3b are essential for de novo methylation and mammalian development ", *Cell*, vol. 99, no. 3, pp. 247-257.

Olsen, J.C. (2001) "EIAV, CAEV and other lentivirus vector systems", *Somatic cell and molecular genetics*, vol. 26, no. 1-6, pp. 131-145.

Ott, M.G., Schmidt, M., Schwarzwaelder, K., Stein, S., Siler, U., Koehl, U., Glimm, H., Kuhlcke, K., Schilz, A., Kunkel, H., Naundorf, S., Brinkmann, A., Deichmann, A., Fischer, M., Ball, C., Pilz, I., Dunbar, C., Du, Y., Jenkins, N.A., Copeland, N.G., Luthi, U., Hassan, M., Thrasher, A.J., Hoelzer, D., von Kalle, C., Seger, R. and Grez, M. (2006) "Correction of X-linked chronic granulomatous disease by gene therapy, augmented by insertional activation of MDS1-EVI1, PRDM16 or SETBP1 ", *Nature medicine*, vol. 12, no. 4, pp. 401-409.

Otto, E., Jones-Trower, A., Vanin, E.F., Stambaugh, K., Mueller, S.N., Anderson, W.F. and McGarrity, G.J. (1994) "Characterization of a replication-competent retrovirus

resulting from recombination of packaging and vector sequences ", *Human Gene Therapy,* vol. 5, no. 5, pp. 567-575.

Palaniappan, C., Fuentes, G.M., Rodriguez-Rodriguez, L., Fay, P.J. and Bambara, R.A. (1996) "Helix structure and ends of RNA/DNA hybrids direct the cleavage specificity of HIV-1 reverse transcriptase RNase H ", *The Journal of biological chemistry,* vol. 271, no. 4, pp. 2063-2070.

Palii, S.S., Van Emburgh, B.O., Sankpal, U.T., Brown, K.D. and Robertson, K.D. (2008) "DNA methylation inhibitor 5-Aza-2'-deoxycytidine induces reversible genome-wide DNA damage that is distinctly influenced by DNA methyltransferases 1 and 3B ", *Molecular and cellular biology,* vol. 28, no. 2, pp. 752-771.

Paull, T.T., Rogakou, E.P., Yamazaki, V., Kirchgessner, C.U., Gellert, M. and Bonner, W.M. (2000) "A critical role for histone H2AX in recruitment of repair factors to nuclear foci after DNA damage ", *Current biology : CB,* vol. 10, no. 15, pp. 886-895.

Pfeifer, A. and Verma, I.M. (2001) "Gene therapy: promises and problems", *Annual review of genomics and human genetics,* vol. 2, pp. 177-211.

Polager, S., Kalma, Y., Berkovich, E. and Ginsberg, D. (2002) "E2Fs up-regulate expression of genes involved in DNA replication, DNA repair and mitosis ", *Oncogene,* vol. 21, no. 3, pp. 437-446.

Pontoglio, M., Faust, D.M., Doyen, A., Yaniv, M. and Weiss, M.C. (1997) "Hepatocyte nuclear factor 1alpha gene inactivation impairs chromatin remodeling and demethylation of the phenylalanine hydroxylase gene ", *Molecular and cellular biology,* vol. 17, no. 9, pp. 4948-4956.

Pruss, D., Bushman, F.D. and Wolffe, A.P. (1994) "Human immunodeficiency virus integrase directs integration to sites of severe DNA distortion within the nucleosome core ", *Proceedings of the National Academy of Sciences of the United States of America,* vol. 91, no. 13, pp. 5913-5917.

Qasim, W., Gaspar, H.B. and Thrasher, A.J. (2009) "Progress and prospects: gene therapy for inherited immunodeficiencies ", *Gene therapy,* vol. 16, no. 11, pp. 1285-1291.

Qvarnstrom, O.F., Simonsson, M., Johansson, K.A., Nyman, J. and Turesson, I. (2004) "DNA double strand break quantification in skin biopsies ", *Radiotherapy and oncology : journal of the European Society for Therapeutic Radiology and Oncology,* vol. 72, no. 3, pp. 311-317.

Ramezani, A., Hawley, T.S. and Hawley, R.G. (2008) "Reducing the genotoxic potential of retroviral vectors", *Methods in molecular biology (Clifton, N.J.),* vol. 434, pp. 183-203.

Ricke, R.M., van Ree, J.H. and van Deursen, J.M. (2008) "Whole chromosome instability and cancer: a complex relationship ", *Trends in genetics : TIG*, vol. 24, no. 9, pp. 457-466.

Rieke, W.O. (1962) "The in vivo reutilization of lymphocytic and sarcoma DNA by cells growing in the peritoneal cavity ", *The Journal of cell biology*, vol. 13, pp. 205-216.

Robertson, K.D. (2001) "DNA methylation, methyltransferases, and cancer ", *Oncogene*, vol. 20, no. 24, pp. 3139-3155.

Robertson, K.D. and Wolffe, A.P. (2000) "DNA methylation in health and disease ", *Nature reviews.Genetics*, vol. 1, no. 1, pp. 11-19.

Rodrigues, A; Paula, M; Coroadinh; Chapter 2, V. (2011) "Production of Retroviral and Lentiviral Gene Therapy Vectors: Challenges in the Manufacturing of Lipid Enveloped Virus"

Roe, T., Reynolds, T.C., Yu, G. and Brown, P.O. (1993) "Integration of murine leukemia virus DNA depends on mitosis ", *The EMBO journal*, vol. 12, no. 5, pp. 2099-2108.

Rogakou, E.P., Pilch, D.R., Orr, A.H., Ivanova, V.S. and Bonner, W.M. (1998) "DNA double-stranded breaks induce histone H2AX phosphorylation on serine 139 ", *The Journal of biological chemistry*, vol. 273, no. 10, pp. 5858-5868.

Rohdewohld, H., Weiher, H., Reik, W., Jaenisch, R. and Breindl, M. (1987) "Retrovirus integration and chromatin structure: Moloney murine leukemia proviral integration sites map near DNase I-hypersensitive sites ", *Journal of virology*, vol. 61, no. 2, pp. 336-343.

Rowe, H.M., Friedli, M., Offner, S., Verp, S., Mesnard, D., Marquis, J., Aktas, T. and Trono, D. (2013) "De novo DNA methylation of endogenous retroviruses is shaped by KRAB-ZFPs/KAP1 and ESET ", *Development (Cambridge, England)*, vol. 140, no. 3, pp. 519-529.

Rowh, M.A., DeMicco, A., Horowitz, J.E., Yin, B., Yang-Iott, K.S., Fusello, A.M., Hobeika, E., Reth, M. and Bassing, C.H. (2011) "Tp53 deletion in B lineage cells predisposes mice to lymphomas with oncogenic translocations ", *Oncogene*, vol. 30, no. 47, pp. 4757-4764.

Sakurai, Y., Komatsu, K., Agematsu, K. and Matsuoka, M. (2009) "DNA double strand break repair enzymes function at multiple steps in retroviral infection ", *Retrovirology*, vol. 6, pp. 114-4690-6-114.

Sarkies, P. and Sale, J.E. (2012) "Cellular epigenetic stability and cancer ", *Trends in genetics : TIG*, vol. 28, no. 3, pp. 118-127.

Scherdin, U., Rhodes, K. and Breindl, M. (1990) "Transcriptionally active genome regions are preferred targets for retrovirus integration ", *Journal of virology*, vol. 64, no. 2, pp. 907-912.

Schmidt, M., Zickler, P., Hoffmann, G., Haas, S., Wissler, M., Muessig, A., Tisdale, J.F., Kuramoto, K., Andrews, R.G., Wu, T., Kiem, H.P., Dunbar, C.E. and von Kalle, C. (2002) "Polyclonal long-term repopulating stem cell clones in a primate model ", *Blood*, vol. 100, no. 8, pp. 2737-2743.

Schroder, A.R., Shinn, P., Chen, H., Berry, C., Ecker, J.R. and Bushman, F. (2002) "HIV-1 integration in the human genome favors active genes and local hotspots ", *Cell*, vol. 110, no. 4, pp. 521-529.

Schvartzman, J.M., Sotillo, R. and Benezra, R. (2010) "Mitotic chromosomal instability and cancer: mouse modelling of the human disease ", *Nature reviews.Cancer*, vol. 10, no. 2, pp. 102-115.

Seger, R.A. (2008) "Modern management of chronic granulomatous disease ", *British journal of haematology*, vol. 140, no. 3, pp. 255-266.

Shafiei, F., Rahnama, F., Pawella, L., Mitchell, M.D., Gluckman, P.D. and Lobie, P.E. (2008) "DNMT3A and DNMT3B mediate autocrine hGH repression of plakoglobin gene transcription and consequent phenotypic conversion of mammary carcinoma cells ", *Oncogene*, vol. 27, no. 18, pp. 2602-2612.

Sharma, S., Miyanohara, A. and Friedmann, T. (2000) "Separable mechanisms of attachment and cell uptake during retrovirus infection ", *Journal of virology*, vol. 74, no. 22, pp. 10790-10795.

Shibata, A., Barton, O., Noon, A.T., Dahm, K., Deckbar, D., Goodarzi, A.A., Lobrich, M. and Jeggo, P.A. (2010) "Role of ATM and the damage response mediator proteins 53BP1 and MDC1 in the maintenance of G(2)/M checkpoint arrest ", *Molecular and cellular biology*, vol. 30, no. 13, pp. 3371-3383.

Shin, D.S., Chahwan, C., Huffman, J.L. and Tainer, J.A. (2004) "Structure and function of the double-strand break repair machinery ", *DNA repair*, vol. 3, no. 8-9, pp. 863-873.

Shrivastav, M., De Haro, L.P. and Nickoloff, J.A. (2008) "Regulation of DNA double-strand break repair pathway choice ", *Cell research*, vol. 18, no. 1, pp. 134-147.

Skalka, A.M. and Katz, R.A. (2005) "Retroviral DNA integration and the DNA damage response ", *Cell death and differentiation*, vol. 12 Suppl 1, pp. 971-978.

Smith, G.C. and Jackson, S.P. (1999) "The DNA-dependent protein kinase ", *Genes & development*, vol. 13, no. 8, pp. 916-934.

Somia, N. and Verma, I.M. (2000) "Gene therapy: trials and tribulations", *Nature reviews.Genetics,* vol. 1, no. 2, pp. 91-99.

Stein, S., Ott, M.G., Schultze-Strasser, S., Jauch, A., Burwinkel, B., Kinner, A., Schmidt, M., Krämer, A., Schwäble, J., Glimm, H., Koehl, U., Preiss, C., Ball, C., Martin, H., Göhring, G., Schwarzwaelder, K., Hofmann, W., Karakaya, K., Tchatchou, S., Yang, R., Reinecke, P., Kühlcke, K., Schlegelberger, B., Thrasher, A.J., Hoelzer, D., Seger, R., von Kalle, C. and Grez, M. (2010) "Genomic instability and myelodysplasia with monosomy 7 consequent to EVI1 activation after gene therapy for chronic granulomatous disease ", *Nature medicine,* vol. 16, no. 2, pp. 198-204.

Stocking, C., Bergholz, U., Friel, J., Klingler, K., Wagener, T., Starke, C., Kitamura, T., Miyajima, A. and Ostertag, W. (1993) "Distinct Classes of Factor-Independent Mutants can be Isolated after Retroviral Mutagenesis of a Human Myeloid Stem Cell Line ", *Growth Factors,* vol. 8, no. 3, pp. 197 <last_page> 209.

Strebel, K. (2003) "Virus-host interactions: role of HIV proteins Vif, Tat, and Rev ", *AIDS (London, England),* vol. 17 Suppl 4, pp. S25-34.

Summers, K.C., Shen, F., Sierra Potchanant, E.A., Phipps, E.A., Hickey, R.J. and Malkas, L.H. (2011) "Phosphorylation: the molecular switch of double-strand break repair ", *International journal of proteomics,* vol. 2011, pp. 373816.

Sun, Y., Mi, W., Cai, J., Ying, W., Liu, F., Lu, H., Qiao, Y., Jia, W., Bi, X., Lu, N., Liu, S., Qian, X. and Zhao, X. (2008) "Quantitative proteomic signature of liver cancer cells: tissue transglutaminase 2 could be a novel protein candidate of human hepatocellular carcinoma ", *Journal of proteome research,* vol. 7, no. 9, pp. 3847-3859.

Suzuki, Y. and Craigie, R. (2007) "The road to chromatin - nuclear entry of retroviruses ", *Nature reviews.Microbiology,* vol. 5, no. 3, pp. 187-196.

Swanton, C., Nicke, B., Schuett, M., Eklund, A.C., Ng, C., Li, Q., Hardcastle, T., Lee, A., Roy, R., East, P., Kschischo, M., Endesfelder, D., Wylie, P., Kim, S.N., Chen, J.G., Howell, M., Ried, T., Habermann, J.K., Auer, G., Brenton, J.D., Szallasi, Z. and Downward, J. (2009) "Chromosomal instability determines taxane response ", *Proceedings of the National Academy of Sciences of the United States of America,* vol. 106, no. 21, pp. 8671-8676.

Tan, H.H. and Porter, A.G. (2009) "p21(WAF1) negatively regulates DNMT1 expression in mammalian cells ", *Biochemical and biophysical research communications,* vol. 382, no. 1, pp. 171-176.

Tang, H., Kuhen, K.L. and Wong-Staal, F. (1999) "Lentivirus replication and regulation ", *Annual Review of Genetics,* vol. 33, pp. 133-170.

Tao, Q. and Robertson, K.D. (2003) "Stealth technology: how Epstein-Barr virus utilizes DNA methylation to cloak itself from immune detection ", *Clinical immunology (Orlando, Fla.)*, vol. 109, no. 1, pp. 53-63.

Tarantal, A.F., Lee, C.I., Ekert, J.E., McDonald, R., Kohn, D.B., Plopper, C.G., Case, S.S. and Bunnell, B.A. (2001) "Lentiviral vector gene transfer into fetal rhesus monkeys (Macaca mulatta): lung-targeting approaches ", *Molecular therapy : the journal of the American Society of Gene Therapy*, vol. 4, no. 6, pp. 614-621.

Tarantal, A.F., McDonald, R.J., Jimenez, D.F., Lee, C.C., O'Shea, C.E., Leapley, A.C., Won, R.H., Plopper, C.G., Lutzko, C. and Kohn, D.B. (2005) "Intrapulmonary and intramyocardial gene transfer in rhesus monkeys (Macaca mulatta): safety and efficiency of HIV-1-derived lentiviral vectors for fetal gene delivery ", *Molecular therapy : the journal of the American Society of Gene Therapy*, vol. 12, no. 1, pp. 87-98.

Telesnitsky A, G.S. (1997) "Reverse Transcriptase and the Generation of Ret... [Retroviruses. 1997] - PubMed - NCBI ", *In Retroviruses*, , pp. 121-160.

Themis, M., May, D., Coutelle, C. and Newbold, R.F. (2003) "Mutational effects of retrovirus insertion on the genome of V79 cells by an attenuated retrovirus vector: implications for gene therapy ", *Gene therapy*, vol. 10, no. 19, pp. 1703-1711.

Themis, M., Waddington, S.N., Schmidt, M., von Kalle, C., Wang, Y., Al-Allaf, F., Gregory, L.G., Nivsarkar, M., Themis, M., Holder, M.V., Buckley, S.M., Dighe, N., Ruthe, A.T., Mistry, A., Bigger, B., Rahim, A., Nguyen, T.H., Trono, D., Thrasher, A.J. and Coutelle, C. (2005) "Oncogenesis following delivery of a nonprimate lentiviral gene therapy vector to fetal and neonatal mice", *Molecular therapy : the journal of the American Society of Gene Therapy*, vol. 12, no. 4, pp. 763-771.

Thomas, C.E., Ehrhardt, A. and Kay, M.A. (2003) "Progress and problems with the use of viral vectors for gene therapy", *Nature reviews.Genetics*, vol. 4, no. 5, pp. 346-358.

Thompson, L.H. and Schild, D. (1999) "The contribution of homologous recombination in preserving genome integrity in mammalian cells ", *Biochimie*, vol. 81, no. 1-2, pp. 87-105.

Thrasher, A.J., Gaspar, H.B., Baum, C., Modlich, U., Schambach, A., Candotti, F., Otsu, M., Sorrentino, B., Scobie, L., Cameron, E., Blyth, K., Neil, J., Abina, S.H., Cavazzana-Calvo, M. and Fischer, A. (2006) "Gene therapy: X-SCID transgene leukaemogenicity ", *Nature*, vol. 443, no. 7109, pp. E5 <last_page> E6.

Trono, D. (2000) "Lentiviral vectors: turning a deadly foe into a therapeutic agent ", *Gene therapy*, vol. 7, no. 1, pp. 20-23.

Tsai, K.Y., Hu, Y., Macleod, K.F., Crowley, D., Yamasaki, L. and Jacks, T. (1998) "Mutation of E2f-1 suppresses apoptosis and inappropriate S phase entry and extends survival of Rb-deficient mouse embryos ", *Molecular cell*, vol. 2, no. 3, pp. 293-304.

Ugolini, S., Mondor, I. and Sattentau, Q.J. (1999) "HIV-1 attachment: another look ", *Trends in microbiology*, vol. 7, no. 4, pp. 144-149.

Uren, A.G., Kool, J., Berns, A. and van Lohuizen, M. (2005) "Retroviral insertional mutagenesis: past, present and future ", *Oncogene*, vol. 24, no. 52, pp. 7656-7672.

van Attikum, H. and Gasser, S.M. (2009) "Crosstalk between histone modifications during the DNA damage response ", *Trends in cell biology*, vol. 19, no. 5, pp. 207-217.

van Gent, D.C., Hoeijmakers, J.H. and Kanaar, R. (2001) "Chromosomal stability and the DNA double-stranded break connection ", *Nature reviews.Genetics*, vol. 2, no. 3, pp. 196-206.

Varmus, H.E. (1982) "Form and function of retroviral proviruses ", *Science (New York, N.Y.)*, vol. 216, no. 4548, pp. 812-820.

Verma, I.M. and Weitzman, M.D. (2005) "Gene therapy: twenty-first century medicine", *Annual Review of Biochemistry*, vol. 74, pp. 711-738.

Vertino, P.M., Yen, R.W., Gao, J. and Baylin, S.B. (1996) "De novo methylation of CpG island sequences in human fibroblasts overexpressing DNA (cytosine-5-)-methyltransferase ", *Molecular and cellular biology*, vol. 16, no. 8, pp. 4555-4565.

Vijaya, S., Steffen, D.L. and Robinson, H.L. (1986) "Acceptor sites for retroviral integrations map near DNase I-hypersensitive sites in chromatin ", *Journal of virology*, vol. 60, no. 2, pp. 683-692.

Vogt, P.K. (1997) "Historical Introduction to the General Properties of Retroviruses " in *Retroviruses* , eds. J.M. Coffin, S.H. Hughes and H.E. Varmus,Cold Spring Harbor (NY).

von Laer, D., Baum, C. and Protzer, U. (2009) "Antiviral gene therapy ", *Handbook of Experimental Pharmacology*, vol. (189):265-97. doi, no. 189, pp. 265-297.

Waddington, C.H. (2012) "The epigenotype. 1942 ", *International journal of epidemiology*, vol. 41, no. 1, pp. 10-13.

Waddington, S.N., Nivsarkar, M.S., Mistry, A.R., Buckley, S.M., Kemball-Cook, G., Mosley, K.L., Mitrophanous, K., Radcliffe, P., Holder, M.V., Brittan, M., Georgiadis, A., Al-Allaf, F., Bigger, B.W., Gregory, L.G., Cook, H.T., Ali, R.R., Thrasher, A., Tuddenham, E.G., Themis, M. and Coutelle, C. (2004) "Permanent phenotypic

correction of hemophilia B in immunocompetent mice by prenatal gene therapy ", *Blood,* vol. 104, no. 9, pp. 2714-2721.

Walsh, C.E. (1999) "Fetal gene therapy ", *Gene therapy,* vol. 6, no. 7, pp. 1200-1201.

Wang, L., Takabe, K., Bidlingmaier, S.M., Ill, C.R. and Verma, I.M. (1999) "Sustained correction of bleeding disorder in hemophilia B mice by gene therapy ", *Proceedings of the National Academy of Sciences of the United States of America,* vol. 96, no. 7, pp. 3906-3910.

Ward, I.M., Minn, K., van Deursen, J. and Chen, J. (2003) "p53 Binding protein 53BP1 is required for DNA damage responses and tumor suppression in mice ", *Molecular and cellular biology,* vol. 23, no. 7, pp. 2556-2563.

Wederell, E.D., Bilenky, M., Cullum, R., Thiessen, N., Dagpinar, M., Delaney, A., Varhol, R., Zhao, Y., Zeng, T., Bernier, B., Ingham, M., Hirst, M., Robertson, G., Marra, M.A., Jones, S. and Hoodless, P.A. (2008) "Global analysis of in vivo Foxa2-binding sites in mouse adult liver using massively parallel sequencing ", *Nucleic acids research,* vol. 36, no. 14, pp. 4549-4564.

Weller, S.K., Joy, A.E. and Temin, H.M. (1980) "Correlation between cell killing and massive second-round superinfection by members of some subgroups of avian leukosis virus ", *Journal of virology,* vol. 33, no. 1, pp. 494-506.

Wilk, T., Gross, I., Gowen, B.E., Rutten, T., de Haas, F., Welker, R., Krausslich, H.G., Boulanger, P. and Fuller, S.D. (2001) "Organization of immature human immunodeficiency virus type 1 ", *Journal of virology,* vol. 75, no. 2, pp. 759-771.

Wu, J., Prindle, M.J., Dressler, G.R. and Yu, X. (2009) "PTIP regulates 53BP1 and SMC1 at the DNA damage sites ", *The Journal of biological chemistry,* vol. 284, no. 27, pp. 18078-18084.

Wu, X., Li, Y., Crise, B. and Burgess, S.M. (2003) "Transcription start regions in the human genome are favored targets for MLV integration ", *Science (New York, N.Y.),* vol. 300, no. 5626, pp. 1749-1751.

Yamagata, Y., Parietti, V., Stockholm, D., Corre, G., Poinsignon, C., Touleimat, N., Delafoy, D., Besse, C., Tost, J., Galy, A. and Paldi, A. (2012) "Lentiviral transduction of CD34(+) cells induces genome-wide epigenetic modifications ", *PloS one,* vol. 7, no. 11, pp. e48943.

Yang, Z.Q., Streicher, K.L., Ray, M.E., Abrams, J. and Ethier, S.P. (2006) "Multiple interacting oncogenes on the 8p11-p12 amplicon in human breast cancer ", *Cancer research,* vol. 66, no. 24, pp. 11632-11643.

Yu, S.F., von Ruden, T., Kantoff, P.W., Garber, C., Seiberg, M., Ruther, U., Anderson, W.F., Wagner, E.F. and Gilboa, E. (1986) "Self-inactivating retroviral vectors designed for transfer of whole genes into mammalian cells ", *Proceedings of the National Academy of Sciences of the United States of America*, vol. 83, no. 10, pp. 3194-3198.

Zgheib, O., Huyen, Y., DiTullio, R.A.,Jr, Snyder, A., Venere, M., Stavridi, E.S. and Halazonetis, T.D. (2005) "ATM signaling and 53BP1 ", *Radiotherapy and oncology : journal of the European Society for Therapeutic Radiology and Oncology*, vol. 76, no. 2, pp. 119-122.

Zhang, J. and Temin, H.M. (1993) "Rate and mechanism of nonhomologous recombination during a single cycle of retroviral replication ", *Science (New York, N.Y.)*, vol. 259, no. 5092, pp. 234-238.

Zhang, W., Canziani, G., Plugariu, C., Wyatt, R., Sodroski, J., Sweet, R., Kwong, P., Hendrickson, W. and Chaiken, I. (1999) "Conformational changes of gp120 in epitopes near the CCR5 binding site are induced by CD4 and a CD4 miniprotein mimetic ", *Biochemistry*, vol. 38, no. 29, pp. 9405-9416.

Zhang, Y., Proenca, R., Maffei, M., Barone, M., Leopold, L. and Friedman, J.M. (1994) "Positional cloning of the mouse obese gene and its human homologue ", *Nature*, vol. 372, no. 6505, pp. 425-432.

Zhao, Z., Wu, Q., Cheng, J., Qiu, X., Zhang, J. and Fan, H. (2010) "Depletion of DNMT3A suppressed cell proliferation and restored PTEN in hepatocellular carcinoma cell ", *Journal of biomedicine & biotechnology*, vol. 2010, pp. 737535.

Zheng, L., Flesken-Nikitin, A., Chen, P.L. and Lee, W.H. (2002) "Deficiency of Retinoblastoma gene in mouse embryonic stem cells leads to genetic instability ", *Cancer research*, vol. 62, no. 9, pp. 2498-2502.

Zufferey, R., Donello, J.E., Trono, D. and Hope, T.J. (1999) "Woodchuck hepatitis virus posttranscriptional regulatory element enhances expression of transgenes delivered by retroviral vectors ", *Journal of virology*, vol. 73, no. 4, pp. 2886-2892.

Zufferey, R., Dull, T., Mandel, R.J., Bukovsky, A., Quiroz, D., Naldini, L. and Trono, D. (1998) "Self-inactivating lentivirus vector for safe and efficient in vivo gene delivery", *Journal of virology*, vol. 72, no. 12, pp. 9873-9880.

Appendix 1

original article

The Fetal Mouse Is a Sensitive Genotoxicity Model That Exposes Lentiviral-associated Mutagenesis Resulting in Liver Oncogenesis

Ali Nowrouzi[1], Wing T Cheung[2], Tingting Li[3,4], Xuegong Zhang[3,4], Anne Arens[1], Anna Paruzynski[1], Simon N Waddington[5], Emma Osejindu[6], Safia Reja[6], Christof von Kalle[7], Yoahe Wang[8], Faisal Al-Allaf[2,9], Lisa Gregory[2], Matthew Themis[10], Maxine Holder[11], Niraja Dighe[2], Alaine Ruthe[2], Suzanne MK Buckley[5], Brian Bigger[12], Eugenio Montini[13], Adrian J Thrasher[10], Robert Andrews[14], Terry P Roberts[6], Robert F Newbold[6], Charles Coutelle[2], Manfred Schmidt[1] and Mike Themis[2,6]

[1]National Centre for Tumorigenesis (NCT), Heidelberg Technology park TP4, Heidelberg, Germany; [2]Gene Therapy Research Group, Section of Cell and Molecular Biology, Imperial College, London, UK; [3]Bioinformatics Division, TNLIST and Department of Automation, Tsinghua University, Beijing, China; [4]Peking University Medical School, Peking, China; [5]Institute for Women's Health, University College London, London, UK; [6]Brunel Institute for Cancer Genetics and Pharmacogenomics, Division of Biosciences, Brunel University, Uxbridge, UK; [7]Division of Experimental Hematology, Cincinnati Children's Hospital Medical Center, Cincinnati, Ohio, USA; [8]Cancer Research UK, Queen Mary's School of Medicine & Dentistry at Barts & The London John Vane Science Centre, London, UK; [9]Department of Medical Genetics, Faculty of Medicine, Umm Al-Qura University, Makkah, Saudi Arabia; [10]Molecular Immunology- Unit, Institute of Child Health, London, UK; [11]Apoptosis and Proliferation Control Laboratory, Cancer Research UK, London, UK; [12]Stem Cell & Neurotherapies Group, Faculty of Medical and Human Sciences, University of Manchester, Manchester, UK; [13]San Raffaele Telethon Institute for Gene
[Q1] *Therapy, HSR-TIGET, Safety of Gene Therapy and Insertional Mutagenesis Research Unit, Milan, Italy; [14]Wellcome Trust Sanger Institute, Cambridge, UK*

Genotoxicity models are extremely important to assess retroviral vector biosafety before gene therapy. We have developed an *in utero* model that demonstrates that hepatocellular carcinoma (HCC) development is restricted to mice receiving nonprimate (np) lentiviral vectors (LV) and does not occur when a primate (p) LV is used regardless of woodchuck post-translation regulatory element (WPRE) mutations to prevent truncated X gene expression. Analysis of 839 npLV and 244 pLV integrations in the liver genomes of vector-treated mice revealed clear differences between vector insertions in gene dense regions and highly expressed genes, suggestive of vector preference for insertion or clonal outgrowth. In npLV-associated clonal tumors, 56% of insertions occurred in oncogenes or genes associated with oncogenesis or tumor suppres-sion and surprisingly, most genes examined (11/12) had reduced expression as compared with control livers and tumors. Two examples of vector-inserted genes were the *Park 7* oncogene and *Uvrag* tumor suppressor gene. Both these genes and their known interactive partners had differential expression profiles. Interactive partners were assigned to networks specific to liver disease and HCC via ingenuity pathway analysis. The fetal mouse model not only exposes the genotoxic potential of vectors intended for gene therapy but can also reveal genes associated with liver oncogenesis.

Received 9 February 2012; accepted 26 September 2012; advance online publication 00 Month 2012. doi:10.1038/mt.2012.224

Introduction

Stable integration into the host genome by retrovirus vectors (RV) has rendered these vehicles as ideal candidates for permanent therapeutic gene delivery. Because active genes in the host are considered targets for insertion, RV infection carries the risk of mutation lead-ing to oncogenesis, as demonstrated in preclinical models and gene therapy clinical trials.[1–3] *In vitro* clonal assays and *in vivo* models have been adapted to assess the genotoxic potential of individual viral vectors.[4,5] Those models that include a tumor prone mouse model have been successfully used to target oncogenes and tumor-suppressor genes on RV or transposon integration and have been demonstrated to be capable of revealing vector-related genotoxic factors that include vector insertion preferences, vector dose, and configuration and possible transgene involvement in oncogenesis.[6–9] Although self-inactivating (SIN) lentiviral vectors (LV) are gener-ally considered safer than γ-RV for gene therapy[10,11] recently, clonal expansion has been associated with LV following integration into the *HMGA2* gene accompanied by highly elevated *HMGA2* expres-sion in a patient treated for β-thalassaemia.[12]

Currently, little is known about the potential for presumably subtle RV or LV-mediated side effects on the host following non-targeted, somatic gene transfer where several unperturbed cell types with differing spatial and temporal gene expression profiles are exposed to the risk of insertional mutagenesis. Hence, there is an important need for models to predict the side effects of gene therapy application directly *in vivo*.

In a previous report, we described our unexpected finding that MF-1 outbred mice treated *in utero* at the E16 fetal stage of development with SIN configuration nonprimate equine infectious

A.N. and W.T.C. contributed equally to this research.
M.S. and M.T. are equally contributing senior authors.
Correspondence: *Michael Themis, Division of Biosciences, Gene Therapy and Genotoxicity Group, Heinz Wolff Building, Brunel University, idge, Middlesex, UK. Email: Michael.themis@brunel.ac.uk*

anemia virus (EIAV) LVs developed hepatocellular carcinomas (HCCs) at high frequency, whereas mice treated in a compara-tive setting with a SIN primate HIV-1-based vector did not. These mice have a normal genetic background and are not predisposed to tumor development. As the majority of the HCCs found were clonal derived with provirus insertions in or close to *RefSeq* genes that were mostly associated with cancer, we suspected insertional mutagenesis to have caused liver disease.[13] This was suspected because during development genes involved in cell cycle, differ-entiation, metabolism, and defense are in a highly transcriptional and proliferative state; so, we hypothesized that RV and LV inser-tion may have occurred in such genes that control these processes that are known to be involved in oncogenesis.[14]

It was, however, suggested that differences between the trun-cated X gene sequences included in the woodchuck post-translation regulatory element (WPRE) that would allow X expression from the nonprimate (np) LV vector but not the primate (p) LV vector could be the cause of the different outcomes in the fetally treated adult mice because the X gene in its wild-type form is known to be involved in HCC development.[15]

The findings presented here, follow on from our previous work and describe the usefulness of the MF-1 mouse that is a fully immunocompetent outbred strain that is not predisposed to tumor development as genotoxicity model. In this study, we first address the question of possible vector-associated WPRE involve-ment in HCC and report that even with WPRE mutations in the npLV similar to those used in the pLV to abolish X gene expres-sion, HCC still develops at high frequency.

We next profile the insertion sites of the npLV and pLV-based vectors and relate these to the genes that are transcriptionally active in the fetus to find clues as to the cause of oncogenesis restricted to the npLV. We also show that tumor development is not only associated with the EIAV LV used but also with an alternative npLV based on the feline immunodeficiency virus (FIV) gene therapy vector. Our data suggest that LV application to the mouse fetus *in utero* can be valuable to identify gene ther-apy vectors with genotoxic potential before clinical application and useful to discover genes involved in complex liver disease pathways.

Results

Tumor development in fetal mice treated with nonprimate LV

We investigated the involvement of the truncated X (*tX*) gene in the WPRE sequence to cause oncogenesis in the *in utero* treated mice by using LVs with and without mutations in the promoter and start codon of the *tX* gene to prevent *tX* expression. The hypothesis that *tX* was the cause of oncogenesis was based on the previously shown fact that EIAV SMART npLVs without these mutations were associated with HCC, whereas the HIV HR'SIN-cPPT-S-FIX-W pLV with these mutations was not. Hence, a modified-SMART vector, SMART 2ZW with X promoter, and start codon mutations were tested alongside the original non-*tX*– mutated SMART 2Z vector in fetal mice. In addition, we used the original pLV HIV-based vector HR'SIN-cPPT-S-FIX-W and a pLV HIV-based vector RRL.SIN-CMV-FIX without the *tX* mutations. In addition, to determine whether oncogenesis was restricted to the EIAV SMART 2 npLV, we introduced a FIV-derived vector pLION11-hAAT-eGFP into our study as an alternative npLV that had *tX* mutations identical to those described previously HR'SIN-cPPT-S-FIX-W.[16] Each vector was injected into E16 gestation fetal mice at similar doses shown in **Table 1**. Vector configura-tions are shown in **Figure 1**. All animals were palpated weekly to determine tumor development, and those suspected to be tumor positive were subjected to internal examination- by laparotomy. Liver tumors were found only in SMART 2Z (*n* = 4/6), SMART 2ZW (*n* = 4/10), and pLionII-hAAT-eGFP (*n* = 3/8)-treated ani-mals from 127 to 715 [Q2] days of age and not in the HIV pLV-treated mice (*n* = 31) (**Table 1** and **Figure 2**). One of the FIV-treated mice developed an ovarian tumor without sign of a liver tumor and was killed at day 715. No tumors developed in the vector buffer treated control animals (*n* = 3). Only one mouse at an age of 568 days of >500 untreated MF-1 mice ranging from 3 months to 2 years of age was identified with a spontaneously occurring HCC in our laboratory. Survival data for mice used in this study are shown in **Supplementary Figure S1** and includes mice treated with SMART 2hFIX previously described that developed HCCs.[13]

Histological examination of tumors and vector gene expression

Mouse tumors, their respective normal livers, and control unin-fected mouse livers were subjected to histological examination to characterize their liver architecture. Each of the liver tumors was identified as a HCC represented by trabecular architecture, cellu-lar polymorphism, and abnormal mitosis (**Figure 2i–n**). Normal liver [Q3] staining for β-galactosidase expression by the CMV promoter in SMART 2Z and SMART 2ZW closely matched our previously reported findings using the SMART 2Z vector after *in utero* injec- [Q4] tion with 10% of hepatocytes showing positive for β-galactosidase expression.[17] GFP expression driven by the hAAT promoter in pLionII-hAAT-eGFP and the CMV promoter in RRL.SIN-CMV-GFP provided obvious GFP fluorescence, in 50% and 20% of hepatocytes, respectively, in the mice treated with these vec-tors [Q5] (measured at 3.5 and 5 months, respectively) (**Figure 2g,h**). Human factor IX gene expression in the blood of mice treated with HR'SIN-cPPT-S-FIX-W ranged between 2.1–23.7% (week 1 bleed) and 2.1–39.75% (week 71 bleed) of the hFIX levels found in normal human plasma nearly matched our findings by enzyme-linked immunosorbent assay in mice treated with this vector.[18] Although we found high-hFIX levels driven by RRL.SIN-CMV-FIX in D17 cells infected *in vitro* with this LV, in mice fetally treated with this vector, low levels of hFIX gene expression was found by enzyme-linked immunosorbent assay in two of six mice at 0.3% and 0.4% of normal human FIX levels at 1 month and no expression was found at the 6-month time point. Immunostaining of hepatocytes for *hFIX* expression by RRL.SIN-CMV-FIX found ~10% hepatocyte transduction (data not shown).

HCCs are composed of clonally derived cells mixed with polyclonal cells

To determine vector clonality in HCCs, Southern analysis of pro-virus integration was performed that resulted in distinct bands for the SMART 2 vectors representative of clonally derived genomic DNA (**Supplementary Figure S2)**. No bands were identified in

Table 1 Details of mice injected with lentivirus vectors

Vector/mouse identification	Titer (per fetus)	Age at killing	Liver tumor	VCN
Control buffers				
A	N/A	819	No	N/A
B	N/A	810	No	N/A
C	N/A	715	No	N/A
[a]SMART 2hFIX				
1	2.7×10^7	348	Y	Tumors T1+T2 (5 each)
2	2.7×10^7	231	Y	4
3	2.7×10^7	230	Y	2
4	2.7×10^7	238	Y	5
5	2.7×10^7	154	Y	13
6	2.7×10^7	376	Y	N/D
7	2.7×10^7	355	Y	N/D
8	2.7×10^7	299	Y	3
9	2.7×10^7	239	N	N/D
10	2.7×10^7	406	N	N/D
SMART 2Z				
1	3.8×10^7	487	Y	9
2	1.2×10^7	369	N	N/A
3	1.2×10^7	573	Y	6
4	1.2×10^7	531	Y	3
5	1.2×10^7	712	N	N/D
6	$1.2 \times x\ 10^7$	644	Y	Tumors T1+T2 (3 each)
NL	1.2×10^7	N/A	N	8.7 ± SE 0.23 (n = 4)
SMART 2ZW (mutated *tX*)				
7	4.2×10^7	127	Y	Tumors T1+T2 (7 each)
8	1.4×10^7	162	N	N/A
9	1.4×10^7	279	Y	Tumors T1 (9)+T2 (10)
10	1.4×10^7	369	Y	2
11	4.2×10^7	714	N	N/D
12	1.4×10^7	537	Y	Tumors T1+T2(3 each)
13	1.4×10^7	627	N	N/D
14	1.4×10^7	502	N	N/D
15	1.4×10^7	640	N	N/D
16	1.4×10^7	447	N	N/D
NL	1.2×10^7	N/A	N	14.5 ± SE 2.3 (n = 4)
pLionII-hAAT-eGFP (mutated *tX*)				
17	1.0×10^7	484	Y	Tumors T1 (8)+ T2 (9)
18	1.0×10^7	433	Y	Tumors T1 (1)+T2 (6)
19	1.0×10^7	273	Y	Tumors T1 (2)+T2 (10)
20	1.0×10^7	341	N	N/D
21	1.0×10^7	622	N	N/D
22	1.0×10^7	715	[b]N	2
23	1.0×10^7	715	N	N/D
24	1.0×10^7	677	N	N/D
NL	1.0×10^7	N/A	N	5.5 ± SE 0.31 (n = 4)
HR'SIN-cPPT-S-FIX-W (mutated *tX*)				
25–50 (NL)	1.0×10^7	>666	N	0.9 ± SE 0.15 (n = 6)
RRL.SIN-CMV/-FIX				
56 (NL)	1.0×10^7	>666	N	0.6 ± SE 0.22 (n = 6)

MF-1 fetal mice were injected on day 16 (E16) of gestation with VSV-G pseudotyped lentiviral vectors vectors after titration, or with vector buffer only. Survival to birth of mice treated with these vectors routinely exceeded 90%. Treated mice were examined by palpation and those with suspected tumors underwent laparotomy. Those bearing tumors were killed for further analysis. Tumors that were found positive for distinct provirus bands following Southern analysis are listed as clonal and VCNs are shown. No tumors were found in mice treated with the vector buffer only (n = 3) or with HR'SIN-cPPT-S-FIX-W (n = 25), and RRL.SIN-CMV-FIX (n = 6).

Q-PCR analysis of VCNs in tumor DNAs agreed with those determined by Southern analysis. VCNs with SEM were also determined using Q-PCR on normal livers (NL) of SMART 2Z (n = 4), SMART 2ZW (n = 4), pLION11-hAAT-eGFP (n = 4), HR'SIN-cPPT-S-FIX-W (n = 6), and RRL.SIN-CMV-FIX (n = 6) infected mice. Animals were allowed to reach 666 or above days of age before killing based on the maximum age of tumor onset that we reported previously.[13] All mice were monitored on a daily basis as per Home Office regulations and per license stipulations. EIAV vector preparations were generated and titered by Oxford BioMedica. Vectors with mutated truncated X (*tX*) are shown.

EIAV, equine infectious anemia virus; N/A, not applicable; N/D, not determined; SIN, self-inactivating; VCN, vector copy numbers.

[a]Mice shown from original study.[13] [b]Mouse developed a clonal ovarian tumor and no liver tumor.

[Q6

the DNA of the suspected bone tumor that developed in a SMART 2ZW -treated animal (mouse 15) (**Supplementary Figure S2)**, and we suspected the bone tumors in this mouse either to have arisen spontaneously or may have had lost vector sequences during development. Each of the liver tumors in the pLionII-hAAT-eGFP FIV-treated mice were also found to be clonal (data not shown) as was the ovarian tumor that developed in the pLionII-hAAT-eGFP-treated mouse where no liver tumor was identified (mouse 22). By this analysis, we found vector copy numbers (VCN) in the EIAV and FIV-derived tumors were between 1–6 and 1–5, respectively.

Despite loading equal amounts of SMART 2 vector-derived tumor DNAs (10 μg) to agarose gels before Southern analysis and repeating several times (n = 5), band intensities differed significantly after hybridization. This suggested the tumors were composed of clonal cells mixed with heterogeneous polyclonal cell populations present in the tumor masses **(Supplementary Figure S2)**. This was also obvious by the speckled β-galactosidase expression identified macroscopically in these tumors (**Figure 2**). In contrast, tumors that developed in FIV-treated mice had clear banding patterns after Southern analysis with no variations in band intensities (data not shown). GFP expression in these tumors was also highly intense and uniform throughout each tumor (data not shown).

The animals treated in this study received similar vector doses (between 1×10^7–4.2×10^7 vector particles); however, only EIAV and FIV vector-treated mice developed tumors (**Table 1**). VCN averages were measured using real-time PCR. VCNs with SEM for SMART 2Z were found to be 8.7 ± SE 0.23 (n = 4), SMART 2ZW 14.5 ± SE 2.3 (n = 4), pLION11- hAAT-eGFP 5.5 ± SE 0.31 (n = 4), HR'SIN-cPPT-S-FIX-W 0.9 ± SE 0.15 (n = 6), and for RRL.SIN-CMV-FIX 0.6 ± SE 0.22 (n = 6). The VCNs found in the HIV LV-treated animals closely matched those in our previous studies;[13,18] however, the SMART 2 VCNs found

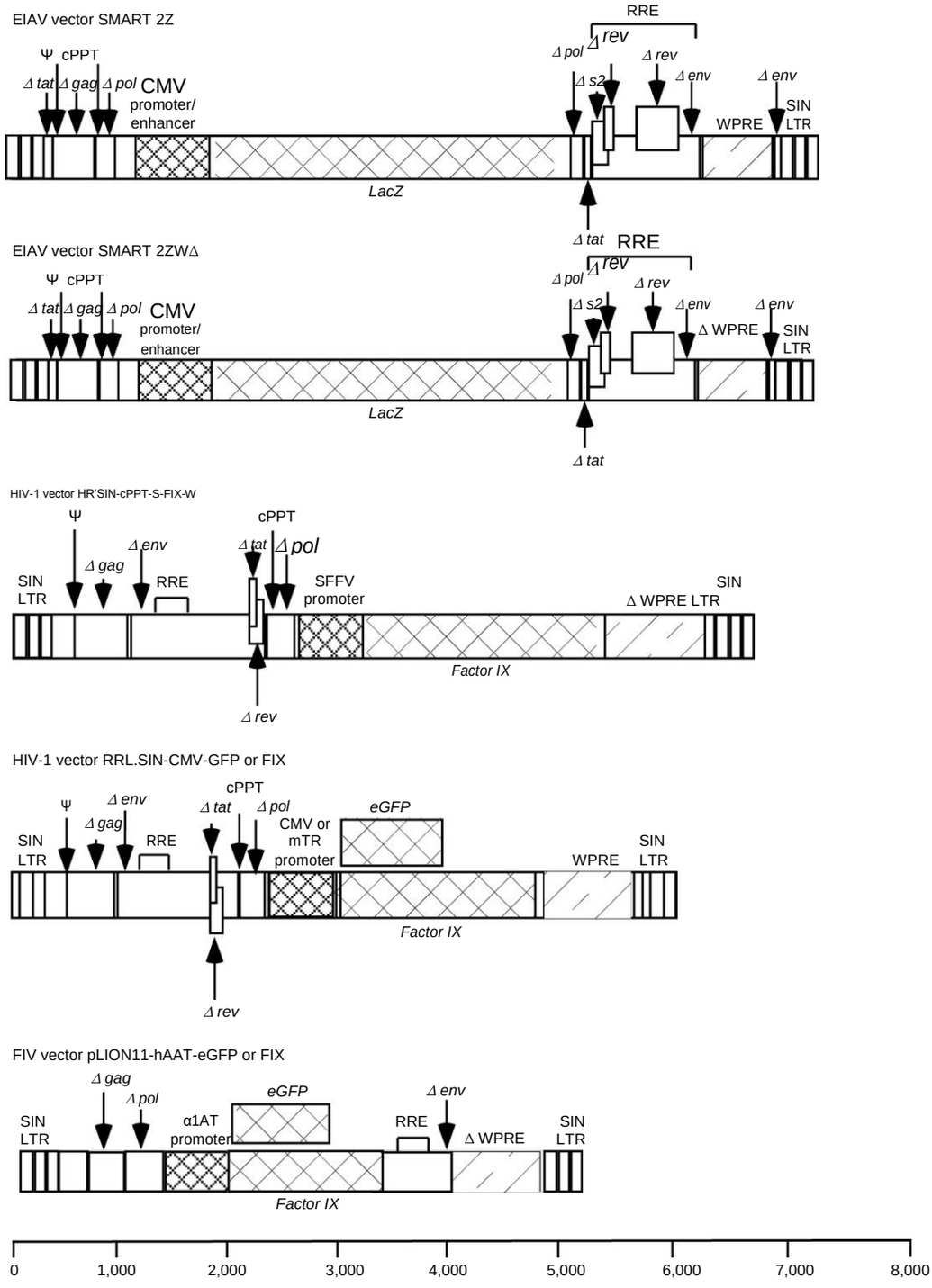

Figure 1 Schematic representation of lentivirus vectors. Equine infectious anemia virus (EIAV) SMART 2Z, and SMART 2ZW , HIV HR'SIN-cPPT-S-FIX-W and RRL.SIN-CMV-FIX/GFP and FIV pLION11-hAAT-GFP vector genomes. Each vector has been previously described.[13,18,33] SMART 2ZW is identical to SMART 2Z except that it carries mutations in the X gene promoter and start codon present in the woodchuck post-translation regulatory element to abrogate *tX* gene expression. The pLION11-hAAT-eGFP vector is based on the FIV and carries identical mutations in the X gene promoter and start codon in HR'SIN-cPPT-S-FIX-W as previously described.[16] The RRL.SIN-CMV/-FIX or GFP vectors like SMART 2Z do not have mutations in the X gene to prevent *tX* expression. Each vector contains SIN LTR configuration and cPPT. An internal SFFV promoter in HR'SIN-cPPT-S-FIX-W drives human factor IX (hFIX) gene expression; SMART 2Z and SMART 2ZW use the CMV promoter to drive β-galactosidase gene expression; pLION11-hAAT-GFP drives GFP expression using the human α1 antitrypsin promoter; and in RRL.SIN-CMV/-FIX or GFP the CMV promoter drives hFIX expression-. FIV, feline immune-deficiency virus; SIN, self-inactivating.

in this study appeared significantly higher than in our previous study where we first described oncogenesis with these vectors. These findings demonstrate the difficulties we experienced in controlling vector dose to the liver following vector administration at this gestation. VCNs in the tumors of the npLV-treated mice were in good agreement with those found by Southern analysis. The ages of the mice that developed tumors are provided in **Table 1**. Using this data and that from our original study no correlation was found between VCN and age of liver tumor onset. Measurement of the clonality of these tumors is

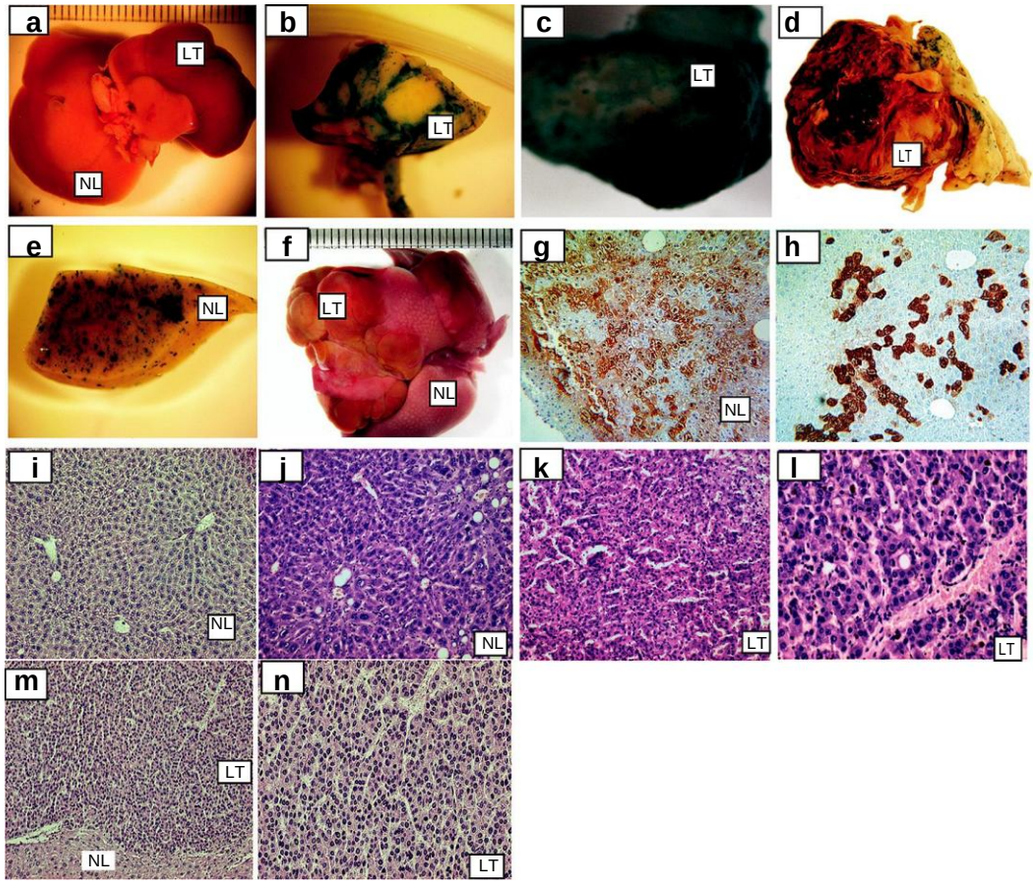

Figure 2 Macroscopic and microscopic analysis. Representative photomicrographs of tumors that developed in the fetally treated adult mice.These appear to closely match those described in our previous study as solid masses surrounded by normal liver tissue. (**a)** SMART 2ZW -treated mouse 10 liver with tumor (killed at 369 days) (original magnification ×10); (**b**) β-galactosidase expression in EIAV mouse 10 tumor (original magnification ×40); **(c)** SMART 2ZW infected mouse 9 (killed at day 279) tumor with speckled staining of cells in foci positively expressing β-galactosidase (original mag-nification ×40); **(d)** SMART 2ZW -infected mouse 7 (killed at day 127) tumor also with speckled β-galactosidase expression (original magnification ×40); **(e)** EIAV mouse 7 normal liver stained for β-galactosidase expression (original magnification ×40). (**f**) Representative liver tumors that developed in mouse 18 treated with feline immunodeficiency virus vector pLION11-hAAT-eGFP (original magnification ×10); (**g**) Anti-GFP immunostaining of mouse 18 hepatocytes infected by pLION11-hAAT-eGFP. Approximately 50% of cells appear positively for GFP expression (original magnification ×100); (**h**) Immunostaining for GFP in RRL.SIN-CMV-GFP infected cells shows ~20% express GFP (original magnification ×100). Histological analysis; (**i**) Representative normal liver tissue of a vector buffer only treated mouse at 715 days with fatty degeneration and normal hepatocyte morphol-ogy (hematoxylin and eosin staining, original magnification ×100); (**j**) Liver of EIAV SMART 2Z-treated mouse 4 killed at 531 days also with normal hepatocyte morphology and fatty degeneration (hematoxylin and eosin staining, original magnification ×100); (**k**) Mouse 4 hepatocellular carcinoma (HCC) showing a trabecular architecture of tumor cells (hematoxylin and eosin staining, original magnification ×100); (**l**) High-power magnification of EIAV SMART 2Z mouse 1, killed at 487 days, HCC with abnormal mitosis and dysplastic cells around central vein (hematoxylin and eosin staining, original magnification ×200); (**m**) EIAV SMART 2Z W-treated mouse 7 killed at 127 days with HCC showing a cross-section of the liver with a border between normal liver and tumor (hematoxylin and eosin staining, original magnification ×40); (**n**) Mouse 7 HCC with widespread polymorphic tumor cells (hematoxylin and eosin staining, original magnification ×100). All livers of HIV HR'SIN-cPPT-S-FIX-W and RRL.SIN-CMV-FIX pLV HIV-treated mice appeared normal morphologically and histologically. EIAV, equine infectious anemia virus; LV, lentiviral vectors; SIN, self-inactivating.

provided below that followed the identification of SMART 2 insertions in genes in tumors by linear amplification-mediated (LAM) PCR and DNA sequencing.

Tumor insertions occur in cancer-associated genes at high frequency

Then, we examined tumor clonality in greater detail by identifying the positions of virus insertions with respect to *RefSeq* genes in the mouse genome using LAM PCR and DNA sequencing. In total, provirus-genomic DNA junctions were sequenced from five EIAV-derived tumors; two by Sanger and Coulson sequencing, two by 454 pyrosequencing, and one by both methods. Insertion sites were also retrieved from six FIV-derived

To generate sets of provirus integrants from the normal liv-ers of EIAV and HIV-treated mice, we used LAM PCR and 454 pyrosequencing on the normal livers of the three SMART 2-treated mice (from which we had retrieved vector insertions from their tumors) and on two normal livers from HR'SIN-cPPT-S-FIX-W-treated animals. These data were then used for comparative analy-sis of the insertion profiles between EIAV and HIV vectors in the fetal mouse genome. Of note, this data were generated at the end of the study at the time of killing and may be influenced by clonal outgrowth in the liver caused by vector genotoxicity.

To obtain vector insertions, all LAM-PCR amplicon sequences were aligned to the mouse genome using BLAST (http://www. ncbi.nlm.nih.gov/genome/seq/MmBlast.html) and BLAT searches [09] (http://genome.ucsc.edu). Using a

integration site sequencing confirmed the clonal nature of the developed HCCs mixed with nonclonal cells. As deep sequencing efficiently retrieves integration sites from polyclonal cell populations not involved in tumor formation in addition to those involved in tumorigenesis, we subtracted tumor versus nontumor relevant integrants by using the retrieval frequency of each integrant. The higher the identical sequence count for each integrant, the higher the likelihood of it being clonal and tumor associated. Using sequence count data we were then able to calculate the per-centage of cells with clonal insertions in the three deep sequenced tumors relative to all infected cell populations in each tumor. For the three tumors examined, these percentages were 25.7, 49.9, and 3.9. These values, however, do not include untransduced cells recruited to the tumors.

Using each sequencing method, from the five EIAV and six FIV-associated tumors, we obtained a total of 16 and 23 clonal integrations in *RefSeq* genes, respectively. Of these, 56% were either in known oncogenes, associated with oncogenes, or involved in tumor suppression. We next identified the molecular function and role in biological processes for each gene using the gene ontology (GO) database. Each gene was also examined for inclusion in the Mouse Retroviral Tagged Cancer Gene Database (RTCGD, http://RTCGD.ncifcrf.gov) and for its relationship to oncogenesis (**Supplementary Table S1**). A total of 25 genes were found with known involvement in cancer and 13 specifically with HCC. Seven of these genes or family members were also found listed in the RTCGD.

Using both sequencing methods after LAM PCR on one of the tumors examined (mouse 1T2 from our previous study), both agreed that *Park 7*, *Uvrag*, and *Rabgef* genes were the clonal integra-tion sites in this tumor (these genes were represented with closely matching sequence count by the 454 method). It is worth noting that *Park7* is an oncogene and known to be involved in HCC;[19,20] and *Uvrag* is a tumor suppressor important to autophagy[21] and also involved in liver cancer.

We used locus-specific Q-PCR to measure the levels of clonality in two of the three tumors where LAM PCR followed by 454 sequencing had provided the identification of genes with EIAV LV insertions with high-sequence counts. From tumor 6T1 with insertions in *Pah*, *loc382044*, and *Acvr2a*, we measured the abundance of DNA-containing SMART 2Z in *Pah*; and from tumor 1T2 with insertions in *Rabgef*, *Rnf 13*, *Uvrag*, and *Park 7*, we mea-sured the abundance of DNA-containing SMART 2Z in *Uvrag*. These genes were chosen due to their proximity of the vector to the gene that provided ideal conditions to design primer/probe sets for Q-PCR analysis. From this analysis using GAPDH as the gene locus which would be expected in 100% of cells, we found the abundance of *Pah* and *Uvrag* insertions to be 35% ± 0.33 and 16% ± 0.23, respectively. Of note, these data reflect clonality in these tumors as compared with cell populations that are nonclonal with or without vector insertions.

Comparison of EIAV and HIV vector integration profiles in normal livers

At E16 to day 3 after birth, the period of time when vector integration was expected to have been completed, gene expres-sion in the fetus is highly complex with many genes in a highly transcriptionally active state.[14] These genes are known to be involved in control of liver development and proliferation and with known involvement in HCC.[14] We suspected, therefore, that insertion into these genes by a potentially genotoxic vector may initiate outgrowth of subsets of cells and lead to liver disease. We therefore characterized and compared the insertion profiles of EIAV and HIV LVs in normal livers to look at differences in inser-tion site selection that could have contributed to clonal outgrowth and oncogenesis in the EIAV-treated mice.

A total of 839 EIAV and 244 HIV nonredundant insertions were retrieved. Of these, 642 (76.5%) and 193 (79%) insertions of EIAV and HIV, respectively, were located in or close to *RefSeq* genes (within a window of 100 kb), which is in agreement with previous investigations of the insertion site frequencies into *RefSeq* genes by these vectors.[10,11,22–24] Using the 839 EIAV and 244 HIV nonredundant unique insertions, we made comparisons using the following parameters: (i) region within the inserted gene and relative to transcription start site, (ii) distance from the CpG island, (iii) regional CG content, (iv) chromosome preferences, and (v) regional gene density. Common insertions: hot spots for each vector were also identified. First, independent and random-ized insertion data sets for EIAV and HIV were created by setting each vector insertion site randomly across the genome.[25]

As previously described for these LV vectors, each preferably integrated into the transcription unit and not near the transcrip-tion start site or CpG islands (**Supplementary Figure S3a,b**).[10,11] In addition, as already described, EIAV and HIV insertions posi-tively correlated with AT rich region selection ($P < 0.001$)[11,26] with a 35–45% GC content around insertions using windows of 100, 250, 500, 750, and 1 kb on either side of each integrant. The 1 kb interval is shown as representative of every window that has iden-tical behavior **(Supplementary Figure S3c)**. For both vectors, in contrast to the random set, we found an uneven chromosomal distribution that was independent of chromosome size and gene density with HIV insertions in regions with lower gene density (0–59 genes/5 × 10^6 bp) than EIAV (30–120 genes/5 × 10^6 bp) ($P < 0.0001$) (**Supplementary Figure S3d,e**).

We then tried to identify hotspots of EIAV insertions in common insertion sites within a narrow 500 bp interval. Insertions were found in several genes located on different chromosomes one of which was in *Uvrag* that we already identified in a clonal HCC from our original study 13. Of note, GO assignment of the EIAV common insertion sites showed their gene products to be relevant to development, cell death, cycle, proliferation DNA replication/ repair, cell signaling, and cancer (http://www.ncbi.nlm.nih.gov/) **(Supplementary Table S2)**. Although HIV preference for insertion hotspots have been previously described,[11,23] we found no integration hotspots for the HR'SIN-cPPT-S-FIX-W HIV vector even when we broadened our investigation for hotspots in a 100 kb interval around each insertion site. Using this insertion site, window EIAV hotspots were found in *Park7*, *Cyp3A11*, and *Mrpl23* genes in addition to the *Uvrag* gene that was also identified in the clonal tumors[13] **(Supplementary Table S2)**. The hotspot region with most vector insertions (using the 500 bp interval) contained 13 EIAV insertions between the *Ankrd17* and *Alb* genes clustered in a 115.3 kbp region on chromosome 5. In the 1 Mbp region around this region, we found six more EIAV insertions in the closely located *Afm*, *Rassf6*,

and *Cxcl1* cluster of genes **(Supplementary Figure S4)**. These genes are among the most highly expressed during fetal development[14] suggesting the insertion hotspots may represent a preference for EIAV integration in highly transcriptionally active genes of the fetal mouse. Alternatively, the identification of these hotspots may be as the result of clonal outgrowth of cells containing these insertions promoted by EIAV integration.

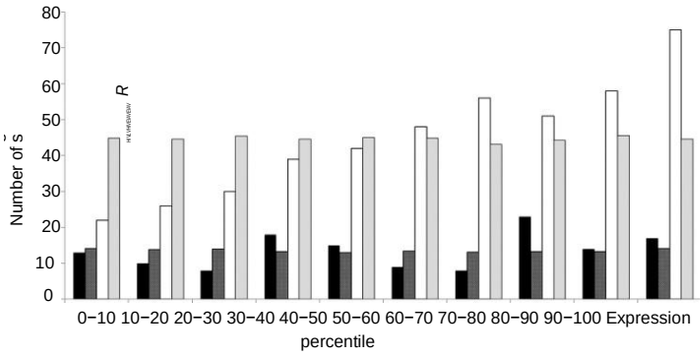

Figure 3 Vector insertions relative to fetal gene expression. A horizon-tal representation was generated between gene ontologies (GOs) of *RefSeq* genes with vector integrations during the E16 to postnatal day 3 (when integration was expected to occur) period and GOs of genes differentially expressed by 1.5-fold and above or decreased by 1/1.5-fold and below the average of all times points from E11.5 to adulthood in our fetal develop-ment microarray. GOs of EIAV and HIV RefSeq insertions were obtained using the Babelomics platform (http://babelomics.bioinfo.cipf.es) $-\log^{10}$ *P* values >1.3 are taken as significant (*P* < 0.05 after Benjamini Hotchberg correction).[27] The number of genes in each Ref Seq GO was plotted, with the number of genes in the GOs of the random data set, against the expression levels of GOs representing the differentially expressed genes during the E16 to day 3 period. The expression levels of genes within each GO are represented in percentiles from low to high for each time point. Significant differences were identified for each vector compared with the random data (*P* value <0.001). EIAV insertion appears only in genes that are highly expressed whereas HIV vector insertions appear not to follow this trend with a more specific gene profile. The random data set shows no preference for gene expression levels of GOs. EIAV LV, infected data set (clear bar); EIAV R, random insertion data set (gray column); HIV LV, infected data set (black bar); HIV R, random data set (chequered bar). EIAV, equine infectious anemia virus; LV, lentiviral vectors.

Correlation between vector insertions and gene expression in the fetus

To make comparisons between the LV gene insertion profiles and gene expression at the time of infection (E16 to day 3 after birth period), we aligned the unique 642 EIAV and 193 HIV RefSeq inser-tions with genes differentially expressed (either 1.5 up or 1/1.5-fold down) in the fetus. Using our previously reported microarrays cov-ering expression levels over these time points[14] and our RefSeq inser-tion site data, we made horizontal representations between the GOs for each gene data set. GOs were obtained using http://babelomics. bioinfo.cipf.es (log 10 *P* values >1.3 are taken as significant, *P* value <0.05 after Benjamini Hotchberg correction).[27] This was repeated with the random insertion data (*P* values set at the 95% confidence interval) to determine significant deviation between experimental and random data sets (**Figure 3**). In contrast to HIV insertions and the random data set (*P* value <0.001) consistently for each gestational day, EIAV insertions appeared in genes with high levels of expres-sion. This suggested, once again, that either different sets of genes were chosen for integration by each vector or that cells with genes carrying EIAV insertions became predominant in the liver possibly as a result of clonal outgrowth associated with vector genotoxicity.

To determine the importance of the genes found with vector insertions, the GOs representing RefSeq insertions were subjected to Ingenuity Pathways Knowledge Base software (IPA) analysis that provides information on biological processes overrepresented in each data set. *P* values $<10^{-20}$ or lower were used to select highly significant overrepresentation after Benjamini Hotchberg correction[27] with a *P* value <0.05 cutoff and a minimum of three gene transcripts represented from each category (**Figure 4**). Importantly, only EIAV insertions were found with statistical significance in the GO categories containing genes responsible for multiple genetic disorders and genes associated with cellular growth and prolif-eration, hepatic system development, and function, gene expres-sion, and cancer. In line with the absence of tumor development in HR'SIN-cPPT-S-FIX-W HIV-treated mice, insertions by this vec-tor were not found in these categories but restricted to genes that are associated with neuronal disorders (*n* = 104).

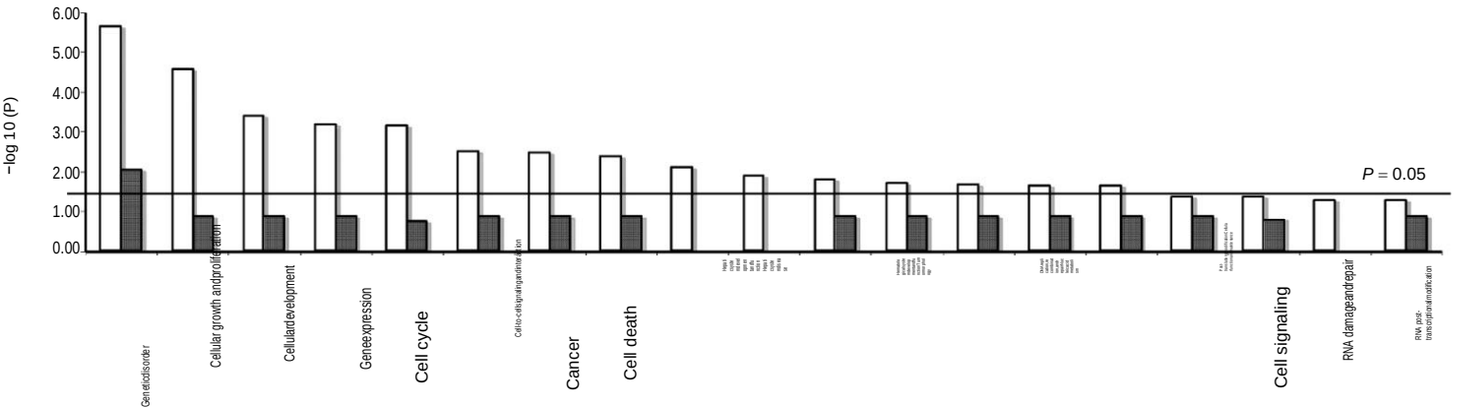

Figure 4 Analysis of the GO terms of *RefSeq* genes overrepresented in infected mouse livers by EIAV and HIV vectors. Ingenuity Pathways Knowledge Base software (IPA) was used to provide information on the enrichment of biological function and disease processes within given GO categories representing the inserted *RefSeq* genes. Fisher's exact test was used for *P* values of overrepresented genes in a given GO category compared with a random sample gene set (*P* value <0.05). Statistical significance is represented as $-\log^{10}$ *P* value and threshold of *P* = 0.05 is shown. *P* values $<10^{-20}$ or lower were used to select highly significant biological networks and GO pathways after multiple comparison error correction using the Benjamini Hotchberg method[27] and three or more genes per data set. Only the EIAV vector appeared in categories associated with cellular growth and proliferation, cancer, hepatic system development and function, and gene expression. EIAV, clear boxes and HIV, dark boxes. EIAV, equine infectious anemia virus.

Finally, we aligned our EIAV and HIV-insertion data sets with a human HCC microarray database of 65 liver disease samples of disease groups representing the stepwise oncogenic process from preneoplastic lesions of cirrhosis and dysplasia to HCC and also includes 10 healthy tissue samples.[20] Matches were found common to cell adhesion, DNA replication, and apoptosis (**Supplementary Table S3**). Although none of the GO matches after Benjamini Hotchberg correction were found to be statistically significant (*P* value 0.05 cutoff) interestingly, only EIAV and not HIV insertions aligned with genes known to be involved in cellular proliferation that are also highly expressed during fetal development and associated with cancer. This included the *Park7*, *Bre*, and *Ep300* genes that were identified as hotspots for insertion and of which two were found (*Park7* and *Bre*) as clonal insertions in liver tumors.

Characterization of gene expression in representative vector-associated HCCs

We next performed microarrays on the clonal tumors of the three representative mice that were used for insertion site retrieval (1T2, 6T1, and 9T1) for a comparison of global differential gene expression between each tumor and their respective normal liver tissue. We included in this analysis, comparison with a spontaneous HCC of an untreated 568-day-old mouse that served as an uninfected HCC control. Using the top 500 differentially expressed genes between these tumors and normal livers (with a negative Log 2 ratio fold change cutoff of 1.5 or 1/1.5, *P* value <0.05 after Benjamini Hochberg correction), we initially created heat-maps to represent each differential gene expression profile (**Supplementary Figure S5)**. These profiles appeared quite different between each tumor and the spontaneous HCC. The difference between gene expressions in these tumors was also evident when comparing overrepresented GO functions. In line with HCC, genes involved mainly in oxidative reduction in mouse 1T2, mouse 9T1, and the spontaneous HCC were most significantly represented. This was not seen in mouse 6T1 and this with other differences in enriched GOs between these tumors suggested the involvement of alternative biosynthetic pathways to oncogenesis (**Supplementary Figure S5)**.

Genes in clonal tumors carrying vector insertions are differentially expressed

We examined the influence of vector insertion on gene expression using a representative selection of genes from the clonal tumors of EIAV and FIV vector-treated animals by real-time PCR of reverse transcribed purified mRNAs. Comparisons of gene expression levels were restricted to the gene with a provirus insertion in the tumor and the same gene in the respective normal liver tissue of the same animal to avoid variations in gene expression levels between mice of different ages and sexes. The control tumor used in this analysis without provirus insertion in the gene under investigation was also gender matched (**Table 2**). This selection encompassed known oncogenes or genes associated with cancer or specifically HCC (*Pah*, *Park7*, *Acvr2a*, *Mark 3*, *Rabgef1*, *Tnfrs19*, *Pscd3*) and a tumor suppressor gene (*Uvrag*). We found *Park7*, *Uvrag*, *Pah*, *Bre*, *Katna1*, *Nek9*, *Coro7*, and *Tnfrs19* gene expression reduced relative to controls. The *Acvr2a*, *Mrpl23*, and *Pscd3* genes were increased in expression relative to the normal liver but significantly lower in expression than their control-matched tumors suggesting that they are upregulated in HCC but lower possibly as a result of vector insertion. *Mark3* gene expression was found only slightly elevated and we did not find altered gene expression of *Rabgef1*.

Because our profiling of EIAV insertions in normal livers showed vector integrations mainly in highly expressed genes in the fetus, we compared the normal expression levels of the vector-inserted genes, at E16-day3 period, we found differential expression using real-time PCR in clonal tumors with representative genes known to be either expressed at high or at low levels naturally in the mouse at this developmental period. As compared with the pregnancy-specific glycoprotein 19 (*Psg19*) gene that is expressed at low levels during this period, the inserted genes are normally expressed at between 5 and 229-fold greater levels. As compared with the expression of the albumin (*Alb*) gene, however, which is very highly expressed dur-ing this period their normal expression was lower by between 5 and 206-fold. This analysis did not, therefore, discriminate EIAV prefer-ence for insertion only into very highly expressed genes.

Mouse 1T2 tumor inserted genes and their related partners are found in networks associated with liver disease

We next chose a representative tumor (mouse 1T2) to investigate how virus integration may be associated with oncogenesis. This

Table 2 Differential expression of genes and gene pathways in tumors

	Fold change ± SEM		
Vector/gene	**Tumor with insertion**	**Tumor without insertion**	**Normal liver**
EIAV			
Park7	0.70 ± 0.16	1.03 ± 0.14	1 ± 0.10
Uvrag	0.59 ± 0.11	0.95 ± 0.14	1 ± 0.11
Mrpl23	5.11 ± 0.22	27.53 ± 0.08	1 ± 0.26
Pah	0.35 ± 0.18	3.7 ± 0.06	1 ± 0.06
Acvr2	1.3 ± 0.19	10.79 ± 0.07	1 ± 0.26
Bre	0.5 ± 0.04	0.99 ± 0.07	1 ± 0.07
Mark3	1.44 ± 0.05	1.13 ± 0.03	1 ± 0.02
Katna1	0.81 ± 0.06	0.57 ± 0.11	1 ± 0.03
FIV			
Pscd3	3.88 ± 0.06	33.67 ± 0.02	1 ± 0.19
Coro7	0.11 ± 0.19	19.48 ± 0.02	1 ± 0.07
Nek9	0.11 ± 0.22	3.78 ± 0.11	1 ± 0.06
Tnfrs19	N/E	2.69 ± 0.20	1 ± 0.15

Genes transcriptionally dysregulated following vector integration are shown. Real-time PCR on reverse transcribed mRNAs isolated from SMART 2Z, SMART 2ZW , and pLION11-hAAT-eGFP-infected tumors using primer/probe sets (Applied Biosystems) specific for the gene under analysis shows altered gene expression levels relative to normal respective tissues and a gender-matched tumor without insertion in the gene of interest. Normal liver gene expression was set at 100% shown as 1. Relative levels of gene transcription are given for EIAV SMART 2hFIX insertions in *Park7* and *Uvrag* of mouse 1T2, SMART 2Z insertions in *Pah* and *Acvr2a* of mouse 6T1, SMART 2ZW insertions in *Bre, Mark3,* and *Katna1* of mouse 7T1 and FIV pLION11-hAAT-eGFP insertions in *Pscd3* of mouse 19T2, *Coro7* of mouse 18T2, *Nek9* of mouse 18T1, and *Tnfrs19* of mouse 22 ovarian tumor. Values shown represent the mean of 3 or more measurements with SEM. Confidence intervals were set at 95% and *P* values of <0.01 or below were taken as statistically significant.

EIAV, equine infectious anemia virus; FIV, feline immune-deficiency virus; N/E, no expression detected. [Q12

mouse was chosen for the analysis because first we had characterized its tumor with elevated expression of genes associated with oxidative stress, which is a hallmark of HCC and second as insertions in the *Park7* oncogene and *Uvrag* tumor suppressor gene were found in this tumor. Although there were additional inser-tions in the *Mrpl23* and *Rabgef1* genes, *Rabgef1* was not found differentially expressed and there is no association between *Mrpl23* and cancer. Third, we had identified *Park7* in the human HCC database and *Uvrag* that is also associated with cancer. Finally, these genes were also identified as hotspots for insertion and were found reduced in expressed by real-time PCR.

Initially, we found interactive partners to *Park 7* and *Uvrag* genes using the STRING (http://string-db.org/) database that provides information on predicted protein–protein interactions that includes direct (physical) and indirect (functional) associations to identify interactive genes (with significant associated combined scores 0.4 confidence level). We then collated gene expression levels from our microarray of this tumor according to a *P* value significance cut-off of <0.05 (after Benjamini Hochberg correction) rather than 1.5 negative log 2 fold cutoff to maximize our data set. We next identi-fied differential expression of the interactive partners of *Park 7* and *Uvrag* in our microarray database of this tumor (**Supplementary Figure S6 and Supplementary Table S4**).

Finally, we subjected these gene sets to IPA network analysis that directly links them to pathways involved in liver disease and cancer of the liver. The pathways identified included apoptosis of hepatocytes, repair of DNA, liver tumorigenesis, hepatocyte proliferation, cell cycle progression, transcription, and HCC (**Figure 5**).

Discussion

The potential for RV and LV-mediated side effects following non-targeted, somatic gene transfer is still unknown. We suspect that a significant genotoxic risk could be present following *in vivo* gene transfer to several cell types with different spatial and temporal profiles of gene expression by vectors that are known to prefer to integrate into gene promoters and/or active gene transcription units. In contrast to *ex-vivo* gene therapy, the *in vivo* approach does not rely on cell engraftment for survival and proliferation and therefore, it is possible that a significant population of cells harboring provirus "hits" into cancer-related genes could sur-vive after gene transfer which theoretically increases the risk of

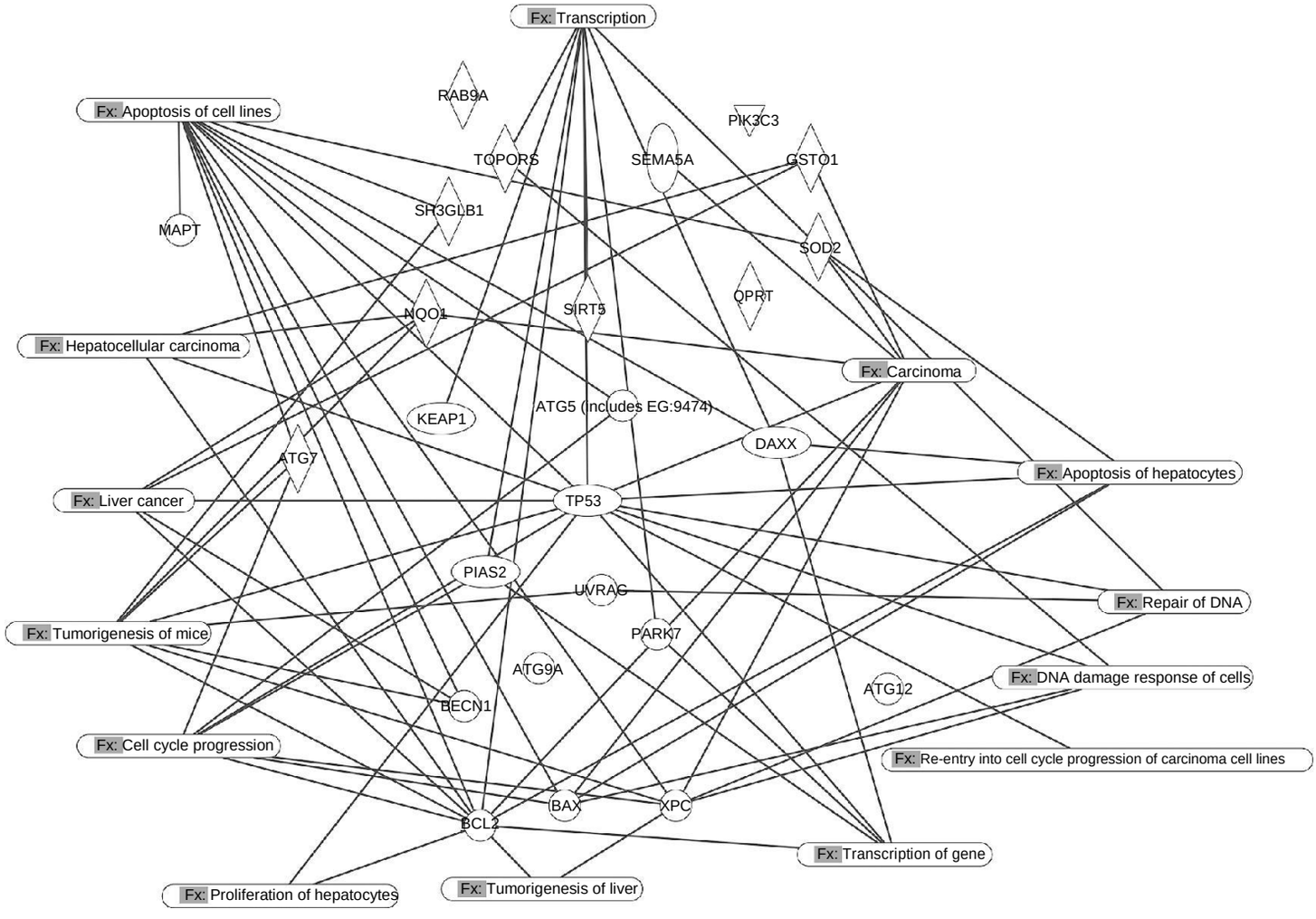

Figure 5 Biological networks and functional pathways linking *Park7* and *Uvrag* genes. IPA network analysis of *Park7* and *Uvrag* from (mouse 1T2) found with significant differential expression in the microarray from these mice compared with their respective controls and ranked by fold change ($-\log^2$ ratio, cutoff *P* value <0.05 after Benjamini Hochberg correction). Networks show interactive genes linked to pathways that include apoptosis in the liver, DNA repair, liver tumorigenesis, hepatocyte proliferation, cell cycle progression, transcription, and hepatocellular carcinoma (HCC). Their detailed involvement in HCC requires further investigation.

insertional mutagenesis leading to oncogenesis. Genotoxicity models *in vivo* are, therefore, essential to reflect this risk following somatic gene therapy.

In an earlier study, we found oncogenesis associated with SMART 2 and 3 EIAV-based nonprimate (np) LV vectors but not with the HR'SIN-cPPT-S-FIX-W HIV-1-derived primate (p) LV 13. Because the X gene present on the WPRE in its full-length form is known to be involved in HCC, our initial goal was to determine if the *tX* is involved in oncogenesis. This suspicion was supported by differences in *tX* gene configurations between the HR'SIN-cPPT-S-FIX-W pLV vector with mutations to prevent *tX* expression and the SMART 2 npLV without these mutations. Because we found liver tumors in mice treated with the mutated form of SMART 2 and also with an alternative npLV FIV vector, pLION11-hAAT-eGFP carrying mutations identical to HR'SIN-cPPT-S-FIX-W ruled out *tX* gene involvement in oncogenesis. Furthermore, mice treated with the RRL.SIN-CMV-FIX vector without these mutations did not develop tumors following fetal gene transfer.

The fetal mouse has many highly expressed genes that con-trol cellular proliferation and differentiation that are also known to be associated with HCC.[14] The MF-1 mouse is not genetically predisposed to cancer and we have found that this outbred mouse strain allows life-long vector presence with transgene expression. On the basis of our findings that EIAV and FIV npLVs but not HIV LVs are associated with liver cancer, we propose this model to be a sensitive platform to test for vector-associated genotoxic-ity. In addition, as high transcriptional activity is known to have a potentially strong influence on LV integration,[23,24] we suspected that the difference in oncogenic outread between these vectors may be due to differences in their insertion site preferences in the mouse genome. It is important to note that comparisons of inser-tions sites were made between EIAV and HIV LVs at the end point of our study and would therefore include any bias in the clonal outgrowth of cells caused by a genotoxic vector.

LV-insertion profiles that have been described in previous studies[10–11,24] were also evident in the fetally treated mouse liver in this study. These included preference for the transcription unit, insertion away from the transcription start site, and CpG islands that represent gene promoter regions, and insertion into AT rich DNA. Of note, we found SMART 2 vector insertions appearing in gene dense regions to a much greater extent than HR'SIN-cPPT-S-FIX-W and clearly different patterns of insertions in particular chromosomes were evident between the LVs. This is in contrast to previous work using different immortal cell lines that revealed hotspots for HIV in different human chromosomes and no hotspots for EIAV integration.[11,23] In the fetus, hotspots for SMART 2 insertion were found in several genes whereas none were found for HR'SIN-cPPT-S-FIX-W. These hotspots (using a 500 bp interval) included several unique SMART 2 integrations narrowly clustered on chromosome 5 in genes surrounding the albumin locus known to be highly expressed before birth in the mouse.[14] This suggested, once again, that the EIAV vector has a preference for highly expressed genes or possibly that our iden-tification of these hotspots may be influenced by cellular prolif-eration as a result of clonal outgrowth mediated by SMART 2 genotoxicity.

Our global insertion site profile of SMART 2 integrations in highly expressed genes was also confirmed by our horizontal GO comparative analysis that showed insertion sites occurring in highly expressed genes around the E16 period of development. The fact that SMART 2 integration may have influenced cellular outgrowth was further supported by our IPA analysis that identi-fied the GOs of genes with insertions of this vector and not the HIV vector in categories associated with cellular proliferation, hepatic system development and function, gene expression, and liver cancer. Interestingly, the *Uvrag* tumor suppressor gene and the *Park 7* oncogene, *Cyp3a11*, and *Mrpl23* genes that were identi-fied as hotspots for insertion at the 500 bp and 100 kb intervals, respectively, were also found in clonal tumors with SMART 2 integrations.

Our analysis of vector copy number following *in utero* gene transfer shows that it is difficult to control vector delivery to the liver during *in utero* gene transfer as VCN varied widely between LVs. A potential reason for the difference in HIV and EIAV VCNs found, even though similar vector doses of VSV-G envelope pseudotyped vectors were used (10^7 IU/fetus), may be associated with the required level of the epithelium-derived growth factor LEDGF/p75 required by each LV to tether the vector genome to its site of integration. High-level LEDGF/p75 expression is believed to influence integration into actively transcribed regions of DNA 22, and EIAV LV infection levels have been found significantly impaired by reduced levels of LEDGF/p75 as compared with HIV LV in murine cells depleted for LEDGF/p75 (50-fold versus five-fold, respectively). In the fetal mouse relative to the adult LEDGF/p75, expression is fivefold greater and if EIAV is more dependant on LEDGF/p75 than HIV, then high level LEDGF/p75 expression may account for high EIAV VCN. It would be interesting to determine the role of LEDGF/p75 expression also on FIV integration. Low HIV VCN may also be the reason for the absence of oncogenesis in the HIV-treated mice; however, in our previous study HIV VCN was similar to that found for EIAV, yet neither the HR'SIN-cPPT-S-FIX-W nor RRL.SIN-CMV-FIX HIV vectors were associated with oncogenesis. VCN may not necessarily be very accurate in measuring genotoxicity as in our previous work, we found that even at undetectable VCN levels measured by Q-PCR, one mouse still developed an HCC carrying a clonal SMART 2 insertion.[13] Importantly, our measurement of high EIAV and FIV VCNs ver-sus low HIV VCN may once again be influenced by npLV driven clonal outgrowth of cells and only measurement of VCN at an early time point followed by comparison with the data presented in this work would address this issue.

For our comparative real-time PCR analysis of gene expres-sion levels, we measured the level of gene expression of genes in tumors carrying provirus insertions within the gene. This was compared to the level of expression of each gene in the respec-tive normal liver of the mouse bearing a tumor and matched mouse tumors without insertions in the gene under investigation. Although we used gender and age-matched controls, we are aware that this allowed only limited statistical analysis of the data. To circumvent this difficulty to some degree, we performed real-time PCR on samples harvested from at least four different sites in each tumor and normal liver tissue. We also realize that although our microarray analysis used gender-matched mouse tumor controls,

these were not of identical ages and it is likely that in each tumor, different pathways may be responsible for the development of liver cancer. Furthermore, even though high-density microarray anal-ysis is believed capable to confirm altered levels of gene expres-sion found by real-time PCR, this is not always possible for every gene set under investigation[28] and we therefore, did not expect to be able to achieve accurate matches between every differentially expressed gene examined by the two techniques as was sometimes the case during our analysis.

Nonetheless, assuming our observations were mediated by vector genotoxicity, we linked the *Park7* and *Uvrag* genes that car-ried viral insertions, showed reduced in expression by Q-PCR, with their interactive partners using the STRING database in a representative tumor, and identified these genes in our tumor microarray. Applying this data set to IPA analysis, we determined which gene networks could have been involved in oncogenesis. Although this identified genes belonging to pathways involved in liver disease, cancer, and specifically HCC, that may have differ-ential expression influenced by vector integration, we cannot rule out that these genes may be altered in expression as a result of effects not related to vector integration. Hence, we are still only able to speculate that insertion by SMART 2 in the *Park7* onco-gene and *Uvrag* tumor suppressor gene in the same tumor may have initiated neoplasia.

A possible mechanism behind mutagenesis in the treated mice by SMART 2 and pLION11-hAAT-eGFP vector is the configura-tion of splice donor and acceptor sites in these vectors. Aberrant splicing is known to cause altered oncogene expression as was shown in the tumor prone model.[9] Interestingly, both SMART 2Z and pLION11-hAAT-eGFP have splice donor and acceptor sites some distance apart either side of the transgene and promoter as opposed to HR'SIN-cPPT-S-FIX-W where both splice sites are 5′ to the transgene and promoter. The importance of the splice acceptor in SMART 2 and pLION11-hAAT-eGFP just 5′ of WPRE is yet to be investigated. In theory, splicing of cellular genes with the vector, if in the appropriate orientation, could result in WPRE being introduced onto cellular RNA which could result in pro-longed RNA half live and increased gene expression. Alternatively, splicing could also result in nonfunctional truncated proteins thereby effectively reducing gene expression.

In summary and following on from our previous report, we conclude in this study that the X gene is not directly involved in oncogenesis after *in utero* gene transfer. We find genes mostly downregulated following SMART 2 and pLION11-hAAT-eGFP insertion and that the EIAV vector either has a preference for highly expressed genes and gene dense regions or may have caused clonal outgrowth of cells following integration. We aim to deter-mine this by comparing our current insertion site profiles with those of mice killed at a 2-week time point following SMART 2 administration before clonal outgrowth could occur.

We believe, therefore, this highly transcriptionally active and proliferative model with an unperturbed genetic background to be a particularly sensitive alternative animal system to test for genotox-icity following *in vivo* gene transfer as demonstrated here by signifi-cant differences in the genotoxic potential between the LVs tested. We propose this model as highly useful to screen novel therapeutic integrative vectors intended for safe clinical gene therapy. Due to its sensitivity, this model may even be extended to nonintegrating vectors that are currently considered safe because they only rarely integrate in the genome in a more randomly manner.[29] Although we have not observed oncogenesis associated with the HIV-derived vectors used in this study, we cannot rule out that these vectors may be genotoxic in an alternative model and hence we cannot assume them to be completely safe. As for any genotoxicity model, conclu-sions about vector safety drawn from this fetal mouse model should be made with caution as it may not be capable of accurately repre-senting the likelihood of insertional mutagenesis in humans follow-ing LV-mediated gene transfer. However, as HCC is such a common disease being the fifth most common cancer in humans, we also propose that the fetal model may also be considered as a useful tool to research the cause of this disease.

Materials and Methods

Animal procedures and tissue harvests. MF1 mice were used for *in utero* injection. All animal work was carried out in accordance with UK Home Office regulation and was compliant with the guidelines of the Imperial College London ethical review committee. Details of the animal proce-dures and harvests used have been previously described.[13] Sampling was performed by dissection of four parts of each tissue to be investigated.

Vector production and titration. EIAV SMART 2 lentivectors were pro-duced using transient transfection of human embryonic kidney 293T cells and titered as previously described.[30,31] X-gal staining was performed using standard procedures.[17] No replication competent virus was identified using the method described by Martin-Rendon *et al*.[32] EIAV vector preparations were generated and titered by Oxford BioMedica. [Q13] Recombinant HR'SIN-cPPT-S-FIX-W HIV vectors were also produced by transient transfections of 293T cells and titered using a commercial immunoassay kit for p24 gag (Beckman Coulter, High Wycombe, UK) as previously described[18] that routinely provided concentrations with a range 20–40 ng/μl of p24 protein. Generation of the HR'SIN-cPPT-S-FIX-W vector carrying the human factor IX (hFIX) cDNA after replacement of GFP from pHR'SIN-cPPT-SEW has also been described.[18] Virus titers were calculated using batches of HR'SIN-cPPT-S-FIX-W hFIX- and pHR'SIN-cPPT-SEW eGFP-lentivirus prepared in parallel. Fluorescence-activated cell sorting analysis of cells after infection by eGFP-lentivirus [Q14] yielded a titer of 5×10^8 infectious particles/ml.

pLION11-hAAT-eGFP FIV particles were generated as previously described using the 293T packaging cell line.[33] HR'SIN-cPPT-S-FIX-W and pLION11-hAAT-eGFP vector particles were concentrated 100-fold by ultracentrifugation at 50,000 g for 90 minutes at 4 °C. The pellet was resuspended in serum-free X-VIVO10 (BioWhittaker Europe, Verviers, Belgium) and stored at −80 °C.

Fluorescence-activated cell sorting analysis of cells after infection by pLION11-hAAT-eGFP yielded a titer of 1×10^9 infectious particles (TU)/ml. All viruses used were pseudotyped using the VSV-G envelope.

Measurement of hFIX antigen (hFIX:Ag) expression. Plasma samples con-taining hFIX:Ag after collection of 100 μl of mouse blood in Na Citrate and centrifugation was measured using a specific hFIX:Ag enzyme-linked immunosorbent assay as directed by the manufacturer (Roche Diagnostics, Mannheim, Germany). Human FIX reference supplied with the kit was used to create standard curve measurements of diluted hFIX:Ag for direct comparability. Mouse plasma samples were assayed at 50-fold dilution.

Immunohistochemistry. Liver tissue fixed in 25% formalin overnight, transferred to 70% ethanol, and processed into paraffin was used to detect GFP expression. GFP was detected after microwaving in citrate buffer then incubation with rabbit anti-eGFP (A-6455, Molecular Probes, Eugene, Oregon) as previously described.[18]

Quantitative of VCN by real-time PCR. Lentiviral copy number in DNA samples was also determined using primer/probe sets designed to recog-nize the human FIX cDNA (for HR'SIN-cPPT-S-FIX-W) or the EIAV and FIV packaging signals in SMART 2 and pLION11-hAAT-eGFP, respec-tively. Quantitative PCR was performed using an ABI PrismR7900HT sequence detector (Applied Biosystems, Warrington, UK) as previously described.[13] Absolute quantification was used to mathematically deter-mine the viral load by comparing a range of standards concentrations. The range of standards was derived from a reliable tumor sample with a known copy number via Southern blot analysis. The genomic DNA was diluted twofold from a starting concentration of 500 ng to provide a range of 500–15.625 ng. CT values were obtained using probes specific to the

[Q15] GAPDH housekeeping gene, the WPRE virus vector sequences common to HR'SIN-cPPT-S-FIX-W and pLION11-hAAT-eGFP and the packaging signal (Ψ) of the SMART 2 vector. Raw CT values from tumors and normal livers were normalized against those of the standard curve.

The amplification was carried out in a final volume of 20 µl in which each reaction contained 18 µl of TaqMan Universal PCR Master Mix (Amperase UNG, AmpliTaq Gold polymerase, dNTP, Applied Biosystems), [Q16] 100 mmol/l of each primer and probe, and 31.25 ng of genomic DNA. All samples were tested in triplicate and the variation between the CT of each duplicate was ≤0.5 Ct. The total number of genomes was recorded for each concentration in the dilution series. A standard curve was constructed with Log10 genome values plotted against CT values for each concentration and a linear regression equation plotted. For unknown samples, VCNs were interpolated from the standard curve. For each unknown sample, the number of vector copies per genome (diploid) was calculated using the average CT values (per concentration) and linear regression values (slope and intercept) from the standard curve.

Real-time PCR to determine the effects of LV provirus insertion on inserted genes. RNAs were extracted using TRI reagent (Sigma Aldrich, Gillingham, UK) on tissue samples followed by chloroform extraction and isopropanol precipitation. RNAs were purified before cDNA syn-thesis using an Agilent Technology Company kit (Agilent technologies, Stratagene, Stockport, UK) as per the manufacturers instructions. Purified RNA was prepared using a High Capacity cDNA reverse transcription kit (Applied Biosystems). A reverse transcriptase master mix was prepared with RT buffer, dNTP mix, RT random primers, MultiScribe Reverse transcriptase, RNase inhibitor, and nuclease-free distilled water accord-ing to manufacturer's instructions (Applied Biosystems) was used for cDNA synthesis using 125 ng of total RNA. cDNA of 2 µl was used with PCR Mastermix and TaqMan Assays (Amperase UNG, AmpliTaq Gold polymerase, dNTP, Applied Biosystems). All reactions were carried out in triplicate on an ABI Prism7900HT real-time PCR instrument (Applied Biosystems) using primer/probe sets designed for each gene under exami-nation obtained from Applied Biosystems. Absolute Quantification (stan-dard curve) reactions were used to optimize the TaqMan reactions using serially diluted cDNA samples (500–15.625 ng/µl). Relative quantification was performed on quadruplicate PCR reactions using the Ct method.[34] Data were analyzed with SDS software and cycle thresholds obtained were normalized ribosomal 18S expression (control) and calibrated to normal tissue and a gender-matched tumor control for relative quantification.

Locus-specific PCR was performed on two genes from two tumors which were identified by LAM PCR/454 and Sanger and Coulson sequencing methods. Primer/probe sets for *Pah* and *Uvrag* genes and the 5′ LTR of the SMART 2 vector were as follows: 1. Uvrag, Forward 5′-G TACCTTGCAGGC TTTAATTGTCC-3′, Reverse 5′-AAGGTTATGAGAGCATCAGCAAC-3′. Product 293 bp. Probe FAM 5′-CGCCTGGCTCCAGCGGCACC-3′ Tamra. Pah, Forward 5′-CCTAGATAGAATCTTTCAGTTTGG-3′, Reverse 5′- CC TTTGGGTTATACAAGGTT ATG-3′. Product 266 bp. Probe 5′-CCTCA GTGCCACAAATTCAGGCTGC-3′. 5′ FAM, 3′ Tamra. EIAV-5′ LTR primer 5′-GTTATACAAGGTTATGAGAGC-3′. PCR products were tested to identify the correct product sizes before Q-PCR. Genomic DNAs were subjected to amplifications as described above. CT values using primer/probes specific to the GAPDH housekeeping gene were used to calculate the presence of a gene in 100% of the genomes of cells in each tumor. The CTs of each gene under investigation was compared with that of GAPDH to obtain the percentage of the locus-specific virus/gene representing clonally derived cells. All samples were tested in quadruplicate and CT SDs were used to represent SEMs. DNA from normal livers from each mouse and an uninfected mouse were used as negative controls to show no amplifications.

Amplification of vector-genomic DNA junctions. Genomic DNA was extracted from tumors as previously described.[13] LAM-PCR: linear amplification for the SMART 2 EIAV vector was performed as previously described.[35,36]

LAM-PCR of genomic DNA adjacent to the pLION11-hAAT-eGFP vector was also performed using 100 ng of genomic DNA and 2.5 U Taq polymerase using the following two biotinylated primers of sequences found in the 5′ LTR: 5′-GTT CTC GGC CCG GAT TCC-3′ and 5′-CCC GGA TTC CGA GAC CTC-3′ (50 µl final volume). Cycle parameters of 95 °C for 5 minutes (single cycle) followed by 95 °C for 60 seconds, 60 °C for 45 seconds, 72 °C 90 seconds for 50 cycles, 72 °C for 10 minutes. 2.5 U additional Taq polymerase was added and the PCR run for another 50 cycles. PCR products were captured using the Dynabeads kilobase binder kit (Dynal, Oslo, Norway) and the second DNA strand was synthesized using Klenow (Invitrogen, Carlsbad, CA) with random hexanucleotides (Invitrogen, Paisley, UK) (20 µl reaction mixture) at 37 °C for 1 hour. The double stranded DNA was digested with Tsp509I and a linker oligonucleotide added (5′-GAC CCG GGA GAT CTG AAT TCA GTG GCA CAG CAG TTA GG-3′ and 5′-AAT TCC TAA CTG CTG TGC CAC TGA ATT CAG ATC-3′) followed by ligation with Fast Link DNA Ligase kit (Epicentre Technologies, Madison, Wisconsin) for 15 minutes at room temperature. The DNA was denatured with 0.1 mol/l NaOH before two rounds of PCR using the same conditions as the linear amplification with primers: FIV LTR 5′-CTC GAC AGG GTT CAA TCT C-3′ and linker 5′- GAC CCG GGA GAT CTG AAT TC-3′ followed by nested PCR primers: FIV LTR 5′-CTC AAA AGT CCT CAA CAA AG-3′ and linker 5′ GAT CTG AAT TCA GTG GCA CAG-3′. PCR products were separated on 3% agarose gels and DNA fragments were isolated using a Quiex II gel extraction kit (Qiagen, Crawley, UK) and cloned into a TOPO TA plasmid cloning kit (Invitrogen) as per the manufacturer's instructions. Bacterial colonies containing DNA fragments corresponding to those seen in the second round PCR were sequenced using the FIV-specific nested primer (Leicester University, Leicester, UK). EIAV and HIV-insertion sites cloned by LAM PCR and nonrestrictive PCR techniques obtained using 100–300 ng of sample genomic DNA were sequenced by deep parallel pyrosequencing (GS FLX/454: Roche, Mannheim, Germany) then subjected to Blas2Seq and the Smith-Waterman algorithm as previously described.[37]

Sequences were aligned with the mouse genome (*Mus musculus* genome) assembly July 2007 (NCBI37/mm9, UCSC *M. musculus* genome version 8) using UCSC BLAT genome browser (http://genome.ucsc.edu) or BLAST (http://www.ncbi.nlm.nih.gov/genome/seq/MmBlast.html). The molecular function and role in biological processes of each integration near to or within a *RefSeq* gene (within a 100 kb window) was determined using the Gene Ontology database and identified with potential to be a candidate gene involved in tumorigenesis. Candidate genes were searched against the Mouse Retroviral Tagged Cancer Gene Database (RTCGD; http://RTCGD.ncifcrf.gov).

Determination of lentivirus copy number by Southern analysis. Southern analysis of genomic tumor DNA was carried out as previously described.[13] Briefly, 10 µg of genomic DNAs were digested with Hind III that allows the EIAV provirus and adjacent mouse 3′ genomic DNA to be identified after separation in 0.6% agarose gels and hybridization with a 625 bp WPRE probe excised from the pSMART 2Z plasmid. The FIV vector was probed with a 700 bp GFP probe. Probes were routinely produced using a random primed labeling kit (Mega-prime system Amersham, UK) with a-32P-CTP.

Autoradiographs were used to visualize provirus bands on Hybond N+ nylon membranes (Amersham).

Microarrays. Total RNA was isolated from liver tissues using Trizol reagent (Invitrogen) then subjected to gene expression profiling using an Illumina mouse sentrix-8 microarray chip from Illumina recognizing 25,000 sequences to provide a measurement of genes whose expression had been up or downregulated with high sensitivity. The gene expression values were extracted using the GenomeStudio software and filtered according to fluorescence above chip background. Data were quantile normalized(82) and analyzed using the bioconductor http://www.bioconductor.org/, http://www.bioconductor.org/packages/2.0/bioc/html/lumi.html lumi and limma packages(83). Data were *P* value adjusted(40) to yield a sorted list

[Q17] of differentially expression genes.

GO function analysis of microarrays. The Gene Ontology file (version: 1.513; Date: 09/29/2009) and the mouse annotation file (gene_associa-tion.mgi. version: 1.806; Date: 01/15/2010) were downloaded from http:// www.geneontology.org. We selected the top 500 significantly differen-tially expressed genes and ranked these by fold change (log2 ratio, *P* value <0.05). Hypergeometric distributions were used to detect overrepresented or underrepresented biological process terms in the study set compared with the population set. Here, the population set was constructed using all genes in the microarray of mouse 1T2 13, mouse 6T1, and mouse 9T1 tumors and a spontaneous HCC that occurred in a 568-days-old mouse. Probabilities obtained by hypergeometric distributions were subject to Benjamini Hotchburg correction.[27]

Randomized data set generation. To assess whether insertion sites where assigned to chromosomes randomly, randomization was carried out 100-times to yield 100 randomized counts of vector inserts per chromosomes. A *t*-test (95% confidence) was performed between the single observed count of sites per chromosome and the randomized population of 100 counts. Similarly, for CG content and gene density statistics, randomized data were generated across the genome. To determine the nature of vector insertion distances from transcription start site and regions within genes, *t*-tests were performed between observed data and those data generated from sites assigned to random locations, 100-times, within the gene.

Analysis of biological networks by Ingenuity Pathway Analysis (IPA).

Network analysis was performed on lists of genes generated from the earlier analyses described above as being differentially expressed. IPA (Ingenuity Systems, Redwood City, CA) that contains data of individually curated relationships between gene objects (e.g., genes, mRNAs, and proteins) was used for the identification of the biological processes that are significantly overrepresented to generate significant biological networks and pathways. Statistical significance of the biological overrepresentation was determined using Fisher's exact *P* value based on the relative overrepresentation of a minimum of three genes in the particular pathway as compared with a random sample of genes (*P* value cutoff of <0.05). Scores corresponding to $P < 10^{-20}$ or lower after Benjamini Hotchburg correction were used to select highly significant biological networks.

SUPPLEMENTARY MATERIAL

Figure S1. Survival of cohorts treated with lentivirus vectors.
Figure S2. Representative Southern analysis of tumors and respective

[Q18] normal livers.
Figure S3.
Figure S4. Linear representation of the regional hotspot for EIAV SMART 2 vector insertion in chromosome 5.
Figure S5. Global analysis of tumor gene expression.
Figure S6. Gene pathways associated with provirus-integrated genes
Park 7 and *Uvrag*
Table S3. Alignment of RefSeq insertions with human HCC samples.
Table S4. Microarray of differentially expressed genes belonging to pathways associated with genes with altered expression identified by real-time PCR.

ACKNOWLEDGMENTS

We are grateful to Eithan Galun, Goldyne Savad Institute of Gene Therapy,Hadassah Hebrew University Hospital, Jerusalem, 91120, Israel for providing pLION11-hAAT-eGFP virus containing supernatant. This work was funded by Imperial College London, a Wellcome Trust Value in People award and a Brunel University BRIEF award.

REFERENCES

1. Hacein-Bey-Abina, S, Von Kalle, C, Schmidt, M, McCormack, MP, Wulffraat, N, Leboulch, P *et al*. (2003). LMO2-associated clonal T cell proliferation in two patients after gene therapy for SCID-X1. *Science* **302**: 415–419.
2. Howe, SJ, Mansour, MR, Schwarzwaelder, K, Bartholomae, C, Hubank, M, Kempski, H *et al*. (2008). Insertional mutagenesis combined with acquired somatic mutations causes leukemogenesis following gene therapy of SCID-X1 patients. *J Clin Invest* **118**: 3143–3150.
3. Ott, MG, Schmidt, M, Schwarzwaelder, K, Stein, S, Siler, U, Koehl, U *et al*. (2006). Correction of X-linked chronic granulomatous disease by gene therapy, augmented by insertional activation of MDS1-EVI1, PRDM16 or SETBP1. *Nat Med* **12**: 401–409.
4. Montini, E, Cesana, D, Schmidt, M, Sanvito, F, Ponzoni, M, Bartholomae, C *et al*. (2006). Hematopoietic stem cell gene transfer in a tumor-prone mouse model uncovers low genotoxicity of lentiviral vector integration. *Nat Biotechnol* **24**: 687–696.
5. Modlich, U, Bohne, J, Schmidt, M, von Kalle, C, Knöss, S, Schambach, A *et al*. (2006). Cell-culture assays reveal the importance of retroviral vector design for insertional genotoxicity. *Blood* **108**: 2545–2553.
6. Nienhuis, AW, Dunbar, CE and Sorrentino, BP (2006). Genotoxicity of retroviral integration in hematopoietic cells. *Mol Ther* **13**: 1031–1049.
7. Baum, C, Düllmann, J, Li, Z, Fehse, B, Meyer, J, Williams, DA *et al*. (2003). Side effects of retroviral gene transfer into hematopoietic stem cells. *Blood* **101**: 2099–2114.
8. Modlich, U, Kustikova, OS, Schmidt, M, Rudolph, C, Meyer, J, Li, Z *et al*. (2005). Leukemias following retroviral transfer of multidrug resistance 1 (MDR1) are driven by combinatorial insertional mutagenesis. *Blood* **105**: 4235–4246.
9. Montini, E, Cesana, D, Schmidt, M, Sanvito, F, Bartholomae, CC, Ranzani, M *et al*. (2009). The genotoxic potential of retroviral vectors is strongly modulated by vector design and integration site selection in a mouse model of HSC gene therapy. *J Clin Invest* **119**: 964–975.
10. Wu, X, Li, Y, Crise, B and Burgess, SM (2003). Transcription start regions in the human genome are favored targets for MLV integration. *Science* **300**: 1749–1751.
11. Hacker, CV, Vink, CA, Wardell, TW, Lee, S, Treasure, P, Kingsman, SM *et al*. (2006). The integration profile of EIAV-based vectors. *Mol Ther* **14**: 536–545.
12. Cavazzana-Calvo, M, Payen, E, Negre, O, Wang, G, Hehir, K, Fusil, F *et al*. (2010). Transfusion independence and HMGA2 activation after gene therapy of human ß-thalassaemia. *Nature* **467**: 318–322.
13. Themis, M, Waddington, SN, Schmidt, M, von Kalle, C, Wang, Y, Al-Allaf, F *et al*. (2005). Oncogenesis following delivery of a nonprimate lentiviral gene therapy vector to fetal and neonatal mice. *Mol Ther* **12**: 763–771.
14. Li, T, Huang, J, Jiang, Y, Zeng, Y, He, F, Zhang, MQ *et al*. (2009). Multi-stage analysis of gene expression and transcription regulation in C57/B6 mouse liver development. *Genomics* **93**: 235–242.
15. Kingsman, SM, Mitrophanous, K and Olsen, JC (2005). Potential oncogene activity of the woodchuck hepatitis post-transcriptional regulatory element (WPRE). *Gene Ther* **12**: 3–4.
16. Zanta-Boussif, MA, Charrier, S, Brice-Ouzet, A, Martin, S, Opolon, P, Thrasher, AJ *et al*. (2009). Validation of a mutated PRE sequence allowing high and sustained transgene expression while abrogating WHV-X protein synthesis: application to the gene therapy of WAS. *Gene Ther* **16**: 605–619.
17. Waddington, SN, Mitrophanous, KA, Ellard, FM, Buckley, SM, Nivsarkar, M, Lawrence, L *et al*. (2003). Long-term transgene expression by administration of a lentivirus-based vector to the fetal circulation of immuno-competent mice. *Gene Ther* **10**: 1234–1240.
18. Waddington, SN, Nivsarkar, MS, Mistry, AR, Buckley, SM, Kemball-Cook, G, Mosley, KL *et al*. (2004). Permanent phenotypic correction of hemophilia B in immunocompetent mice by prenatal gene therapy. *Blood* **104**: 2714–2721.
19. Wu, F, Liang, YQ and Huang, ZM (2009). (The expression of DJ-1 gene in human hepatocellular carcinoma and its relationship with tumor invasion and metastasis). *Zhonghua Gan Zang Bing Za Zhi* **17**: 203–206.
20. Wurmbach, E, Chen, YB, Khitrov, G, Zhang, W, Roayaie, S, Schwartz, M *et al*. (2007). Genome-wide molecular profiles of HCV-induced dysplasia and hepatocellular carcinoma. *Hepatology* **45**: 938–947.
21. Liang, C, Feng, P, Ku, B, Oh, BH and Jung, JU (2007). UVRAG: a new player in autophagy and tumor cell growth. *Autophagy* **3**: 69–71.
22. Marshall, HM, Ronen, K, Berry, C, Llano, M, Sutherland, H, Saenz, D *et al*. (2007). Role of PSIP1/LEDGF/p75 in lentiviral infectivity and integration targeting. *PLoS ONE* **2**: e1340.
23. Schröder, AR, Shinn, P, Chen, H, Berry, C, Ecker, JR and Bushman, F (2002). HIV-1 integration in the human genome favors active genes and local hotspots. *Cell* **110**: 521–529.
24. Mitchell, RS, Beitzel, BF, Schroder, AR, Shinn, P, Chen, H, Berry, CC *et al*. (2004). Retroviral DNA integration: ASLV, HIV, and MLV show distinct target site preferences.
PLoS Biol **2**: E234.
25. Dhami, P, Saffrey, P, Bruce, AW, Dillon, SC, Chiang, K, Bonhoure, N *et al*. (2010). Complex exon-intron marking by histone modifications is not determined solely by nucleosome distribution. *PLoS ONE* **5**: e12339.

26. Ciuffi, A, Llano, M, Poeschla, E, Hoffmann, C, Leipzig, J, Shinn, P *et al*. (2005). A role for LEDGF/p75 in targeting HIV DNA integration. *Nat Med* **11**: 1287–1289.
27. Benjamini YaH, Y. (1995). Controlling the false discovery rate:a practical and powerful approach to mulitiple testing. *J Roy Statist Soc Ser* **B57**: 289–300.
28. Dallas, PB, Gottardo, NG, Firth, MJ, Beesley, AH, Hoffmann, K, Terry, PA *et al.* (2005). Gene expression levels assessed by oligonucleotide microarray analysis and quantitative real-time RT-PCR – how well do they correlate? *BMC Genomics* **6**: 59.
29. Mátrai, J, Cantore, A, Bartholomae, CC, Annoni, A, Wang, W, Acosta-Sanchez, A *et al*. (2011). Hepatocyte-targeted expression by integrase-defective lentiviral vectors induces antigen-specific tolerance in mice with low genotoxic risk. *Hepatology* **53**: 1696–1707.
30. Mitrophanous, K, Yoon, S, Rohll, J, Patil, D, Wilkes, F, Kim, V *et al*. (1999). Stable gene transfer to the nervous system using a non-primate lentiviral vector. *Gene Ther* **6**: 1808–1818.
31. Olsen, JC (1998). Gene transfer vectors derived from equine infectious anemia virus. *Gene Ther* **5**: 1481–1487.

32. Ciuffi, A, Llano, M, Poeschla, E, Hoffmann, C, Leipzig, J, Shinn, P *et al*. (2005). A role for LEDGF/p75 in targeting HIV DNA integration. *Nat Med* **11**: 1287–1289.
33. Benjamini YaH, Y. (1995). Controlling the false discovery rate:a practical and powerful approach to mulitiple testing. *J Roy Statist Soc Ser* **B57**: 289–300.
34. Dallas, PB, Gottardo, NG, Firth, MJ, Beesley, AH, Hoffmann, K, Terry, PA *et al.* (2005). Gene expression levels assessed by oligonucleotide microarray analysis and quantitative real-time RT-PCR – how well do they correlate? *BMC Genomics* **6**: 59.
35. Mátrai, J, Cantore, A, Bartholomae, CC, Annoni, A, Wang, W, Acosta-Sanchez, A *et al*. (2011). Hepatocyte-targeted expression by integrase-defective lentiviral vectors induces antigen-specific tolerance in mice with low genotoxic risk. *Hepatology* **53**: 1696–1707.
36. Mitrophanous, K, Yoon, S, Rohll, J, Patil, D, Wilkes, F, Kim, V *et al*. (1999). Stable gene transfer to the nervous system using a non-primate lentiviral vector. *Gene Ther* **6**: 1808–1818.

37. Olsen, JC (1998). Gene transfer vectors derived from equine infectious anemia virus. *Gene Ther* **5**: 1481–1487.